UNIVERSITÀ DEGLI STUDI DI MILANO

DIPARTIMENTO DI BIOSCIENZE

PhD School In Molecular And Cellular Biology

XXXV Cycle

Academic Year 2021-2022

The *Arabidopsis thaliana* ABC transporters TAP1, NAP8 and ATH12 extrude peptides from chloroplasts and are linked to chloroplast protein homeostasis maintenance.

Scientific tutor:

Prof. Paolo Pesaresi

Nicolaj Jeran

R12476

INDEX

RIASSUNTO

Il cloroplasto è l'organello fotosintetico delle alghe verdi e delle piante. Il cloroplasto originò da un antenato simile ai cianobatteri tramite un antico evento endosimbiontico, in maniera simile a quanto accaduto per il mitocondrio. Come vestigi delle sue origini, il cloroplasto possiede un genoma che ancora esprime poche proteine plastidiali. Come diretta conseguenza, il proteoma del cloroplasto è un mosaico di proteine codificate dal nucleo e dal cloroplasto stesso. Questo richiede un importante scambio di informazioni tra i due genomi, per coordinare l'espressione genica per la biogenesi del cloroplasto e per adattarlo alle esigenze fisiologiche e ai cambiamenti nell'ambiente. La segnalazione retrograda è una collezione di vie molecolari generate dal cloroplasto per informare il nucleo del suo stato di sviluppo e funzionale. Lo studio delle vie di segnalazione retrograda coinvolte nella comunicazione di una perturbata omeostasi plastidiale è un campo di ricerca recente e dinamico. Nei nematodi, la via di segnalazione retrograda della omeostasi proteica mitocondriale si affida all'estrusione di peptidi, prodotti dalla degradazione delle proteine danneggiate, da parte del trasportatore ABC HAF-1 localizzato sulla membrana interna del mitocondrio. HAF-1 è omologo al trasportatore di peptidi mitocondriale MDL1 di lievito, che se rimosso causa sensibilità al calore. In questo lavoro, i trasportatori ABC del cloroplasto di *Arabidopsis thaliana* TAP1, NAP8 e ATH12, non ancora caratterizzati, sono stati identificati come i più vicini omologhi sia di MDL1 che di HAF-1. La presenza di questi trasportatori è necessaria ai cloroplasti per estrudere peptidi quando esposti a calore, e ognuno di loro, è in grado di complementare la sensibilità al calore del mutante di lievito *⊿mdl1*. Piante mutanti nei tre corrispettivi geni sono più sensibili a condizioni che perturbano l'omeostasi proteica plastidiale. Coerentemente, il mutante triplo fallisce nel accumulare a livello di proteina, ma non a livello di trascritto, la chaperona plastidiale CLPB3, , quando esposto ad alte temperature, suggerendo un possibile ruolo per questi trasportatori nella regolazione post-

trascrizionale di CLPB3 e, in generale, nella protezione contro le minacce verso la omeostasi proteica del cloroplasto.

ABSTRACT

The chloroplast is the photosynthesising organelle of green algae and plants. The chloroplast originated from an ancient endosymbiosis event with a cyanobacteria-like ancestor, similar to what occurred for the mitochondrion. As vestiges of its origin, the chloroplast retains its genome which still encodes a few plastid proteins. As a direct consequence, the chloroplast proteome is a mosaic of nuclear- and plastid-encoded proteins. This requires an important exchange of information between the two genomes, to coordinate gene expression for chloroplast biogenesis and organelle adaptation to internal or external variations. Retrograde signalling is a collection of pathways generated by the chloroplast to inform the nucleus about its developmental and operational status. The study of the molecular pathways involved in the communication of perturbed plastid protein homeostasis is a recent and dynamic research field. In nematodes, a retrograde signalling pathway triggered by the deterioration of the mitochondrial protein homeostasis relies on the extrusion of peptides, produced by the proteolysis of the damaged proteins, by the HAF-1 ABC transporter on the mitochondrial envelope, paving the way for peptides as possible signalling molecules. HAF-1 is the homolog of the MDL1 mitochondrial peptide transporter of yeast, which if removed causes sensitivity to heat. In this work, TAP1, NAP8 and ATH12 uncharacterized ABC transporters of the chloroplast in *Arabidopsis thaliana* were identified as the closest homologues of both HAF-1 and MDL1. The presence of the transporters is required to extrude peptides from chloroplasts upon heat exposure and each of them could complement the heat sensitivity of *⊿mdl1* null mutant in yeast. Triple mutant plants exhibit higher sensitivity to conditions that challenged the plastid protein homeostasis, such as high temperature. Coherently, triple mutant plants failed the up-regulation of CLPB3 plastid chaperone at the protein level, but not of the corresponding transcripts, upon exposure to high temperatures, suggesting a

possible role for these transporters in the post-transcriptional regulation of CLPB3 and, overall, in the protection of chloroplast protein homeostasis against threats.

INTRODUCTION

Chloroplasts are photosynthesizing organelles

The primary energy source for life on Earth is sunlight. Solar electromagnetic radiation is absorbed and transformed into chemical energy, stored as carbohydrates, by a chemical reaction, called photosynthesis. Eukaryotic organisms can perform this reaction, thanks to the chlorophyll-containing chloroplast, a specialized form of plastid. Plastids are extremely plastic organelles that, starting from the undifferentiated proplastid, can develop in several types according to developmental and environmental cues (Fig. 1). Nevertheless, the chloroplast is the most ancient kind of plastid that, in addition to providing nutrients to the cell, is also pivotal for the biosynthesis of a plethora of essential compounds and the perception of both biotic and abiotic challenges (Lopez-Juez and Pyke, 2005; Jarvis and López-Juez, 2013).

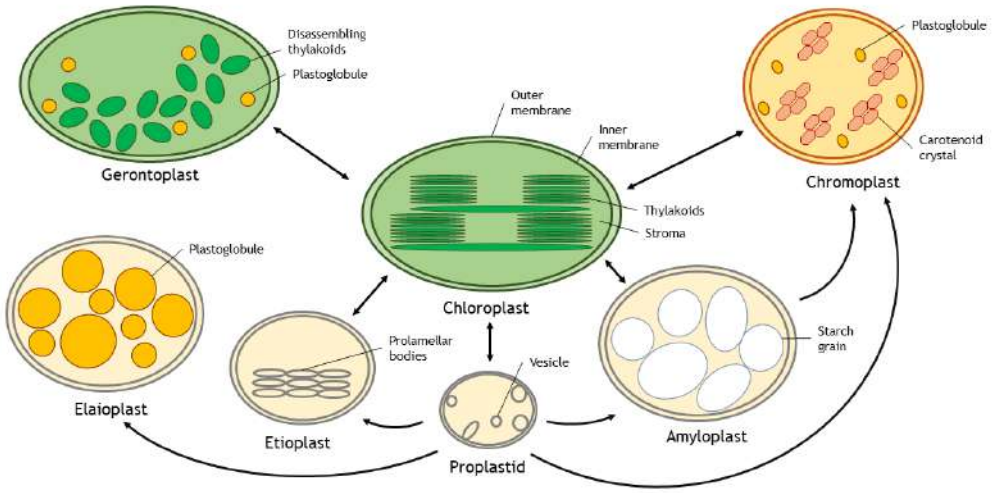

Figure 1 – Common types of plastids present in land plants. Plastids are extremely plastic organelles that, starting from the undifferentiated proplastid, can develop in several types according to developmental and environmental cues. Some of the types of plastids can redifferentiate into other types as indicated by the arrows. The differentiation implies the plastid proteome reorganization. Chloroplasts are the photosynthesising form of plastids. Etioplasts produce chlorophyll precursors in darkness forming prolamellar bodies that upon light-

driven induction rapidly develop into chloroplasts. Gerontoplasts are chloroplasts undergoing senescence processes. Chromoplasts are plastids accumulating huge amounts of carotenoid pigments often found Amyloplasts and elaioplasts have storage functions, accumulating starch granules or lipid-containing plastoglobuli, respectively (Jarvis and López-Juez, 2013).

The typical chloroplast of land plants is shaped as a lens with a diameter between 5 and 10 μm and a thickness of 3-4 μm. According to the cell type and the species, chloroplasts number varies from a few to hundreds. Chloroplasts are defined by an envelope composed of the outer and the inner membranes, separated by the intermembrane space. The envelope is the interface that mediates the exchange of substances and information between the organelle and the cytoplasm of the cell. The outer membrane is permeable to molecules up to 10 kDa, whereas the inner membrane confers selectivity to the chloroplast (Flügge, 2001). The inner membrane delimits the stroma, a protein-rich aqueous environment, that acts as cytosol of the organelle. It is the site of the carbon fixation reactions, it contains the chloroplast genetic machinery and the thylakoids, the internal membranous system. The thylakoids form a complex interconnected compartment, which encloses the lumen (Mustárdy and Garab, 2003).

Embedded in the thylakoids are large protein complexes which provide a scaffold on which chlorophylls are precisely positioned to absorb photons and transfer their energy to the reaction centres of the two photosystems (Grondelle et al., 1994). Photosystem II exploits this energy to extract from water molecules their electrons producing oxygen as a by-product (McEvoy and Brudvig, 2006). These electrons flow from photosystem II to photosystem I through the electron transport chain (Gould and Izawa, 1973). Electrons from photosystem II are accepted by the plastoquinone, an aromatic and lipophilic molecule. Once reduced, the plastoquinol diffuses in the thylakoid membrane towards the cytochrome b_6f where it is oxidized donating its electrons. The electron transfer between the photosystem II and the cytochrome through the plastoquinone pool pumps protons into the lumen establishing a pH gradient across the thylakoid membranes (Okamura et al., 2000).

In turn, the cytochrome transfers the electrons to the photosystem I through the small copper-containing water-soluble protein plastocyanin (Gross, 1993). The proton gradient is then dissipated by the ATP-synthase which converts the electro-chemical gradient into ATP (Boyer, 1997). At last, electrons are transferred to the $NADP^+$ which is reduced to NADPH by the photosystem I and ferredoxin (Karplus et al., 1991). ATP and NADPH are invested in the Calvin-Benson cycle, where the RuBisCO enzyme fixes carbon dioxide molecules into triose phosphate intermediates which ultimately are converted into glucose in the cytoplasm (Cleland et al., 1998).

Chloroplasts originated from an ancient endosymbiosis

Similar to what occurred to the mitochondrion, the chloroplast also originated from an endosymbiosis event, roughly 1,5 billion years ago between a eukaryotic host and a photosynthetic cyanobacteria-like prokaryote (Sagan, 1967; Dorrell and Howe, 2012). An extraordinary diversity of photosynthetic eukaryotic species arose from this event. Those that derived by the primary endosymbiosis are grouped in the Archaeplastida clade and share the presence of primary plastids, which are surrounded by an envelope composed of two lipid bilayers: the innermost deriving from the cyanobacteria-like ancestor and the outermost descending from the host eukaryotic cell (Dyall et al., 2004; Dorrell and Howe, 2012). Three major lineages based on the characteristics of their photosynthetic organelles can be recognised within the Archaeplastida: Glaucophyta, Rhodophyta and Chloroplastida (Adl et al., 2005). The Glaucophyta possesses the most basal plastid, called cyanelle, that still has, as vestiges of its prokaryotic ancestry, the peptidoglycan wall and the typical cyanobacterial pigments phycobilins, in addition to chlorophylls. The Rhodophyta has the rhodoplast which lacks the ancestral peptidoglycan wall but still contains phycobilins and chlorophylls. Lastly, the Chloroplastida, in which the green algae (Chlorophyta) and the land plants (Embryophyta) groups are placed, exhibits the most derived kind of plastid, the chloroplast (Leebens-Mack et al., 2019).

The establishment of a properly functioning photosynthesising organelle from the endosymbiotic relationship between the host eukaryotic cell and cyanobacteria-like prokaryotic cells required millions of years and several attempts to stabilize the relationship. The first endosymbiosis events were most likely very unstable and led to the quick lysis of the bacteria within the eukaryotic cytoplasm. Eventually, the released prokaryotic DNA was integrated into the eukaryotic genome (Dagan and Martin, 2006). This newly acquired genetic material was, at first, impossible to express by the eukaryotic system due to the prokaryotic regulatory elements, and thus, it simply accumulated within the host genome for a long time as non-functioning nuclear plastid DNA or nuptDNA. This transfer of genetic material, from both plastids and mitochondria, still occurs nowadays (Huang, 2005). With time, the prokaryotic DNA sequences mutated until they could be expressed by the eukaryotic system. In this way, these newly nuclear-encoded proteins, derived from the genetic material of previous unsuccessful endosymbionts, could now be used by the present endosymbionts, providing chances to prolong and modulate the relationship. This phenomenon has likely occurred multiple times before a modern photosynthetic organelle finally emerged (Howe et al., 2008).

The massive horizontal transfer of genetic material in favour of the nucleus deprived the plastid genome of genes (Bock and Timmis, 2008). In *Arabidopsis thaliana*, the plastome (*i.e.* the plastid genome) bears only 130 genes encoding for tRNAs, rRNAs and 85 proteins mainly involved in the photosynthetic process and the plastid gene expression, instead, the other 2-3000 plastid-localised proteins are nuclear-encoded (Lopez-Juez and Pyke, 2005). The reason why a small fraction of the genes is still encoded by the plastome is not certain, however, a few explanations have been hypothesised. For example, those genes encoding for highly hydrophobic proteins, difficult to be imported into the chloroplast, would be favoured to be maintained within the plastome (Daley and Whelan, 2005). Another hypothesis is based on the observation that most of the plastid-encoded proteins have functions

in energy metabolism. Indeed, being the photosynthetic process harmful to the involved proteins, their genes would have been retained within the plastome to assure a faster protein turnover (Allen, 2015). A plastid capable to perform autonomously *de novo* protein synthesis would be able to rapidly satisfy its own particular needs, whereas an exclusively centralized production of plastid proteins in the cytosol would force the entire pool of the cellular chloroplasts to adapt to any given perturbation, even if their operativity is satisfactory (Allen and Martin, 2016). Accordingly, the local protein synthesis requires RNA polymerase, tRNA, rRNA and ribosomal proteins, so also those genes were retained in the chloroplast (Maier et al., 2013). Despite all of this, both the photosynthetic apparatus and the plastid transcriptional and translational machinery still necessitate nuclear-encoded factors to be functional.

Chloroplast and nucleus exchange information

As briefly resumed above, the origin and the evolutionary history of the chloroplast have shaped its proteome as a mosaic of proteins, encoded by two physically separated genomes. Notably, nuclear- and plastid-encoded proteins assemble in hybrid multimeric complexes, requiring precise stoichiometry. The fact that plastid-localised proteins are almost completely nuclear-encoded places the nucleus in control over the plastid for its biogenesis, differentiation and maintenance, however, at the same time, chloroplasts need to influence the nucleus. As a consequence of this context, plant cells evolved effective communication mechanisms that can be divided into anterograde pathways (*i.e.* nucleus-to-chloroplast) and retrograde pathways (*i.e.* chloroplast-to-nucleus) (Fig. 2). The anterograde control mainly consists of nuclear-encoded plastid-localised proteins involved in the transcription and translation of the plastid genetic material. On the other hand, the chloroplast, through various retrograde signals, communicates developmental, functional and environmental information. The nucleus reacts to the retrograde signals by generating an anterograde correction, that is the

modulation of its gene expression that results in the production of those nuclear-encoded plastid proteins that can meet the chloroplast needs (Woodson and Chory, 2008; Jarvis and López-Juez, 2013; Hernández-Verdeja and Strand, 2018; Loudya et al., 2020).

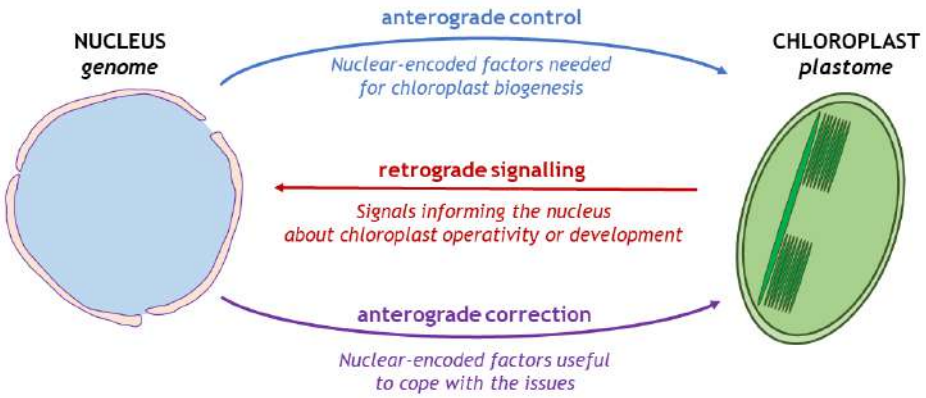

Figure 2 – Schematic representation of the reciprocal exchange of information between the nucleus and the chloroplast. The anterograde control mainly consists of nuclear-encoded plastid-localised proteins involved in the transcription and translation of the plastid genetic material. The chloroplast can emanate several kinds of signals, collectively known as retrograde signalling, that transmit developmental, functional and environmental information. The anterograde correction is the result of the reprogramming of the nuclear gene expression according to those signals.

Examples of anterograde control mechanisms

The composition and the regulation of the chloroplast transcriptional and translational machinery are bright examples of the anterograde control exerted by the nucleus and the complexity of the interplay between the nucleus and the chloroplast. The chloroplast has at least two very different RNA polymerases: the multimeric Plastid Encoded Polymerase (PEP) and the monomeric Nuclear Encoded Polymerase (NEP) (Börner et al., 2015). The PEP enzyme had been inherited by the cyanobacteria-like ancestors and, consequently, it strongly resembles the typical prokaryotic enzyme. The core enzyme is composed of α, β, β' and β" subunits encoded by *rpoA*, *rpoB*, *rpoC1* and *rpoC2* genes, respectively, which are conserved in the plastome, as suggested by the name of the polymerase (Hajdukiewicz et al., 1997). All these genes are essential for proper chloroplast

biogenesis, as mutations disrupting any of them result in albino or yellowish phenotypes (Pfannschmidt et al., 2015). Like any prokaryotic RNA polymerase, PEP requires σ factors to recognize promoters and to initiate transcription (Tiller and Link, 1995). In contrast to the core PEP subunits, plastid σ factors are nuclear-encoded (*SIG1-6* genes in *A. thaliana*) and have both specialised roles and overlapping functions (Lysenko, 2007; Woodson et al., 2013; Chi et al., 2015). In addition to plastid σ factors, also the nuclear-encoded PEP-associated proteins (PAPs) are essential for PEP activity (Steiner et al., 2011). These proteins appear to be a unique evolutionary achievement of land plants, as no orthologous have been identified in the green algae *Chlamydomonas reinhardtii* (Surzycki, 1969; Pfalz and Pfannschmidt, 2013). The chloroplast NEP enzyme, or RPOTp, is another important component of the nuclear anterograde control over the plastid. In *Arabidopsis*, three *RPOT* genes are found in the nuclear genome. *RPOT1* produces the RNA polymerase of mitochondria, called RPOTm. *RPOT2* encodes an enzyme that is targeted to both the mitochondrion and the chloroplast while the *RPOT3* gene produces the chloroplast RNA polymerase. NEP is a monomeric phage-derived RNA polymerase, probably originated by the duplication of the *RPOT1* gene, which is mainly responsible for the transcription of plastid housekeeping genes, among them the PEP-encoding genes, reinforcing further the nuclear control over the plastid gene expression (Hedtke et al., 1997; Hedtke et al., 2000). Moreover, several transcripts of plastid-encoded genes require additional processing to fully maturate, mediated by a plethora of nuclear-encoded proteins, mostly unknown (Jacobs and Kück, 2011). Among these, the pentatricopeptide repeat proteins can bind RNA, stabilize it and perform transcript maturation or transcript editing. These functions could be essential for plant viability (Kotera et al., 2005; Schmitz-Linneweber and Small, 2008a; Tadini et al., 2018).

As it happens for the transcriptional machinery, also the chloroplast ribosome shares several features with that of bacteria (Mache, 1990). Both bacterial

and plastid ribosomes sediment at 70S and are formed by a small 30S and a large 50S subunit that consists of rRNAs and ribosomal proteins, named RPSs or RPLs based on the ribosomal subunit they belong to. In *Arabidopsis thaliana*, the chloroplast ribosome is composed of 57 proteins. As for many chloroplast protein complexes, the genes encoding for the ribosomal proteins are found both in the plastid genome and in the nuclear genome. The plastid genome codes for 21 ribosomal proteins which correspond to roughly two-fifth of the total ribosomal proteins (Sugiura, 1995; Yamaguchi et al., 2000; Yamaguchi and Subramanian, 2000; Olinares et al., 2010; Tiller and Bock, 2014). Almost all the chloroplast ribosomal proteins have an orthologue in *E. coli* however, some differences in ribosome composition are known. *E. coli* Rpl25 and Rpl30 proteins are not found in chloroplasts. In some species, including spinach, chloroplast RPL23 is substituted by the corresponding protein of the cytosolic 80S ribosome subunit. Finally, PSRP2, PSRP3, PSRP5 and PSRP6 are identified as plastid-specific ribosomal proteins and therefore have no orthologues in bacteria (Bubunenko et al., 1994; Yamaguchi et al., 2000; Yamaguchi and Subramanian, 2000; Tiller and Bock, 2014; Bieri et al., 2017; Zoschke and Bock, 2018). In addition to these differences in ribosome composition, the conserved chloroplast ribosomal proteins present N- and C-terminal extensions, together with internal expansions, that are responsible for the establishment of new interactions with rRNAs, mRNAs, ribosomal proteins and regulatory factors that are exclusive features of the chloroplast (Ahmed et al., 2016; Bieri et al., 2017; Graf et al., 2017). Being a large part of the anterograde control, many nuclear-encoded plastid ribosomal proteins are essential for chloroplast biogenesis and, consequently, their mutation often results in the arrest of embryo development or severe pale phenotypes and stent growth of seedlings (Romani et al., 2012).

Main sources of retrograde signals

As said, the production of nuclear-encoded plastid proteins which directly influence the plastid gene expression is known as the anterograde control, which

sets the chloroplast biogenesis and its genetic material under the regulation of the nucleus. Nevertheless, the chloroplast emits a collection of signals, to transmit information to the nucleus and eventually modify the nuclear gene expression and, consequently, the composition of nuclear-encoded plastid proteins. Together, these signals are collectively indicated as retrograde signalling that can be distinct into "biogenic control" and "operational control" referring to those signals sent during the differentiation of plastids or those released from mature chloroplasts in response to physiological needs and environmental fluctuations, respectively (Chan et al., 2016; Hernández-Verdeja and Strand, 2018). To date, several main sources of retrograde signals can be traditionally defined, the main ones being the activity of the electron transport chain coupled with ROS development, the biosynthesis of tetrapyrroles and the plastid gene expression (Inaba et al., 2011; de Souza et al., 2017; Hernández-Verdeja and Strand, 2018).

Overall, the signals that can be correlated with the activity of the electron transport chain appear to be mediated by the plastoquinone pool or by the photosystem I acceptor site along with a variety of redox compounds such as NADPH, thioredoxin and glutathione. However, the regulation of gene expression by this pathway seems inconsistent among different organisms (Pesaresi et al., 2007). In the green algae *Dunaliella tertiolecta* the regulation is thought to be coupled with the plastoquinone pool, while in *Chlamydomonas reinhardtii* it is mediated by the photosystem I (Escoubas et al., 1995; Shao et al., 2006). In *Arabidopsis thaliana* gene modulation in response to short-term light fluctuation depends on the photosystem I but the plastoquinone pool could have a role in long-term adaptation (Fey et al., 2005). In addition, expression studies on ASCORBATE PEROXIDASE 2 upon high-light treatment first suggested H_2O_2 as a possible messenger (Karpinski et al., 1999).

Studies performed on the green algae *Chlamydomonas reinhardtii* demonstrated that cells treated with inhibitors of the late steps of the tetrapyrrole biosynthesis failed to accumulate transcripts of the light-harvesting complex (Beck et al., 2006). These observations suggested that some intermediates of the tetrapyrrole biosynthesis trigger the selective inhibition of nuclear gene expression encoding plastid proteins. Similar to this, treatments with norflurazon, an inhibitor of the phytoene desaturase hampering carotenoid biosynthesis, causes chloroplasts to bleach and lead to the repression of photosynthesis-associated nuclear genes (*PhANGs*) in *Arabidopsis thaliana*. The use of norflurazon-based screens led to the identification of five mutants unable to repress *PhANGs* expression in these conditions. All of the mutated genes encode plastid-located proteins and were indicated as *GUN* (*Genomes UNcoupled*) genes (Susek et al., 1993; Mochizuki et al., 2001; Koussevitzky et al., 2007). *GUN1* produces a pentatricopeptide protein, a class of proteins usually able to interact with RNAs and often involved in their maturation in chloroplasts (Koussevitzky et al., 2007; Schmitz-Linneweber and Small, 2008a). *GUN2* and *GUN3* genes encode a heme oxygenase and a phytochromobilin synthase, respectively, required for heme conversion into phytochromobilin. Their mutation results in the accumulation of heme (Susek et al., 1993; Mochizuki et al., 2001). *GUN4* and *GUN5* produce an Mg-ProtoIX-binding protein and the H subunit of the Mg-chelatase, respectively. Both enzymes are involved in chlorophyll biosynthesis and consequently, the mutants are paler than the wild type (Mochizuki et al., 2001). Successively, *gun6*, a gain of function mutant overexpressing the ferrochelatase 1, upstream to GUN2 and GUN3 enzymes, was found (Woodson et al., 2011). *GUN2* to *GUN6* genes are all involved in tetrapyrrole biosynthesis and the respective mutants have defects in the relative abundance of the related metabolites, suggesting a positive role of tetrapyrroles for *PhANGs* regulation during chloroplast biogenesis (Woodson et al., 2011; Hernández-Verdeja and Strand, 2018).

Historically, studies on the barley mutants *albostrians* and *Saskatoon*, which exhibit albino or variegated phenotypes due to mutations in nuclear genes, had first suggested the possibility that the plastid gene expression generates retrograde signals (Bradbeer et al., 1979). In these mutants, although the cytosolic ribosomes were functional, the activity of plastid-located enzymes was reduced, together with the expression of photosynthesis-associated nuclear genes (*PhANGs*) (Bradbeer et al., 1979; Hess et al., 1994). Instead, the expression of the nuclear gene encoding for the NEP RNA polymerase of the chloroplast was increased (Emanuel et al., 2004). Similar results were obtained with the employment of inhibitors of chloroplast transcription or translation such as lincomycin that, in plants, specifically inhibits chloroplast protein synthesis leading to albino seedlings (Thomson and Ellis, 1972; Inaba et al., 2011). The use of this drug has revealed that the already cited *gun1* mutant is unable to repress *PhANGs* expression, a unique feature among the *gun* mutants that display this phenotype only if treated with norfluorazon, suggesting that GUN1 could have a role in retrograde signalling due to altered plastid gene expression. Indeed, in contrast to the other GUN proteins, GUN1 is not related to tetrapyrrole biosynthesis but it is a pentatricopeptide protein (Koussevitzky et al., 2007). As described earlier, pentatricopeptide proteins are usually associated with RNA maturation and regulation of plastid gene expression (Pfalz et al., 2006; Schmitz-Linneweber and Small, 2008b). However, despite that GUN1 appeared to bind DNA *in vitro*, immunoprecipitation assays performed *in vivo* have failed to detect any stable interaction of GUN1 with nucleic acids (Tadini et al., 2016). Instead, GUN1 seems to be rather engaged in the regulation, possibly through protein-protein interactions, of several plastid molecular mechanisms such as tetrapyrrole biosynthesis, plastid transcription, translation, ROS regulation and protein homeostasis (Colombo et al., 2016; Tadini et al., 2016; Wu et al., 2019; Tadini et al., 2020b; Tadini et al., 2020a; Fortunato et al., 2022).

The knowledge regarding the chloroplast retrograde signals has been deepened during the past years but several aspects remain enigmatic. Notably, in land plants, a specific signalling molecule is still unidentified and, indeed, the retrograde signalling system should be considered as a complex network of signals and pathways that are mostly unknown (Inaba et al., 2011; Hernández-Verdeja and Strand, 2018).

Chloroplast proteome biogenesis, maintenance and degradation

Up to 95% of plastid-localised proteins are nuclear-encoded. This implies that a constant bulk of plastid proteins must be sorted, imported into the chloroplast and processed for maturation. Additionally, mature proteins in the chloroplast require proper folding and continuous quality check. Finally, old or terminally damaged proteins must be removed (Paila et al., 2015; van Wijk, 2015; Nishimura et al., 2016; Fu et al., 2022; Rochaix, 2022). In addition to the physiological protein turnover, the photosynthetic process makes the chloroplast a difficult environment for the organellar protein structures. The absorption of photons and the electron flow require proteins to be highly functional, to guarantee safe energy conversion avoiding ROS production (Suzuki et al., 2012). Thus, to achieve a regular import of nuclear-encoded proteins and their maintenance, chloroplasts are equipped with complex import machinery, numerous chaperones and a plethora of proteases (Flores-Pérez and Jarvis, 2013; Paila et al., 2015; Nishimura et al., 2016).

Import of nuclear-encoded plastid proteins

The nuclear-encoded plastid precursor proteins are discernible from those that are resident in the cytoplasm by the first N-terminal portion of their amino acid sequences which act as a chloroplast-specific targeting signal called chloroplast transit peptide (cTP). The exact features that define a chloroplast transit peptide are still poorly understood since no consensus sequence can be identified even though it is possible to detect it *in silico* (Emanuelsson et al., 2000; Bruce, 2001). The

chloroplast transit peptide recruits cytosolic sorting factors, such as HSP70, HSP90 and/or 14-3-3 proteins to bring the precursor protein to the translocon complex on the surface of the chloroplast (Lee et al., 2013). HSP70 and HSP90 also interact with CHIP (Carboxyl-terminal Hsp70-Interacting Protein), a highly conserved cytosolic E3 ligase (Ballinger et al., 1999). Together, these proteins exert a chloroplast protein quality control by targeting unwanted chloroplast precursors to the proteasome to prevent their accumulation in the cytosol (Lee et al., 2009).

The translocon complex can be described as two molecular gates embedded on the outer and inner membranes of the chloroplast, which eventually interact to form a channel allowing the precursor proteins in the cytoplasm to cross the chloroplast envelope and reach the stroma (Paila et al., 2015). The translocon components placed on the outer membrane are called TOC proteins (Translocon at the Outer membrane of the Chloroplast), while those constituting the complex on the inner membrane are known as TIC proteins (Translocon at the Inner membrane of the Chloroplast). Both group names are followed by numbers indicating the molecular mass in kDa of the corresponding proteins (Schnell et al., 1997).

TOC159 and TOC34 are membrane-bound GTPase receptors which establish the first interactions with the client precursor protein (Chang et al., 2012). The client protein is then inserted into TOC75 which forms the TOC channels thanks to its β-barrel structure (Li and Chiu, 2010). Upon insertion into TOC75, the client protein engages the TIC complex since the translocon proteins on both membranes physically interact (Schnell and Blobel, 1993). Recent studies have highlighted that the ubiquitin-dependent modification of proteins located on the chloroplast outer membrane is a pivotal event, at the basis of chloroplast adaptation to stress conditions. SP1 E3 ubiquitin ligase is embedded in the outer envelope of the chloroplast and, by ubiquitination of TOC components, confers the ability to isolate the chloroplasts from the bulk of plastid precursor proteins in the cytoplasm,

thus modulating the quantity and the quality of the imported precursor proteins (Ling and Jarvis, 2015). The SP2 outer-membrane protein, thanks to its β-barrel architecture, provides a channel through which ubiquitinated TOC components can be extracted and eventually delivered to the proteasome, a process indicated as CHLOroplast-Associated protein Degradation (CHLORAD). The extraction is carried out by the cytosolic CDC48 AAA+ protein, which is also the motor of the similar degradation process known as the Endoplasmic Reticulum-Associated protein Degradation (ERAD) pathway, which inspired the name of the chloroplastic one (Ling et al., 2012; Chen et al., 2020).

Despite that several components of the TIC complex have been characterized, the precise nature of the import machinery of the inner membrane is still not fully understood (Paila et al., 2015). The so-called TIC110 complex is formed by at least TIC20, TIC21, TIC22, TIC40 and TIC110 proteins that were shown to associate with client precursor proteins and with TOC complexes (Kessler and Blobel, 1996; Kouranov et al., 1998; Chou et al., 2003). TIC20 and TIC21 share similar structural organization and topology, both displaying four α-helices, and are thought to form the TIC channel (Teng et al., 2006; Kovács-Bogdán et al., 2011). TIC110 contains two N-terminal α-helices and a large C-terminal region which protrudes into the stroma (Jackson et al., 1998). It is still unclear if TIC110 could be part of the TIC channel, however, a portion close to the transmembrane helices of the stromal domain binds directly transit peptides providing a docking site for the client proteins emerging from the TIC channel, whereas the rest of the stromal domain could serve as a scaffold for the interaction of stromal chaperones involved in the import process (Inaba et al., 2003; Paila et al., 2015).

The motor of the TIC110 translocon complex has been identified in CLPC stromal chaperone, a member of the AAA+ protein family (ATPases Associated with various cellular Activities) which forms a hexameric ring through which the

emerging polypeptide chain is pulled (Nielsen et al., 1997). TIC40 mediates the interaction between CLPC and TIC110 and stimulates the ATPase activity of CLPC (Chou et al., 2006). However, several pieces of evidence indicate that also the stromal chaperone with ATPase activity cpHSC70 (chloroplast Heat Shock Cognate protein of 70 kDa) is a central component of the protein import motor and could provide a second import pathway, parallel with the TIC40/CLPC system (Su and Li, 2010; Paila et al., 2015). More recently, another heteromeric complex associated with the TIC complex, referred to as 2-MD complex, that functions as an ATP-dependent import motor was found in *Arabidopsis thaliana* and is composed of the plastid-encoded Ycf2 protein, four nuclear-encoded FTSH-like proteins and the nuclear-encoded FTSH12 and it appears to have a complementary role with that of the TIC110 complex (Kikuchi et al., 2018).

A second 1 MDa protein complex has been found associated with precursor client proteins at the inner membrane and TOC elements. It is composed of TIC20 and TIC21, which are also part of the TIC110 complex, TIC56, TIC100 nuclear-encoded proteins and the plastid-encoded Tic214/Ycf1 protein, (Kikuchi et al., 2009). Tic214 displays six α-helices, is the first putative import component found to be encoded by the plastome and, in tobacco, is essential for plant viability (Drescher et al., 2000; Kikuchi et al., 2013). Interestingly, the components not shared with the TIC110 complex are absent in Glaucophyta and Rhodophyta algae lineages and the Poaceae land plant family, suggesting that the 1 MDa complex is not required in all plastids (Drescher et al., 2000). It has been proposed that the TIC110 complex and the 1 MDa complex could be two independent channels for precursor proteins, however, since they share the TIC20 and TIC21 components and both complexes were identified as associated with the same precursor client proteins, it seems reasonable that they could function coordinately for import (Kikuchi et al., 2013; Paila et al., 2015).

Main chaperones and proteases of the chloroplast

To generate and maintain a fully functional chloroplast proteome a variety of proteases are required for several purposes including removal of chloroplast transit peptides, cleavage of the N-terminal methionine from plastid-encoded proteins, additional N- or C-terminal cleavages for protein maturation, degradation of unfolded, damaged or aggregated proteins and removal of unwanted proteins upon developmental or environmental changes. The main known chloroplast proteases and their direct chaperones, which function as adaptors, can be divided into the ATP-dependent and the ATP-independent proteins. The ATP-dependent group includes members from the LON, CLP and FTSH families, all classified in the larger AAA+ (ATPases Associated with various cellular Activities) protein family, whereas the ATP-independent members are from the DEG family (van Wijk, 2015). The ATP-dependent members of the AAA+ superfamily bind and hydrolyse ATP to power the conformational changes useful for unfolding the protein substrates and, in *Arabidopsis thaliana*, the FTSH and CLP proteins are the major conserved multimeric protease complexes of the chloroplast. Both proteolytic systems evolved from prokaryotic ancestors and are conserved in all kingdoms of life (Nishimura et al., 2016).

The FTSH (Filamentation Temperature Sensitive) family comprises numerous membrane-embedded metalloproteases composed of one or two transmembrane N-terminal domains, the ATPase domain and the proteolytic domain with a zinc-binding motif (Fig. 3). These metalloproteases must interact in homo- or hetero-hexamers to form the catalytic chamber that can control the access of substrates (van Wijk, 2015). *Arabidopsis thaliana* genome encodes twelve *FTSH* genes, nine of them targeted to the chloroplast (Nishimura et al., 2016). The four major isoforms are embedded in the thylakoids, with the catalytic domain facing the stroma. The thylakoid FTSHs are divided into type A, consisting of FTSH1 and FTSH5, and type B, containing FTSH8 and FTSH2. The removal of all type A or

type B proteases results in albino phenotypes (Yu et al., 2004; Zaltsman, 2005). FTSH2 and FTSH5 are the first and the second most abundant FTSH isomers in the chloroplast as reflected by their loss-of-function mutants, resulting in increasingly severe variegated phenotypes on true leaves indicating their importance in thylakoid development. The severity of the phenotypes correlates with the physiological abundance of the lost protease. Indeed, the *ftsh2* mutant shows leaves with large white sectors, while in the *ftsh5* mutant variegations are less extended. Coherently, the double mutant results in an enhanced variegated phenotype with only a few small green sectors. Additionally, both mutants show increased sensitivity to high light. Conversely, *ftsh1* and *ftsh8* mutants and the double mutant are wild-type-like (Takechi et al., 2000; Sakamoto et al., 2002; Sakamoto et al., 2003; Zaltsman, 2005). The FTSH6 sub-plastidial localisation is still uncertain, however, it has been linked with the regulation of thermomemory in *Arabidopsis* (van Wijk, 2015; Sedaghatmehr et al., 2016). FTSH7, FTSH9, FTSH11 and FTSH12 are localised at the chloroplast's inner membrane. FTSH7 and FTSH9 are thought to form a complex, although no additional information is available (Wagner et al., 2012). FTSH12 has been mentioned above as part of the novel 2-MD complex involved in protein import that comprises Ycf2 and four FTSHi proteins, which, lacking the zinc-binding motif, are not catalytically active but retain the chaperone activity (Kikuchi et al., 2018). FTSH11 forms homohexamer at the chloroplast inner membrane and its loss has little or no impact on developing plantlets kept under standard growth conditions. Nevertheless, FTSH11 is important to cope with heat exposure, as the knock-out mutant displays hampered growth and sharp decreases in the photosynthetic performance, if cultivated at temperatures higher than 30°C (Chen et al., 2006; Chen et al., 2018). Detailed analyses of the mutant revealed its interactions with proteins involved in photosynthesis and import, as probable targets, and the chaperones HSP70, CPN60 and CLPB3, as putative substrate-delivery partners (Adam et al., 2019).

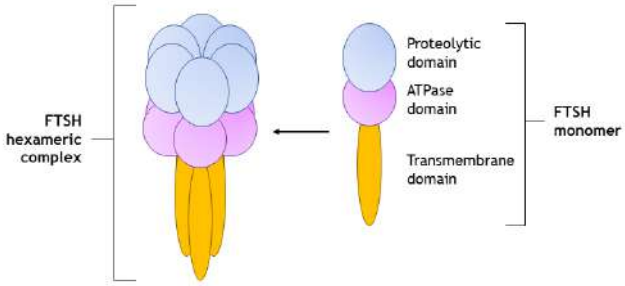

Figure 3 – Simplified representation of an FTSH protease. A single monomer is composed of a transmembrane domain, an ATPase domain and the proteolytic domain which coordinates a zinc ion. To form a functional FTSH protease, monomers must form a hexameric complex. In *A. thaliana* chloroplasts can be found both homo- and hetero-complexes.

The serine-type CLP (CaseinoLytic Protease) machinery is the most abundant stromal protease of the chloroplast and it is composed of several subunits organised in rings (Fig. 4). The proteolytic core consists of two asymmetric heptameric rings. The P-ring contains the catalytically active subunits CLPP3, CLPP4, CLPP5 and CLPP6 in a 1:2:3:1 ratio. The R-ring is composed of the catalytic plastid-encoded subunit ClpP1 and the catalytically inactive CLPR1, CLPR2, CLPR3 and CLPR4 proteins in a 3:1:1:1:1 ratio (Olinares et al., 2011a). The various *clpp* and *clpr* null mutants in *Arabidopsis thaliana* exhibit several phenotypes affecting embryogenesis, seedling development and chloroplast biogenesis (Kim et al., 2013). The unique plastid-encoded ClpP1 subunit has been studied in tobacco and it is essential for leaf development (van Wijk, 2015). Loss of *CLPP4* and *CLPP5* is incompatible with life, as the respective mutant embryos cannot complete their development. The knock-out mutants *clpr2*, *clpr4* and *clpp3* arrest their development at the cotyledon stage however, when cultivated in heterotrophic conditions, they can complete the life cycle. Interestingly, the *clpr1* mutant displays only a mild virescent phenotype because its functions can be partially replaced by CLPR3, resulting in a hampered CLP complex (Kim et al., 2009; Kim et al., 2013). Protein substrates are delivered to the proteolytic core by hexameric rings with chaperone functions composed of CLPC1, CLPC2 and/or CLPD subunits. These HSP100

class proteins present a C-terminal Protease Binding Domain (PBM) which mediates the interactions with the proteolytic rings. The unfoldase activity of the hexamer linearizes the target polypeptide facilitating its proteolytic degradation by the CLP core rings (Lee et al., 2007; van Wijk, 2015). The knock-out mutations in *CLPC1* result in small pale plants, while *clpc2* and *clpd* plants have no phenotype (Constan et al., 2004; Sjögren et al., 2004). CLPC chaperones have been found associated with the TIC complex and could function as a motor for the translocon machinery (Chou et al., 2006; Paila et al., 2015). Additionally, they could be involved in protein quality control during the import process by recruiting the CLP core protease at the translocon to degrade misfolded proteins generated during their import (Nishimura et al., 2016).

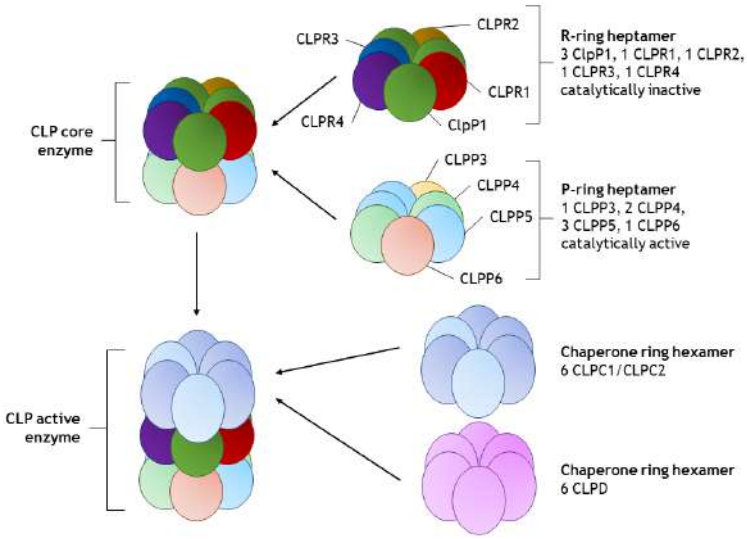

Figure 4 – Simplified representation of CLP protease complex subunits. The CLP core enzyme is composed of two heptameric rings, the R- and the P-ring. The R-ring is catalytically inactive and contains three ClpP1, one CLPR1, one CLPR2, one CLPR3 and one CLPR4 subunit. The P-ring is catalytically active and features one CLPP3, two CLPP4, three CLPP5 and one CLPP6 subunit. The ClpP1 protein is the only one encoded by the plastome. The chaperone rings are composed of CLPC1/C2 or CLPD proteins. By interacting with the core enzyme, these rings deliver the substrates to the core enzymes. They promote CLP activity by ATP hydrolysis.

Another important plastid HSP100 chaperone is CLPB3. Similar to CLPC/D chaperones, also CLPB3 forms homohexameric rings, although it lacks the PBD sequence preventing its interaction with the CLP proteolytic core. *CLPB3* depletion results in seedlings which germinate but soon die when grown on soil, or in severe albinotic phenotype with thylakoid-deficient plastids when the seedlings germinated on a sugar-containing medium. Additionally, *clpb3* mutants possess no tolerance to increasing temperatures. Indeed, plants exposed to heat selectively up-regulate *CLPB3* transcripts while exhibiting no changes in *CLPC/D* expression (Myouga et al., 2006; Lee et al., 2007). The biochemical characterization of CLBP3 demonstrated that it has high affinity with protein aggregates and it acts as an unfoldase contributing to dissolve aggregates or to linearize its targets allowing for their re-folding, functioning either alone or with the aid of cpHSP70/J20 chaperone system (Pulido et al., 2016; Parcerisa et al., 2020). These pieces of evidence point to two diversified roles for CLPC/D and CLPB3 chaperones. The cpHSP70/J20 chaperone system functions as a hub that can dispatch its misfolded clients either to the CLPC/D ring, which linearizes them for their final degradation by the CLP protease core or to CLPB3, which actively promotes the acquisition of their native conformations (Pulido et al., 2016).

Degradation of chloroplasts

Chloroplasts are expensive organelles to maintain and, when damaged, can be an additional source of hazard to cells, especially under stressful environmental conditions, starvation or during senescence. Recent investigations revealed a variety of pathways that cells employ to commit old or damaged chloroplasts for degradation, achieving the maintenance of a functional pool of chloroplasts and the redistribution of nutrients/resources (Woodson, 2016; Woodson, 2022). Chloroplast portions or whole organelles can be delivered to the central vacuole by vesicle-mediated pathways. Some pathways work with autophagosome-derived vesicles. Autophagy is an ancient process for the degradation of cellular components

in eukaryotic cells that requires the involvement of conserved ATG proteins, and therefore, these degradation pathways are also referred to as ATG-dependent. The other pathways that instead are executed by vesicles unrelated to the autophagosome formation are indicated as ATG-independent (Fu et al., 2022). In some cases, chloroplasts have been observed to bud large vesicles directly in the vacuole, known as "bleb". This event is triggered by the activity of the cytosolic PUB4 E3 ubiquitin ligase that tags yet unidentified outer-membrane chloroplast proteins. Indeed, PUB4 removal suppresses chloroplast degradation and cell death in the mutant *fc2*, which accumulates excessive $^1O_2$, and promotes greening in the double mutant *gun1 ftsh5*, which is defective in protein quality control mechanisms (Woodson et al., 2011; Jeran et al., 2021; Lemke et al., 2021).

Chloroplast protein homeostasis as a source of retrograde signals

The development of a repressible chloroplast gene expression system that specifically depletes *ClpP1* expression in the green algae *Chlamydomonas reinhardtii*, granted the ability to induce an imbalance of the chloroplast protein homeostasis and study the cellular reaction to the event (Ramundo et al., 2014). Several consequences arose in cells depleted of the CLP protease complex. They stopped their proliferation and displayed progressive impairment of the photosynthetic performance. Coherently, the expression of nuclear-encoded genes involved in these processes was repressed. Conversely, the expression of nuclear genes encoding chloroplast chaperones and proteases, and their accumulation at the protein level, were steadily up-regulated. The accumulation of these proteins in chloroplasts can counteract and mitigate protein aggregation and damage (Ramundo et al., 2014; Ramundo and Rochaix, 2014). Several studies in *Arabidopsis thaliana* describe similar phenomena. Indeed, mutants lacking FTSH or CLP proteins exhibit chloroplast proteomes highly enriched in chaperones, proteases and ROS detoxifiers (Kim et al., 2009; Kim et al., 2013; Adam et al., 2019; Dogra et al., 2019). Taken together, these pieces of evidence strongly suggest that the perturbation of the chloroplast

protein homeostasis triggers the generation of retrograde signals that promote the nuclear production of plastid-localised protein quality control factors. These molecular mechanisms are considered a chloroplast version of the Unfolded Protein Response, a molecular mechanism first discovered in the yeast endoplasmic reticulum when unfolded proteins accumulated due to defective folding capacity, and successively found also in mitochondria of mammalian cells (Cox et al., 1993; Zhao et al., 2002; Ramundo et al., 2014; Llamas et al., 2017; Qureshi et al., 2017; Dogra et al., 2019).

The signalling pathways mediating the UPR in the endoplasmic reticulum are very conserved and are well-studied (Hetz et al., 2015). Instead, the research in the field of mitochondrial UPR was only recently boosted with the characterization of a peptide-mediated mitochondrion-to-nucleus retrograde signalling pathway in the roundworm *Caenorhabditis elegans* (Fig. 5) (Haynes et al., 2007; Haynes et al., 2010). More into detail, the exposure of the animals to heat causes mitochondrial proteins to damage and unfold. Unfolded proteins are prone to aggregate, therefore, the mitochondrial soluble AAA+ CLPXP protease complex promptly degrades them into peptides. These 6 to 20 residues long peptides are eventually extruded into the cytoplasm, where promote the nuclear translocation of the ATFS1 transcription factor activating the expression of UPR-related genes. The peptide efflux depends on the ABC transporters HAF-1, localised at the inner membrane of the mitochondria (Haynes et al., 2010). Strikingly, HAF-1 is orthologous to the previously reported ABC transporter MDL1 from *Saccharomyces cerevisiae* which also mediates peptide extrusion from mitochondria upon heat incubation (Young et al., 2001). These results have encouraged the re-evaluation of the human ABCB10 mitochondrial transporter which possesses a fair sequence identity with both MDL1 and HAF-1. ABCB10 also localises at the inner membrane of the mitochondrion, and its activity has been associated with oxidative stress protection although it is not clear yet if its substrates are peptides, heme intermediates or both (Liesa et al., 2012).

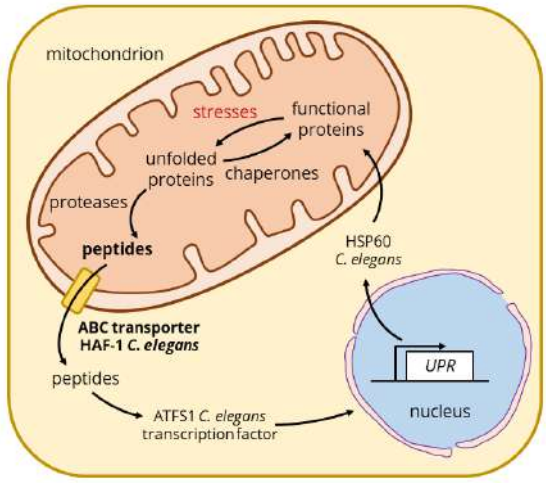

Figure 5 – Graphical summary of the mitochondrial UPR described in *C. elegans*. Upon heat, mitochondrial proteins are damaged and their unfolding is promoted. In these conditions, protein aggregates could form threatening mitochondria functionality. The mitochondrial proteases degrade the damaged proteins into peptides. The resulting peptides are then extruded into the cytoplasm by the ABC transporter HAF-1, localised at the inner membrane of the mitochondria. In the cytoplasm, the peptides promote the translocation of the ATFS1 transcription factor into the nucleus activating the expression of UPR-related genes (Haynes et al., 2010).

ABC proteins

The ABC (ATP-Binding Cassette) proteins constitute one of the largest protein families found in all living organisms (Higgins, 1992; Henikoff et al., 1997). The vast majority of the ABC proteins act as transporters, as their general structure features two transmembrane domains, which delineate a pore in the membrane, and two soluble nucleotide-binding domains, which power substrates export. The transmembrane domains are generally composed of four or six hydrophobic α-helices that appear to determine, or at least contribute, to the substrate selectivity of the transporter. Nevertheless, the transmembrane domains of even closely related ABC transporters exhibit low levels of sequence similarity, unlike the nucleotide-binding domains which are strongly conserved and give the name to the protein family (Higgins, 1992; Sánchez-Fernández et al., 2001; Martinoia et al., 2002; Kang et al., 2011). The survey of the superfamily reveals the modular construction of the ABC transporters. The four core domains may be encoded by individual genes, by

one gene encoding for a half-transporter (composed of a nucleotide-binding domain and a transmembrane domain) which then homodimerizes, by two genes each encoding half-transporters that form heterodimers or by a single gene coding for a full-transporter. In addition, the organization of the domains in both half-transporters and full-transporters is defined as forward, if the transmembrane domain lies in the N-terminal portion and the nucleotide-binding domain is in the C-terminal region, or as reverse in the opposite case (Higgins, 1992; Sánchez-Fernández et al., 2001; Kang et al., 2011).

Based on their domains structure and phylogenetic relationships and, following the nomenclature system in use for animal transporters, the *Arabidopsis thaliana* ABC proteins are currently classified into eight subfamilies, that re-organises the previous nomenclature system (Fig. 6). The ABCA subfamily comprises eleven forward half-transporters, previously part of the ABC Two Homolog (ATH) group, and one forward full-transporter, from the ABC One Homolog (AOH). The ABCB subfamily includes twenty-one forward full-transporters, former MultiDrug Resistance (MDR), and seven forward half-transporters, previously belonging to the Transporter Associated with antigen Processing (TAP) and Transporter of the Mitochondrion (ATM) subfamilies. The ABCC contains fifteen forward full-transporters before indicated as Multidrug Resistance-associated Proteins (MRP), that exhibit an additional N-terminal transmembrane domain. The ABCD subfamily is represented by one forward half-transporter and one forward full-transporters previously named Peroxisomal Membrane Proteins (PRP) due to their subcellular localisation. The ABCE and the ABCF subfamilies consist of three and five members, respectively, that lack any transmembrane domains and are, probably, involved in other functions than transport. The ABCG is the largest subfamily and it groups twenty-eight reverse half-transporters, formerly indicated as White-Brown Complex homolog (WBC), and twelve reverse full-transporters, named Pleiotropic Drug Resistance (PDR). Lastly, the ABCI subfamily contains twenty-one proteins

that fold in single transmembrane, nucleotide-binding or accessory domains that, at least some of them, can assemble into multi-subunit transporters, similar to what occurs in prokaryotes (Sánchez-Fernández et al., 2001; Verrier et al., 2008; Kang et al., 2011).

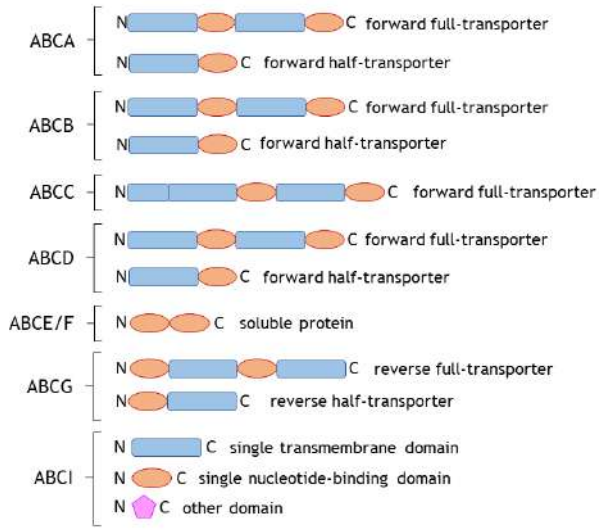

Figure 6 – Simplified graphical representation of the ABC protein subfamilies. ABCA, ABCB and ABCD families contain forward full- or half-transporters. ABCC family groups forward full-transporters with an additional N-terminal transmembrane domain. ABCE and ABCF families are composed of soluble proteins with no transmembrane domains. In the ABCG family are found reverse full- or half-transporters. The ABCI family contains proteins that represent single domains, that can interact to form complete transporters. Blue rectangles represents transmembrane domains, red circles indicate nucleotide binding domains.

AIM OF THE PROJECT

Several pieces of evidence support the notion that the chloroplast proteome adapts in response to perturbed protein homeostasis to re-establish its optimal functional state. Protein homeostasis perturbations can be due to genetic defects that hinder the molecular mechanisms involved with the generation and maintenance of the proteome or can result from external challenges. Either way, proteome modification requires the nuclear gene expression to be re-programmed to cope with the issues. To date, the modality by which the chloroplast communicates to the nucleus the onset of challenges to its protein homeostasis has been partially elucidated, but it is still an open topic that can be investigated deeply.

Chloroplasts and mitochondria share similar molecular features due to their common evolutionary origin that forces the coordination of the organellar genomes with the nuclear genome, which provides almost completely for the proteins of the organelles. In *Caenorhabditis elegans*, a retrograde signalling pathway deputed to the communication of folding stress in mitochondria and generated by the degradation of damaged mitochondrial proteins and by the consequent extrusion of the proteolytic products has been characterized. The translocation of the peptides is associated with the presence of the HAF-1 ABC transporter in the envelope of the mitochondria, and its loss correlates with increased sensitivity to protein homeostasis threats. Moreover, HAF-1 is the homolog of the MDL1 ABC transporter in *Saccharomyces cerevisiae*, which exerts the same peptide-translocation activity from mitochondria into the cytosol. Additionally, ABC peptide transporters have also been found in human cells, such as the TAP transporter, which is involved in the immunological response, or the TAPL transporter which scavenges peptides from the cytosol into the lysosome.

ABC transporters are part of a vast, ancient and conserved superfamily of proteins that can recognize a plethora of substrates and translocate them across

several biological membranes mediating a variety of functions. *Arabidopsis thaliana* genome encodes 130 ABC proteins which are mostly uncharacterized and none of them is reported to have peptide as substrate.

In light of this, it can be hypothesised the existence of a chloroplast retrograde signalling pathway comparable to that described in mitochondria. Therefore, this work aims to:

1. Identify, in *Arabidopsis thaliana*, the ABC transporter that could mediate peptide extrusion from chloroplasts.
2. Detection and characterization of the putative peptide efflux from chloroplasts.
3. Characterize the biological function of such transporter, particularly in response to plastid protein homeostasis perturbations.
4. Attempt to link the function of the transporter with a putative retrograde signalling pathway generated by protein degradation within the chloroplast and mediated by the extrusion of the peptides.

To achieve these goals, a bioinformatic approach will be employed to identify candidate proteins and their respective genes starting from the amino acid sequences of HAF-1 and MDL1 peptide ABC transporters. The plastid-localisation of the candidate proteins will be then verified by confocal microscopy. The detection of peptide efflux from chloroplasts and its possible abolishment will be performed directly on intact chloroplasts, isolated from wild-type and mutant plants, subjected to stress able to promote protein degradation employing an experimental approach inspired by the work accomplished for the characterization of the mitochondrial peptide efflux. The putative extruded plastid peptides will be characterized by mass spectrometry. The mutants exhibiting a reduction in efflux will be further investigated to test their sensitivity to plastid protein homeostasis challenges.

RESULTS AND DISCUSSION

Identification of candidate plastid peptide ABC transporters in *A. thaliana*

It has been shown that the mitochondrial-located ABC transporters HAF-1 from *C. elegans* and MDL1 from *S. cerevisiae* are capable of releasing peptide-based signalling molecules into the cytosolic compartment upon heat exposure (Young et al., 2001; Augustin et al., 2005; Arnold et al., 2006; Haynes et al., 2010). On the other hand, the plastid-located counterpart of such peptide transporters, together with a peptide-mediated communication pathway, has been postulated but remains unknown (Olinares et al., 2011b). To computationally identify candidate plastid peptide transporters, the SwissProt protein sequence database of *A. thaliana* was interrogated by BLASTp searches employing as queries the amino acid sequences of both HAF-1 and MDL1. The analyses produced 87 and 80 significant protein hits (E value < 0,05) from HAF-1 and MDL1 queries, respectively, all annotated as ABC transporters. Hits were then arbitrarily filtered for BLAST scores higher than 100 and plastid localization according to SUBA5 database information. Among all the hits from both searches, three common uncharacterized candidates satisfied both criteria: TAP1 (Transporter associated with Antigen processing Protein) had the highest score, followed by NAP8 (Non-intrinsic ABC Protein 8 or TAP-related protein 1) and ATH12 (ABC Two Homolog 12).

Table 1 – Summary of BLASTp searches. The output of the BLASTp searches using either MDL1 or HAF-1 aminoacidic sequences as queries against the *Arabidopsis thaliana* proteome from the SwissProt database. Only hits predicted to localise in the plastid and with a BLASTp score higher than 100 are reported. TAP1, NAP8 and ATH12 proteins were the unique hits satisfying both criteria. The AGI codes and protein names are reported. E value indicates the probability of a random match. BLASTp Score indicates the overall strength of the matches.

ID Araport	Protein name	E value	BLASTp Score	Coverage	Identity %	Positives %	Total length
MDL1 as query							
AT1G70610	TAP1	1,39E-81	272	0,71	34,87	55,51	700
AT5G03910	ATH12	6,74E-50	184	0,72	31,53	49,71	634
AT4G25450	NAP8	3,37E-47	177	0,33	40,69	61,9	714
HAF-1 as query							
AT1G70610	TAP1	6,56E-78	262	0,84	32,19	54,91	700
AT4G25450	NAP8	1,28E-52	192	0,71	30,54	48,60	714
AT5G03910	ATH12	7,37E-43	163	0,69	29,22	49,59	634

Plant ABC proteins are currently subdivided into 8 subfamilies, according to their topology, domain composition and phylogenetic relationship (Sánchez-Fernández et al., 2001; Verrier et al., 2008; Kang et al., 2011). To assign the identified candidates to an ABC protein subfamily, the amino acid sequences of TAP1, NAP8 and ATH12 were prompted in CCTOP and ScanProsite tools (de Castro et al., 2006; Aszí O Dobson et al., 2015). For comparison, the sequences of HAF-1 and MDL1 were included as well. All of the proteins were predicted to possess an N-terminal transmembrane domain (TMD), composed of six α-helices and a C-terminal nucleotide-binding domain (NBD) (Fig. 7 A). TargetP software was employed to highlight the organelle transit peptides required for mitochondrial or plastid localisation (Fig. 7 A). The obtained data established that all of the analysed proteins have identical domain compositions and topologies, compatible with their classification in the ABCB half-transporter subclass. This is in agreement with a previously published complete survey of the Arabidopsis ABC proteins where TAP1, NAP8 and ATH12 proteins are also named ABCB26, ABCB28 and ABCB29, respectively, and cluster into a distinct group (Kang et al., 2011).

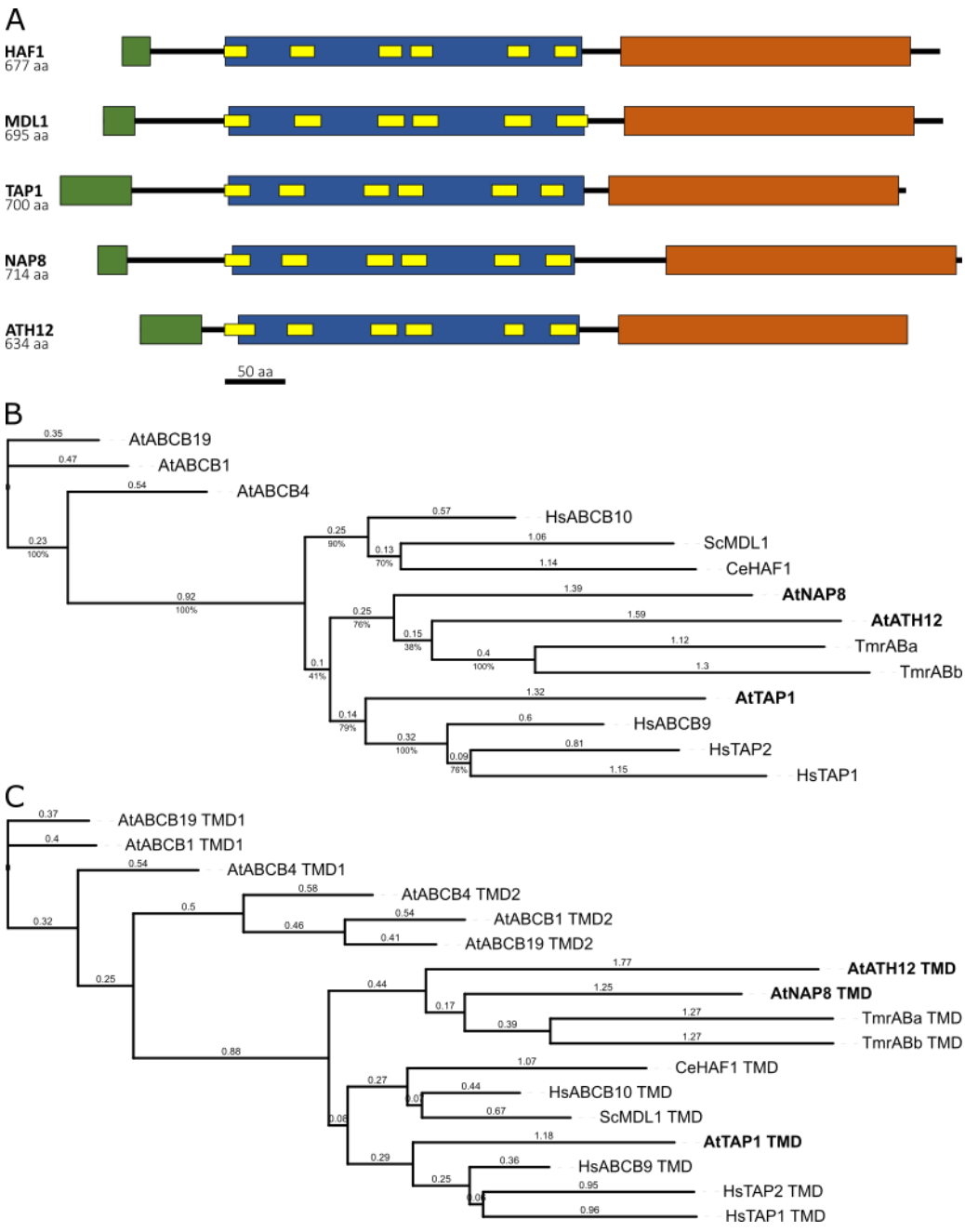
A
HAF1
677 aa
MDL1
695 aa
TAP1
700 aa
NAP8
714 aa
ATH12
634 aa
50 aa
B
AtABCB19
AtABCB1
AtABCB4
HsABCB10
ScMDL1
CeHAF1
AtNAP8
AtATH12
TmrABa
TmrABb
AtTAP1
HsABCB9
HsTAP2
HsTAP1
C
AtABCB19 TMD1
AtABCB1 TMD1
AtABCB4 TMD1
AtABCB4 TMD2
AtABCB1 TMD2
AtABCB19 TMD2
AtATH12 TMD
AtNAP8 TMD
TmrABa TMD
TmrABb TMD
CeHAF1 TMD
HsABCB10 TMD
ScMDL1 TMD
AtTAP1 TMD
HsABCB9 TMD
HsTAP2 TMD
HsTAP1 TMD

Figure 7 – *In silico* analyses of candidate ABC transporters. A) Graphical representation of the indicated ABC transporters. Chloroplast Transit Peptide (green), transmembrane domain (TMD, blue), nucleotide-binding domain (NBD, orange) and transmembrane helices (yellow) are reported. To better show the similarities, models have been aligned by the first amino acid of their first transmembrane helix. Protein models are drawn to scale. **B)** Phylogenetic tree based on the alignment of the amino acid sequences from the indicated ABC transporters. AtABCB1, AtABCB4 and AtABCB19 were included as outgroups. Percentages represent branch probability based on 100 bootstrap repetitions. Numbers over branches indicate the phylogenetic distance. Tm, *T. thermophilus*; Sc, *S. cerevisiae*; At, *A. thaliana*; Ce, *C. elegans*; Hs, *H. sapiens*. **C)** Phylogenetic tree based on the alignment of the amino acid sequences from the transmembrane domains (TDM) of the indicated ABC transporters.

To further corroborate *in silico* the homology of the candidate proteins, their amino acid sequences were analysed with the multiple sequence alignment (MSA) tool MUSCLE (Edgar, 2004). The analysis was performed including the sequences of a subset of known peptide transporters found in several organisms, together with the sequences of the Arabidopsis auxin transporters MDR1 (ABCB1), MDR4 (ABCB4) and MDR11 (ABCB19) as outgroup (Table 2). Subsequently, the analysis was further processed through the PhyML software, which estimates maximum likelihood phylogenies from MSA data (Guindon et al., 2009). TAP1, NAP8 and ATH12 were clustered among the known peptide transporters, whereas, MDR proteins were not (Fig. 7 B). TAP1 was arranged with the human peptide transporters TAP1 (ABCB2), TAP2 (ABCB3) and TAPL (TAP-like protein, ABCB9), whereas, NAP8 and ATH12 were grouped with TmrAB peptide transporters found in *Thermus thermophilus*. MDL1, HAF-1 and ABCB10 transporters, found in the mitochondria of yeast, roundworm and human, respectively, formed a group of their own. The NBD is the most conserved domain in the ABC proteins, instead, the TMD is very variable, even among proteins from the same species (Sánchez-Fernández et al., 2001). Therefore, to rule out the possibility that TAP1, NAP8 and ATH12 were misleadingly clustered, the same analysis was repeated with the sequences of the TMD portions from each transporter. The obtained phylogenetic tree was strikingly alike (Fig. 7 C).

Table 2 – List of the ABC proteins employed in the MSA analysis. The protein names, the organism of origin, subcellular localisation, a brief description and the references found in the literature are reported in the table. All of the transporters are confirmed peptide transporters, except for the human ABCB10 protein, which substrate is still to be experimentally verified, and the *A. thaliana* MDR auxin transporters, here used as an outgroup.

Protein name	Organism	Subcellular localisation	Description	Reference
TmrABa TmrABb	*Thermo thermophilus*	plasma membrane	Functional homologues of the human TAP complex. The two proteins heterodimerise.	(Nöll et al., 2017)
MDL1	*Saccharomyces cerevisiae*	mitochondria	It forms homodimers. The null mutant is sensitive to heat.	(Young et al., 2001; Jarolim et al., 2013)
HAF-1	*Caenorhabditis elegans*	mitochondria	It forms homodimers. It mediates retrograde signalling in response to proteostasis perturbations by extruding peptides originated by protease activity.	(Haynes et al., 2010)
ABCB10	*Homo sapiens*	mitochondria	It forms homodimers. It is proposed to translocate peptides and could be involved in the response to ROS.	(Liesa et al., 2012)
TAP1 (ABCB2) TAP2 (ABCB3)	*Homo sapiens*	endoplasmic reticulum	The two proteins heterodimerise. The TAP complex transfers peptides derived from the antigen processing into the ER lumen contributing to the immunological response.	(Nijenhuis and Hämmerling, 1996; Lehnert et al., 2016)
TAPL (ABCB9)	*Homo sapiens*	lysosome, endoplasmic reticulum	It forms homodimers. It is involved in the removal of peptides from the cytoplasm into lysosomes and ER lumen.	(Wolters et al., 2005; Zhao et al., 2008)
MDR1 (ABCB1) MDR11 (ABCB19) MDR4 (ABCB4)	*Arabidopsis thaliana*	plasma membrane	Full-transporters mediating auxin export and the associated signalling.	(Noh et al., 2001; Lin and Wang, 2005; Santelia et al., 2005)

The sequence similarity of TAP1, NAP8 and ATH12 with HAF-1 suggests that they could function as peptide transporters involved in the generation of retrograde signalling. Additionally, they were computationally predicted to be plastid-located and, in virtue of their TMD, they should be embedded in a lipid bilayer. Therefore, TAP1, NAP8 and ATH12 are expected to localise in the

chloroplast envelope. To validate this hypothesis, the coding sequences of the candidate proteins were cloned in frame with that of *GFP* or *RFP* genes under the control of the *CaMV 35S* constitutive promoter to obtain C-terminally tagged proteins. The coding sequence of *TIC20*, encoding for a subunit of the Inner membrane Translocon Complex of the chloroplast, was cloned as well as a marker of the plastid envelope. The produced constructs were then introgressed into wild-type plants by Agrobacterium-mediated transformation. Transformed plants were subsequently crossed to generate Arabidopsis lines co-expressing GFP or RFP tagged proteins as follows: *oeTAP1-GFP oeTIC20-RFP*, *oeTAP1-GFP oeNAP8-RFP*, *oeTAP1-GFP oeATH12-RFP*. Leaf tissue from these plants was then analysed via Confocal Laser Scanning Microscopy (Fig. 8). The signal from TAP1-GFP appeared to be surrounding the fluorescence of plastid chlorophylls, resembling the RFP signal from the TIC20 chimaera. Moreover, NAP8-RFP and ATH12-RFP signals were ring-shaped and perfectly overlapped with that from TAP1-GFP. In accordance with these experimental observations, TAP1, NAP8 and ATH12 were found in the envelope fraction by a mass-spectrometry-based analysis of the chloroplast proteome (Ferro et al., 2010). Taken together, these observations are compatible with the role envisaged for TAP1, NAP8 and ATH12 as plastid envelope-located peptide transporters, similar to what is described for mitochondrial-located peptide extruders HAF-1 and MDL1.

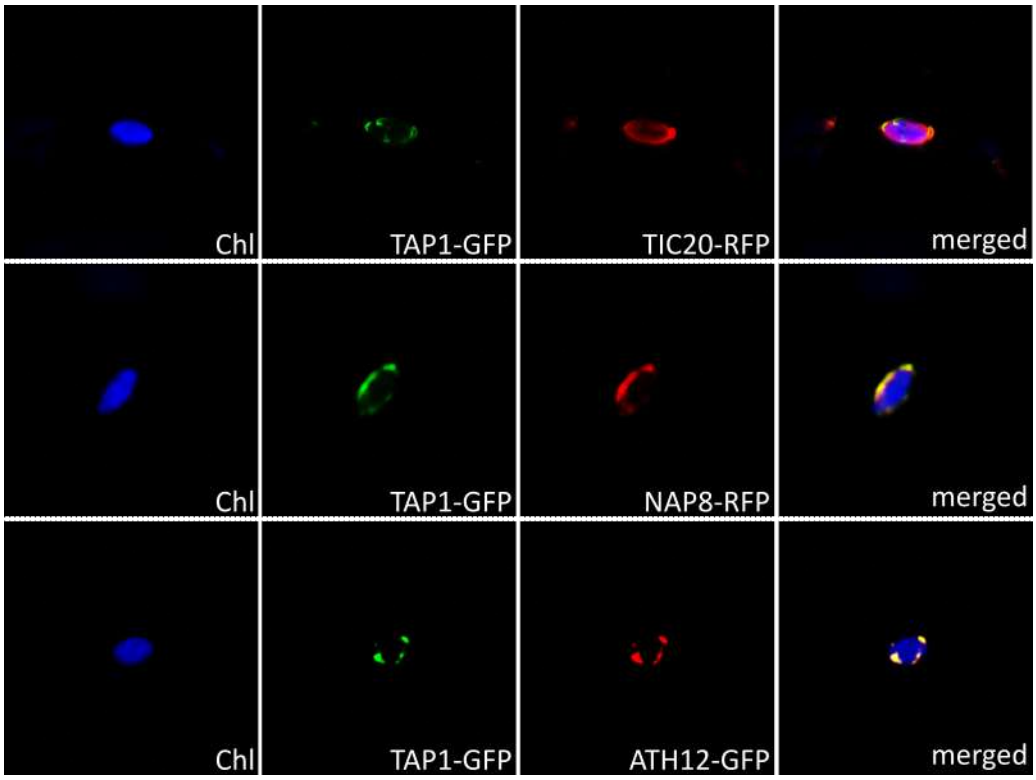

Figure 8 – Localisation of candidate peptide ABC transporters. Mesophyll cells from *oeTAP1-GFP oeTIC20-RFP*, *oeTAP1-GFP oeNAP8-RFP*, *oeTAP1-GFP oeATH12-RFP* transgenic lines observed under the confocal microscope. Blue channel: chlorophyll autofluorescence (Chl); green channel: GFP signal; red channel: RFP signal.

TAP1, NAP8 and ATH12 mediate peptide efflux from chloroplasts

To investigate the molecular and physiological function of the candidate transporters, single mutants bearing a T-DNA inserted in *TAP1* (AT1G70610), *NAP8* (AT5G03910) and *ATH12* (AT4G25450) gene loci were acquired from the Nottingham Arabidopsis Stock Centre. The exact insertion sites in each mutant were experimentally verified by PCR amplification followed by Sanger sequencing. The *tap1-1* allele resulted to bear the T-DNA insertion within the third intron, the T-DNA in the *nap8-1* allele fell in the fourth intron and *ath12-1* allele had it in the tenth exon (Fig. 9 A). The position of T-DNAs within the locus suggested the disruption of the respective genes. The single mutants were then crossed to yield all the possible combinations of double mutants and, subsequently, the triple mutant was generated. No obvious phenotypes were noticeable in any of the mutants when grown under standard conditions (Fig. 9 B). The absence of phenotype, however, is in line with what was observed in the *mdl1⊿* and *haf-1* mutants in yeast and nematode, respectively, which behaved as the wild type under standard growth conditions (Young et al., 2001; Haynes et al., 2010). Nevertheless, both these mutants struggled if their protein homeostasis was perturbed (Haynes et al., 2010; Jarolim et al., 2013).

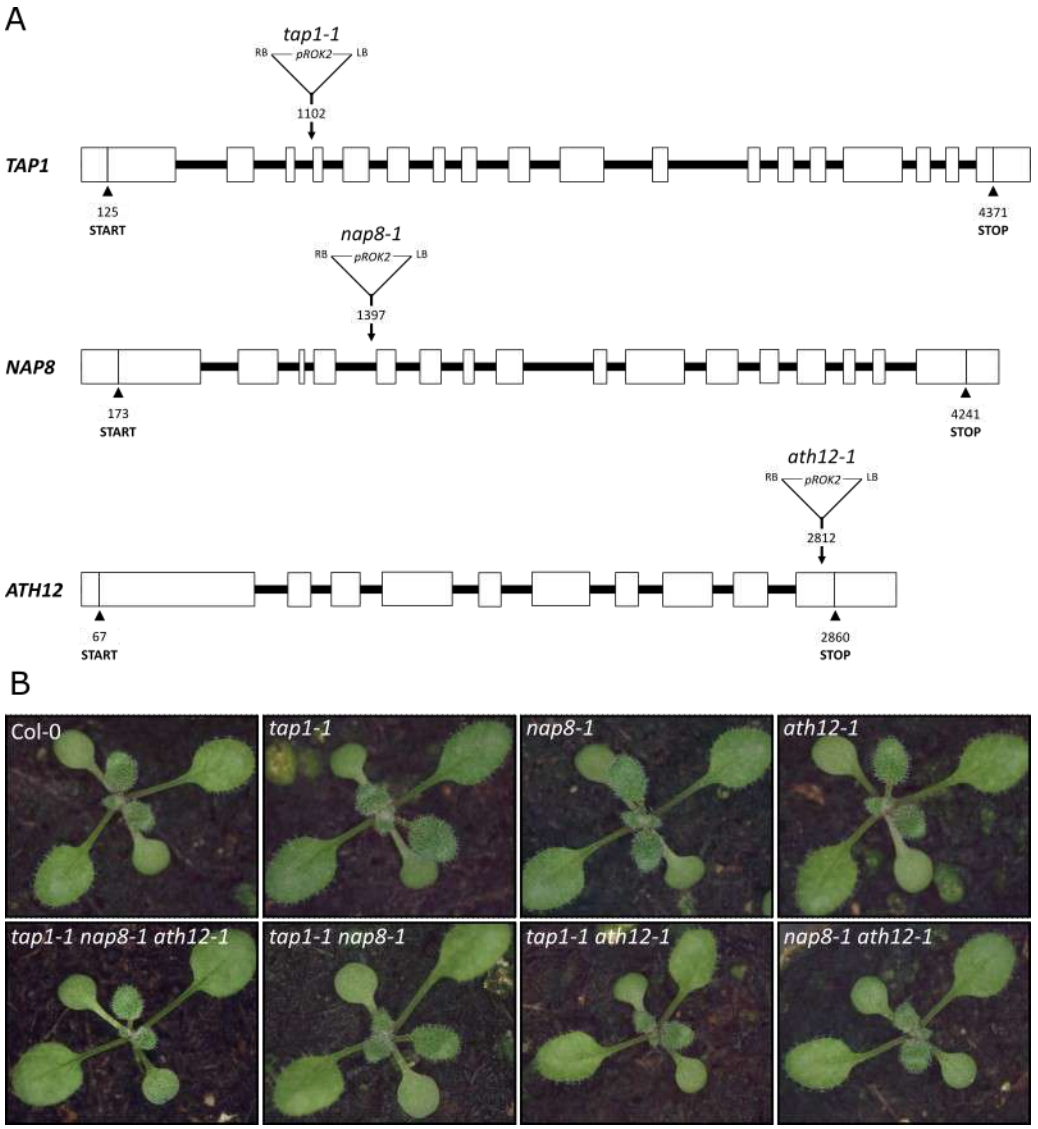

Figure 9 – T-DNA insertional lines in candidate genes. A) Schematic representations of the indicated genes. Exons are represented as white boxes and introns as black lines. Models are in scale. T-DNA insertion sites, start and stop codons are indicated. T-DNAs are not in scale. **B)** Pictures of 12 days old plants of the indicated genotypes grown on soil under long-day photoperiod.

Wild-type purified mitochondria that were exposed to heat in an incubation buffer containing ATP extruded peptides, whereas the mitochondria isolated from *mdl1⊿* and *haf-1* mutants were deficient in this function (Young et al., 2001; Haynes et al., 2010). The proposed role for TAP1, NAP8 and ATH12 ABC proteins, the closest plastid-localised homologues of both MDL1 and HAF-1 peptide transporters, is the translocation of peptides from chloroplasts, possibly mediating a retrograde signalling pathway in response to stress. If this holds true, an increment in plastid-derived peptides would be detected in the incubation buffer in which isolated intact chloroplasts are resuspended when exposed to heat, similar to what was observed from mitochondria of yeast and nematode, instead, this molecular phenotype would be abolished when mutant chloroplasts are treated. Therefore, to test this hypothesis, the experimental procedure performed to detect the peptide efflux from purified mitochondria upon heat incubation was adapted for chloroplasts (Haynes et al., 2010). Chloroplasts were isolated from wild-type and mutant plants through Percoll gradients (Seigneurin-Berny et al., 2008). Isolated chloroplasts were then incubated at 45° C to perturb the protein homeostasis, by promoting protein misfolding and degradation, and possibly triggering peptide efflux. ATP was added to the samples to support the ATP-dependent peptide transport. As a control, wild-type chloroplasts were incubated at 25° C with ATP or, at 45° C in the absence of ATP. After the treatment, chloroplasts were pelleted and supernatants were collected. Samples were cleaned through a 30 kDa cut-off filter and successively processed with a solid-phase extraction column, to allow enrichment in low molecular weight peptides. Finally, peptide concentration in each sample was evaluated by UV spectrometry at 280 nm (Fig. 10 A). When treated at 45° C with ATP, wild-type chloroplasts produced a peptide extrusion of about twice the amount of the control samples, where no heat or ATP was applied. The lack of one or two of the transporters did not significantly affect the level of retrieved peptides in the supernatants. Instead, when subjected to the same treatment,

chloroplasts devoid of all three transporters extruded half the amount of peptides in comparison with wild-type chloroplasts. The peptide efflux from triple mutant was comparable to the one from untreated wild-type chloroplasts, in the presence of ATP, or treated wild-type chloroplasts without ATP. These results suggest that the identified putative plastid-located peptide transporters promote peptide efflux upon heat treatment. Moreover, all three TAP1, NAP8 and ATH12 transporters contribute to the total peptide efflux from chloroplasts upon heat exposure in an ATP-dependent manner, showing functional redundancy and possible substrate overlap. Hence, from now on TAP1, NAP8 and ATH12 proteins will be collectively indicated as PPTs (Plastid Peptide Transporters) and *ppts* would be used in place of *tap1 nap8 ath12* name.

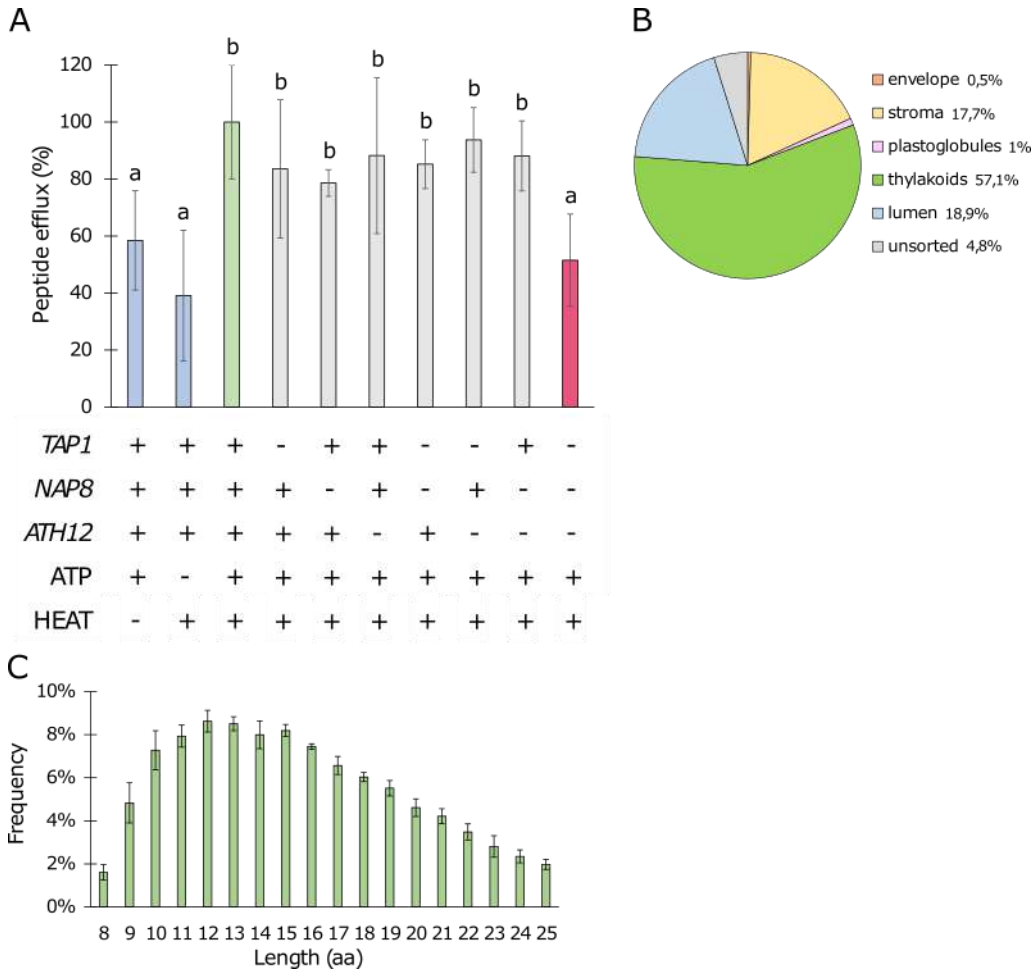

Figure 10 – Chloroplast peptide efflux A) UV quantification of peptides recovered from the supernatants after 1 hour of heat-incubation. Averages and standard deviations are shown. The value of wild-type chloroplasts treated with heat and ATP has been set as 100% (green). Control samples are indicated in blue. Samples from single double mutants are in grey. The triple mutant sample is indicated in red. Statistical significance has been calculated with ANOVA one-way test and Tukey's posthoc analysis. **B)** Pie chart indicating the distribution by the origin of peptides recovered from the supernatant of wild-type chloroplasts. **C)** Distribution of the length of peptides recovered from the supernatant of wild-type chloroplasts.

Peptides recovered from heat-treated wild-type chloroplasts were analysed by mass spectrometry, to attempt sequence identification. The average total number of detected peptides from 2 independent experiments was 10629, derived from 481 different proteins (Table 3). Only proteins identified by peptides found in both replicates were considered. 99,2% of the peptides mapped on the amino acid sequences of plastid proteins, indicating that the chloroplast samples were virtually pure. The majority of the plastid-derived peptides (57,1%) originated from thylakoid proteins (Fig. 10 B). Luminal proteins contributed to the production of 18,9% of the peptides, whereas the stromal proteins supplied 17,7% (Fig. 10 B). The remaining portions of peptides were attributed to proteins localised in plastoglobules (1%), envelope (0,5%) or unsorted ones (4,8%) (Fig. 10 B). About 50% of the peptides belonged to the Photosystem II proteins, the subunits of its antenna complexes or the oxygen-evolving complex. According to the literature, these proteins are both highly abundant in chloroplasts, tightly regulated by proteases and prone to suffer severe damage upon heat treatments (Allakhverdiev et al., 2008). Among all recovered peptides in wild-type heat-treated plants, the length ranged from 8 to 25 amino acids, with the average peptide being 15 amino acids long (Fig. 10 C). This feature is remarkably similar to those previously reported for the peptide released by both MDL1 and HAF-1 (Augustin et al., 2005; Haynes et al., 2010).

Table 3 – Subset of the first 20 most represented proteins originating the detected peptides from heat-treated wild-type chloroplasts. In the table are reported the AGI code, the protein ID from the Uniprot database, the protein names and the sub-plastidial localisation according to the PPDB database of the first twenty most represented peptide-producing proteins. The average amount of peptides detected from 2 independent experiments and the percentage (%) relative to the total amount of peptides for each protein are indicated.

Araport ID	Uniprot ID	Protein name	PPDB localisation	AVG Count	%
ATCG00280	P56778	psbC	thylakoid	578	5,48
AT5G66570	P23321	PSBO1	lumen	508	4,81
AT2G39730	P10896	RCA	stroma	386	3,66
AT3G50820	Q9S841	PSBO2	lumen	378	3,58
ATCG00270	P56761	psbD	thylakoid	372	3,52
AT1G06680	Q42029	PSBP1	thylakoid	334	3,16
AT4G05180	Q41932	PSBQ2	lumen	293	2,77
AT4G21280	Q9XFT3	PSBQ1	lumen	286	2,71
ATCG00680	P56777	psbB	thylakoid	241	2,28
AT5G01530	Q07473	LHCB4.1	thylakoid	219	2,07
AT3G08940	Q9XF88	LHCB4.2	thylakoid	214	2,02
ATCG00020	P83755	psbA	thylakoid	209	1,98
AT1G03600	Q9LR64	PSB27-1	thylakoid	155	1,46
AT1G79040	P27202	PSBR	thylakoid	153	1,45
AT1G29930	P04778	LHCB1.3	thylakoid	146	1,38
AT2G34420	Q39141	Lhb1B2	thylakoid	131	1,24
AT3G46780	Q9STF2	PTAC16	thylakoid	129	1,22
AT4G10340	Q9XF89	LHCB5	thylakoid	129	1,22
ATCG00710	P56780	psbH	thylakoid	115	1,09
AT4G01050	Q9M158	STR4	thylakoid	112	1,06

However, the diminished peptide extrusion from triple mutant chloroplasts could be attributed to differences in the protein degradation rate rather than peptide extrusion. To rule out this possibility, the relative abundance of proteins was monitored in heat-treated chloroplasts in the presence of ATP through western blot. Chloroplasts from the wild type and the triple mutant were sampled before the treatment, after 30 minutes and at the end of the incubation at 45° C. Samples incubated with ATP but not exposed to heat and chloroplasts heat-treated without ATP were included as a control (Fig. 11). PSBO and LHCB4 proteins were selected as targets since a high amount of their peptides was found in the previous analysis. The relative abundance of both proteins decreased gradually during the treatment in both chloroplast populations, indicating that the diminished peptide efflux in the triple mutant chloroplasts is to be attributed to the absence of the transporters rather than impaired proteolysis. Notably, the presence of ATP alone did not cause protein degradation. Instead, protein stability is lost if heat is applied even in the absence of ATP, which could be due to both heat-induced cleavage and the activity of ATP-independent proteases, such as DEG (Allakhverdiev et al., 2008; van Wijk, 2015). In addition, the peptide efflux data have shown that the extrusion activity of heated wild-type chloroplasts was not increased without ATP (Fig. 10 A). Taken together, these data suggest that proteolysis is promoted by heat even in the absence of ATP, nevertheless, in these conditions, the extrusion of the resulting peptides is hampered.

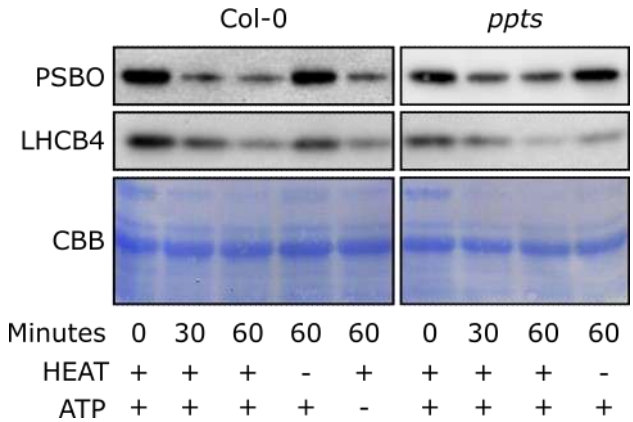

Figure 11 – Protein degradation in wild-type and *ppts* mutant chloroplasts. Immunoblots performed on wild-type and triple mutant chloroplasts incubated as indicated using antibodies raised against PSBO and LHCB4 plastid proteins. Coomassie blue staining has been used as a loading control.

PPTs can functionally replace MDL1 in *S. cerevisiae*

MDL1 ABC transporter of *S. cerevisiae* mitochondria mediates the extrusion of peptides upon heat treatment into the cytoplasm (Young et al., 2001; Augustin et al., 2005). Peptide production and extrusion have been involved in the regulation of gene expression (Arnold et al., 2006). Moreover, the *mdl1⊿* mutant strain is heat-sensitive as revealed by a high-throughput screen, indicating that MDL1 activity is involved in conferring the ability to survive high temperatures (Jarolim et al., 2013). Since TAP1, NAP8 and ATH12 ABC transporters appeared to contribute to the plastid peptide efflux upon heat treatment (Fig. 10 A), it could be possible that the heat-sensitive phenotype of *mdl1⊿* mutant could be rescued by the introduction of *TAP1*, *NAP8* and/or *ATH12* genes.

To test this hypothesis, genetically modified yeast strains expressing either *TAP1*, *NAP8* or *ATH12* coding sequences in place of the endogenous *MDL1* gene were generated. Three different recombination cassettes have been designed to bear the *TAP1*, *NAP8* or *ATH12* coding sequences (devoid of chloroplast transit peptides) together with the *KANMX* resistance and cloned in a plasmid for propagation in *E. coli*. Each recombination cassette was flanked upstream and downstream by 40 bp stretches homologous to the desired recombination sites in the yeast genome. The recombination sites were designed to drive the replacement of the entire *MDL1* coding sequence downstream of the mitochondrial transit peptide, allowing for the expression of the Arabidopsis proteins targeted to the mitochondria. A similar recombination cassette bearing the *KANMX* resistance only was designed to replace completely the *MDL1* locus. The wild-type yeast strain BY4741 was then transformed with the described DNA cassettes to yield *mdl1⊿ TAP1*, *mdl1⊿ NAP8* and *mdl1⊿ ATH12* transgenic strains and the null mutant *mdl1⊿*. The proper recombination of the constructs was verified by PCR amplification and sequencing.

The wild type and the obtained mutant strains were incubated in growing conditions (28° C, 250 rpm) until the exponential phase was reached. Then, cell cultures were divided into two subcultures (Mock and Heat). Before splitting, aliquots were collected, serial diluted and plated on a complete medium as T0 samples. The Mock cultures were incubated in the previous growing conditions as a control. The Heat cultures were incubated at 45° C, instead. After 2 hours both cultures were sampled, and cells were plated on Petri dishes kept at 28° C for 3 days to allow colony formation. The obtained colonies were then manually counted to compare the T0 sample with the Mock and the Heat ones to estimate cell growth (expressed as a ratio) in the two conditions (Fig. 12 A). All the yeast strains grew similarly when incubated at 28° C, while (Fig. 12 B) the temperature raised at 45° C caused cell loss in all cultures. However, the *mdl1*⊿ Heat sample produced about -60% of colonies relative to the T0 sample whereas, the wild type and, importantly, all the transgenic strains resulted in about -30% of negative growth (Fig. 12 B). These results indicate that TAP1, NAP8 or ATH12 can rescue the heat-sensitive phenotype of the *mdl1*⊿ mutant, demonstrating that each one of them can functionally replace MDL1 protein in extruding peptides from mitochondria.

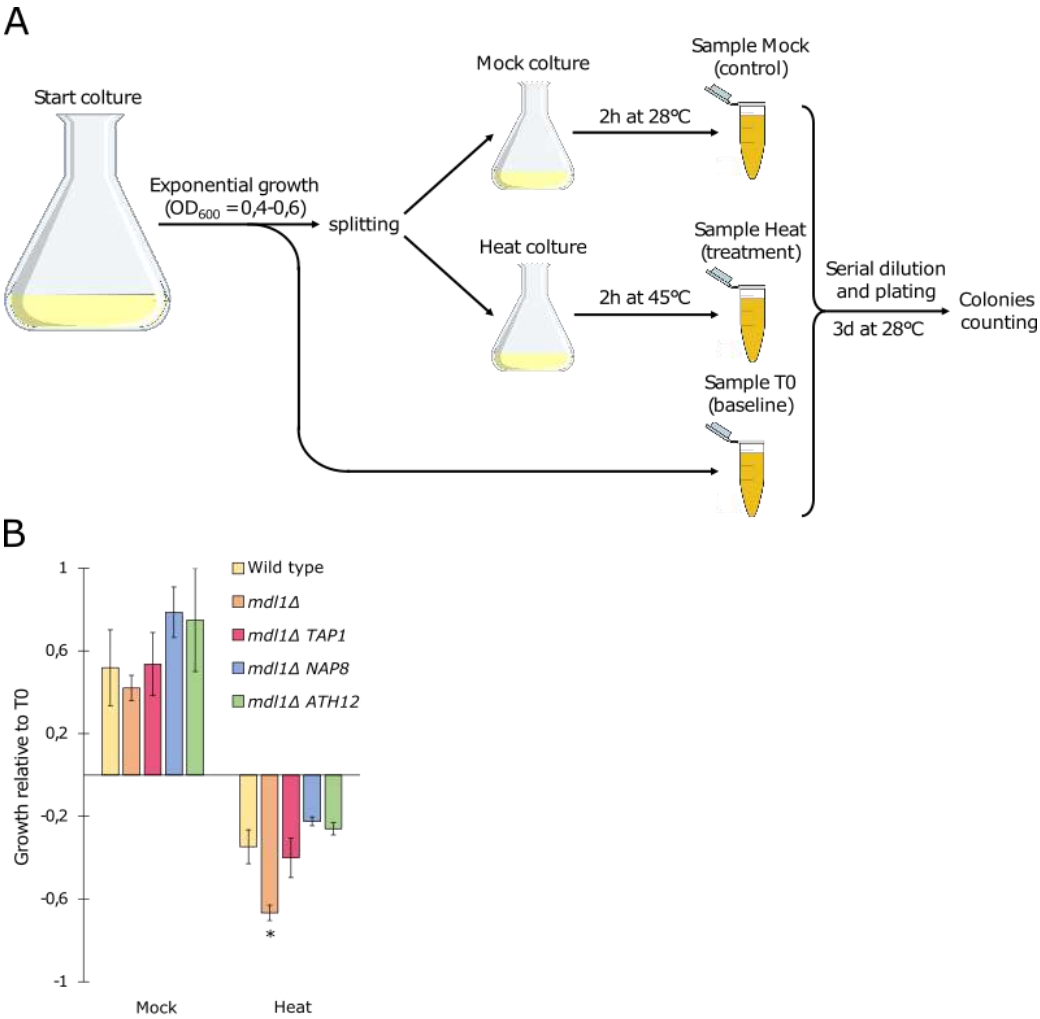

Figure 12 – TAP1, NAP8 and ATH12 can functionally replace MDL1. A) Schematic representation of the experimental workflow. **B)** Growth relative to the T0 sample for the indicated yeast strains. Averages and standard deviations are shown. The asterisk indicates statistical significance relative to the wild type (Student's t-test p-value < 0,05).

The *ppts* triple mutant displays enhanced sensitivity to alterations of chloroplast protein homeostasis

The previously described data support the model that TAP1, NAP8 and ATH12 mediate peptide extrusion from chloroplasts upon heat exposure, similar to what was observed in mitochondria of both nematode and yeast (Young et al., 2001; Haynes et al., 2010). In addition, the mutants lacking the peptide transporters in mitochondria resulted to be more susceptible to heat incubation, a condition that perturbs the protein homeostasis of the organelle (Haynes et al., 2010; Jarolim et al., 2013). Notably, PPTs were found to rescue the heat-sensitive phenotype of the yeast mutant (Fig. 12 B). In light of this, *ppts* triple mutant plants, being unable to generate a peptide efflux from chloroplasts, could also be more sensitive to high temperatures. To test this, the photosynthetic efficiency (F_v/F_m) of heat-treated plants was evaluated since this parameter has been reported to be a good indicator of plant health and to correlate with heat tolerance/sensitivity (Allakhverdiev et al., 2008; Chen et al., 2018). 15 days old plants grown under standard conditions were subjected to two different heat treatments. At first, plants were incubated at 45° C for 2 hours in the dark (HS). In a second treatment, plants were first acclimated (1,5 hours at 37° C in the dark and 2 hours of recovery in standard conditions) before the incubation (ACHS). Acclimation has been demonstrated to increase heat tolerance by inducing the expression of heat-shock proteins that protect the cellular environment (Chen et al., 1990; Havaux, 1993). To measure reference values, a 2-hour-long incubation in the dark without shifts in temperature was performed (Mock). The *ftsh11* mutant was included in the analysis, as it lacks a transmembrane protease involved in thermotolerance and protein quality control (Chen et al., 2006; Chen et al., 2018; Adam et al., 2019). Overall, the HS treatment determined a reduction in the photosynthetic parameter F_v/F_m in all plants when compared to the mock, while the acclimation affected positively the endurance to the heat stress, as expected (Fig. 13 A). Wild-type photosynthetic efficiency decreased strongly after

the HS treatment, while acclimation allowed it to endure better heat incubation, mitigating the impairment of photosynthetic parameters. The F_v/F_m values reduction was enhanced in the *ftsh11* mutant in both treatments. Interestingly, the *ppts* triple mutant appeared less capable to recover after heat exposure than the wild type in both conditions. The greatest reduction in wild-type plants was observed in plants that endured direct heat treatment. Instead, plants first subjected to acclimation had the parameter F_v/F_m slightly lowered relative to the wild type (Fig. 13 A).

To challenge the *ppts* triple mutant with alternative-to-heat plastid protein homeostasis perturbations, the sensitivity to methyl viologen (MV) was evaluated as well. Also known as Paraquat herbicide, MV is an oxidative agent that induces protein misfolding by promoting ROS development and carbonylation (Manning-Bog et al., 2002; Nyström, 2005; Pulido et al., 2017). Wild-type, *ppts* and *ftsh11* plants were sown on MS synthetic medium containing 1 or 2 μM MV and their photosynthetic efficiency were evaluated after 9 days of growth (Fig. 13 B). The wild type was marginally affected by the presence of MV, as its photosynthetic efficiency decreased slightly compared to that observed in the mock. On the other hand, the *ftsh11* mutant was significantly more sensitive to the chemical treatment. Remarkably, if the photosynthesis of *ppts* triple mutant was just slightly diminished at 1 μM MV relative to the wild type, it was greatly affected in 2 μM MV-treated samples. These results indicate that the PPTs-mediated peptide efflux from chloroplast participates at least in part with the defence of the chloroplast physiology against conditions that threaten the plastid protein homeostasis.

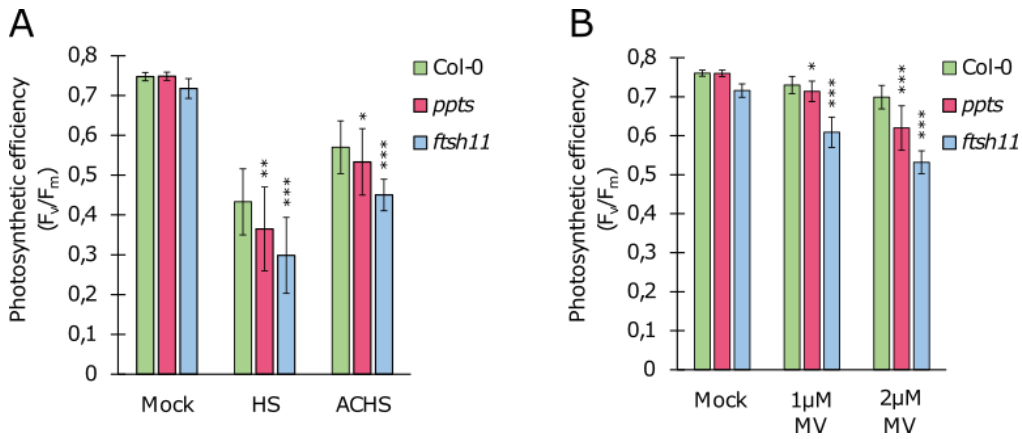

Figure 13 – The *ppts* triple mutant is sensitive to plastid protein homeostasis perturbations A) Photosynthetic efficiency measurements performed on 15 days old plants 2 days after the treatments. Averages and standard deviations are shown. Asterisks indicate statistical significance relative to the wild type (Student's t-test p-value: * < 0,05; ** < 0,01; *** < 0,001). **B)** Photosynthetic efficiency measurements performed on 9 days old plants grown on medium containing the indicated concentration of methyl viologen (MV). Averages and standard deviations are shown. Asterisks indicate statistical significance relative to the wild type in the same condition (Student's t-test p-value: * < 0,05; ** < 0,01; *** < 0,001).

The absence of PPTs causes an altered accumulation of CLPB3 chaperone in chloroplasts

The *ppts* triple mutant was found to be sensitive to both heat and MV treatments, which are known to induce protein instability (Manning-Bog et al., 2002; Feller, 2010). As described in previous sections, the depletion of the *HAF-1* gene in *C. elegans* leads to increased sensitivity to mitochondrial proteostasis perturbations. This phenotype was due to the abolishment of the peptide-mediated retrograde signalling that ultimately is required for HSP60 mitochondrial chaperone up-regulation upon heat stress (Haynes et al., 2010). In *A. thaliana*, the nuclear-encoded plastid-located CLPB3 chaperone is up-regulated when the chloroplast protein homeostasis is challenged (Myouga et al., 2006; Lee et al., 2007; Llamas et al., 2017). Indeed, the CLPB3 plastid chaperone has the important function of resolving aggregates of unfolded proteins in the stroma to avoid their toxic accumulation (Llamas et al., 2017; Parcerisa et al., 2020). Hence, CLPB3 relative abundance was evaluated as a marker of ongoing protein homeostasis maintenance and possible chloroplast UPR molecular marker.

First, the amount of CLPB3 was probed via immunoblotting in total protein samples harvested from 15 days old wild-type and *ppts* triple mutant plants that were grown on soil in standard conditions. Notably, on average, the amount of CLPB3 in the *ppts* triple mutant was about 65% more abundant than the wild type (Fig. 14 A and B). It was noticed that chloroplasts from the *ppts* triple mutant were still able to perform proteolysis upon heat exposure (Fig. 11) despite the hampered peptide efflux. In yeast, it was demonstrated that mitochondria constantly extrude peptides resulting from normal protein turnover (Augustin et al., 2005). Therefore, taken together, these results suggest that the absence of PPTs could be *per se* a source of plastid proteostasis alteration, possibly due to the not-extruded peptides derived from plastid protein turnover.

Next, the ability to up-regulate CLPB3 was evaluated in response to stress. According to the observations made previously, *ppts* triple mutant plants directly exposed to 2 hours long heat treatments were particularly more sensitive than the wild type (Fig. 13 A). Thus, wild-type and triple mutant plants grown in standard conditions were moved in a pre-heated incubator at 45° C for 2 hours to deliver the heat shock. After the treatment, plants were allowed to recover back to standard conditions. Plants were sampled before the heat shock (preHS), immediately after the treatment (2h HS), after 1 hour of recovery (1h Rec) and after 2 additional hours of recovery (3h Rec). Total proteins were then extracted, fractionated on SDS-PAGE and probed with CLPB3-specific antibodies. In the wild type, CLPB3 gradually increased its accumulation in all the considered time points reaching, in the 3h Rec time point, about 3-fold the amount of the preHS sample (Fig. 14 C and D). Instead, the *ppts* triple mutant failed to over-accumulate CLPB3 during the same time window. Importantly, CLPB3 in the treated mutant decreased to the preHS sample by about 70% (Fig. 14 C and D). To understand whether gene expression was altered as well, the expression of the *CLPB3* gene was tested by qRT-PCR at the preHS and 1h Rec time points. Remarkably, the detected amount of *CLPB3* transcripts in both wild type and *ppts* triple mutant were comparable, which increased about 4-fold after 1 hour of recovery from the heat treatment (Fig. 14 E). According to these results, CLPB3 is steadily up-regulated in the wild type upon exposure of the plants to heat. Such up-regulation is lost in the *ppts* triple mutant at the protein level, whereas transcripts accumulation appeared unperturbed, thus providing pieces of evidence that PPTs could be involved in the positive post-transcriptional regulation of CLPB3 upon stresses which eventually confers higher tolerance to elevated temperatures.

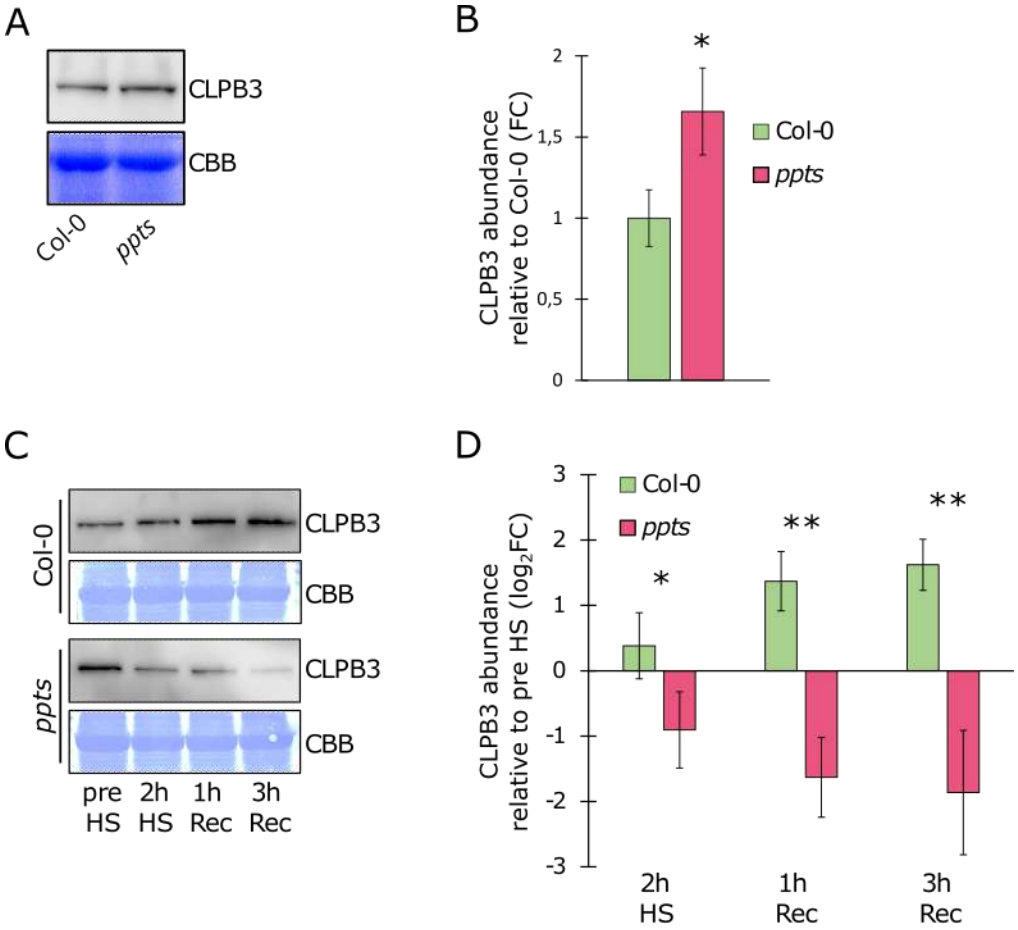

Figure 14 – The regulation of CLPB3 abundance in chloroplasts is altered in *ppts* triple mutant. **A)** Immunoblot against CLPB3 on total protein extracts from 15 days old wild-type and *ppts* triple mutant plants. Coomassie blue staining was used as a loading control. B) Quantification of the CLPB3 relative abundance shown in A. Averages and standard deviations are shown. The asterisk indicates statistical significance relative to the wild type (Student's t-test p-value < 0,05). **C)** Immunoblots against CLPB3 on total protein extract obtained from 15 days old wild-type and *ppts* triple mutant plants before treatment (preHS), after 2 hours heat treatment (2h HS), after 1 hour recovery (1h Rec) and after 2 additional hours (3h Rec). Coomassie blue staining was used as a loading control. **D)** Quantification of CLPB3 relative abundance expressed as a logarithm. Averages and standard deviations are shown. Asterisks indicate statistical significance relative to the wild type (Student's t-test p-value: * < 0,01; ** < 0,001). **E)** Relative expression of *CLPB3* gene at the indicated time points. Averages and standard deviations are shown.

Genetic interactions of *ppts* triple mutant with mutants impaired in plastid proteases

In the effort to provide a plastid-specific perturbation of the chloroplast protein homeostasis, a genetic approach was employed by introgressing mutations in plastid proteases into the *ppts* triple mutant background. In these conditions, possible genetic interactions between the hampered plastid proteolytic machinery and the putative peptide-mediated response could be revealed. Three mutants in plastid proteases had been selected for this purpose. The *ftsh11* mutant was described in the previous section. The highly variegated *ftsh2* mutant lacks a thylakoidal transmembrane protease located on the thylakoid membranes. It is required for the biogenesis and the preservation of photosystem II and in its absence, the chloroplast protein quality control mechanisms are triggered as a compensatory response (Takechi et al., 2000; Dogra et al., 2019). Finally, the virescent *clpr1* has the CLP multisubunit stromal protease hampered since it lacks a non-catalytic subunit of the core enzyme (Pulido et al., 2016; Llamas et al., 2017; Pulido et al., 2017). Quadruple mutants were generated by manual crossing and isolated through PCR-based screening. The obtained quadruple mutants displayed no major differences from the phenotypes observed in the parental single mutants (Fig. 15 A). Nevertheless, their photosynthetic efficiencies were measured to evaluate if the functionality of chloroplasts was further perturbed by the concomitant absence of the transporters. Measurements were performed on plants grown on soil under standard conditions for 15 days. Interestingly, all of them displayed a modest decrease in the F_v/F_m values relative to the single mutants (Fig. 15 B), indicating the existence of genetic interactions between the protease activity and the peptide extrusion in chloroplasts and supporting a common role in maintenance of plastid protein homeostasis

CLPB3 accumulation was altered in *ppts* triple mutant plants, either in the absence of stresses or after heat treatment (Fig. 14). To test whether CLPB3

accumulation was somehow affected also in these conditions, its relative abundance was evaluated as well (Fig. 15 C). As previously observed, the *ppts* triple mutant accumulated more CLPB3 relative to the wild type. The same was observed for all three mutants in plastid proteases. This was already detected by mass spectrometry analyses in mutant backgrounds defective in the proteolytic activity mediated by the protease of interest (Kim et al., 2013; Adam et al., 2019; Dogra et al., 2019). Remarkably, CLPB3 was found to be less accumulated in *ftsh ppts* mutants, whereas in *ppts clpr1* background it was more abundant. Such a result further supports the interactions in place between protein degradation, peptide extrusion and the activation of protein quality control systems.

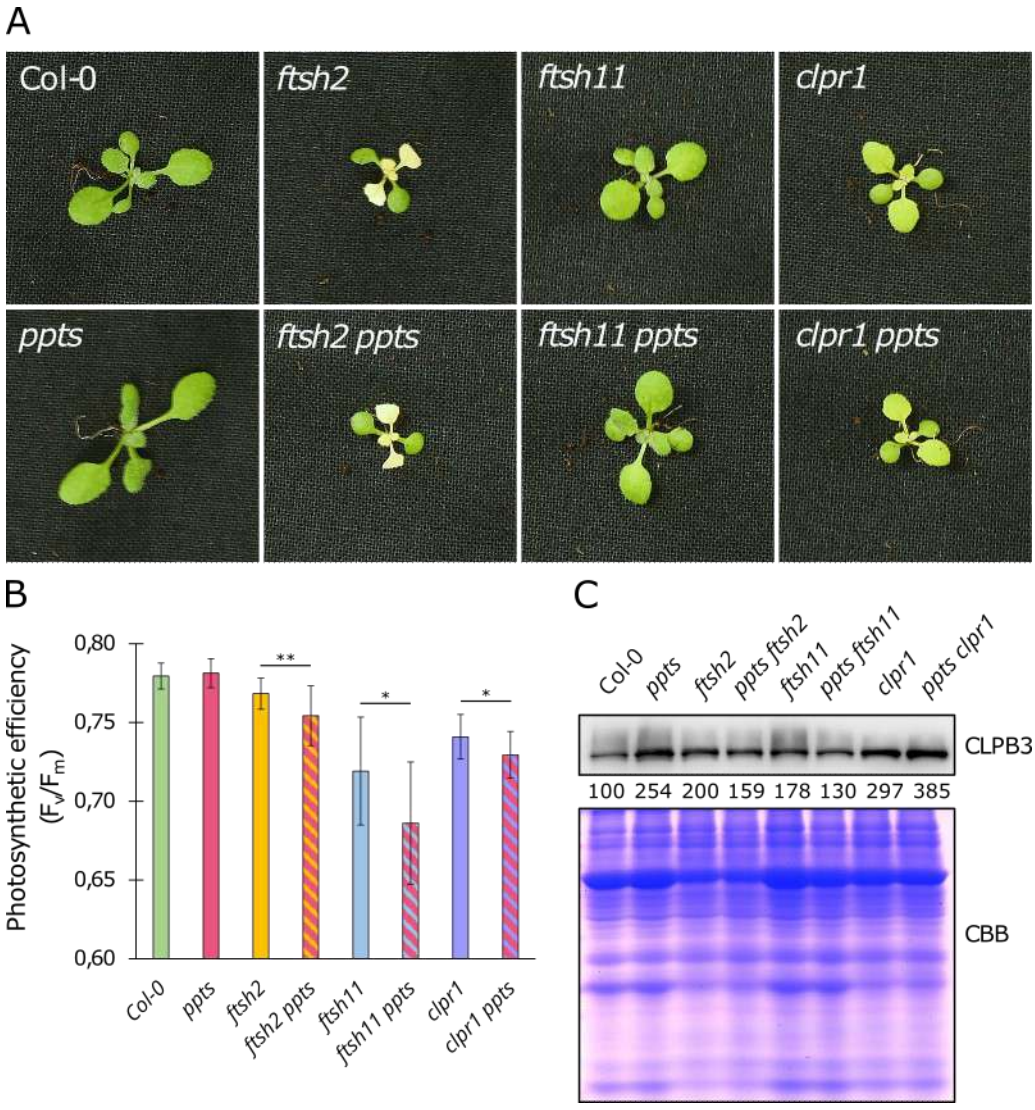

Figure 15 – Genetic interactions of *ppts* with mutants in plastid proteases. A) Pictures of 15 days old plants of the indicated genotypes. **B)** Photosynthetic efficiency measurements performed on plants shown in C. Averages and standard deviations are shown. Asterisks indicate statistical significance relative to the single mutant of reference (Student's t-test p-value: * < 0,05; ** < 0,01). **C)** Immunoblot against CLPB3 on total protein extracts from 15 days old plants of the indicated genotypes. Coomassie blue staining was used as a loading control.

CONCLUSIONS AND FUTURE PERSPECTIVES

In this work, the ability of chloroplasts to extrude peptides upon heat treatment was investigated and linked to the presence, in the chloroplast envelope, of TAP1, NAP8 and ATH12 ABC proteins and thus, here collectively designated as PPTs, Plastid Peptide Transporters. Additionally, plants lacking all PPTs were found more sensitive to conditions that pose challenges to chloroplast protein homeostasis and are defective in the post-transcriptional regulation of CLPB3 plastid unfoldase.

PPTs proteins were identified as the closest plastid-located homologues of MDL1 and HAF-1 mitochondrial peptide transporters (Young et al., 2001; Haynes et al., 2010). The *in silico* analysis of PPTs amino acid sequences revealed that each one possesses an N-terminal TMD composed of 6 transmembrane α-helices and a C-terminal NBD. These observations, together with the data from a complete survey of the *Arabidopsis* ABC protein, agreed with the classification of PPTs among the ABCB half-transporters subclass (Kang et al., 2011). The localisation of PPTs in the chloroplast envelope was experimentally corroborated by confocal microscopy observations of mesophyll tissue expressing PPTs fluorescent chimaeras. A mass spectrometry analysis has also reported PPTs in the chloroplast envelope fraction (Ferro et al., 2010).

The PPT-dependent peptide efflux from isolated intact chloroplasts was triggered by heat and the presence of ATP in the incubation buffer. This is consistent with the putative molecular function of PPTs (transport of substrate coupled with ATPase activity) in mediating the export of the peptides derived from protein degradation in chloroplasts. This efflux was hampered in chloroplasts isolated from *ppts* triple mutant plants, while those purified from single or double mutants were still able to emit peptides, indicating that all three transporters exert the same peptide-extrusion activity in the chloroplast envelope. The same conclusions could be drawn from the results obtained by the yeast complementation

assay. Indeed, the heat sensitivity of *mdl1*Δ was rescued by introducing any coding sequence among the *PPT* genes corroborating further that the PPTs function is translocating peptides between two compartments (Jarolim et al., 2013). From a future perspective, the purification of PPT proteins would be instrumental to test their activity also *in vitro* by coupling the ATP hydrolysis with the presence of their substrate (*i.e.* peptides) as recently reported (Saxberg et al., 2021).

The mass spectrometry analysis of the peptides extruded by wild-type chloroplasts revealed that their length is comparable with that of the peptides extruded by yeast and nematode mitochondria, suggesting that peptide ABC transporters share an evolutionarily conserved mechanism of action, at least for substrate recognition, despite little sequence similarity can be detected in this kind of proteins (Sánchez-Fernández et al., 2001; Augustin et al., 2005; Haynes et al., 2010). This observation is also consistent with the successful complementation observed in yeast. The extruded peptides were prevalently originated by proteins forming or associated with Photosystem II, such as PsbC, LHCB4, and PSBO, to name a few. Coherently, these proteins are particularly abundant in chloroplasts and are fragile under heat stress (Allakhverdiev et al., 2008). In comparison, the peptides extruded from the mitochondria of yeast and nematodes originated especially from proteins forming the respiratory chain complexes, the TCA cycle or the ATP-synthase which could be considered as mitochondrial equivalent (Augustin et al., 2005; Haynes et al., 2010).

As mentioned, the observations through confocal microscopy of mesophyll tissue co-expressing PPTs fluorescence-tagged chimerae, revealed, in addition to their plastid-localisation, that PPTs are close suggesting possible interactions. Indeed, PPTs, being half-transporters and, thus, requiring a partner molecule to produce a complete functional transporter, could either form homodimers, as in the case of MDL1 and HAF-1 or heterodimers, as occurs for TAP1 and TAP2 in *H.*

sapiens (Nijenhuis and Hämmerling, 1996; Young et al., 2001; Haynes et al., 2010). The results obtained from both the peptide-efflux detection and the yeast complementation assay support the idea that PPTs form homodimers, as the presence of just one of the proteins was sufficient to either produce an efflux from chloroplasts or to complement the yeast heat sensitivity (Young et al., 2001; Haynes et al., 2010). Nevertheless, these observations provide indirect pieces of evidence for this conclusion which will be reinforced by a Split-ubiquitin screen (Grefen et al., 2007).

In *C. elegans*, the *haf-1* mutant was found to be sensitive to a variety of mitochondrial protein homeostasis perturbations and its ability to induce a mtUPR was abolished (Haynes et al., 2010). The *ppts* triple mutant, lacking the three PPTs from chloroplasts, resulted to be vulnerable as well to both heat and MV treatments. In addition, the introgression of mutations in chloroplast proteases, namely FTSH2, FTSH11 and CLPR1, within the *ppts* mutant background led to diminished photosynthetic performances as well in the quadruple mutants. This is in agreement with the overall sensitivity of *ppts* to perturbed protein homeostasis. These observations are coherent with the hypothesised role of PPTs as mediators of a retrograde signalling pathway involved in the response against chloroplast protein homeostasis alterations. Indeed, although no changes at the transcript level were detected, upon heat shock, *ppts* mutant plants failed to upregulate CLPB3 proteins in chloroplasts. CLPB3 resolves aggregates of unfolded proteins in the stroma, therefore, the higher sensitivity of *ppts* could be linked to the decreased amount of CLPB3 and consequently to a loss of its protective action during the early events of the cellular response to heat. Currently, it is not clear how the peptide efflux contributes to CLPB3 regulation after heat treatment. Additionally, it remains to investigate if PPTs activity influences nuclear gene expression. The transcriptome analysis of the *ppts* triple mutant both under standard conditions and after heat

treatment will be performed to identify PPTs-dependent genes and to correlate the PPTs-mediated peptide efflux with the retrograde signalling.

Interestingly, CLPB3 was also found to accumulate in larger amounts in *ppts* mutants than wild-type leaves before any external challenge was applied. This indicates the presence of an already deteriorated protein homeostasis in chloroplasts (Llamas et al., 2017; Parcerisa et al., 2020). Since it was observed that protein degradation is unaffected by PPTs absence, it is reasonable to speculate that peptide concentration is increased within chloroplasts of *ppts* mutants. Peptides can interact with proteins affecting their activity, folding, interaction and stability, therefore, accumulating peptides within chloroplasts could provoke the imbalance in the plastid protein homeostasis and trigger another retrograde signal which ultimately leads to higher CLPB3 accumulation (Ferro et al., 2014). It was interesting to observe that the removal of the considered plastid proteases from the *ppts* mutant genetic background resulted in two different outcomes of CLPB3 accumulation in plants grown in standard conditions. Loss of FTSH proteases (both FTSH2 or FTSH11) correlated with a diminished accumulation of CLPB3, instead, if the CLP protease complex was hindered, CLPB3 accumulation was even higher. The experiments here described are not sufficient to explain in detail the reason behind these differences and further investigation is required, however, it is tempting to speculate that the removal of either FTSH2 or FTSH11 could lead to a decreased rate of proteolysis and the consequentially reduced accumulation of peptides, compensating for the lack of PPTs (Adam et al., 2019; Dogra et al., 2019). Instead, the higher amount of CLPB3 in the *clpr1 ppts* quadruple mutant could be due to the additive effect that arose from the malfunctioning CLP complex and the abolition of a putative PPTs-mediated retrograde signalling.

In conclusion, the data here reported can delineate a working model in which PPTs are peptide transporter located on the chloroplast envelope (Fig. 16).

Under standard growing conditions, PPTs could contribute to the removal of peptides originated by the normal protein turnover from the stroma. Upon challenges to the chloroplast protein homeostasis, peptide production is increased due to a higher proteolysis rate of the accumulating damaged proteins. The resulting peptides are then extruded from chloroplasts into the cytoplasm by PPTs. This event has somehow a role in regulating CLPB3 post-transcriptionally leading to its higher accumulation in chloroplasts. The failed CLPB3 upregulation could be responsible for the higher sensitivity of *ppts* triple mutant to the chloroplast protein homeostasis.

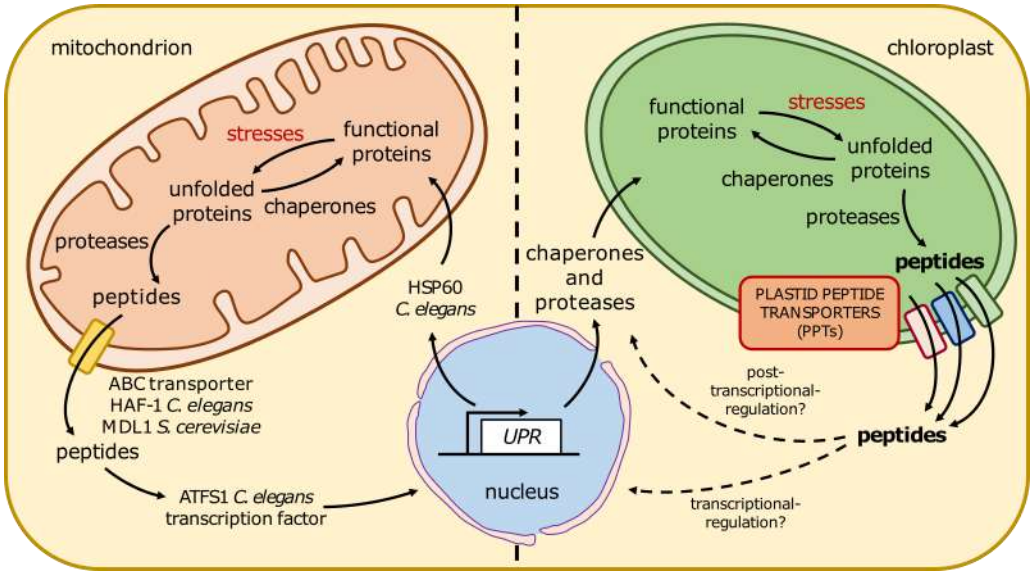

Figure 16 – The working model of a putative PPTs-mediated retrograde signalling pathway. On the left is reported, as a comparison, a graphical summary of the mitochondrial retrograde pathway mediated by HAF-1 and extruded peptides (Haynes *et al.*, 2010). Stress caused by heat promotes protein unfolding and degradation. The resulting peptides are then extruded into the cytoplasm by HAF-1. This event favours the translocation of the ATFS1 transcription factor in the nucleus, where it triggers the expression of mtUPR-related genes (*e.g. HSP60*). On the right is depicted the proposed working model in *Arabidopsis thaliana*. Heat exposure causes plastid protein degradation. Fueled by ATP, PPTs export peptides out of the chloroplast. It is still unclear if peptides act as signalling molecules influencing nuclear gene expression or if are part of a post-transcriptional regulation mechanism, or both. Nevertheless, *ppts* triple mutant plants fail to promote CLPB3 chaperone accumulation in chloroplasts upon heat treatment and are sensitive to perturbation of protein homeostasis induced by heat or methyl viologen. Additionally, the concomitant removal of plastid proteases with PPTs decreases the photosynthetic performance of the chloroplasts and results in CLPB3 misregulation at the protein level.

MATERIALS AND METHODS

Plant material and growth conditions

Arabidopsis thaliana Col-0 ecotype plants both wild type and T-DNA mutant lines were cultivated in pots within growth chambers under standard conditions (16 h at 100 μmol photons m^{-2} s^{-1} light and 8 h dark, at 22°C temperature). T-DNA insertion sites were determined by sending the PCR-amplified genomic regions of interest to a company for Sanger-based sequencing analyses. Multiple mutants were generated by manual crossing and identified by PCR-based segregation analyses of F2 populations. The mutant lines are listed in Table 4.

Plants tested for heat and methyl viologen (Sigma) sensitivity were grown in Petri dishes containing synthetic medium (Murashige and Skoog salt 0,4% w/v; Phyto agar 1,5% w/v) with the addition, where indicated, of 1 or 2 μM MV. Heat treatments on entire 15 days old plants grown in Petri dishes were performed by incubating the Petri dishes in dark at 45°C for 2 h. Acclimation was performed in the same way at 37°C for 1,5 h when indicated.

Table 4 – List of T-DNA mutant lines employed in this work.

ID Araport	Gene	Allele	Line	Reference
AT1G70610	*TAP1*	*tap1-1*	SALK_085664	this work
AT4G25450	*NAP8*	*nap8-1*	SALK_151551	this work
AT5G03910	*ATH12*	*ath12-1*	SALK_052673	this work
AT2G30950	*FTSH2*	*ftsh2-2*	SAIL_253_A03	(Tadini et al., 2020b)
AT5G53170	*FTSH11*	*ftsh11*	SALK_033047	(Adam et al., 2019)
AT1G49970	*CLPR1*	*clpr1-2*	SALK_088407	(Llamas et al., 2017)

Accession numbers

The Arabidopsis Genome Initiative accession numbers for the *A. thaliana* genes mentioned in this work can be found at TAIR (https://www.arabidopsis.org): *TAP1* (AT1G70610), *NAP8* (AT4G25450), *ATH12* (AT5G03910), *FTSH2* (AT2G30950), *FTSH11* (AT5G53170), *CLPR1* (AT1G49970), *TIC20-II* (AT2G47840), *PP2AA3* (AT1G13320), *CLPB3* (AT5G15450), *LHCB4* (AT5G01530), *PSBO1* (AT5G66570).

Genomic DNA isolation from *Arabidopsis thaliana*

Genomic DNA was isolated from *A. thaliana* leaves or cotyledons. Samples DNA extraction buffer (200 mM Tris-HCl pH 7.5, 250 mM NaCl, 25 mM EDTA and 0.5% (w/v) SDS) and precipitated with 0,8 volumes of isopropanol at 16,000 g for 20 minutes. The pellet was then washed in 70% ethanol and resuspended in 200 µl of ddH_2O.

Total RNA isolation

The total RNA was extracted from liquid-nitrogen-freeze ground samples using one volume of extraction buffer (300 mM NaCl, 50 mM TRIS-HCl pH 7,5, 20 mM EDTA, 0,5% SDS) and one volume of Acid Phenol followed by solubilization at 55°C for 5 minutes. Samples were centrifuged for 2 min at 16000 g at 4°C and the aqueous phases were collected and washed twice in chloroform. The chloroform-cleaned aqueous phases were collected and mixed with one volume of 8 M LiCl, incubated for two hours at -20°C and centrifuged for 60 minutes at 4°C at 16000 g. The pellet was then washed twice with 75% ethanol and resuspended in 80 µl of DEPC-treated water. Samples were used fresh or stored at -20°C for future analyses.

Standard PCR, High Fidelity PCR and RT-qPCR

For genotyping of plant material 1 µl of DNA was used as a template for PCR analysis. For this purpose, the PCR was performed in a total volume of 20 µl

containing 2 µl of 10x PCR-buffer (Promega), 250 µM dNTPs, 100 µM for each primer, 0,5 units of GoTaq polymerase (Promega). The PCR product was then loaded on a 1% agarose gel.

cDNA for RT-qPCR analyses or cloning procedures were obtained from 1 µg of total RNA processed with iScript™ gDNA Clear cDNA Synthesis Kit (BioRad) for genomic DNA digestion and first-strand cDNA synthesis.

The genes of interest for cloning procedures were amplified from Col-0 cDNA with the Q5 High-Fidelity DNA Polymerase (NEB). Reactions were performed in a total volume of 50 µl each. The reaction contained 10 µl colourless reaction buffer 10X, 200 µM of each primer, 250 µM dNTPs and 1 unit of Q5 High-Fidelity DNA Polymerase. The PCR products were loaded on a 1% agarose TAE (150 mM Tris-HCl, 1.74 M Acetic acid, 1 mM EDTA) gel and then cut from the gel and purified via the Qiagen gel extraction kit following the producer's instructions.

RT-qPCR analyses were performed on a CFX96 Real-Time system (Bio-Rad), using SYBR Green Master Mix (BioRad). Data obtained from three biological and three technical replicates were analysed with the CFX Maestro software (BioRad). Used primers are listed in Table 5.

Table 5 – List of primers for *Arabidopsis thaliana* sequences used in this work. Underscored sequences annealed on T-DNA left borders. wt: wild-type locus; mut: T-DNA insertion; goi: gene of interest; ref: internal reference for RT-qPCR.

Target	Forward sequence (5' to 3')	Reverse sequence (5' to 3')	Note
Primers used for genotyping			
TAP1	TTCAGTGGCATACGAGGATGC	CAGCATATCACCAATGTGCAC	wt
	GCGTGGACCGCTTGCTGCAACTC	CAGCATATCACCAATGTGCAC	mut
NAP8	AAGGGTTTTGATCCAGAAGG	CCTGACTACCGAAGATAGAC	wt
	GCGTGGACCGCTTGCTGCAACTC	CCTGACTACCGAAGATAGAC	mut
ATH12	TCAAAAAGGCATAACTAGGG	TACAGAGATCTCACGACAGG	wt
	TCAAAAAGGCATAACTAGGG	GCGTGGACCGCTTGCTGCAACTC	mut
FTSH2	CGCTTTTGATTGGTGGTTTG	CGTCAACACTTACCTGCACC	wt
	GCATCTGAATTTCATAACCAATCTCGATACAC	CGTCAACACTTACCTGCACC	mut
FTSH11	TCCTCCTCTCCATACTTCTTCG	CATGGTAACAATACCAGTGCG	wt
	GCGTGGACCGCTTGCTGCAACTC	CATGGTAACAATACCAGTGCG	mut
CLPR1	GTGGGCTTTTGCCTTCAC	GAAGCATGCCAAAAGACGAG	wt
	GTGGGCTTTTGCCTTCAC	GCGTGGACCGCTTGCTGCAACTC	mut
Primers used for RT-qPCR			
CLPB3	TGAATGCTGCAAGGTCAATC	ACACGTGCCAGCTGTAAC	goi
PP2A	GACAAGGTTCACTCAATCCG	TCGGATCCCATTACTGGAGC	ref
Primers used for cloning procedures			
TAP1	*ATGGCTCAGCAAGTACTCGG	**ATAAGACGGCATCGTTTTGTCTC	-
NAP8	*ATGGCGTCTGCAACGACTC	**ACTCAAAGGCTAGTCTCTGAGTG	-
ATH12	*ATGTCATTTCTCCTCCTAACACCG	**AAATCACGAGTCCAGCTGATG	-
TIC20	*ATGGCGTCTCTGTGCCTTTC	**AGAGTTGTCTACCGGCGGC	-
attB1 site	GGGGACAAGTTTGTACAAAAAAGCAGGCT*		
attB2 site	GGGGACCACTTTGTACAAGAAAGCTGGGT**		

Cloning procedure and transgenic lines generation

First, an entry clone (pDONR207, Invitrogen) was produced using BP ClonaseII enzyme mix reaction (see the Invitrogen GATEWAY™ instruction manual). After purification of the donor vector from *E. coli* (QIAprep Spin Miniprep Kit, following producer's instructions) the LR reaction (LR Clonase II enzyme mix, Invitrogen) was used to clone the gene of interest in the GFP (pB7FWG2) and RFP

(pB7RWG2) destination vectors. GFP- or RFP-tagged transgenic lines were generated by Agrobacterium-mediated transformation of wild-type plants, manual crossing and PCR-based segregation analyses. Primer sequences employed in this thesis are listed in Table 4.

Chloroplasts isolation and heat treatment

Intact chloroplasts were isolated from leaves (5 g fresh weight) harvested from mature plants according to previous work (Kunst, 1998), with a few changes. Samples were homogenized in 250 mL of homogenization buffer (45 mM sorbitol, 20 mM Tricine-KOH pH 8,4, 10 mM EDTA, 10 mM $NaHCO_3$ and 0,1% (w/v) BSA fraction V, supplemented with proteinase inhibitor cocktail (cOmplete™, COEDTAF-RO, Roche), filtered through a single-layer of Miracloth (Millipore) and centrifuged for 7 min at 700 *g* at 4°C. The pellet was gently resuspended in resuspension buffer (300 mM sorbitol, 200 mM Tricine-KOH pH 8,4, 2,5 mM EDTA and 5 mM $MgCl_2$). The suspension was centrifuged using a two-step Percoll gradient (40%-80% (v/v) in resuspension buffer) at 4°C and 6500 g for 20 min. Intact chloroplasts were collected at the interface of the percoll gradient and washed once with the resuspension buffer. Samples were then normalized on the chlorophyll quantity. Samples were heat treated at 45°C for 1h with a pre-heated thermoblock. 3 mM ATP was added to the sample just before treatment. After stress delivery, samples were centrifuged at 1000 g for 8 min. Supernatants were used for peptide quantification and identification. Pellets were used for protein degradation tests via immunoblots. Both fractions were immediately frozen in liquid nitrogen and stored at -80°C until use.

Peptides purification, quantification and identification

Samples were first purified using Ultra-0.5 Centrifugal Filter Devices (Amicon) and further purified and concentrated using the SPE Clean-up Kit (Waters). Peptides were quantified through UV spectrometry at 280 nm. A

calibration curve was realised using MS Compatible Yeast and Human Protein Extracts (Promega) as a reference for peptide quantification. Normality and one-way ANOVA test and Tukey HSD were performed using https://www.statskingdom.com/. Standard parameters were used as indicated by the tool.

Peptide detection was performed through Q Exactive™ Hybrid Quadrupole-Orbitrap™ Mass Spectrometer (LC-MS/MS). Three independent biological replicas were performed. Raw data were processed with MaxQuant v. 1.5.3.31, using default settings. Peptide-producing proteins were identified with the *Arabidopsis thaliana* protein UniProt database (www.uniprot.org) and their subcellular localisation was determined with The Plant Proteome Database (http://ppdb.tc.cornell.edu/).

Protein Sample Preparation and Immunoblot Analyses

For immunoblot analyses, plant tissues or purified chloroplasts were homogenized in Laemmli sample buffer (20% v/v glycerol, 4% w/v SDS, 160 mM Tris-HCl pH 6,8, 10% v/v 2-mercaptoethanol) to a final concentration of 0,1 mg μL−1 (fresh weight/Laemmli sample buffer). Samples were incubated at 65 °C for 15 min and, after a centrifugation step at 16000 *g* for 10 min, the supernatant was incubated at 95 °C for 5 min. Samples were used fresh or stored at -20°C for future analyses. Protein extracts corresponding to 4 mg (fresh-weight) seedlings were loaded onto SDS–PAGE (10% [w/v] acrylamide) gels and transferred to polyvinylidene-difluoride (PVDF) filters (0.20 μm pore size). Replicate membranes were immuno-decorated with specific antibodies. The antibody specific for CLPB3, LHCB4 and PSBO were obtained from Agrisera. Secondary antibodies Anti-rabbit conjugated with HRP were obtained from Thermo. Immunodetection was performed using the ChemiDoc imaging system (BioRad). Signals were quantified with ImageLab software (BioRad) in at least three biological replicates.

Photosynthetic efficiency measurements

Photosynthetic efficiency was evaluated using a Walz Imaging PAM fluorometer (https://walz.com). The maximum quantum yield of the photosystem 2 (F_v/F_m) was measured from plants previously dark-adapted for 20 minutes. Measurements were repeated at least in three biological replicates.

Yeast strains generation

All yeast strains obtained in this work were derived from the *Saccharomyces cerevisiae* BY4741 (genetic background S288C) strain, kindly donated by Prof. Federico Lazzaro. For the generation of *mdl1*Δ *TAP1*, *mdl1*Δ *NAP8* and *mdl1*Δ *ATH12* strains, the DNA recombination cassettes were synthesised by the Duolix company. The cassettes contain upstream coding sequences of *TAP1*, *NAP8* or *ATH12* without the portion coding for the respective chloroplast transit peptides. Downstream, lies the *KANMX* locus from the pFA6a plasmid which confers to yeast cells resistance against the G-418 kanamycin derivative for selection. Each recombination cassette was flanked upstream and downstream by 40 bp stretches homologous to the desired recombination sites in the yeast genome (Table 5). The recombination sites were designed to drive the replacement of the entire *MDL1* coding sequence downstream of the mitochondrial transit peptide, allowing for the expression of the Arabidopsis proteins targeted to the mitochondria. The recombination cassettes were additionally flanked by *EcoRI* restriction sites and cloned into the pSEVA18 plasmid. For this purpose, the CDS of *NAP8* was edited by substituting the thymine 1416 with cytosine to disrupt an internal *EcoRI* restriction site without altering the amino acid encoded by the edited codon. The obtained plasmids were then propagated in *E. coli*. Finally, the EcoRI digestion of the purified plasmids provided the linear DNA utilized for yeast transformation. Instead, the recombination cassette employed for the generation of the *mdl1*Δ null mutant strain was obtained by High-Fidelity PCR amplification of the *KANMX* locus using the pFA6a plasmid as a template. The used primers were designed to

add 40 bp homologous able to replace completely the *MDL1* locus through homologous recombination (Table 5). Yeast transformation was carried out by the lithium acetate/single-stranded carrier DNA/polyethylene glycol method (Gietz and Woods, 2002). Strains selection was performed on a YPD medium containing 200 μg/ml G-418. The in-frame correct insertion of the recombination cassettes was confirmed through PCR amplification and Sanger sequencing.

Table 6 – DNA sequences employed for yeast homologous recombination.

Target	Sequence (5' to 3')	Notes
Recombination sites		
MDL1 mTP	GTTGTTGCGAAGTCAATTCGCATCAGCAAG TGCACTATAT	Used to replace in frame *MDL1* with *TAP1*, *NAP8* or *ATH12*
downstream *MDL1*	ACTGTGGCATAGAAAAGTGATTCCATACTG CGGCAACTTC	Used to replace in frame *MDL1* with *TAP1*, *NAP8* or *ATH12*
upstream *MDL1*	CATTGAAATTTTACTAAGTTAAAGAAGAGG AAGGGCTCCA	Used to delete *MDL1*
Primers used for the generation of the recombination cassette for the generation of the *mdl1Δ* null mutant		
upstream *MDL1*	CATTGAAATTTTACTAAGTTAAAGAAGAGGAAGGGCTCCAGACATGGAGGCCCA GAATAC	
downstream *MDL1*	ACTGTGGCATAGAAAAGTGATTCCATACTGCGGCAACTTCCAGTATAGCGACCA GCATTCAC	

Yeast heat-shock treatment

Heat-shock treatments were performed as explained, with few changes (Jarolim et al., 2013). Yeast cultures were grown (28° C, 250 rpm) until the exponential phase was reached (0,5-0,6 OD_{600}). Then, cultures were divided into two subcultures (Mock and Heat). Before splitting, aliquots were collected, serial diluted and plated on a complete YPD medium as T0 samples. The Mock cultures were incubated in the previous growing conditions as a control. The Heat cultures were

incubated at 45° C instead. After 2 hours both cultures were sampled, and cells were plated on Petri dishes kept at 28° C for 3 days to allow colony formation. The obtained colonies were then manually counted to compare the T0 sample with the Mock and the Heat ones to estimate cell growth (expressed as a ratio) in the two conditions.

REFERENCES

Adam Z, Aviv-Sharon E, Keren-Paz A, Naveh L, Rozenberg M, Savidor A, Chen J (2019) The Chloroplast Envelope Protease FTSH11 – Interaction With CPN60 and Identification of Potential Substrates. Front Plant Sci **10**: 428

Adl SM, Simpson AGB, Farmer MA, Andersen RA, Anderson OR, Barta JR, Bowser SS, Brugerolle G, Fensome RA, Fredericq S, et al (2005) The new higher level classification of eukaryotes with emphasis on the taxonomy of protists. J Eukaryot Microbiol **52**: 399–451

Ahmed T, Yin Z, Bhushan S (2016) Cryo-EM structure of the large subunit of the spinach chloroplast ribosome. Sci Rep **6**: 1–13

Allakhverdiev SI, Kreslavski VD, Klimov V V., Los DA, Carpentier R, Mohanty P (2008) Heat stress: An overview of molecular responses in photosynthesis. Photosynth Res **98**: 541–550

Allen JF (2015) Why chloroplasts and mitochondria retain their own genomes and genetic systems: Colocation for redox regulation of gene expression. Proc Natl Acad Sci **112**: 10231–10238

Allen JF, Martin WF (2016) Why have organelles retained genomes? Cell Syst **2**: 70–72

Arnold I, Wagner-Ecker M, Ansorge W, Langer T (2006) Evidence for a novel mitochondria-to-nucleus signalling pathway in respiring cells lacking i-AAA protease and the ABC-transporter Mdl1. Gene **367**: 74–88

Aszí O Dobson L´, Istv´ I, Reményi I, Reményi R, Tusnády E, Tusnády T (2015) CCTOP: a Consensus Constrained TOPology prediction web server. Nucleic Acids Res **43**: W408–W412

Augustin S, Nolden M, Müller S, Hardt O, Arnold L, Langer T (2005)

Characterization of peptides released from mitochondria: Evidence for constant proteolysis and peptide efflux. J Biol Chem **280**: 2691–2699

Ballinger CA, Connell P, Wu Y, Hu Z, Thompson LJ, Yin L-Y, Patterson C (1999) Identification of CHIP, a Novel Tetratricopeptide Repeat-Containing Protein That Interacts with Heat Shock Proteins and Negatively Regulates Chaperone Functions. Mol Cell Biol **19**: 4535–4545

Beck CF, Freiburg D-, Grimm B (2006) Involvement of Tetrapyrroles in Cellular Regulation. Adv Photosynth Respir **25**: 223–235

Bieri P, Leibundgut M, Saurer M, Boehringer D, Ban N (2017) The complete structure of the chloroplast 70S ribosome in complex with translation factor pY. EMBO J **36**: 475–486

Bock R, Timmis JN (2008) Reconstructing evolution: Gene transfer from plastids to the nucleus. BioEssays **30**: 556–566

Börner T, Aleynikova AY u., Zubo YO, Kusnetsov V V. (2015) Chloroplast RNA polymerases: Role in chloroplast biogenesis. Biochim Biophys Acta **1847**: 761–769

Boyer PD (1997) The ATP synthase - A splendid molecular machine. Annu Rev Biochem **66**: 717–749

Bradbeer JW, Atkinson YE, Börner T, Hagemann R (1979) Cytoplasmic synthesis of plastid polypeptides may be controlled by plastid-synthesised RNA [20]. Nature **279**: 816–817

Bruce BD (2001) The paradox of plastid transit peptides: Conservation of function despite divergence in primary structure. Biochim Biophys Acta - Mol Cell Res **1541**: 2–21

Bubunenko MG, Schmidt J, Subramanian AR (1994) Protein substitution in

chloroplast ribosome evolution a eukaryotic cytosolic protein has replaced its organelle homologue (L23) in spinach. J Mol Biol **240**: 28–41

de Castro E, Sigrist CJA, Gattiker A, Bulliard V, Langendijk-Genevaux PS, Gasteiger E, Bairoch A, Hulo N (2006) ScanProsite: detection of PROSITE signature matches and ProRule-associated functional and structural residues in proteins. Nucleic Acids Res **34**: W362–W365

Chan KX, Phua SY, Crisp P, McQuinn R, Pogson BJ (2016) Learning the Languages of the Chloroplast: Retrograde Signaling and Beyond. Annu Rev Plant Biol **67**: 25–53

Chang WL, Soll J, Bolter B (2012) The gateway to chloroplast: Re-defining the function of chloroplast receptor proteins. Biol Chem **393**: 1263–1277

Chen J, Burke JJ, Velten J, Xin Z (2006) FtsH11 protease plays a critical role in Arabidopsis thermotolerance. Plant J **48**: 73–84

Chen J, Burke JJ, Xin Z (2018) Chlorophyll fluorescence analysis revealed essential roles of FtsH11 protease in regulation of the adaptive responses of photosynthetic systems to high temperature. BMC Plant Biol **18**: 1–13

Chen Q, Lauzon LM, DeRocher AE, Vierling E (1990) Accumulation, stability, and localization of a major chloroplast heat-shock protein. J Cell Biol **110**: 1873–1883

Chen Q, Yu F, Xie Q (2020) Insights into endoplasmic reticulum-associated degradation in plants. New Phytol **226**: 345–350

Chi W, He B, Mao J, Jiang J, Zhang L (2015) Plastid sigma factors: Their individual functions and regulation in transcription. Biochim Biophys Acta - Bioenerg **1847**: 770–778

Chou ML, Chu CC, Chen LJ, Akita M, Li HM (2006) Stimulation of transit-

peptide release and ATP hydrolysis by a cochaperone during protein import into chloroplasts. J Cell Biol **175**: 893–900

Chou ML, Fitzpatrick LM, Tu SL, Budziszewski G, Potter-Lewis S, Akita M, Levin JZ, Keegstra K, Li HM (2003) Tic40, a membrane-anchored co-chaperone homolog in the chloroplast protein translocon. EMBO J **22**: 2970–2980

Cleland WW, Andrews TJ, Gutteridge S, Hartman FC, Lorimer GH (1998) Mechanism of Rubisco: The Carbamate as General Base. Chem Rev **98**: 549–562

Colombo M, Tadini L, Peracchio C, Ferrari R, Pesaresi P (2016) GUN1, a Jack-Of-All-Trades in Chloroplast Protein Homeostasis and Signaling. Front Plant Sci. doi: 10.3389/fpls.2016.01427

Constan D, Froehlich JE, Rangarajan S, Keegstra K (2004) A stromal Hsp100 protein is required for normal chloroplast development and function in arabidopsis. Plant Physiol **136**: 3605–3615

Cox JS, Shamu CE, Walter P (1993) Transcriptional induction of genes encoding endoplasmic reticulum resident proteins requires a transmembrane protein kinase. Cell **73**: 1197–1206

Dagan T, Martin W (2006) The tree of one percent. Genome Biol. doi: 10.1186/gb-2006-7-10-118

Daley DO, Whelan J (2005) Why genes persist in organelle genomes. Genome Biol. doi: 10.1186/gb-2005-6-5-110

Dogra V, Duan J, Lee KP, Kim C (2019) Impaired PSII proteostasis triggers a UPR-like response in the var2 mutant of Arabidopsis. J Exp Bot **70**: 3075–3088

Dorrell RG, Howe CJ (2012) What makes a chloroplast? Reconstructing the establishment of photosynthetic symbioses. J Cell Sci **125**: 1865–1875

Drescher A, Stephanie R, Calsa T, Carrer H, Bock R (2000) The two largest chloroplast genome-encoded open reading frames of higher plants are essential genes. Plant J **22**: 97–104

Dyall SD, Brown MT, Johnson PJ (2004) Ancient invasions: from endosymbionts to organelles. Science **304**: 253–257

Edgar RC (2004) MUSCLE: A multiple sequence alignment method with reduced time and space complexity. BMC Bioinformatics **5**: 1–19

Emanuel C, Weihe A, Graner A, Hess WR, Börner T (2004) Chloroplast development affects expression of phage-type RNA polymerases in barley leaves. Plant J **38**: 460–472

Emanuelsson O, Nielsen H, Brunak S, von Heijne G (2000) Predicting Subcellular Localization of Proteins Based on their N-terminal Amino Acid Sequence. J Mol Biol **300**: 1005–1016

Escoubas JM, Lomas M, LaRoche J, Falkowski PG (1995) Light intensity regulation of cab gene transcription is signaled by the redox state of the plastoquinone pool. Proc Natl Acad Sci **92**: 10237–10241

Feller G (2010) Protein stability and enzyme activity at extreme biological temperatures. J Phys Condens Matter **22**: 323101

Ferro ES, Rioli V, Castro LM, Fricker LD (2014) Intracellular peptides: From discovery to function. EuPA Open Proteomics **3**: 143–151

Ferro M, Brugière S, Salvi D, Seigneurin-Berny D, Court M, Moyet L, Ramus C, Miras S, Mellal M, Le Gall S, et al (2010) AT_CHLORO, a Comprehensive Chloroplast Proteome Database with Subplastidial

Localization and Curated Information on Envelope Proteins. Mol Cell Proteomics. doi: 10.1074/mcp.M900325-MCP200

Fey V, Wagner R, Bräutigam K, Wirtz M, Hell R, Dietzmann A, Leister D, Oelmüller R, Pfannschmidt T (2005) Retrograde plastid redox signals in the expression of nuclear genes for chloroplast proteins of Arabidopsis thaliana. J Biol Chem **280**: 5318–5328

Flores-Pérez Ú, Jarvis P (2013) Molecular chaperone involvement in chloroplast protein import. Biochim Biophys Acta - Mol Cell Res **1833**: 332–340

Flügge U-I (2001) Plant Chloroplasts and Other Plastids. eLS. doi: 10.1038/npg.els.0001678

Fortunato S, Lasorella C, Tadini L, Jeran N, Vita F, Pesaresi P, de Pinto MC (2022) GUN1 involvement in the redox changes occurring during biogenic retrograde signaling. Plant Sci **320**: 111265

Fu Y, Li X, Fan B, Zhu C, Chen Z (2022) Chloroplasts Protein Quality Control and Turnover: A Multitude of Mechanisms. Int J Mol Sci **23**: 7760

Gietz RD, Woods RA (2002) Transformation of yeast by lithium acetate/single-stranded carrier DNA/polyethylene glycol method. Methods Enzymol **350**: 87–96

Gould JM, Izawa S (1973) Studies on the energy coupling sites of photophosphorylation. I. Separation of Site I and Site II by partial reactions of the chloroplast electron transport chain. BBA - Bioenerg **314**: 211–223

Graf M, Arenz S, Huter P, Dönhöfer A, Nováček J, Wilson DN (2017) Cryo-EM structure of the spinach chloroplast ribosome reveals the location of plastid-specific ribosomal proteins and extensions. Nucleic Acids Res **45**: 2887–2896

Grefen C, Lalonde S, Obrdlik P (2007) Split-Ubiquitin System for Identifying Protein-Protein Interactions in Membrane and Full-Length Proteins. Curr Protoc Neurosci. doi: 10.1002/0471142301.ns0527s41

Grondelle R van, Dekker JP, Gillbro T, Sunstrom V (1994) Energy transfer and trapping in phtotosynthesis. Biochem Biophys Acta **1187**: 1–65

Gross EL (1993) Plastocyanin: Structure and function. Photosynth Res **37**: 103–116

Guindon S, Delsuc F, Dufayard JF, Gascuel O (2009) Estimating maximum likelihood phylogenies with PhyML. Methods Mol Biol **537**: 113–137

Hajdukiewicz PTJ, Allison LA, Maliga P (1997) The two RNA polymerases encoded by the nuclear and the plastid compartments transcribe distinct groups of genes in tobacco plastids. EMBO J **16**: 4041–4048

Havaux M (1993) Rapid photosynthetic adaptation to heat stress triggered in potato leaves by moderately elevated temperatures. Plant Cell Environ **16**: 461–467

Haynes CM, Petrova K, Benedetti C, Yang Y, Ron D (2007) ClpP Mediates Activation of a Mitochondrial Unfolded Protein Response in C. elegans. Dev Cell **13**: 467–480

Haynes CM, Yang Y, Blais SP, Neubert TA, Ron D (2010) The Matrix Peptide Exporter HAF-1 Signals a Mitochondrial UPR by Activating the Transcription Factor ZC376.7 in C. elegans. Mol Cell **37**: 529–540

Hedtke B, Börner T, Weihe A (1997) Mitochondrial and chloroplast phage-type RNA polymerases in Arabidopsis. Science **277**: 809–811

Hedtke B, Börner T, Weihe A (2000) One RNA polymerase serving two genomes. EMBO Rep **1**: 435–440

Henikoff S, Greene EA, Pietrokovski S, Bork P, K T, Hood L (1997) Gene Families: The Taxonomy of Protein Paralogs and Chimeras. Science (80-) **278**: 609–614

Hernández-Verdeja T, Strand Å (2018) Retrograde signals navigate the path to chloroplast development. Plant Physiol **176**: 967–976

Hess WR, Müller A, Nagy F, Börner T (1994) Ribosome-deficient plastids affect transcription of light-induced nuclear genes: genetic evidence for a plastid-derived signal. Mol Gen Genet MGG 1994 2423 **242**: 305–312

Hetz C, Chevet E, Oakes SA (2015) Proteostasis control by the unfolded protein response. Nat Cell Biol **17**: 829–838

Higgins CF (1992) ABC Transporters: From Microorganisms to Man. Annu Rev Cell Biol **8**: 67–113

Howe CJ, Barbrook AC, Nisbet RER, Lockhart PJ, Larkum AWD (2008) The origin of plastids. Philos Trans R Soc B Biol Sci **363**: 2675–2685

Huang CY (2005) Mutational Decay and Age of Chloroplast and Mitochondrial Genomes Transferred Recently to Angiosperm Nuclear Chromosomes. Plant Physiol **138**: 1723–1733

Inaba T, Li M, Alvarez-Huerta M, Kessler F, Schnell DJ (2003) atTic110 functions as a scaffold for coordinating the stromal events of protein import into chloroplasts. J Biol Chem **278**: 38617–38627

Inaba T, Yazu F, Ito-Inaba Y, Kakizaki T, Nakayama K (2011) Retrograde Signaling Pathway from Plastid to Nucleus, 1st ed. Int Rev Cell Mol Biol. doi: 10.1016/B978-0-12-386037-8.00002-8

Jackson DT, Froehlich JE, Keegstra K (1998) The hydrophilic domain of tic110, and inner envelope membrane component of the chloroplastic protein

translocation apparatus, faces stromal compartment. J Biol Chem **273**: 16583–16588

Jacobs J, Kück U (2011) Function of chloroplast RNA-binding proteins. Cell Mol Life Sci **68**: 735–748

Jarolim S, Ayer A, Pillay B, Gee AC, Phrakaysone A, Perrone GG, Breitenbach M, Dawes IW (2013) Saccharomyces cerevisiae genes involved in survival of heat shock. G3 Genes, Genomes, Genet **3**: 2321–2333

Jarvis P, López-Juez E (2013) Biogenesis and homeostasis of chloroplasts and other plastids. Nat Rev Mol Cell Biol **14**: 787–802

Jeran N, Rotasperti L, Frabetti G, Calabritto A, Pesaresi P, Tadini L (2021) The PUB4 E3 ubiquitin ligase is responsible for the variegated phenotype observed upon alteration of chloroplast protein homeostasis in arabidopsis cotyledons. Genes (Basel) **12**: 1387

Kang J, Park J, Choi H, Burla B, Kretzschmar T, Lee Y, Martinoia E (2011) Plant ABC Transporters. Arab. B. p e0153

Karpinski S, Reynolds H, Karpinska B, Wingsle G, Mullineaux P (1999) Systemic signalling and acclimatiom on response to excess excitation energy in Arabidopsis. Science (80-) **284**: 654–657

Karplus PA, Daniels MJ, Herriott JR (1991) Atomic structure of ferredoxin-NADP+ reductase: prototype for a structurally novel flavoenzyme family. Science **251**: 60–6

Kessler F, Blobel G (1996) Interaction of the protein import and folding machineries in the chloroplast. Proc Natl Acad Sci U S A **93**: 7684–7689

Kikuchi S, Asakura Y, Imai M, Nakahira Y, Kotani Y, Hashiguchi Y, Nakai Y, Takafuji K, Bédard J, Hirabayashi-Ishioka Y, et al (2018) A Ycf2-FtsHi

heteromeric AAA-ATPase complex is required for chloroplast protein import. Plant Cell **30**: 2677–2703

Kikuchi S, Bédard J, Hirano M, Hirabayashi Y, Oishi M, Imai M, Takase M, Ide T, Nakai M (2013) Uncovering the protein translocon at the chloroplast inner envelope membrane. Science (80-) **339**: 571–574

Kikuchi S, Oishi M, Hirabayashi Y, Lee DW, Hwang I, Nakai M (2009) A 1 -Megadalton translocation complex containing tic20 and tic21 mediates chloroplast protein import at the inner envelope membrane. Plant Cell **21**: 1781–1797

Kim J, Olinares PD, Oh SH, Ghisaura S, Poliakov A, Ponnala L, van Wijk KJ (2013) Modified Clp protease complex in the ClpP3 null mutant and consequences for chloroplast development and function in Arabidopsis. Plant Physiol **162**: 157–179

Kim J, Rudella A, Ramirez Rodriguez V, Zybailov B, Olinares PDB, van Wijk KJ (2009) Subunits of the Plastid ClpPR Protease Complex Have Differential Contributions to Embryogenesis, Plastid Biogenesis, and Plant Development in Arabidopsis. Plant Cell Online **21**: 1669–1692

Kotera E, Tasaka M, Shikanai T (2005) A pentatricopeptide repeat protein is essential for RNA editing in chloroplasts. Nature **433**: 326–330

Kouranov A, Chen X, Fuks B, Schnell DJ (1998) Tic20 and Tic22 are new components of the protein import apparatus at the chloroplast inner envelope membrane. J Cell Biol **143**: 991–1002

Koussevitzky S, Nott A, Mockler TC, Hong F, Sachetto-martins G, Surpin M, Lim J, Mittler R, Chory J (2007) Signals from Chloroplasts Converge to Regulate Nuclear Gene Expression. Science (80-) **316**: 715–719

Kovács-Bogdán E, Benz JP, Soll J, Bölter B (2011) Tic20 forms a channel independent of Tic110 in chloroplasts. BMC Plant Biol **11**: 1–16

Kunst L (1998) Preparation of physiologically active chloroplasts from Arabidopsis. Methods Mol Biol **82**: 43–48

Lee DW, Jung C, Hwang I (2013) Cytosolic events involved in chloroplast protein targeting. Biochim Biophys Acta - Mol Cell Res **1833**: 245–252

Lee S, Lee DW, Lee Y, Mayer U, Stierhof YD, Lee S, Jürgens G, Hwang I (2009) Heat shock protein cognate 70-4 and an E3 ubiquitin ligase, CHIP, mediate plastid-destined precursor degradation through the ubiquitin-26S proteasome system in Arabidopsis. Plant Cell **21**: 3984–4001

Lee U, Rioflorido I, Hong SW, Larkindale J, Waters ER, Vierling E (2007) The Arabidopsis ClpB/Hsp100 family of proteins: Chaperones for stress and chloroplast development. Plant J **49**: 115–127

Leebens-Mack JH, Barker MS, Carpenter EJ, Deyholos MK, Gitzendanner MA, Graham SW, Grosse I, Li Z, Melkonian M, Mirarab S, et al (2019) One thousand plant transcriptomes and the phylogenomics of green plants. Nature **574**: 679–685

Lehnert E, Mao J, Mehdipour AR, Hummer G, Abele R, Glaubitz C, Tampé R (2016) Antigenic Peptide Recognition on the Human ABC Transporter TAP Resolved by DNP-Enhanced Solid-State NMR Spectroscopy. J Am Chem Soc **138**: 13967–13974

Lemke MD, Fisher KE, Kozlowska MA, Tano DW, Woodson JD (2021) The core autophagy machinery is not required for chloroplast singlet oxygen-mediated cell death in the Arabidopsis thaliana plastid ferrochelatase two mutant. BMC Plant Biol **21**: 1–20

Li H, Chiu C-C (2010) Protein Transport into Chloroplasts. Annu Rev Plant Biol **61**: 157–180

Liesa M, Qiu W, Shirihai OS (2012) Mitochondrial ABC transporters function: The role of ABCB10 (ABC-me) as a novel player in cellular handling of reactive oxygen species. Biochim Biophys Acta - Mol Cell Res **1823**: 1945–1957

Lin R, Wang H (2005) Two Homologous ATP-Binding Cassette Transporter Proteins, AtMDR1 and AtPGP1, Regulate Arabidopsis Photomorphogenesis and Root Development by Mediating Polar Auxin Transport. Plant Physiol **138**: 949–964

Ling Q, Huang W, Baldwin A, Jarvis P (2012) Chloroplast biogenesis is regulated by direct action of the ubiquitin-proteasome system. Science (80-) **338**: 655–659

Ling Q, Jarvis P (2015) Regulation of chloroplast protein import by the ubiquitin E3 ligase SP1 is important for stress tolerance in plants. Curr Biol **25**: 2527–2534

Llamas E, Pulido P, Rodriguez-Concepcion M (2017) Interference with plastome gene expression and Clp protease activity in Arabidopsis triggers a chloroplast unfolded protein response to restore protein homeostasis. PLoS Genet **13**: 1–28

Lopez-Juez E, Pyke KA (2005) Plastids unleashed: Their development and their integration in plant development. Int J Dev Biol **49**: 557–577

Loudya N, Okunola T, He J, Jarvis P, López-Juez E (2020) Retrograde signalling in a virescent mutant triggers an anterograde delay of chloroplast biogenesis that requires GUN1 and is essential for survival. Philos Trans R Soc B Biol Sci **375**: 20190400

Lysenko EA (2007) Plant sigma factors and their role in plastid transcription. Plant Cell Rep **26**: 845–859

Mache R (1990) Chloroplast ribosomal proteins and their genes. Plant Sci **72**: 1–12

Maier UG, Zauner S, Woehle C, Bolte K, Hempel F, Allen JF, Martin WF (2013) Massively convergent evolution for ribosomal protein gene content in plastid and mitochondrial genomes. Genome Biol Evol **5**: 2318–2329

Manning-Bog AB, McCormack AL, Li J, Uversky VN, Fink AL, Di Monte DA (2002) The Herbicide Paraquat Causes Up-regulation and Aggregation of α-Synuclein in Mice: PARAQUAT AND α-SYNUCLEIN *. J Biol Chem **277**: 1641–1644

Martinoia E, Klein M, Geisler M, Bovet L, Forestier C, Kolukisaoglu Ü, Müller-Röber B, Schulz B (2002) Multifunctionality of plant ABC transporters - More than just detoxifiers. Planta **214**: 345–355

McEvoy JP, Brudvig GW (2006) Water-splitting chemistry of photosystem II. Chem Rev **106**: 4455–4483

Mochizuki N, Brusslan JA, Larkin R, Nagatani A, Chory J (2001) Arabidopsis genomes uncoupled 5 (GUN5) mutant reveals the involvement of Mg-chelatase H subunit in plastid-to-nucleus signal transduction. Proc Natl Acad Sci **98**: 2053–2058

Mustárdy L, Garab G (2003) Granum revisited. A three-dimensional model - Where things fall into place. Trends Plant Sci **8**: 117–122

Myouga F, Motohashi R, Kuromori T, Nagata N, Shinozaki K (2006) An Arabidopsis chloroplast-targeted Hsp101 homologue, APG6, has an essential role in chloroplast development as well as heat-stress response. Plant J **48**: 249–260

Nielsen E, Akita M, Davila-Aponte J, Keegstra K (1997) Stable association of chloroplastic precursors with protein translocation complexes that contain proteins from both envelope membranes and a stromal Hsp100 molecular chaperone. EMBO J **16**: 935–946

Nijenhuis M, Hämmerling GJ (1996) Multiple regions of the transporter associated with antigen processing (TAP) contribute to its peptide binding site. J Immunol **157**: 5467–77

Nishimura K, Kato Y, Sakamoto W (2016) Chloroplast Proteases: Updates on Proteolysis within and across Suborganellar Compartments. Plant Physiol **171**: 2280–2293

Noh B, Murphy AS, Spalding EP (2001) Multidrug Resistance-Like Genes of Arabidopsis Required for Auxin Transport and Auxin-Mediated Development. Plant Cell **13**: 2441

Nöll A, Thomas C, Herbring V, Zollmann T, Barth K, Mehdipour AR, Tomasiak TM, Brüchert S, Joseph B, Abele R, et al (2017) Crystal structure and mechanistic basis of a functional homolog of the antigen transporter TAP. Proc Natl Acad Sci **114**: E438–E447

Nyström T (2005) Role of oxidative carbonylation in protein quality control and senescence. EMBO J **24**: 1311–1317

Okamura M, Paddock M, Graige M., Feher G (2000) Proton and electron transfer in bacterial reaction centers. Biochim Biophys Acta - Bioenerg **1458**: 148–163

Olinares PDB, Kim J, Davis JI, van Wijk KJ (2011a) Subunit stoichiometry, evolution, and functional implications of an asymmetric plant plastid ClpP/R protease complex in Arabidopsis. Plant Cell **23**: 2348–2361

Olinares PDB, Kim J, Van Wijk KJ (2011b) The Clp protease system; A central component of the chloroplast protease network. Biochim Biophys Acta - Bioenerg **1807**: 999–1011

Olinares PDB, Ponnala L, Van Wijk KJ (2010) Megadalton complexes in the chloroplast stroma of Arabidopsis thaliana characterized by size exclusion chromatography, mass spectrometry, and hierarchical clustering. Mol Cell Proteomics **9**: 1594–1615

Paila YD, Richardson LGL, Schnell DJ (2015) New insights into the mechanism of chloroplast protein import and its integration with protein quality control, organelle biogenesis and development. J Mol Biol **427**: 1038–1060

Parcerisa IL, Rosano GL, Ceccarelli EA (2020) Biochemical characterization of ClpB3, a chloroplastic disaggregase from Arabidopsis thaliana. Plant Mol Biol **104**: 451–465

Pesaresi P, Schneider A, Kleine T, Leister D (2007) Interorganellar communication. Curr Opin Plant Biol **10**: 600–606

Pfalz J, Liere K, Kandlbinder A, Dietz KJ, Oelmüller R (2006) pTAC2, -6, and -12 are components of the transcriptionally active plastid chromosome that are required for plastid gene expression. Plant Cell **18**: 176–197

Pfalz J, Pfannschmidt T (2013) Essential nucleoid proteins in early chloroplast development. Trends Plant Sci **18**: 186–194

Pfannschmidt T, Blanvillain R, Merendino L, Courtois F, Chevalier F, Liebers M, Grübler B, Hommel E, Lerbs-Mache S (2015) Plastid RNA polymerases: orchestration of enzymes with different evolutionary origins controls chloroplast biogenesis during the plant life cycle. J Exp Bot **66**: 6957–6973

Pulido P, Llamas E, Llorente B, Ventura S, Wright LP, Rodríguez-Concepción M (2016) Specific Hsp100 Chaperones Determine the Fate of the First Enzyme of the Plastidial Isoprenoid Pathway for Either Refolding or Degradation by the Stromal Clp Protease in Arabidopsis. PLoS Genet. doi: 10.1371/journal.pgen.1005824

Pulido P, Llamas E, Rodriguez-Concepcion M (2017) Both Hsp70 chaperone and Clp protease plastidial systems are required for protection against oxidative stress. Plant Signal Behav **12**: 1–4

Qureshi MA, Haynes CM, Pellegrino MW (2017) The mitochondrial unfolded protein response: Signaling from the powerhouse. J Biol Chem **292**: 13500–13506

Ramundo S, Casero D, Muhlhaus T, Hemme D, Sommer F, Crevecoeur M, Rahire M, Schroda M, Rusch J, Goodenough U, et al (2014) Conditional Depletion of the Chlamydomonas Chloroplast ClpP Protease Activates Nuclear Genes Involved in Autophagy and Plastid Protein Quality Control. Plant Cell **26**: 2201–2222

Ramundo S, Rochaix JD (2014) Chloroplast unfolded protein response, a new plastid stress signaling pathway? Plant Signal Behav **9**: 1–3

Rochaix JD (2022) Chloroplast protein import machinery and quality control. FEBS J **289**: 6908–6918

Romani I, Tadini L, Rossi F, Masiero S, Pribil M, Jahns P, Kater M, Leister D, Pesaresi P (2012) Versatile roles of Arabidopsis plastid ribosomal proteins in plant growth and development. Plant J **72**: 922–934

Sagan L (1967) On the origin of mitosing cells. J Theor Biol **14**: 225-IN6

Sakamoto W, Tamura T, Hanba-Tomita Y, Sodmergen, Murata M (2002) The

VAR1 locus of Arabidopis encodes a choloroplastic FtsH and is responsible for leaf variegation in the mutant alleles. Genes to Cells **7**: 769–780

Sakamoto W, Zaltsman A, Adam Z, Takahashi Y (2003) Coordinated Regulation and Complex Formation of YELLOW VARIEGATED1 and YELLOW VARIEGATED2, Chloroplastic FtsH Metalloproteases Involved in the Repair Cycle of Photosystem II in Arabidopsis Thylakoid Membranes. Plant Cell **15**: 2843–2855

Sánchez-Fernández R, Davies TGE, Coleman JOD, Rea PA (2001) The Arabidopsis thaliana ABC Protein Superfamily, a Complete Inventory. J Biol Chem **276**: 30231–30244

Santelia D, Vincenzetti V, Azzarello E, Bovet L, Fukao Y, Düchtig P, Mancuso S, Martinoia E, Geisler M (2005) MDR-like ABC transporter AtPGP4 is involved in auxin-mediated lateral root and root hair development. FEBS Lett **579**: 5399–5406

Saxberg AD, Martinez M, Fendley GA, Zoghbi ME (2021) Production of a human mitochondrial ABC transporter in E. coli. Protein Expr Purif **178**: 105778

Schmitz-Linneweber C, Small I (2008a) Pentatricopeptide repeat proteins: a socket set for organelle gene expression. Trends Plant Sci **13**: 663–670

Schmitz-Linneweber C, Small I (2008b) Pentatricopeptide repeat proteins: a socket set for organelle gene expression. Trends Plant Sci **13**: 663–670

Schnell DJ, Blobel G (1993) Identification of intermediates in pathway of protein import into chlotoplasts and thier localization to envelop contact sites. J Cell Biol **120**: 103–115

Schnell DJ, Blobel G, Keegstra K, Kessler F, Ko K, Soll J (1997) A consensus

nomenclature for the protein-import components of the chloroplast envelope. Trends Cell Biol **7**: 303–304

Sedaghatmehr M, Mueller-Roeber B, Balazadeh S (2016) The plastid metalloprotease FtsH6 and small heat shock protein HSP21 jointly regulate thermomemory in Arabidopsis. Nat Commun. doi: 10.1038/ncomms12439

Seigneurin-Berny D, Salvi D, Dorne AJ, Joyard J, Rolland N (2008) Percoll-purified and photosynthetically active chloroplasts from Arabidopsis thaliana leaves. Plant Physiol Biochem **46**: 951–955

Shao N, Vallon O, Dent R, Niyogi KK, Beck CF (2006) Defects in the cytochrome b6/f complex prevent light-induced expression of nuclear genes involved in chlorophyll biosynthesis. Plant Physiol **141**: 1128–1137

Sjögren LLE, MacDonald TM, Sutinen S, Clarke AK (2004) Inactivation of the clpC1 gene encoding a chloroplast Hsp100 molecular chaperone causes growth retardation, leaf chlorosis, lower photosynthetic activity, and a specific reduction in photosystem content. Plant Physiol **136**: 4114–4126

de Souza A, Wang J-Z, Dehesh K (2017) Retrograde Signals: Integrators of Interorganellar Communication and Orchestrators of Plant Development. Annu Rev Plant Biol **68**: 85–108

Steiner S, Schroter Y, Pfalz J, Pfannschmidt T (2011) Identification of Essential Subunits in the Plastid-Encoded RNA Polymerase Complex Reveals Building Blocks for Proper Plastid Development. Plant Physiol **157**: 1043–1055

Su P-H, Li H (2010) Stromal Hsp70 Is Important for Protein Translocation into Pea and Arabidopsis Chloroplasts. Plant Cell Online **22**: 1516–1531

Sugiura M (1995) The chloroplast genome. Essays Biochem **30**: 49–57

Surzycki SJ (1969) Genetic functions of the chloroplast of Chlamydomonas

reinhardi: effect of rifampin on chloroplast DNA-dependent RNA polymerase. Proc Natl Acad Sci U S A **63**: 1327–34

Susek RE, Ausubel FM, Chory J (1993) Signal transduction mutants of arabidopsis uncouple nuclear CAB and RBCS gene expression from chloroplast development. Cell **74**: 787–799

Suzuki N, Koussevitzky S, Mittler R, Miller G (2012) ROS and redox signalling in the response of plants to abiotic stress. Plant, Cell Environ **35**: 259–270

Tadini L, Ferrari R, Lehniger M-K, Mizzotti C, Moratti F, Resentini F, Colombo M, Costa A, Masiero S, Pesaresi P (2018) Trans-splicing of plastid rps12 transcripts, mediated by AtPPR4, is essential for embryo patterning in Arabidopsis thaliana. Planta **248**: 257–265

Tadini L, Jeran N, Pesaresi P (2020a) GUN1 and Plastid RNA Metabolism: Learning from Genetics. Cells **9**: 2307

Tadini L, Peracchio C, Trotta A, Colombo M, Mancini I, Jeran N, Costa A, Faoro F, Marsoni M, Vannini C, et al (2020b) GUN1 influences the accumulation of NEP-dependent transcripts and chloroplast protein import in Arabidopsis cotyledons upon perturbation of chloroplast protein homeostasis. Plant J **101**: 1198–1220

Tadini L, Pesaresi P, Kleine T, Rossi F, Guljamow A, Sommer F, Mühlhaus T, Schroda M, Masiero S, Pribil M, et al (2016) GUN1 Controls Accumulation of the Plastid Ribosomal Protein S1 at the Protein Level and Interacts with Proteins Involved in Plastid Protein Homeostasis. Plant Physiol **170**: 1817–30

Takechi K, Sodmergen, Murata M, Motoyoshi F, Sakamoto W (2000) The yellow variegated (var2) locus encodes a homologue of FtsH, an ATP-

dependent protease in arabidopsis. Plant Cell Physiol **41**: 1334–1346

Teng YS, Su YS, Chen LJ, Lee YJ, Hwang I, Li HM (2006) Tic21 is an essential translocon component for protein translocation across the chloroplast inner envelope membrane. Plant Cell **18**: 2247–2257

Thomson WW, Ellis RJ (1972) Inhibition of grana formation by lincomycin. Planta **108**: 89–92

Tiller K, Link G (1995) σ-Like Plastid Transcription Factors. Methods Mol Biol **37**: 337–348

Tiller N, Bock R (2014) The translational apparatus of plastids and its role in plant development. Mol Plant **7**: 1105–1120

Verrier P, Bird D, Burla B, Dassa E, Forestier C, Geisler M, Klein M, Kolukisaoglu Ü, Lee Y, Martinoia E, et al (2008) Plant ABC proteins – a unified nomenclature and updated inventory. Trends Plant Sci **13**: 151–159

Wagner R, Aigner H, Funk C (2012) FtsH proteases located in the plant chloroplast. Physiol Plant **145**: 203–214

van Wijk KJ (2015) Protein Maturation and Proteolysis in Plant Plastids, Mitochondria, and Peroxisomes. Annu Rev Plant Biol **66**: 75–111

Wolters JC, Abele R, Tampé R (2005) Selective and ATP-dependent translocation of peptides by the homodimeric ATP binding cassette transporter TAP-like (ABCB9). J Biol Chem **280**: 23631–23636

Woodson JD (2016) Chloroplast quality control - balancing energy production and stress. New Phytol **212**: 36–41

Woodson JD (2022) Control of chloroplast degradation and cell death in response to stress. Trends Biochem Sci. doi: 10.1016/j.tibs.2022.03.010

Woodson JD, Chory J (2008) Coordination of gene expression between organellar and nuclear genomes. Nat Rev Genet **9**: 383–395

Woodson JD, Perez-Ruiz JM, Chory J (2011) Heme synthesis by plastid ferrochelatase i regulates nuclear gene expression in plants. Curr Biol **21**: 897–903

Woodson JD, Perez-Ruiz JM, Schmitz RJ, Ecker JR, Chory J (2013) Sigma factor-mediated plastid retrograde signals control nuclear gene expression. Plant J **73**: 1–13

Wu GZ, Meyer EH, Richter AS, Schuster M, Ling Q, Schöttler MA, Walther D, Zoschke R, Grimm B, Jarvis RP, et al (2019) Control of retrograde signalling by protein import and cytosolic folding stress. Nat Plants **5**: 525–538

Yamaguchi K, Von Knoblauch K, Subramanian AR (2000) The plastid ribosomal proteins. IDENTIFICATION OF ALL THE PROTEINS IN THE 30 S SUBUNIT OF AN ORGANELLE RIBOSOME (CHLOROPLAST)*. J Biol Chem **275**: 28455–28465

Yamaguchi K, Subramanian AR (2000) The plastid ribosomal proteins. Identification of all the proteins in the 50 S subunit of an organelle ribosome (chloroplast). J Biol Chem **275**: 28466–28482

Young L, Leonhard K, Tatsuta T, Trowsdale J, Langer T (2001) Role of the ABC transporter Mdl1 in peptide export from mitochondria. Science (80-) **291**: 2135–2138

Yu F, Park S, Rodermel SR (2004) The Arabidopsis FtsH metalloprotease gene family: Interchangeability of subunits in chloroplast oligomeric complexes. Plant J **37**: 864–876

Zaltsman A (2005) Two Types of FtsH Protease Subunits Are Required for

Chloroplast Biogenesis and Photosystem II Repair in Arabidopsis. PLANT CELL ONLINE **17**: 2782–2790

Zhao C, Haase W, Tampé R, Abele R (2008) Peptide specificity and lipid activation of the lysosomal transport complex ABCB9 (TAPL). J Biol Chem **283**: 17083–17091

Zhao Q, Wang J, Levichkin I V., Stasinopoulos S, Ryan MT, Hoogenraad NJ (2002) A mitochondrial specific stress response in mammalian cells. EMBO J **21**: 4411–4419

Zoschke R, Bock R (2018) Chloroplast translation: Structural and functional organization, operational control, and regulation. Plant Cell **30**: 745–770

APPENDIX

During the three years of fellowship as a PhD student under Prof. Paolo Pesaresi's supervision, I have also contributed to research activities regarding chloroplast biogenesis and the retrograde communication of chloroplasts which resulted in published research and review articles and in the submission of a research article which is currently under the revision process.

Published articles

⌘ Lasorella C, Fortunato S, Dipierro N, Jeran N, Tadini L, Vita F, Pesaresi P, de Pinto MC (2022) Chloroplast-localized GUN1 contributes to the acquisition of basal thermotolerance in *Arabidopsis thaliana*. Frontiers in Plant Science, 13, 5319.

(Accepted manuscript under preparation for final publication, the Authors' proof is attached).

In this work, we investigate the heat-shock response in Arabidopsis wild-type and *gun1* plantlets subjected to 2 hours of incubation at 45°C. My direct contribution was: the analysis of the photosynthetic efficiency, the biochemical analysis regarding the accumulation of plastid-precursor proteins in the cytosol and the editing of the manuscript.

⌘ Fortunato S, Lasorella C, Tadini L, Jeran N, Vita F, Pesaresi P, de Pinto MC (2022) GUN1 involvement in the redox changes occurring during biogenic retrograde signaling. Plant Sci 320: 111265

https://doi.org/10.1016/j.plantsci.2022.111265

In this work, we focused on the interplay between GUN1 and redox regulation during biogenic retrograde signalling. My direct contribution was: the production of biological material which was then employed for the analyses, the bioinformatic analysis of already published gene expression datasets and the editing of the manuscript.

⌘ Jeran N, Rotasperti L, Frabetti G, Calabritto A, Pesaresi P, Tadini L (2021) The PUB4 E3 ubiquitin ligase is responsible for the variegated phenotype observed upon alteration of chloroplast protein homeostasis in arabidopsis cotyledons. Genes (Basel) 12: 1387

https://doi.org/10.3390/genes12091387

In this work, we have analysed the Arabidopsis double mutant *gun1 ftsh5*. The double mutant seedlings display both variegated cotyledons and true leaves. We attempted to suppress this phenotype by introgressing second-site mutations in genes involved in plastid translation, plastid folding/import and cytosolic protein ubiquitination. My direct contribution was: the isolation of the mutants, the physiological and biochemical analyses of the mutants, the preparation of the figures and the drafting of the manuscript.

⌘ Barbato R, Tadini L, Cannata R, Peracchio C, Jeran N, Alboresi A, Morosinotto T, Bajwa AA, Paakkarinen V, Suorsa M, et al (2020) Higher order photoprotection mutants reveal the importance of ΔpH-dependent photosynthesis-control in preventing light induced damage to both photosystem II and photosystem I. Sci Rep. doi: 10.1038/s41598-020-62717-1

https://10.1038/s41598-020-62717-1

In this work, we have generated a number of higher-order mutants by crossing genotypes bearing defects in each of the short-term photoprotection mechanisms, with the final aim to obtain a direct comparison of their role and efficiency in photoprotection. My direct contribution was: the growth rate analysis of mutants, the preparation of the figures and the drafting of the manuscript.

⌘ Tadini L, Jeran N, Pesaresi P (2020) GUN1 and Plastid RNA Metabolism: Learning from Genetics. Cells 9: 2307

https://doi.org/10.3390/cells9102307

In this review, we discuss the recently identified links between plastid RNA metabolism and retrograde signalling by providing a new and extended concept of GUN1 activity, which integrates the multitude of functional, genetic and physical interactions reported in the last years. My direct contribution was: the bioinformatic analysis of already published gene expression datasets, the preparation of the figures and the editing of the manuscript.

⌘ Tadini L, Jeran N, Peracchio C, Masiero S, Colombo M, Pesaresi P (2020) The plastid transcription machinery and its coordination with the expression of nuclear genome: Plastid-Encoded Polymerase, Nuclear-Encoded Polymerase and the Genomes Uncoupled 1-mediated retrograde communication. Philos Trans R Soc B Biol Sci 375: 20190399

https://doi.org/10.1098/rstb.2019.0399

In this review, we discuss chloroplast transcription regulation and its coordination with the expression of photosynthesis-associated nuclear genes. Particular attention is given to the link between NEP and PEP activity and the GUN1-mediated chloroplast-to-nucleus retrograde signalling. My direct contribution was: the preparation of the included figure and table, the drafting of part of the manuscript and the editing of the manuscript.

frontiers | Frontiers in Plant Science

TYPE Original Research
PUBLISHED xx xx 2022
DOI 10.3389/fpls.2022.1058831

OPEN ACCESS

EDITED BY
Laura De Gara,
Campus Bio-Medico University, Italy

REVIEWED BY
Rosa M. Rivero,
Center for Edaphology and Applied Biology of Segura (CSIC), Spain
Karin Krupinska,
University of Kiel, Germany
Piotr Gawroński

Q3 *CORRESPONDENCE
Maria Concetta de Pinto
mariaconcetta.depinto@uniba.it

†These authors have contributed equally to this work

SPECIALTY SECTION
This article was submitted to Plant Abiotic Stress, a section of the journal Frontiers in Plant Science

RECEIVED 30 September 2022
ACCEPTED 05 December 2022
PUBLISHED xx xx 2022

CITATION
Lasorella C, Fortunato S, Dipierro N, Jeran N, Tadini L, Vita F, Pesaresi P and de Pinto MC (2022) Chloroplast-localized GUN1 contributes to the acquisition of basal thermotolerance in *Arabidopsis thaliana*. *Front. Plant Sci.* 13:1058831. doi: 10.3389/fpls.2022.1058831

Chloroplast-localized GUN1 contributes to the acquisition of basal thermotolerance in *Arabidopsis thaliana*

Cecilia Lasorella[1†], Stefania Fortunato[1†], Nunzio Dipierro[1], Nicolaj Jeran[2], Luca Tadini[2], Federico Vita[1], Paolo Pesaresi[2] and Maria Concetta de Pinto[1*]

[1]Department of Biology, University of Bari Aldo Moro, Bari, Italy, [2]Department of Biosciences, University of Milano, Milano, Italy

Heat stress (HS) severely affects different cellular compartments operating in metabolic processes and represents a critical threat to plant growth and yield. Chloroplasts are crucial for heat stress response (HSR), signaling to the nucleus the environmental challenge and adjusting metabolic and biosynthetic functions accordingly. GENOMES UNCOUPLED 1 (GUN1), a chloroplast-localized protein, has been recognized as one of the main players of chloroplast retrograde signaling. Here, we investigate HSR in Arabidopsis wild-type and *gun1* plantlets subjected to 2 hours of HS at 45°C. In wild-type plants, Reactive Oxygen Species (ROS) accumulate promptly after HS, contributing to transiently oxidize the cellular environment and acting as signaling molecules. After 3 hours of physiological recovery at growth temperature (22°C), the induction of enzymatic and non-enzymatic antioxidants prevents oxidative damage. On the other hand, *gun1* mutants fail to induce the oxidative burst immediately after HS and accumulate ROS and oxidative damage after 3 hours of recovery at 22°C, thus resulting in enhanced sensitivity to HS. These data suggest that GUN1 is required to oxidize the cellular environment, participating in the acquisition of basal thermotolerance through the redox-dependent plastid-to-nucleus communication.

KEYWORDS

heat stress, GENOMES UNCOUPLED 1, reactive oxygen species, redox regulation, retrograde signaling, thermotolerance

Introduction

Plants are constantly exposed to abiotic stresses throughout their entire life cycle, which heavily impact growth and yield. The effects of climate change increase the frequency and intensity of extreme events such as heat waves, compromising plant development and crop productivity irreversibly (Bita and Gerats, 2013). Among abiotic stresses, heat stress (HS) is considered one of the most detrimental for plants, since extreme temperature fluctuations cause impairment in essential biochemical and physiological processes (Hasanuzzaman et al., 2013). As sessile organisms, plants sense and respond to adverse environmental conditions activating defense systems (Zhu, 2016). The study of the mechanisms involved in plant perception and response to heat has, therefore, a great relevance in the actual climatic scenario.

Considering that photosynthesis-related processes are sensitive to thermal fluctuations, chloroplasts have been proposed as sensors of HS (Sun and Guo, 2016). Among the chloroplast protein complexes, the photosystem II, its oxygen-evolving complex, the electron transport chain and the carbon fixation system are particularly prone to damage due to high temperatures (Allakhverdiev et al., 2008). Furthermore, heat stress reduces the content of photosynthesis-associated pigments and alters cell membrane stability by protein denaturation and lipid peroxidation (Wise et al., 2004; Wahid et al., 2007; Allakhverdiev et al., 2008). The HS-mediated damage to photosynthetic apparatus inhibits the excitation energy transfer and the electron transport in the chloroplast, leading to an overproduction of Reactive Oxygen Species (ROS) and to an imbalance of redox homeostasis (Wang et al., 2018). ROS are produced in plastids in the forms of singlet oxygen, superoxide anion ($O_{2}^{\cdot-}$), hydroxyl radicals and hydrogen peroxide (H_2O_2) (Noctor et al., 2002). ROS accumulation is controlled by scavenging and antioxidant machinery, including enzymes such as superoxide dismutase (SOD), catalases (CAT), ascorbate peroxidases (APX), and low molecular weight metabolites, like ascorbate (ASC), glutathione (GSH), tocopherols and carotenoids (Foyer and Noctor, 2013; Das et al., 2015). Although ROS were initially recognized as toxic by-products, a large number of evidence has shown the important role that these molecules may have in many essential plant processes (Farnese et al., 2016; Mittler, 2017). The role of ROS as oxidants or components of redox signaling mostly depends on a fine balance between the production and scavenging of these molecules in different organelles (Mittler, 2017).

In response to stress conditions, ROS can leave their production sites and, acting as secondary messengers, activate several signaling events (Pogson et al., 2008; Suzuki et al., 2012; Sgobba et al., 2015). In response to high temperatures, for instance, ROS act as retrograde signals, transmitting to the nucleus the redox alterations occurring in plastids (Singh et al., 2015; Hu et al., 2020);. In particular, ROS have been observed to elicit and regulate antioxidant enzymes and Heat Shock Proteins (HSPs) (Nishizawa et al., 2006; Volkov et al., 2006; Dickinson et al., 2018). Moreover, the presence of heat shock elements (HSE) in the promoter region of the Arabidopsis *APX1* and *APX2*, together with the increased thermo-sensitivity of Arabidopsis mutants defective in the biosynthetic pathways of antioxidants, supports the idea that a tight connection between ROS homeostasis and acclimation to HS exists (Pnueli et al., 2003; Larkindale et al., 2005).

In the last decades, plastid-localized Genomes Uncoupled (GUN) proteins have been identified as crucial in several processes involved in retrograde signaling (Susek et al., 1993; Mochizuki et al., 2001; Larkin et al., 2003; Strand et al., 2003; Koussevitzky et al., 2007; Woodson et al., 2011). Through chemical alteration of chloroplast biogenesis and physiology by either lincomycin (Lin) or norflurazon (NF) treatments, respectively, six *gun* mutants were isolated (Susek et al., 1993). After exposure to NF, all *gun* mutants expressed photosynthesis-associated nuclear genes (PhANGs), which on the contrary were repressed in wild type seedlings. Thus, it has been assumed that mutations in *GUN* genes led to the uncoupling of nuclear gene expression (NGE) with respect to the functional state of the chloroplast (Nott et al., 2006). GUN1 is a nuclear-encoded pentatricopeptide repeat protein with a C-terminal Small MutS-Relate domain, described as key player of plastid-to-nucleus retrograde signaling, response and adaptation to environmental challenges and plastid development (Koussevitzky et al., 2007; Wu et al., 2018; Pesaresi and Kim, 2019). Based on its amino acid sequence, GUN1 was initially identified as a nucleic acid-binding protein involved in DNA metabolism, gene expression, and DNA repair in the plastids (Koussevitzky et al., 2007). Successively, it has been proposed that GUN1 interacts with proteins rather than with nucleic acids. Among GUN1-interacting proteins, enzymes of the tetrapyrrole biosynthesis pathway and several proteins that participate in plastid gene expression (PGE) and protein homeostasis, such as plastid chaperons, have been identified (Colombo et al., 2016; Tadini et al., 2016; Zhao et al., 2019; Tadini et al., 2020; Wu and Bock, 2021). The identification of GUN1 putative interactors highlighted the role of GUN1 as a hub of multiple retrograde signaling pathways.

Despite the great attention on GUN1 role in the communication between chloroplast and nucleus, little information exists about its involvement in the signaling defense activated in response to HS. Here, we studied the role and interplay of GUN1 and redox signaling in heat stress response (HSR). The results indicate that *gun1* mutants are more sensitive to HS than wild-type plants and suggest that GUN1 could be required for basal thermotolerance, participating in the ROS-dependent oxidization of cellular

environment, which is the basis for communication of plastid impairment to the nucleus.

Materials and methods

Plant materials, growth conditions and heat stress treatment

The Arabidopsis (*Arabidopsis thaliana*, genetic background Col-0) *gun1-102* T-DNA insertion mutant was previously described in Tadini et al. (2016). Wild type (wt) and *gun1-102* (hereafter indicated as *gun1*) seeds were surface-sterilized and sown out on Murashige and Skoog medium (Duchefa, Haarlem, The Netherlands) supplemented with 2% (w/v) sucrose and 1.5% (w/v) Phyto-Agar (Duchefa). After 2 days of stratification at 4°C in the dark, plantlets were grown in a growth chamber for 15 days (22°C, 80 µmol m^{-2} sec^{-1} on 16 h/8 h light/dark cycles).

On day 15, Arabidopsis wild-type and *gun1* plants were exposed to heat stress (45°C for 2 hours) according to Ling et al. (2018). To allow short-term and long-term physiological recovery, plants were then incubated in growth conditions (22° C) for 3 hours or 2 days, respectively. Samples for analysis were collected before HS (C), immediately after HS treatment, and after 3 hours (R) and 2 days (2d-RHS) of physiological recovery. Control plants for the experiments of 2d-RHS were collected after 17 days of growth at 22°C. Each biological replicate consisted of 90 plantlets per condition. Five biological replicates per timepoint were used while each experiment was repeated at least three times.

To measure root length in control, HS and recovery conditions, agar plates were oriented vertically in comparable growth conditions described above. To determine pigment contents leaves were separated from the roots, frozen in liquid nitrogen and stored at -80°C until analysis.

Determination of pigment content and maximum quantum yield of PSII

For pigment quantification, leaf samples (50 mg) were ground in liquid nitrogen with 80% acetone (1:20 w/v) and the homogenates centrifuged at 20,000 g for 20 minutes at 4°C. The supernatant absorbances at 663.2, 646.8 and 470 nm were spectrophotometrically measured according to Zhang and Kirkham (1996). Content of chlorophyll a (Chl a) and chlorophyll b (Chl b), as well as total carotenoids (xanthophyll and β-carotene), expressed as µg g^{-1} fresh weight, were calculated according to Lichtenthaler (1987):

$$\text{Chlorophylla} = \left(12.25 \times A_{663.2}\right) - \left(2.79 \times A_{646.8}\right)$$

$$\text{Chlorophyllb} = \left(21.50 \times A_{646.8}\right) - \left(5.10 \times A_{663.2}\right)$$

$$\text{Carotenoids} = (100 \times A_{470} - 1{,}82 \times \text{Chla} - 85.2 \times \text{Chl b})/198$$

The maximum quantum yield of PSII (*Fv/Fm*) was measured by using the Imaging PAM (Walz, Effeltrich, Germany) as described in Tadini et al. (2012).

Proteasome activity

Proteasome activity was determined spectrofluorometrically by using the fluorogenic substrate Suc-LLYY-NH-AMC (Calbiochem), according to Paradiso et al. (2020). Arabidopsis plantlets were ground in liquid nitrogen and homogenized in a 1:3 (w/v) ratio with extraction buffer (50 mM Hepes-KOH, pH 7.2, 2 mM DTT, 2 mM ATP, 250 mM sucrose). After centrifugation at 20,000xg for 15 min at 4°C, supernatants were collected. 660 µL of samples, with 1mg mL^{-1} protein concentration, were mixed with 40 µL of assay buffer (100 mM Hepes-KOH, pH 7.8, 5mM $MgCl_2$, 10 mM KCl, 2 mM ATP). After 15 min of incubation at 30°C in the dark, the reaction was started by the addition of the fluorogenic substrate. The release of amino-methyl-coumarin (360 nm ex/460 nm em) was monitored between 0 and 120 min by RF-6000 spectrofluorophotometer (Shimadzu Corporation, Japan). Protein concentration was measured using Protein Assay System (Bio-Rad, Hercules, CA, USA) according to Bradford (1976), with serum albumin as standard.

Determination of ROS and oxidative markers

In situ O_2^- and H_2O_2 accumulation in leaves was detected with nitroblue tetrazolium (NBT) and 3,3-diaminobenzidine (DAB), respectively, as described in Fortunato et al. (2022). The staining intensity was digitally acquired and quantified by ImageJ software (https://imagej.nih.gov/ij/). The relative O_2^- and H_2O_2 levels were calculated as the percentage of NBT- and DAB-stained area of leaves, respectively.

The level of lipid peroxidation was evaluated in terms of malondialdehyde (MDA) content determined by the TBA reaction, as described by Paradiso et al. (2008). The amount of MDA-TBA complex was calculated using an extinction coefficient of 155 mM^{-1} cm^{-1}.

Protein oxidation was spectrophotometrically determined by measuring the content of carbonyl-groups reacting with dinitrophenylhydrazine (DNPH), according to Romero-Puertas et al. (2002). Carbonyl content was calculated using an extinction coefficient of 22 mM^{-1} cm^{-1}.

Analysis of enzymatic and non-enzymatic antioxidants

For ascorbate (ASC) and glutathione (GSH) analysis, 0.3 g of samples were homogenized at 4°C with 1.8 mL 5% (v/v) trichloroacetic acid. After centrifugation at 18,000 x g for 20 minutes, the supernatants were collected and ASC and GSH levels were determined through the colorimetric assay described in de Pinto et al. (1999).

For quantifying the enzymatic antioxidant activities, 100 mg of samples were ground to fine powder in liquid nitrogen and mixed with 0.4 mL extraction buffer containing 50mM Tris-HCl pH 7.5, 0.05% (w/v) cysteine, 0.1% bovine serum albumin, 1 mM phenylmethanesulfonylfluoride. To determine the ascorbate peroxidase activity, 1 mM ASC was added to the buffer. After centrifugation at 20,000 x g for 20 minutes at 4°C, the supernatants were used for the spectrophotometric analysis.

Superoxide dismutase (SOD, EC 1.15.1.1) and catalase (CAT, EC 1.11.1.6) activities were spectrophotometrically determined following the methods described in Paradiso et al. (2020). Ascorbate peroxidase (APX, EC 1.11.1.11) was assayed according to de Pinto et al. (2000).

For Western Blot analyses of SOD, CAT and APX, total proteins were extracted from plantlets as described by Fortunato et al. (2022) and successively separated by SDS PAGE. Then, proteins were electrophoretically transferred to polyvinylidene fluoride membranes and incubated with the following specific antibodies: L-ascorbate peroxidase primary polyclonal antibody (n. AS08 368, Agrisera Vännäs, Sweden), which recognizes thylakoidal, stromal and cytosolic isoforms; Catalase (peroxisomal marker) primary polyclonal antibody (n. AS09 501, Agrisera Vännäs, Sweden); Fe-SOD primary polyclonal antibody (n. AS06 125, Agrisera Vännäs, Sweden), and the FTSH5 kindly donated by Wataru Sakamoto (Okayama University). As secondary antibody, the horseradish peroxidase (HRP)- conjugate Anti-Rabbit IgG (Promega, Madison, WI, USA) was used. Chemiluminescent signals were detected and quantified by ChemiDoc MP Imaging System and Quantity One® software (Bio-Rad Laboratories, Hercules, CA, USA), respectively.

Quantitative real-time PCR

Total RNA extraction was achieved using the Nippon Genetics Kit according to manufacturer protocol, using 50 mg (fresh weight) of leaf material. RNA concentration was determined by measuring the absorbance at 260 nm with NanoDrop2000 (Thermo Fisher Scientific, USA). cDNA was synthesized from 2µg of total RNA, using the iScript™ cDNA Synthesis Kit purchased by Bio-Rad according to the manufacturer's instructions. Gene expression analysis (qPCR) was performed using the BIO-RAD CFX Connect system (Bio-Rad, Hercules, CA, USA) employing 37.5 ng of cDNA for each reaction and SsoAdvanced Universal SYBR Green Supermix (Bio-Rad), according to the manufacturer's instruction for the detection system (Bio-Rad). *Ubiquitin10* (At4g05320) and *Actin8* (At1g49240) were used as housekeeping genes and three technical replicates were performed for each biological replicate (n=3). In all experiments, no template controls were also used. Housekeeping data were normalized according to Riedel et al. (2014).

Primers for quantitative real-time PCR (qRT-PCR) were designed by using Primer3 software (http://primer3.ut.ee/) and then double-checked using net primer software (http://www.premierbiosoft.com/netprimer/), except for the housekeeper primers (Giuntoli et al., 2017). Primer sequences used for quantitative PCR (qPCR) analyses are reported in Table S1.

Separation of real-time PCR products on 2% (w/v) agarose gels revealed single bands of the expected molecular weight. Relative quantification was performed according to the comparative Ct (threshold cycle) method ($2^{-\Delta\Delta Ct}$); (Livak and Schmittgen, 2001).

Statistical analysis

The data were expressed as the means ± standard error (SE). One-way analysis of variance (ANOVA) followed by a *post-hoc* Tukey's comparison test was used to calculate the difference between genotypes and treatments. Differences were considered statistically significant at a p-value< 0.05. All statistical analyses were performed by Minitab software (Minitab Inc., State College, PA, USA).

Results

Heat stress sensitivity of wild type and *gun1* plantlets

To analyze heat stress sensitivity, growth rate parameters were measured in 17-day-old wild type (wt) and *gun1* mutant plantlets. Plants were grown for 15 days at 22°C and exposed for 2 hours at 45°C (Heat Stress, HS). Plantlets were then incubated transferred in growth conditions to their optimal growth conditions (22°C; see *Materials and methods*) for 2 days to allow physiological recovery (2d-RHS), which was assessed by monitoring the photosynthetic parameter Fv/Fm. As a control (C), wt and *gun1* plants were grown at 22°C for 17 days. The phenotypical analysis showed that, after 2 days of recovery from HS (2d-RHS), *gun1* plantlets were significantly smaller than wt (Figure 1A). The visible phenotype was confirmed by measuring whole plant fresh weight, which resulted significantly decreased in *gun1* plantlets subjected to HS but did not show significant

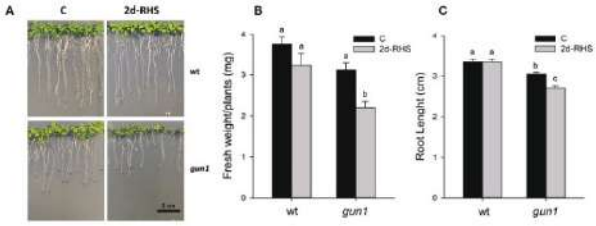

FIGURE 1
Growth parameters of 17-day-old wt and *gun1* plantlets, grown at control temperature (C) or subjected, after 15 days, to Heat Stress (HS; 2 hours at 45°C), followed by long-term recovery (2d-RHS; 2 days at 22°C). **(A)** Representative image of visible phenotypes. **(B)** Fresh Weight and **(C)** Root Length of plantlets measurements. The values are the means ± standard errors of five independent experiments. Different letters indicate significant differences obtained by one-way ANOVA test ($P < 0.05$).

differences in wt plantlets, when compared to the untreated controls (Figure 1B). Root length did not change in HS-treated wt while, on the contrary, *gun1* roots were shorter than wt, already under control conditions, and the exposure to HS further reduced root elongation (Figure 1C). The photosynthetic efficiency, measured as the maximum quantum yield of PSII (*Fv/Fm*), resulted decreased in a similar way in wt and *gun1* plantlets at 2d-RHS, when compared to control conditions (Figure 2A). Consistently, chlorophyll a and b content did not change significantly between wt and *gun1* (Figures 2B, C). On the other hand, a significant drop in carotenoid accumulation occurred in *gun1* mutant only (Figure 2D).

To dissect more in detail the molecular mechanisms underlying *gun1* sensitivity to heat, the transcript level of heat-dependent genes was assessed by quantitative Real-Time PCR (qRT-PCR) in 15 days-old plants before (C), right after the heat stress (HS, 2 hours at 45°C) and upon 3 hours of recovery at 22° C (R), when phenotypic differences were not detectable (Table S2). To this aim, the expression level of heat shock factor A2 (*HsfA2*), a key regulator of the heat stress response, and some heat shock proteins (*HSPs*), was studied. A significant and similar increase in the transcript levels of the nuclear *HsfA2*, the cytosolic *HSP101* and *HSP70* and the chloroplast *HSP26* occurred in response to HS in both wt and *gun1* genotypes. After 3h recovery (R), *HsfA2* and *HSP101* expression decreased in both genotypes, however, the reduction of both transcripts was more marked in *gun1* than in wt (Figures 3A, B). In addition, the expression of *HSP70* and *HSP26* did not change significantly after recovery (R) in wt, unlike in *gun1* (Figures 3C, D). To verify whether in *gun1* mutants heat stress could induce cytosolic folding stress, caused by the accumulation of plastid protein precursors and over-accumulation of cytosolic HSPs, as occurred when the mutants were grown in lincomycin conditions (Wu et al., 2019; Tadini et al., 2020), proteasomal activity and accumulation of FTSH5 plastid protease were analyzed. The proteasome activity in wt and *gun1* plantlets grown in control conditions, upon HS and after recovery did not display significant differences (Figure S1). Moreover, the accumulation of FTSH5 plastid protease pre-protein was not detectable upon HS treatment, while resulted to be accumulating in Lin-treated *gun1* seedlings, suggesting that Lin and HS trigger different non-overlapping signaling mechanisms (Figure S1).

ROS accumulation, oxidative markers, and hydrophilic antioxidants in wild type and *gun1* plantlets during HSR

ROS accumulation in response to HS was different between control and mutant genotypes (Figure 4). Under control conditions, the level of $O_2^{\cdot-}$, visualized by NBT-staining, was significantly higher in *gun1* leaf tissue than in wt (Figure 4A). Nevertheless, in the *gun1* genetic background, the accumulation of $O_2^{\cdot-}$ decreased after HS, reaching bottom values after recovery (R). On the other hand, in wt, HS caused a prompt accumulation of $O_2^{\cdot-}$, which successively decreased during the R phase (Figure 4A). Similarly, in wt, H_2O_2 levels, visualized by DAB-staining, increased after HS and returned to values comparable with control during the recovery (R) (Figure 4B). On the contrary, in *gun1*, H_2O_2 levels did not vary significantly after HS, but showed a high accumulation after recovery (Figure 4B). Furthermore, the level of lipid peroxidation was higher in *gun1* than in wt in control conditions (Figure 5A). This oxidative marker did not vary significantly in response to HS in wt plantlets, whereas it transiently increased in *gun1* mutants, to return to a baseline level after recovery. In wt, protein oxidation increased after HS and returned to values comparable with the control after recovery while, in *gun1* mutant background, the

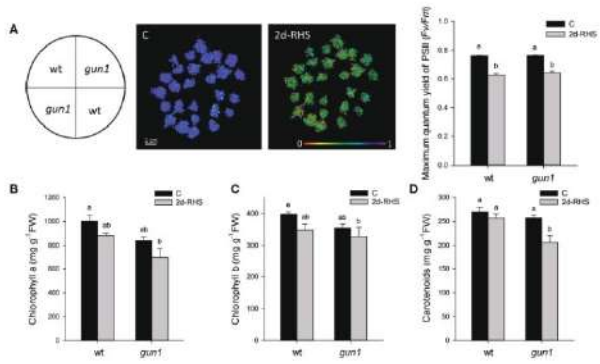

FIGURE 2
Photosynthetic parameters of 17 days-old wt and *gun1* plantlets, grown at control temperature (C) or subjected, after 15 days of growth, to Heat Stress (HS; 2 hours at 45°C), followed by long-term recovery (2d-RHS: 2 days at 22°C). **(A)** Photosynthetic performance of wt and *gun1*. The maximum quantum yield of PSII (*Fv/Fm*) was measured by using the IMAGING PAM (WALZ). **(B)** Chlorophyll a, **(C)** chlorophyll b and **(D)** carotenoids contents were as well determined. The values are the means ± standard errors of five independent experiments. Different letters indicate significant differences obtained by one-way ANOVA test ($P < 0.05$).

total level of protein carbonyl groups did not show significant changes after HS and R (Figure 5B). The total content of two major hydrophilic antioxidants, ascorbate (ASC) and glutathione (GSH), did not vary significantly between wt and *gun1*, under control conditions (Figures 5C, D). In *gun1*, the total content of the two antioxidants did not change either upon HS or after recovery (R). On the other hand, in wt total glutathione levels were lower after HS and both the antioxidants increased after recovery (Figures 5C, D). Moreover, only in wild type seedlings HS reduced the glutathione redox state, which returned to values comparable to control after recovery (Figure 5E).

Behaviour of ROS scavenging enzymes in wild type and *gun1* plantlets upon heat stress

To clarify the different accumulation of ROS in the two genotypes during the HSR, the behavior of the main ROS scavenging enzymes, namely superoxide dismutase (SOD), catalase (CAT) and ascorbate peroxidase (APX), was investigated.

Total SOD activity was similar in wt and *gun1* under control conditions and did not change significantly upon HS in both genotypes. After recovery (R), a rise in SOD activity occurred in wt control only (Figure 6A). The levels of FSD1 protein and transcript were analyzed by immunoblotting and qRT-PCR, respectively (Figures 6B, C). FSD1 protein accumulation was higher in wt than in *gun1* under control conditions. In both genotypes the protein level increased in response to HS, remaining at a higher level than control also after recovery (R) (Figure 6B). In wt plantlets, after HS a decrease in *FSD1* expression occurred, while during the recovery a clear and significant increase in the transcript level was observed (Figure 6C). The two thylakoidal Fe-SOD, *FSD2* and *FSD3* (Myouga et al., 2008), behaved differently when compared to *FSD1* (Figures 6D, E), which besides being present in the stroma of the chloroplast is also localized in the cytoplasm and nuclei (Dvořák et al., 2021). In both the genotypes, HS caused a strong decrease in *FSD2* expression, which remained low in *gun1* and increased in wt after recovery (Figure 6D). On the other hand, *FSD3* expression did not change in *gun1* in response to HS, while in wt decreased after HS and increased after recovery (Figure 6E). HS reduced the expression of cytosolic and chloroplastic copper/zinc superoxide dismutases (*CuZnSD1* and *CuZnSD2*, respectively) in both genotypes. However, after recovery (R), the transcript level of *CuZnSD1* and *CuZnSD2* was partially restored only in wt (Figures 6F, G).

In control conditions, total CAT activity, together with CAT2 protein and transcript levels were lower in *gun1* than in wt (Figure 7). HS caused, however, transient inhibition of CAT activity in wt only (Figure 7A). Despite the decrease in CAT activity observed in wt samples, CAT2 protein and transcript

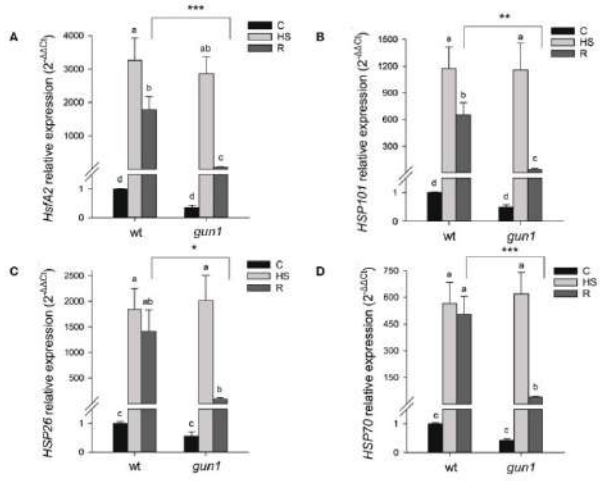

FIGURE 3
Relative expression of **(A)** *HsfA2*, **(B)** *HSP101*, **(C)** *HSP26* and **(D)** *HSP70* in 15 days-old wt and *gun1* plantlets, grown at control temperature (C) or subjected to Heat Stress (HS; 2 hours at 45°C), followed by short recovery (R; 3 hours at 22°C). The expression level of *HsfA2* and *HSPs* was normalized to that of *Ubiquitin10* (At4g05320) and *Actin8* (At1g49240) as internal references. For each sample, gene expression was related to the wt in control conditions **(C)**, set as 1. The values are the means ± SEs from three independent experiments, with three technical replicates for each experiment. Different letters indicate significant differences obtained by one-way ANOVA test ($p < 0.05$). T-test was applied to compare R samples among the genotypes. * $p \leq 0.05$; ** $p \leq 0.01$; *** $p \leq 0.001$.

increased after HS, while did not significantly change in *gun1* (Figures 7B, C).

Moreover, after HS, total APX activity decreased in both genotypes, with a greater intensity in wt than in *gun1*. However, after recovery, APX activity was restored to control (C) level in wt while further decreased in *gun1* (Figure 8A). Western blotting analysis showed that in wt, the accumulation of cytosolic and stromal APX was slightly increased upon HS, while the decrease of thylakoidal isoform was observed. On the other hand, in *gun1* samples, cytosolic and stromal APX isoenzymes showed a progressive decrease while tAPX accumulated in response to HS and decreased in R (Figure 8B).

In wt, the expression of cytosolic *APX1* was strongly reduced after HS and significantly increased after recovery, while in *gun1* not significant changes occurred (Figure 8C). The HS-inducible APX2 showed, however, highly increased expression after HS in both the genotypes. After recovery (R), *APX2* transcript remained high in wt and partially decreased in *gun1* (Figure 8C). At last, the expression of *tAPX* under control conditions was significantly lower in *gun1* than in wt. However, after HS a drop in *tAPX* transcript occurred in wt, while a progressive increase after HS and in R was observed in *gun1* mutants (Figure 8D).

Discussion

Retrograde signaling pathways allow the information flux from plastids to the nucleus. This intra-cellular communication becomes critical during chloroplast biogenesis (biogenic control) and upon alteration of plastid homeostasis in response to environmental stimuli (operational signaling) (Chan et al., 2016). GUN1-dependent signaling has been proposed as one of the main retrograde signaling pathways active during chloroplast biogenesis (Tadini et al., 2020; Shimizu and Masuda, 2021; Wu and Bock, 2021). Nevertheless, multiple evidence suggests that GUN1 also operates in adult plants, contributing to the operational control of chloroplasts (Cheng et al., 2011; Tadini et al., 2016; Guo et al., 2020). Indeed, GUN1 undergoes ta rapid turnover by the Clp protease, unless it becomes stable during the early stages of chloroplast

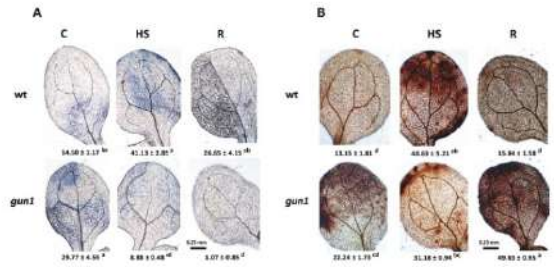

FIGURE 4
Accumulation of superoxide anion ($O_2^{\cdot-}$) and hydrogen peroxide (H_2O_2) in 15 days-old wt and *gun1* plantlets, grown at control temperature (C) or subjected to Heat Stress (HS, 2 hours at 45°C), followed by short recovery (R, 3 hours at 22°C). Representative images of **(A)** $O_2^{\cdot-}$ accumulation, visualized by nitroblue tetrazolium (NBT)-staining and **(B)** H_2O_2 accumulation, visualized by diaminobenzidine (DAB)-staining. $O_2^{\cdot-}$ and H_2O_2 analyses were repeated three times showing reproducible results. The percentage area (± SE) of 60 leaves (20 for each experiment) stained with NBT and DAB, respectively, are indicated. Letters indicate significant differences obtained by one-way ANOVA test ($P < 0.05$).

biogenesis, and under stress conditions that trigger retrograde signaling pathways (Wu et al., 2018; Pesaresi and Kim, 2019).

GUN1 has been reported to be required for cold acclimation, as *gun1* seedlings fail to develop green functional chloroplasts when grown at 4°C (Marino et al., 2019). Moreover, the involvement of GUN1 in response to HS has been previously indicated by showing that *gun1* mutants have reduced basal thermotolerance but do not appear to be impaired in acquired thermotolerance (Miller et al., 2007). In accordance, our data indicate the *gun1* mutants are more sensitive to HS than wt, as demonstrated by the reduced fresh weight and the inhibition of root elongation at 2 days of physiological recovery from HS (Figure 1). Furthermore, at 2d-RHS, despite *gun1* mutants show similar reduction in photosynthetic efficiency than wild type plants, have a reduced content of carotenoids (Figure 2). The decrease in carotenoids content may contribute to higher sensitivity to HS, since these molecules act not only as quenchers of triplet chlorophyll and singlet oxygen but might also stabilize and photo-protect the lipid phase of the thylakoid membranes (Havaux, 1998).

The lowered heat tolerance of *gun1* mutants is not due to cytosolic folding stress, which instead occurs in response lincomycin treatment (Figure S1; Wu et al., 2019; Tadini et al., 2020), suggesting the involvement of a different signaling mechanism. Moreover, the reduced basal thermotolerance of *gun1* mutants cannot be explained by the failure in the induction of *HSPs*, since in *gun1*, *HsfA2* and the cytosolic and chloroplastic *HSPs* analyzed were highly expressed after HS as in wild type plants. However, the higher decrease of *HSPs* after 3 hours of recovery from HS corroborates the idea of a lower thermotolerance of *gun1* mutants compared to wild type plants (Figure 3; Ahn et al., 2004; Charng et al., 2007).

It has been recently reported that during biogenic retrograde signaling, GUN1 mediates the formation of an H_2O_2- dependent oxidized environment, which might represent a redox-mediated communication pathway, aimed to signal the perturbation of chloroplast development (Fortunato et al., 2022).

A plethora of literature data indicate that environmental stresses, including high temperatures, lead to oxidative bursts of $O_2^{\cdot-}$ and/or H_2O_2 in plants (Foyer et al., 1997; Dat et al., 1998; Vallelian-Bindschedler et al., 1998). Accordingly, ROS produced in chloroplasts can work as plastid signals to activate the expression of genes coding for antioxidant enzymes and to fine-tune the stress-responsive apparatus for more effective adaptation to stresses (Sun and Guo, 2016). Chloroplasts have been shown to play an important role in heat-induced ROS accumulation and the subsequent expression of nuclear heat-responsive genes (Hu et al., 2020). The chloroplast-produced H_2O_2 working as signaling molecule for the heat-associated gene expression has been proposed as an interesting model for the generation of diurnal patterns of thermotolerance (Dickinson et al., 2018).

Our results show that in wt, immediately after HS, $O_2^{\cdot-}$ and H_2O_2 values increase, returning to values comparable to control conditions after 3 hours of physiological recovery, while a transient increase in protein oxidation was observed (Figures 4, 5B). This suggests that in this context ROS may contribute to oxidizing the cellular environment temporarily, triggering a signaling cascade. The transient oxidation of cellular environment has been confirmed by the changes in the glutathione redox state, which decreases after HS and returns to values comparable to control during the physiological recovery (Figure 5D). These results are in accordance with recent studies in which the redox-sensitive green fluorescent

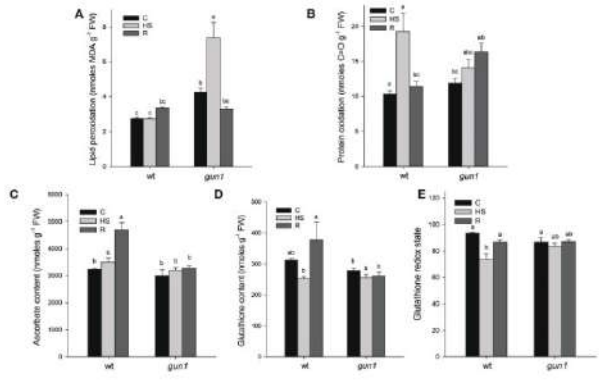

FIGURE 5
Oxidative markers and non-enzymatic antioxidants of Arabidopsis wild type (wt) and *gun1* plantlets, grown at control temperature (C) or subjected to Heat Stress (HS, 2 hours at 45°C), followed by short recovery (R; 3 hours at 22°C). **(A)** Lipid peroxidation, measured as malondialdehyde content and **(B)** protein oxidation measured as total protein carbonyl groups. **(C)** Total ascorbate and **(D)** glutathione contents. **(E)** Glutathione redox state calculated as percentage of the ratio between reduced and total glutathione. The values are the means ± standard errors of five independent experiments. Different letters indicate significant differences obtained by one-way ANOVA test ($P < 0.05$).

protein (roGFP2) was used to show that HS leads to increased oxidation in both cytosol and nucleus compartments. By analyzing transcript profiles of control and heat-stressed plantlets, the authors suggest that heat-induced changes in the nuclear redox state are essential for genetic and epigenetic regulation of HSR (Babbar et al., 2021).

In wt, the transient oxidative burst is also due to the lowered total activity of APX and CAT occurring immediately after HS (Figures 7A, B). Analyzing the protein levels of different APX isoenzymes, it should be noted that, despite the significant decrease of the total activity, the levels of cytosolic and stromal APX proteins increased. At least for the cytosolic APX, two observations could explain this apparent inconsistency: 1) Immediately after HS, the expression level of *APX2* transcript significantly increased, as expected (Figure 8B; Panchuk et al., 2002; Suzuki et al., 2013; Balfagón et al., 2018); 2) It has been reported that after HS, APX1 protein forms high molecular weight complexes, loses the H_2O_2 removal activity, and behaves as chaperone protein. Interestingly, when plants are recovered under physiological conditions, the APX protein returns to dimeric or oligomeric form, recovering its H_2O_2- removal activity required to prevent oxidative damage (Kaur et al., 2021). On the other hand, protein and transcript levels of thylakoidal APX decreased immediately after HS. In this case, the loss or inactivation of tAPX may function as a part of plastid to nucleus retrograde signaling as occurs in light-induced photooxidative stress (Maruta et al., 2012).

Interestingly, also the decrease in CAT activity did not overlap with protein and transcript levels of CAT2, which accumulate immediately after HS. CAT is a peroxisomal enzyme with a pivotal role in redox regulation (Mhamdi et al., 2012). It has been shown that CAT can physically interact with cytosolic stress signaling proteins in plants (Foyer et al., 2020). Thus, it is likely that, upon HS, CAT becomes restrained to the cytosol and mediates redox signaling, as it occurs in mammalians (Walton et al., 2017).

In wt, 3 hours after physiological recovery from HS, both non-enzymatic and enzymatic antioxidants significantly increased, lowering ROS accumulation and preventing oxidative damage (Figures 4–8). In particular, the increase in SOD activity is due to an increase in the expression level of almost all the isoenzymes analyzed and the recovery in APX activity is due to the increased protein and expression level of all APX isoforms (Figure 8).

It is interesting to note that *gun1* mutants grown under physiological conditions show a higher O_2. accumulation and a greater level of lipid peroxidation than wt (Figure 4A), which suggests that *gun1* plastids are more inclined to suffer ROS-mediated damage (Ruckle et al., 2007; Fortunato et al., 2022). After HS, the decrease in O_2. implies the formation of more reactive hydroxyl radicals, which promptly react with lipids,

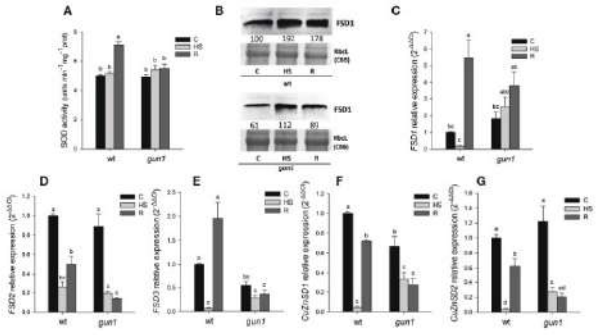

FIGURE 6
Superoxide dismutase (SOD) behavior in 15 days-old wt and *gun1* plantlets, grown at control temperature (C) or subjected to Heat Stress (HS; 2 hours at 45°C), followed by short recovery (R; 3 hours at 22°C). **(A)** Total SOD activity; values are the means ± standard errors (SE) of five independent experiments. Letters indicate significant differences obtained by one-way ANOVA test ($P < 0.05$). **(B)** Representative images from three independent experiments of FSD1 immuno-blotting; each well was loaded with 30 µg of proteins. Coomassie Brilliant Blue (CBB) staining of the gel served as a loading control. Quantification of signals (by Quantity One®) relative to the wt in control conditions (100%) is provided below the panel. Relative expression of **(C)** *FSD1*, **(D)** *FSD2*, **(E)** *FSD3*, **(F)** *CuZnSD1* **(G)** and *CuZnSD2*. The expression level of *SOD* genes was normalized to that of *Ubiquitin10* (At4g05320) and *Actin8* (At1g49240) as internal references. For each sample, gene expression was related to the wt in control conditions (C). Values are expressed as means ± SE from three independent experiments, with three technical replicates for each experiment. Different letters indicate significant differences obtained by one-way ANOVA test ($p < 0.05$).

causing a further increase in lipid peroxidation (Figure 5A; Farmer and Mueller, 2013). However, unlike wt, *gun1* mutants fail to induce an oxidative burst immediately after HS, since no $O_2^{\cdot-}$ neither H_2O_2 accumulate (Figure 4). Consistently, the content of antioxidants and the total activities of SOD and CAT did not show significant differences (Figures 5–7). The absence of a rise in H_2O_2 under HS may contribute to increased

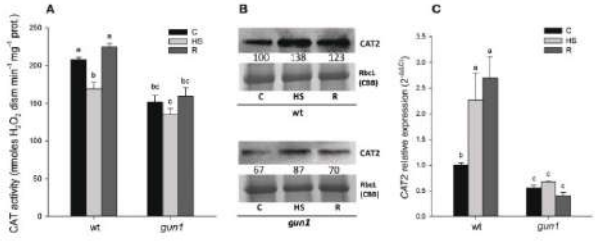

FIGURE 7
Catalase (CAT) behavior in 15 days-old wt and *gun1* plantlets, grown at control temperature (C) or subjected to Heat Stress (HS; 2 hours at 45°C), followed by short recovery (R; 3 hours at 22°C). **(A)** Total CAT activity. Values are the means ± standard errors (SE) of five independent experiments. Letters indicate significant differences obtained by one-way ANOVA test ($P < 0.05$). **(B)** Representative image from three independent experiments of CAT2 immunoblotting, each well was loaded with 30 µg of proteins. CBB staining of the gel is shown as equal loading control. Quantification of signals (by Quantity One®) relative to the wt in control conditions (100%) is provided below the panel. **(C)** Relative expression of *CAT2*. The expression level of *CAT2* was normalized to that of *Ubiquitin 10* (At4g05320) and *Actin8* (At1g49240) as internal references. For each sample, gene expression was related to the wt in control conditions (C). Values are the means ± SE from three independent experiments, with three technical replicates for each experiment. Letters indicate significant differences obtained by one-way ANOVA test ($p < 0.05$).

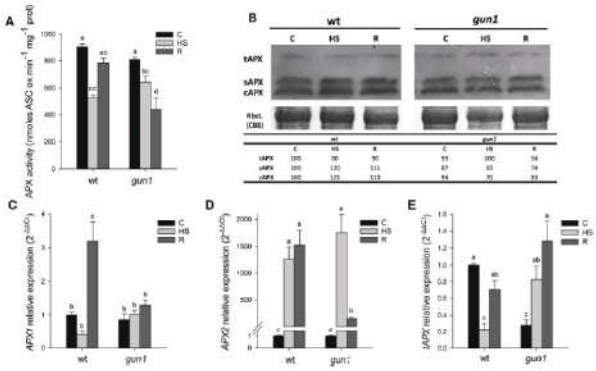

FIGURE 8
Ascorbate peroxidase (APX) behavior in 15 days-old wt and *gun1* plantlets, grown at control temperature (C) or subjected to Heat Stress (HS; 2 hours at 45°C), followed by short recovery (R; 3 hours at 22°C). **(A)** Total APX activity; values indicate means ± standard errors (SE) of five independent experiments. Letters indicate significant differences obtained by one-way ANOVA test ($P < 0.05$). **(B)** Representative image from three independent experiments of APX immuno-blotting; each well was loaded with 30 µg of proteins. CBB staining of the gel served as a loading control. Quantification of signals (by Quantity One®) relative to the wt in control conditions (100%) is provided below the panel. tAPX, sAPX and cAPX are thylakoidal, stromal and cytosolic APX, respectively. Relative expression of **(C)** *APX1*, **(D)** *APX2* and **(E)** *tAPX*. The expression level of APX genes was normalized to that of *Ubiquitin10* (At4g05320) and *Actin8* (At1g49240) as internal references. For each sample, gene expression was related to wt in control conditions (C). Values indicate means ± SE from three independent experiments, with three technical replicates for each experiment. Different letters indicate significant differences obtained by one-way ANOVA test ($p < 0.05$).

heat oxidative damage, as already suggested for *fsd2* and *fsd3* mutants (Bychkov et al., 2022).

In *gun1* mutants, after 3 hours of physiological recovery from HS non-enzymatic antioxidants, as well SOD and CAT activity do not significantly change, whereas a decline in total APX activity occurs, due to the failure in the rescue of the protein levels of chloroplastic and cytosolic APX. As a consequence, H_2O_2 accumulates, becoming responsible for oxidative damage. It has been reported that under photooxidative stress the absence of tAPX more than sAPX causes the accumulation of H_2O_2 and oxidized proteins (Maruta et al., 2010). Moreover, in the absence of the cytosolic APX1, the entire chloroplastic H_2O_2- scavenging system of Arabidopsis is impaired (Davletova et al., 2005), Thus, in *gun1* mutants the absence of the induction of APX1 expression (Figure 8C), could be in part responsible for the failure in thermotolerance acquisition.

However, in *gun1* mutants, the behavior of tAPX deserves more attention; indeed, it should be noted that the expression level of tAPX, which is lower than wt under physiological growth conditions, increased after HS and during the physiological recovery, despite the failure in the accumulation of the protein (Figures 8B, E). These results indicate that the expression of tAPX gene is under the control of the GUN1-mediated signaling pathway, albeit protein amount also appears to be subjected to post-transcriptional regulatory mechanisms that include cytosolic inhibition of protein translation and ubiquitin-mediated protein degradation (Wu et al., 2019; Tadini et al., 2020). This regulation has been described for several *PhANGs*-encoded proteins and, among those, tAPX itself (Wu et al., 2019).

Conclusions

Our data suggest that the transient oxidative burst occurring after HS is mandatory in basal thermotolerance acquisition. Indeed, in wt plants, ROS and oxidation of the cellular environment function as signals to activate the expression of genes adjusting stress-responsive systems for more successful adaptation to HS.

After HS, *gun1* mutants fail to induce ROS accumulation promptly, impairing the proper HSR. This leads to accumulating ROS and oxidative damage during physiological recovery at growth temperature, resulting in enhanced sensitivity to HS.

The results support the idea that GUN1 is required to oxidize the cellular environment, participating in the

acquisition of basal thermotolerance through the redox-dependent plastid-to-nucleus communication.

Our results also indicate a pivotal role of tAPX in GUN1-dependent HSR; further investigation will be aimed at clarifying the mechanisms involved in this signaling pathway.

Data availability statement

The original contributions presented in the study are included in the article/Supplementary Material. Further inquiries can be directed to the corresponding author.

Author contributions

CL, SF, FV, and MP conceived and designed research. CL, SF, ND, NJ, LT, and FV performed the experiments. MP advised on the experiments. CL, SF, LT, FV, and MP drafted the paper. MP and PP funded the project. All authors contributed to the discussion of the data and to the writing and agreed to the published version of the manuscript.

Funding

This project was supported by MUR—Ministero dell'Università e della Ricerca, grant number PRIN-2017, 2017FBS8YN.

Conflict of interest

The authors declare that the research was conducted in the absence of any commercial or financial relationships that could be construed as a potential conflict of interest.

Publisher's note

All claims expressed in this article are solely those of the authors and do not necessarily represent those of their affiliated organizations, or those of the publisher, the editors and the reviewers. Any product that may be evaluated in this article, or claim that may be made by its manufacturer, is not guaranteed or endorsed by the publisher.

Supplementary material

The Supplementary Material for this article can be found online at: https://www.frontiersin.org/articles/10.3389/fpls.2022.1058831/full#supplementary-material

References

Ahn, Y. J., Claussen, K., and Zimmerman, J. L. (2004). Genotypic differences in the heat-shock response and thermotolerance in four potato cultivars. *Plant Sci.* 166, 901–911. doi: 10.1016/j.plantsci.2003.11.027

Allakhverdiev, S. I., Kreslavski, V. D., Klimov, V. V., Los, D. A., Carpentier, R., and Mohanty, P. (2008). Heat stress: An overview of molecular responses in photosynthesis. *Photosynth. Res.* 98, 541–550. doi: 10.1007/s11120-008-9331-0

Babbar, R., Karpinska, B., Grover, A., and Foyer, C. H. (2021). Heat-induced oxidation of the nuclei and cytosol. *Front. Plant Sci.* 11, 617779.

Balfagón, D., Zandalinas, S. I., Baliño, P., Muriach, M., and Gómez-Cadenas, A. (2018). Involvement of ascorbate peroxidase and heat shock proteins on citrus tolerance to combined conditions of drought and high temperatures. *Plant Physiol. Biochem.* 127, 194–199. doi: 10.1016/j.plaphy.2018.03.029

Bita, C. E., and Gerats, T. (2013). Plant tolerance to high temperature in a changing environment: Scientific fundamentals and production of heat stress-tolerant crops. *Front. Plant Sci.* 4. doi: 10.3389/fpls.2013.00273

Bradford, M. (1976). A rapid and sensitive method for the quantitation of microgram quantities of protein utilizing the principle of protein-dye binding. *Anal. Biochem.* 72, 248–254. doi: 10.1006/abio.1976.9999

Bychkov, I. A., Andreeva, A. A., Kudryakova, N. V., Pojidaeva, E. S., and Kusnetsov, V. V. (2022). The role of PAP4/FSD3 and PAP9/FSD2 in heat stress responses of chloroplast genes. *Plant Sci.* 322, 111359. doi: 10.1016/J.PLANTSCI.2022.111359

Chan, K. X., Phua, S. Y., Crisp, P., McQuinn, R., and Pogson, B. J. (2016). Learning the languages of the chloroplast: Retrograde signaling and beyond. *Ann. Rev. Plant Biol.* 67, 25–53. doi: 10.1146/annurev-arplant-043015-111854

Charng, Y.-Y., Liu, H.-C., Liu, N.-Y., Chi, W.-T., Wang, C.-N., Chang, S.-H., et al. (2020). A heat-inducible transcription factor HsfA2 is required for extension of acquired thermotolerance in arabidopsis. *Plant Physiol.* 143, 251–262. doi: 10.1104/pp.106.091322

Cheng, J. A., He, C. X., Zhang, Z. W., Xu, F., Zhang, D. W., Wang, X., et al. (2011). Plastid signals confer arabidopsis tolerance to water stress. *Z. Naturforsch. C.* 66, 47–54. doi: 10.1016/j.jphs.2015.04.006

Colombo, M., Tadini, L., Peracchio, C., Ferrari, R., and Pesaresi, P. (2016). GUN1 a jack-of-all-trades in chloroplast protein homeostasis and signalling. *Front. Plant Sci.* 7, 1427.

Das, P., Nutan, K. K., Singla-Pareek, S. L., and Pareek, A. (2015). Oxidative environment and redox homeostasis in plants: Dissecting out significant contribution of major cellular organelles. *Front. Environ. Sci.* 2. doi: 10.3389/fenvs.2014.00070

Dat, J. F., Foyer, C. H., and Scott, I. M. (1998). Changes in salicylic acid and antioxidants during induced thermotolerance in mustard seedlings. *Plant Physiol.* 118, 1455–1461. doi: 10.1104/pp.118.4.1455

Davletova, S., Rizhsky, L., Liang, H. J., Zhong, S. Q., Oliver, D. J., Coutu, J., et al. (2005). Cytosolic ascorbate peroxidase 1 is a central component of the reactive oxygen gene network of arabidopsis. *Plant Cell* 17, 268–281. doi: 10.1105/tpc.104.026971

de Pinto, M. C., Francis, D., and De Gara, L. (1999). The redox state of the ascorbate-dehydroascorbate pair as a specific sensor of cell division in tobacco BY-2 cells. *Protoplasma* 209, 90–97. doi: 10.1007/BF01415704

de Pinto, M. C., Tommasi, F., and De Gara, L. (2000). Enzymes of the ascorbate biosynthesis and ascorbate-glutathione cycle in cultured cells of tobacco bright

yellow 2. *Plant Physiol. Biochem.* 38, 541–550. doi: 10.1016/S0981-9428(00)00773-7

Dickinson, P. J., Kumar, M., Martinho, C., Yoo, S. J., Lan, H., Artavanis, G., et al. (2018). Chloroplast signaling gates thermotolerance in arabidopsis. *Cell Rep.* 22, 1657–1665. doi: 10.1016/j.celrep.2018.01.054

Dvořák, P., Krasylenko, Y., Ovecka, M., Basheer, J., Zapletalova, V., Samaj, J., et al. (2021). *In vivo* light-sheet microscopy resolves localisation patterns of FSD1 a superoxide dismutase with function in root development and osmoprotection. *Plant Cell Environ.* 44, 68–87. doi: 10.1111/pce.13894

Farmer, E. E., and Mueller, M. J. (2013). ROS-mediated lipid peroxidation and RES-activated signaling. *Annu. Rev. Plant Biol.* 64, 429–450. doi: 10.1146/annurev-arplant-050312-120132

Farnese, F. S., Menezes-Silva, P. E., Gusman, G. S., and Oliveira, J. A. (2016). When bad guys become good ones: The key role of reactive oxygen species and nitric oxide in the plant responses to abiotic stress. *Front. Plant Sci.* 7. doi: 10.3389/fpls.2016.00471

Fortunato, S., Lasorella, C., Tadini, L., Jeran, N., Vita, F., Pesaresi, P., et al. (2022). GUN1 involvement in the redox changes occurring during biogenic retrograde signaling. *Plant Sci.* 320, 111265. doi: 10.1016/j.plantsci.2022.111265

Foyer, C. H., Baker, A., Wright, M., Sparkes, I. A., Mhamdi, A., Schippers, J. H. M., et al. (2020). On the move: Redox-dependent protein relocation in plants. *J. Exp. Bot.* 71, 620–631. doi: 10.1093/jxb/erz330

Foyer, C. H., Lopez-Delgado, H., Dat, J. F., and Scott, I. M. (1997). Hydrogen peroxide-and glutathione-associated mechanisms of acclimatory stress tolerance and signalling. *Physiol. Plant* 100, 241–254.

Foyer, C. H., and Noctor, G. (2013). Redox signaling in plants. *Antioxidants. Redox Signal.* 18, 2087–2090. doi: 10.1089/ars.2013.5278

Giuntoli, B., Shukla, V., Maggiorelli, F., Giorgi, F. M., Lombardi, L., Perata, P., et al. (2017). Age-dependent regulation of ERF-VII transcription factor activity in arabidopsis thaliana. *Plant Cell Environ.* 40, 2333–2346. doi: 10.1111/pce.13037

Guo, J., Zhou, Y., Li, J., Sun, Y., Shangguan, Y., Zhu, Z., et al. (2020). COE 1 and GUN1 regulate the adaptation of plants to high light stress. *Biochem. Biophys. Res. Commun.* 521, 184–189. doi: 10.1016/J.BBRC.2019.10.101

Hasanuzzaman, M., Nahar, K., Alam, M. M., Roychowdhury, R., and Fujita, M. (2013). Physiological biochemical and molecular mechanisms of heat stress tolerance in plants. *Int. J. Mol. Sci.* 14, 9643–9684. doi: 10.3390/ijms14059643

Havaux, M. (1998). Carotenoids as membrane stabilizers in chloroplasts. *Trends Plant Sci.* 3, 147–151. doi: 10.1016/S1360-1385(98)01200-X

Hu, S., Ding, Y., and Zhu, C. (2020). Sensitivity and responses of chloroplasts to heat stress in plants. *Front. Plant Sci.* 11. doi: 10.3389/fpls.2020.00375

Kaur, S., Prakash, P., Bak, D.-H., Hong, S. H., Cho, C., Chung, M.-S., et al. (2021). Regulation of dual activity of ascorbate peroxidase 1 from arabidopsis thaliana by conformational changes and posttranslational modifications. *Front. Plant Sci.* 12. doi: 10.3389/fpls.2021.678111

Q18 Koussevitzky, S., Nott, A., Mockler, T. C., Hong, F., Sachetto-Martins, G., Surpin, M., et al. (2007). Signals from chloroplasts converge to regulate nuclear gene expression. *Science.* doi: 10.1126/science.1140516

Larkin, R. M., Alonso, J. M., Ecker, J. R., and Chory, J. (2003). GUN4 a regulator of chlorophyll synthesis and intracellular signaling. *Science* 299, 902–906. doi: 10.1126/science.1079978

Larkindale, J., Hall, J. D., Knight, M. R., and Vierling, E. (2005). Heat stress phenotypes of arabidopsis mutants implicate multiple signaling pathways in the acquisition of thermotolerance. *Plant Physiol.* 138, 882–897. doi: 10.1104/pp.105.062257

Lichtenthaler, H. K. (1987). Chlorophylls and carotenoids: Pigments of photosynthetic biomembranes. *Methods Enzymol.* 148, 350–382. doi: 10.1016/0076-6879(87)48036-1

Ling, Y., Serrano, N., Gao, G., Atia, M., Mokhtar, M., Woo, Y. H., et al. (2018). Thermopriming triggers splicing memory in arabidopsis. *J. Exp. Bot.* 69, 2659–2675. doi: 10.1093/jxb/ery062

Livak, K. J., and Schmittgen, T. D. (2001). Analysis of relative gene expression data using real-time quantitative PCR and the 2-ΔΔCT method. *Methods* 25, 402–408. doi: 10.1006/meth.2001.1262

Marino, G., Naranjo, B., Wang, J., Penzler, J. F., Kleine, T., and Leister, D. (2019). Relationship of GUN1 to FUG1 in chloroplast protein homeostasis. *Plant J.* 99, 521–535. doi: 10.1111/tpj.14342

Maruta, T., Noshi, M., Tanouchi, A., Tamoi, M., Yabuta, Y., Yoshimura, K., et al. (2012). H2O2-triggered retrograde signaling from chloroplasts to nucleus plays specific role in response to stress. *J. Biol. Chem.* 287, 11717–11729. doi: 10.1074/jbc.M111.292847

Maruta, T., Tanouchi, A., Tamoi, M., Yabuta, Y., Yoshimura, K., Ishikawa, T., et al. (2010). Arabidopsis chloroplastic ascorbate peroxidase isoenzymes play a dual role in photoprotection and gene regulation under photooxidative stress. *Plant Cell Physiol.* 51, 190–200. doi: 10.1093/pcp/pcp177

Mhamdi, A., Noctor, G., and Baker, A. (2012). Plant catalases: Peroxisomal redox guardians. *Arch. Biochem. Biophys.* 525, 181–194. doi: 10.1016/J.ABB.2012.04.015

Miller, G., Suzuki, N., Rizhsky, L., Hegie, A., Koussevitzky, S., and Mittler, R. (2007). Double mutants deficient in cytosolic and thylakoid ascorbate peroxidase reveal a complex mode of interaction between reactive oxygen species plant development and response to abiotic stresses. *Plant Physiol.* 144, 1777–1785. doi: 10.1104/pp.107.101436

Mittler, R. (2017). ROS are good. *Trends Plant Sci.* 22, 11–19. doi: 10.1016/j.tplants.2016.08.002

Mochizuki, N., Brusslan, J. A., Larkin, R., Nagatani, A., and Chory, J. (2001). Arabidopsis genomes uncoupled 5 (GUN5) mutant reveals the involvement of mg-chelatase h subunit in plastid-to-nucleus signal transduction. *PNAS* 98, 2053–2058. doi: 10.1073/pnas.98.4.2053

Myouga, F., Hosoda, C., Umezawa, T., Iizumi, H., Kuromori, T., Motohashi, R., et al. (2008). A heterocomplex of iron superoxide dismutases defends chloroplast nucleoids against oxidative stress and is essential for chloroplast development in arabidopsis. *Plant Cell* 20, 3148–3162. doi: 10.1105/tpc.108.061341

Nishizawa, A., Yabuta, Y., Yoshida, E., Maruta, T., Yoshimura, K., and Shigeoka, S. (2006). Arabidopsis heat shock transcription factor A2 as a key regulator in response to several types of environmental stress. *Plant J.* 48, 535–547. doi: 10.1111/j.1365-313X.2006.02889.x

Noctor, G., Veljovic-Jovanovic, S., Driscoll, S., Novitskaya, L., and Foyer, C. H. (2002). Drought and oxidative load in the leaves of C3 plants: A predominant role for photorespiration? *Ann. Bot.* 89, 841–850. doi: 10.1093/aob/mcf096

Nott, A., Jung, H. S., Koussevitzky, S., and Chory, J. (2006). Plastid-to-nucleus retrograde signaling. *Annu. Rev. Plant Biol.* 57, 739–759. doi: 10.1146/annurev.arplant.57.032905.105310

Panchuk, I. I., Volkov, R. A., and Schöffl, F. (2002). Heat stress- and heat shock transcription factor-dependent expression and activity of ascorbate peroxidase in arabidopsis. *Plant Physiol.* 129, 838–853. doi: 10.1104/pp.001362

Paradiso, A., Berardino, R., De Pinto, M. C., Sanità Di Toppi, L., Storelli, M. M., Tommasi, F., et al. (2008). Increase in ascorbate-glutathione metabolism as local and precocious systemic responses induced by cadmium in durum wheat plants. *Plant Cell Physiol.* 49, 362–374. doi: 10.1093/pcp/pcn013

Paradiso, A., Domingo, G., Blanco, E., Buscaglia, A., Fortunato, S., Marsoni, M., et al. (2020). Cyclic AMP mediates heat stress response by the control of redox homeostasis and ubiquitin-proteasome system. *Plant Cell Environ.* 43, 2727–2742. doi: 10.1111/pce.13878

Pesaresi, P., and Kim, C. (2019). Current understanding of GUN1: a key mediator involved in biogenic retrograde signaling. *Plant Cell Rep.* 38, 819–823. doi: 10.1007/s00299-019-02383-4

Pnueli, L., Liang, H., Rozenberg, M., and Mittler, R. (2003). Growth suppression altered stomatal responses and augmented induction of heat shock proteins in cytosolic ascorbate peroxidase (Apx1)-deficient arabidopsis plants. *Plant J.* 34, 187–203. doi: 10.1046/j.1365-313X.2003.01715.x

Pogson, B. J., Woo, N. S., Förster, B., and Small, I. D. (2008). Plastid signalling to the nucleus and beyond. *Trends Plant Sci.* 13, 602–609. doi: 10.1016/j.tplants.2008.08.008

Riedel, G., Rüdrich, U., Fekete-Drimusz, N., Manns, M. P., Vondran, F. W. R., and Bock, M. (2014). An extended ΔCT-method facilitating normalisation with multiple reference genes suited for quantitative RT-PCR analyses of human hepatocyte-like cells. *PloS One* 9, 2–6. doi: 10.1371/journal.pone.0093031

Romero-Puertas, M. C., Palma, J. M., Gómez, M., Del Río, L. A., and Sandalio, L. M. (2002). Cadmium causes the oxidative modification of proteins in pea plants. *Plant Cell Environ.* 25, 677–686. doi: 10.1046/j.1365-3040.2002.00850.x

Ruckle, M. E., DeMarco, S. M., and Larkin, R. M. (2007). Plastid signals remodel light signaling networks and are essential for efficient chloroplast biogenesis in arabidopsis. *Plant Cell* 19, 3944–3960. doi: 10.1105/tpc.107.054312

Sgobba, A., Paradiso, A., Dipierro, S., de Gara, L., and de Pinto, M. C. (2015). Changes in antioxidants are critical in determining cell responses to short- and long-term heat stress. *Physiol. Plant* 153, 68–78. doi: 10.1111/ppl.12220

Shimizu, T., and Masuda, T. (2021). The role of tetrapyrrole-and GUN1-dependent signaling on chloroplast biogenesis. *Plants* 10, 196. doi: 10.3390/plants10020196

Singh, R., Singh, S., Parihar, P., Singh, V. P., and Prasad, S. M. (2015). Retrograde signaling between plastid and nucleus: A review. *J. Plant Physiol.* 181, 55–66. doi: 10.1016/j.jplph.2015.04.001

Strand, A., Asami, T., Alonso, J., Ecker, J. R., and Chory, J. (2003). Chloroplast to nucleus communication triggered by accumulation of mg-protoporphyrinIX. *Nature* 421, 79–83. doi: 10.1038/nature01204

Sun, A. Z., and Guo, F. Q. (2016). Chloroplast retrograde regulation of heat stress responses in plants. *Front. Plant Sci.* 7. doi: 10.3389/fpls.2016.00398

Susek, R. E., Ausubel, F. M., and Chory, J. (1993). Signal transduction mutants of arabidopsis uncouple nuclear CAB and RBCS gene expression from chloroplast development. *Cell* 74, 787–799.

Suzuki, N., Koussevitzky, S., Mittler, R., and Miller, G. (2012). ROS and redox signalling in the response of plants to abiotic stress. *Plant Cell Environ.* 35, 259–270. doi: 10.1111/j.1365-3040.2011.02336.x

Suzuki, N., Miller, G., Sejima, H., Harper, J., and Mittler, R. (2013). Enhanced seed production under prolonged heat stress conditions in arabidopsis thaliana plants deficient in cytosolic ascorbate peroxidase 2. *J. Exp. Bot.* 64, 253–263. doi: 10.1093/jxb/ers335

Tadini, L., Peracchio, C., Trotta, A., Colombo, M., Mancini, I., Jeran, N., et al. (2020). GUN1 influences the accumulation of NEP-dependent transcripts and chloroplast protein import in arabidopsis cotyledons upon perturbation of chloroplast protein homeostasis. *Plant J.* 101, 1198–1220. doi: 10.1111/tpj.14585

Tadini, L., Pesaresi, P., Kleine, T., Rossi, F., Guljamow, A., Sommer, F., et al. (2016). Gun1 controls accumulation of the plastid ribosomal protein S1 at the protein level and interacts with proteins involved in plastid protein homeostasis. *Plant Physiol.* 170, 1817–1830. doi: 10.1104/pp.15.02033

Tadini, L., Romani, I., Pribil, M., Jahns, P., Leister, D., and Pesaresi, P. (2012). Thylakoid redox signals are integrated into organellar-gene-expression-dependent retrograde signaling in the prors1-1 mutant. *Front. Plant Sci.* 3. doi: 10.3389/fpls.2012.00282

Vallelian-Bindschedler, L., Schweizer, P., Mösinger, E., and Métraux, J. P. (1998). Heat-induced resistance in barley to powdery mildew (Blumeria graminis f.sp.hordei) is associated with a burst of active oxygen species. *Physiol. Mol. Plant Pathol.* 52, 185–199. doi: 10.1006/PMPP.1998.0140

Volkov, R. A., Panchuk, I. I., Mullineaux, P. M., and Schöffl, F. (2006). Heat stress-induced H2O2 is required for effective expression of heat shock genes in arabidopsis. *Plant Mol. Biol.* 61, 733–746. doi: 10.1007/s11103-006-0045-4

Wahid, A., Gelani, S., Ashraf, M., and Foolad, M. R. (2007). Heat tolerance in plants: An overview. *Environ. Exp. Bot.* 61, 199–223. doi: 10.1016/j.envexpbot.2007.05.011

Walton, P. A., Brees, C., Lismont, C., Apanasets, O., and Fransen, M. (2017). The peroxisomal import receptor PEX5 functions as a stress sensor retaining catalase in the cytosol in times of oxidative stress. *Biochim. Biophys. Acta - Mol. Cell Res.* 1864, 1833–1843. doi: 10.1016/J.BBAMCR.2017.07.013

Wang, Q. L., Chen, J. H., He, N. Y., and Guo, F. Q. (2018). Metabolic reprogramming in chloroplasts under heat stress in plants. *Int. J. Mol. Sci.* 19, 849. doi: 10.3390/ijms19030849

Wise, R. R., Olson, A. J., Schrader, S. M., and Sharkey, T. D. (2004). Electron transport is the functional limitation of photosynthesis in field-grown pima cotton plants at high temperature. *Plant Cell Environ.* 27, 717–724. doi: 10.1111/j.1365-3040.2004.01171.x

Woodson, J. D., Perez-Ruiz, J. M., and Chory, J. (2011). Heme synthesis by plastid ferrochelatase i regulates nuclear gene expression in plants. *Curr. Biol.* 21, 897–903. doi: 10.1016/j.cub.2011.04.004

Wu, G. Z., and Bock, R. (2021). GUN control in retrograde signaling: How GENOMES UNCOUPLED proteins adjust nuclear gene expression to plastid biogenesis. *Plant Cell* 33, 457–474. doi: 10.1093/plcell/koaa048

Wu, G. Z., Chalvin, C., Hoelscher, M., Meyer, E. H., Wu, X. N., and Bock, R. (2018). Control of retrograde signaling by rapid turnover of GENOMES UNCOUPLED1. *Plant Physiol.* 176, 2472–2495. doi: 10.1104/pp.18.00009

Wu, G.-Z., Meyer, E. H., Wu, S., and Bock, R. (2019). Extensive posttranscriptional regulation of nuclear gene expression by plastid retrograde signals. *Plant Physiol.* 180, 2034–2048.

Zhang, J., and Kirkham, M. B. (1996). Antioxidant responses to drought in sunflower and sorghum seedlings. *New Phytol.* 132, 361–373. doi: 10.1111/j.1469-8137.1996.tb01856.x

Zhao, X., Huang, J., and Chory, J. (2019). GUN1 interacts with MORF2 to regulate plastid RNA editing during retrograde signaling. *Proc. Natl. Acad. Sci.* 116, 10162–10167.

Zhu, J. K. (2016). Abiotic stress signaling and responses in plants. *Cell* 167, 313–324. doi: 10.1016/j.cell.2016.08.029

Plant Science 320 (2022) 111265

Contents lists available at ScienceDirect

Plant Science

journal homepage: www.elsevier.com/locate/plantsci

GUN1 involvement in the redox changes occurring during biogenic retrograde signaling

Stefania Fortunato [a], Cecilia Lasorella [a], Luca Tadini [b], Nicolaj Jeran [b], Federico Vita [a], Paolo Pesaresi [b], Maria Concetta de Pinto [a,*]

[a] Department of Biology, University of Bari Aldo Moro, Via Orabona 4, Bari 70125, Italy
[b] Department of Biosciences, University of Milano, Milano 20133, Italy

ARTICLE INFO

Keywords:
Antioxidants
Chloroplast biogenesis
GENOMES UNCOUPLED 1
Reactive oxygen species
Redox regulation
Retrograde signaling

ABSTRACT

Chloroplast biogenesis requires a tight communication between nucleus and plastids. By retrograde signals, plastids transmit information about their functional and developmental state to adjust nuclear gene expression, accordingly. GENOMES UNCOUPLED 1 (GUN1), a chloroplast-localized protein integrating several developmental and stress-related signals, is one of the main players of retrograde signaling.

Here, we focused on the interplay between GUN1 and redox regulation during biogenic retrograde signaling, by investigating redox parameters in Arabidopsis wild type and *gun1* seedlings. Our data highlight that during biogenic retrograde signaling superoxide anion ($O_2^{\cdot-}$) and hydrogen peroxide (H_2O_2) play a different role in response to GUN1. Under physiological conditions, even in the absence of a visible phenotype, *gun1* mutants show low activity of superoxide dismutase (SOD) and ascorbate peroxidase (APX), with an increase in $O_2^{\cdot-}$ accumulation and lipid peroxidation, suggesting that GUN1 indirectly protects chloroplasts from oxidative damage. In wild type seedlings, perturbation of chloroplast development with lincomycin causes H_2O_2 accumulation, in parallel with the decrease of ROS-removal metabolites and enzymes. These redox changes do not take place in *gun1* mutants which, in contrast, enhance SOD, APX and catalase activities. Our results indicate that in response to lincomycin, GUN1 is necessary for the H_2O_2-dependent oxidation of cellular environment, which might contribute to the redox-dependent plastid-to nucleus communication.

1. Introduction

Plant development, differentiation and appropriate response to environmental fluctuations require a mutual communication between plastids and the nucleus. By anterograde signaling, the nucleus exerts its control over the chloroplasts, while plastids, through retrograde signaling, transmit information about their developmental and functional state to adjust nuclear gene expression (NGE), accordingly [1,2]. Many components and distinctive pathways of retrograde signaling, controlling chloroplast biogenesis (biogenic control) and plastid homeostasis in response to environmental cues (operational control), have been identified in the last decades. These signaling molecules include carotenoid oxidation products [3], intermediates of tetrapyrrole biosynthesis (TPB) [4–6], carbohydrate metabolites [7,8], isoprenoid precursors [9], phosphoadenosines [10] and reactive oxygen species (ROS) [2,11–13].

The role of ROS as oxidants or components of redox signaling mostly depends on a fine balance between the production and scavenging of these molecules in different organelles [14]. Aerobic metabolism constantly generates ROS in different compartments of plant cells [15,16]. Chloroplasts represent a significant source of ROS, which comprise production of singlet oxygen at photosystem II and superoxide anion ($O_2^{\cdot-}$) at PSI [17]. The signaling activity and the simultaneous prevention of oxidative damage takes place through the control of ROS levels, which is made possible by enzymatic and non-enzymatic antioxidant systems [16,18]. Major non-enzymatic antioxidants include tocopherols, carotenoids, ascorbate (ASC), and glutathione (GSH) [18]. Amongst the enzymatic systems, superoxide dismutases (SOD) catalyze $O_2^{\cdot-}$ dismutation to hydrogen peroxide (H_2O_2).-H_2O_2 is closely controlled by the action of catalases (CAT), ASC peroxidases (APX), class III peroxidases (POD) and thiol-dependent peroxidases (TPX), which include peroxiredoxins [19] and GSH peroxidases (GPX) [20]. APX utilizes ASC to reduce hydrogen peroxide yielding monodehydroascorbate (MDHA), which can be reconverted to ASC by either the action of MDHA

* Corresponding author.
E-mail address: mariaconcetta.depinto@uniba.it (M.C. de Pinto).

https://doi.org/10.1016/j.plantsci.2022.111265
Received 1 November 2021; Received in revised form 18 March 2022; Accepted 21 March 2022
Available online 26 March 2022

reductase (MDHAR) or through the non-enzymatic disproportionation to dehydroascorbate (DHA). Subsequently, DHA reductase (DHAR) reduces DHA to ASC utilizing GSH, which is oxidized to glutathione disulfide (GSSG) and regenerated to GSH by NADPH-dependent GSSSG reductase (GR) [16].

Redox regulation occurring in cell organelles can also regulate retrograde signaling, greatly influencing plant response to external environment changes [15,21–24]. Cellular redox signaling has been proposed as a crucial integrator of retrograde signals deriving from organelles, which permit communication with the nucleus [25].

One of the main biogenic retrograde signaling pathways involves the plastid-localized GENOMES UNCOUPLED (GUN) proteins, identified in experiments where plastid development was chemically inhibited [26]. In these conditions, *gun* mutants failed to repress nucleus-encoded Photosynthesis-Associated Nuclear Genes (PhANGs). Among the six GUN proteins identified, GUN2-GUN6 are directly involved in TPB, giving rise to intermediate molecules with a possible role in biogenic retrograde signaling [6,27–29]. On the other hand, GUN1 is a nuclear encoded pentatricopeptide repeat (PPR) protein, with a C-terminal Small MutS-Relate (SMR) domain, localized in the chloroplast, which takes part in multiple processes to coordinate NGE in response to plastid signals. Since the PPR and SMR proteins are involved in RNA metabolisms and DNA repair and recombination [30,31], GUN1 was initially proposed as a nucleic acid-binding protein acting in either plastid DNA metabolism or repair and involved in plastid gene expression (PGE) [29]. Successive evidence demonstrates that GUN1 interacts with proteins more than with nucleic acids. Co-immunoprecipitation and mass spectrometry studies have detected nearly 300 different GUN1 interacting proteins, involved in several biological processes [32,33], including plastid gene transcription, RNA-editing, translation, protein import and indirectly TPB [34–36].

GUN1 protein level is very low in most plant developmental stages, since Clp protease rapidly degrades the protein after entering the chloroplast [37]. Only during the early stages of chloroplast biogenesis or under stress conditions that perturb plastid protein homeostasis, such as lincomycin (Lin) treatment, GUN1 accumulates to detectable levels [33, 37]. When chloroplast protein synthesis is inhibited by Lin, Clp-protease fails to accumulate, resulting in increased amount of GUN1 protein in the chloroplast [38]. It has been recently proposed that GUN1 functions as a hub by interacting with several protein partners and promoting function by bringing enzymes in proximity with their substrate, or the opposite, inhibiting processes by sequestering specific interactors [35, 39].

Although a growing number of evidence underlines, on one side, the pivotal role of ROS and redox changes and, on the other side, the GUN1 protein in retrograde signaling to our knowledge very few data are present in the literature on the interplay between GUN1 and redox regulation during biogenic retrograde signaling.

Considering these premises, we aimed to study the potential involvement of GUN1 in the control of redox regulation occurring upon activation of GUN1-dependent retrograde signaling. To achieve this goal, we investigated redox parameters in Arabidopsis wild type (Col-0) and *gun1* mutant seedlings grown both in presence and absence of Lin. In particular, the levels of ROS, the main oxidative markers, as well antioxidant metabolites and the major ROS removal enzymes were analyzed. Redox changes observed between Col-0 and *gun1* seedlings in response to lincomycin treatment have provided valuable insights into the role of ROS and redox changes in the biogenic retrograde communication.

2. Materials and methods

2.1. Plant materials and growth conditions

The Arabidopsis (*Arabidopsis thaliana*, genetic background Col-0) *gun1–102* T-DNA insertion mutant was previously described in Tadini et al. [32]. Col-0 and *gun1–102* seeds were surface-sterilized and sown out on Murashige and Skoog medium (Duchefa, Haarlem, The Netherlands) supplemented with 2% (w/v) sucrose and 1.5% (w/v) Phyto-Agar (Duchefa). Lincomycin (Lin) was added at the final concentration of 550 μM. After 2 days incubation at 4 °C in the dark, seedlings were grown for 6 days (80 μmol m^{-2} sec^{-1} on 16 h/8 h dark/light cycles).

2.2. Determination of ROS and oxidative markers

In situ O_2^- and H_2O_2 were detected with nitroblue tetrazolium (NBT) and 3,3-diaminobenzidine (DAB), respectively, as described in Jambunathan (2010) [40] with minor modifications. For anion superoxide visualization, seedlings were vacuum infiltrated (70–100 mbar) for 10 min in NBT-staining solution (50 mM phosphate buffer pH 6.4, 0.1% (w/v) NBT, 10 mM sodium azide). After a further incubation for 15 min with a new NBT-staining solution, seedlings were exposed under cool fluorescent light for 20 min. After the staining, seedlings were bleached by a series of washing steps with 95% ethanol at 45 °C. Superoxide anion was visualized as a blue color produced by NBT precipitation. For H_2O_2 visualization, seedlings were vacuum infiltrated (70–100 mbar) for 5 min with 100 mM phosphate buffer pH 7.4 containing 0.1% 3,3'diaminobenzidine (DAB) (w/v). The seedlings were incubated under vacuum in the dark for 5–6 h until brown precipitates were observed. Successively, stained seedlings were bleached by a series of wash with 95% ethanol at 45 °C. The staining intensity was quantified on digital images by ImageJ software (https://imagej.nih.gov/ij/) as reported in [40]. The relative O_2^- and H_2O_2 levels were determined as percentage of NBT- and DAB-stained area of cotyledons, respectively.

The level of lipid peroxidation was evaluated in terms of malondialdehyde (MDA) content determined by the TBA reaction as described by Paradiso et al. [41]. The amount of MDA-TBA complex was calculated using an extinction coefficient of 155 mM^{-1} cm^{-1}.

Protein oxidation was spectrophotometrically determined by measuring the content of carbonyl-groups reacting with dinitrophenylhydrazine (DNPH), according to Romero Puertas et al. [42]. Carbonyl content was calculated using an extinction coefficient of 22 mM^{-1} cm^{-1}.

For the identification of sulfhydryl groups, proteins were labelled with monobromobimane (mBBr) and separated by sodium dodecyl sulfate (SDS)- Polyacrylamide Gel Electrophoresis (PAGE) according to De Gara et al. (2003) [43]. Quantitative densitometric analyses of the main bands in the gels were performed using Quantity One ™ software (Biorad).

2.3. Analysis of enzymatic and non-enzymatic antioxidants

For the determination of non-enzymatic antioxidants, Arabidopsis seedlings were homogenized with four volumes of cold 5% (w/v) metaphosphoric acid in liquid nitrogen. The homogenates were centrifuged at 20,000 g for 15 min at 4 °C. Supernatants were used to determine contents and redox states of ASC and GSH according to de Pinto et al. [44].

For the determination of enzymatic antioxidants, seedlings were ground in liquid nitrogen and homogenized at 4 °C in a 1:8 (w/v) ratio with the extraction buffer (50 mM Tris–HCl pH 7.5, 0.05% cysteine, 0.1% bovine serum albumin, 1 mM phenylmethanesulfonylfluoride-PMSF). For the determination of APX activity, 1 mM ASC was added to the extraction buffer. Homogenates were centrifuged at 20,000 g for 15 min, and the supernatants were used for spectrophotometric and electrophoretic analyses. Protein concentration was determined according to Bradford [45], using bovine serum albumin as a standard.

Superoxide dismutase (SOD, EC 1.15.1.1) and catalase (CAT, EC 1.11.1.6) activities were spectrophotometrically measured according to Paradiso et al. [46].

Native PAGE of CAT and SOD were performed according to Villani

et al. [47]. After the electrophoretic run, for CAT determination, gels were incubated for 15 min in 5 mM H_2O_2. The gels were washed with distilled water and stained with 1% ferrichloride and 1% ferricynnide solution. CAT isoforms appeared as achromatic bands on a dark-blue background. For SOD, gels were incubated in 36 mM sodium phosphate buffer (pH 7.8), containing 28 μM riboflavin and 28 mM N'-Tetramethyl ethylenediamine for 25 min at room temperature. The gels were washed with distilled water and incubated in the dark for 30 min with a gentle shaker in 36 mM sodium phosphate buffer (pH 7.8), containing 2 mM NBT. After illumination under cool fluorescent light for 15 min, the solution was replaced with 36 mM sodium phosphate buffer (pH 7.8) until achromatic bands on a grey background appeared.

Ascorbate peroxidase (APX, EC 1.11.1.11), dehydroascorbate reductase (DHAR, EC: 1.8.5.1), monodehydroascorbate reductase (MDHAR, EC: 1.6.5.4) and glutathione reductase (GR, EC 1.6.4.2) activities were determined according to de Pinto et al. [48].

Activity of class III peroxidases (POD, EC: 1.11.1.7) was measured following the oxidation of 3,3',5,5'-tetramethylbenzidine (TMB) at 652 nm. The reaction buffer contained 50 mM sodium acetate buffer (pH 5.0), 0.1 mM H_2O_2, and 0.2 mM TMB. The activity was calculated using an extinction coefficient of 26.9 mM^{-1} cm^{-1}.

Glutathione peroxidase (GPX, EC: 1.11.1.9) activity was determined following the NADPH oxidation at 340 nm in a 1 mL reaction mixture composed of 0.1 M Tris-HCl buffer (pH 8.0), 1 mM GSH, 0.2 mM NADPH, 3 U GR and 50 μM H_2O_2. The activity was calculated using an extinction coefficient of 6.2 mM^{-1} cm^{-1}.

2.4. Western Blot of SOD, CAT and APX

Total proteins were extracted from seedlings with 10% (w/v) TCA in a 1:10 (w/v) ratio. The homogenates were centrifuged at 20,000 g for 15 min. Pellets were washed with 1 mL of acetone and resuspended in 100 mM Tris-HCl (pH 7.5), 1 mM EDTA, 2% (w/v) SDS, 1 mM PMSF. Proteins were separated by SDS PAGE and then transferred on a polyvinylidene fluoride membrane, as described by Nigro et al. [49]. Filters were then incubated with the following specific antibodies: L-ascorbate peroxidase primary polyclonal antibody (Agrisera Vännäs, Sweden), which recognizes thylakoidal, stromal and cytosolic isoforms; Catalase (peroxisomal marker) primary polyclonal antibody (Agrisera Vännäs, Sweden); Fe-SOD primary polyclonal antibody (Agrisera Vännäs, Sweden). The secondary antibody used was horseradish peroxidase (HRP)-conjugate Anti-Rabbit IgG (Promega, Madison, WI, USA). Filters were revealed by enhanced chemiluminescence using the Pierce™ ECL Western Blotting Substrate (Thermo Fisher Scientific, Cleveland, OH, USA).

2.5. Differential expression analyses

Differential expression data have been retrieved from published datasets on Gene Expression Repository (GEO; https://www.ncbi.nlm.nih.gov/geo/; GEO accession GSE5770) [29] and analyzed using GEO2R online tool (https://www.ncbi.nlm.nih.gov/geo/geo2r/).

2.6. Statistical analysis

The data were expressed as the means of five different experiments ± standard error (SE). One-way analysis of variance (ANOVA) followed by a post-hoc Tukey's comparison test was used to calculate the difference between genotypes and treatments. Differences were considered statistically significant at a p-value < 0.05. All the statistical analyses were performed by Minitab software (Minitab Inc., State College, PA, USA).

3. Results

3.1. ROS accumulation and oxidative markers differed in wild type and *gun1* seedlings both in presence and absence of Lin

Six-day-old wild type (Col-0) and *gun1* Arabidopsis seedlings grown in the absence of Lin (control conditions, - Lin) did not show any visible phenotypic difference (Fig. 1A). However, under control conditions, the levels of O_2^-, visualized by NBT-staining, were significantly higher in the cotyledons of *gun1* seedlings than in Col-0 (Fig. 1B). On the other hand, H_2O_2 levels, visualized by DAB-staining, did not differ between the two genotypes grown under optimal control conditions (Fig. 1C). In presence of 550 μM Lin, when the proplastid-to-chloroplast transition is completely suppressed (Fig. 1A), O_2^- levels did not change in wild type seedlings but were significantly reduced, i.e. under the limit of detection, in *gun1* cotyledons (Fig. 1B). Conversely, Lin treatment caused a very specific increase in the accumulation of H_2O_2 only in wild type seedlings (Fig. 1C).

Furthermore, under control conditions, the level of lipid peroxidation was higher in *gun1* with respect to wild type seedlings. Interestingly, the Lin treatment did not change lipid peroxidation in Col-0, while the same treatment lowered the level of this oxidative marker in *gun1* seedlings (Fig. 2A). With respect to protein oxidation, the levels of protein carbonyl groups did not show differences between the two genotypes grown under control conditions, while a marked increase occurred in Col-0 seedlings treated with Lin (Fig. 2B). Sulfhydryl groups of proteins, labelled with mBBr and separated by SDS-PAGE, were slightly higher in *gun1* with respect to wild type seedlings grown under control conditions. Treatment with Lin caused a marked oxidation of protein sulfhydryl groups in both genotypes, although more evident in wild type seedlings (Fig. 2C).

3.2. Behavior of ROS scavenging enzymes in wild type and *gun1* seedlings

To clarify the different O_2^- levels found in the two genotypes the activity of SOD was investigated. Under control conditions, total SOD activity in *gun1* was significantly lower than in wild type seedlings. Moreover, Lin treatment did not affect the activity of this enzyme in Col-0, while induced a significant increase in *gun1* seedlings (Fig. 3A). Changes in SOD activity were confirmed by Native PAGE analysis (Fig. 3B), where the SOD isoenzyme activity was lower in *gun1* than in wild type seedlings under control conditions, while both Mn/Fe-SOD and Cu/Zn-SOD activities markedly increased in *gun1* seedlings treated with Lin. A similar behavior could be observed by monitoring the changes in the amount of Fe-SOD protein by immunoblot and densitometric analysis (Fig. 3C).

To explain the different H_2O_2 accumulation in the two genotypes the behavior of the two enzymes directly involved in the removal of this ROS, namely CAT and APX, was investigated (Figs. 4, 5). In control conditions, CAT activity did not differ significantly among the two genotypes (Col-0 and *gun1*), as shown by spectrophotometric analysis and Native PAGE. On the contrary, the presence of Lin in the growth medium induced a significant reduction of CAT activity only in Col-0 seedlings (Figs. 4A, 4B). Interestingly, the protein level of CAT2, analyzed by western blotting, was much higher in *gun1* seedlings under both control and Lin treatment conditions (Fig. 4C).

Regarding APX enzyme, its activity was lower in gun1 seedlings under control conditions; however, the presence of Lin determined a reduction of the enzyme activity in Col-0 and an enhancement in *gun1* mutants (Fig. 5A). Western blotting showed that the various APX isoenzymes behaved differently. Indeed, Lin inhibited the accumulation of thylakoidal APX in both the genotypes, as thylakoid formation itself is inhibited, and caused a clear increase in the cytosolic isoenzymes only in *gun1* seedlings, especially upon Lin treatment (Fig. 5B, C).

The expression analysis of genes coding for different isoforms of SOD, CAT and APX, taken from published microarray experiments as in

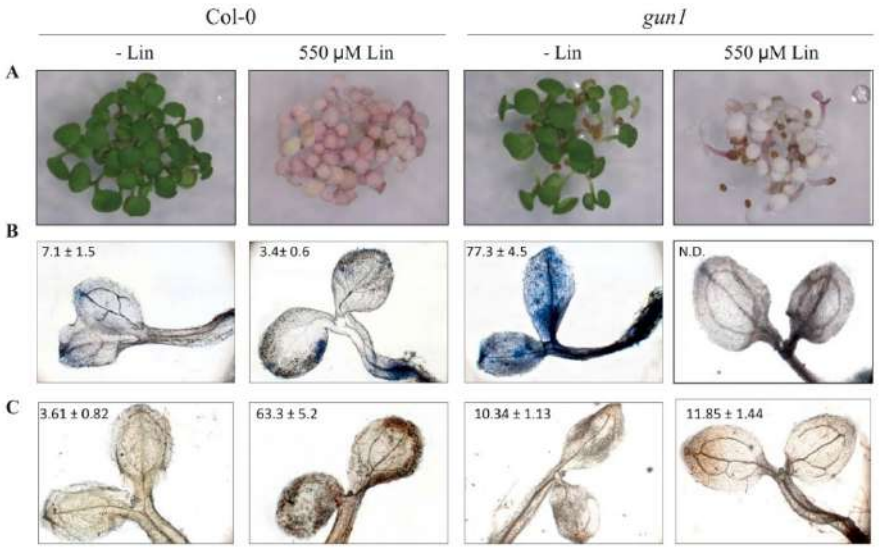

Fig. 1. Accumulation of superoxide anion ($O_2^{\cdot-}$) and hydrogen peroxide (H_2O_2) in Arabidopsis wild type (Col-0) and *gun1* seedlings, grown in the absence or presence of 550 µM lincomycin (Lin). Representative images of **(A)** phenotypes, **(B)** $O_2^{\cdot-}$ accumulation, visualized by nitroblue tetrazolium (NBT)-staining and **(C)** H_2O_2 accumulation, visualized by diaminobenzidine (DAB)-staining. The experiments of $O_2^{\cdot-}$ and H_2O_2 detection were repeated three times showing reproducible results. In (B) and (C) the percentage area ± standard errors of 60 cotyledons (20 for each experiment) stained with NBT and DAB, respectively, is reported inside the images.

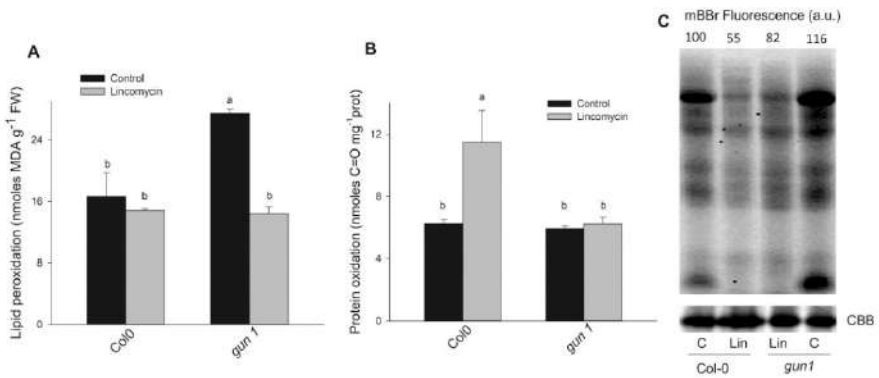

Fig. 2. Oxidative markers in Arabidopsis wild type (Col-0) and *gun1* seedlings after six days of growth in the absence (control) or presence of lincomycin (Lin). **(A)** Lipid peroxidation, measured as malondialdehyde content and **(B)** protein oxidation measured as total protein carbonyl groups. The values are the means ± standard errors of five independent experiments. Different letters indicate significant differences obtained by one-way ANOVA test ($P < 0.05$). **(C)** Representative image from three independent experiments of the levels of sulfhydryl protein groups. Proteins were labelled with monobromobimane (mBBr) and separated by sodium dodecyl sulphate-polyacrylamide gel electrophoresis. Each well was loaded with 100 µg of proteins. To control for loading, gel was stained with Coomassie Brilliant Blue (CBB); quantification of signals (by Quantity One) relative to Col-0 without Lin (100%) is provided above the panel.

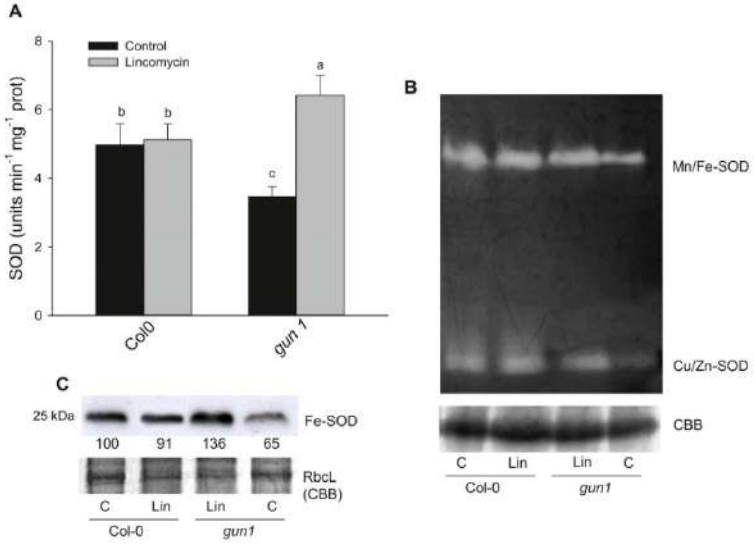

Fig. 3. Superoxide dismutase (SOD) behaviour in wild type (Col-0) and *gun1* seedlings after six days of growth in the absence (control) or presence of lincomycin (Lin). **(A)** Total SOD activity of *Arabidopsis* seedlings (Col-0 and *gun1*), grown in the absence or presence of Lin. The values are the means ± standard errors of five independent experiments. Different letters indicate significant differences obtained by one-way ANOVA test ($P < 0.05$). **(B)** Representative image from three independent experiments of Native Polyacrylamide Gel Electrophoresis of SOD. Each well was loaded with 150 μg of proteins. To control for loading, gel was stained with Coomassie Brilliant Blue (CBB). **(C)** Representative image from three independent experiments of Fe-SOD immunoblotting; each well was loaded with 30 μg of proteins. RcbL band, stained with Coomassie Brilliant Blue (CBB), was used as a loading control between genotypes. The decrease in RcbL in the "Lin" lanes confirmed the action of the treatment. Quantification of signals (by ImageJ) relative to the Col-0 without Lin (100%) is provided below the panel.

Koussevitzky, et al. (2007) [29], showed that genes encoding the plastid-located FSD1, CSD2, tAPX and APX4, as well the gene coding for CAT2, were downregulated by Lin in Col-0 plants. On the other hand, Lin treatment induced the expression of APX2, and CDS3 in *gun1* mutants. Moreover, in Lin-treated plants many of the genes coding for the different SOD (FSD1, FSD2, FSD3, CSD3) and APX (APX2, APX3, APX4, APX6, TAPX) isoforms were upregulated in *gun1* compared to Col-0 (Table S1).

With respect to GPX, its activity did not differ significantly in the two genotypes grown under control conditions., while it appeared to be significantly higher in Lin-treated Col-0 seedlings (Fig. 6A). Lin treatment in Col-0 seedlings caused a repression of genes encoding the chloroplastic GPXs, namely GPX1 and GPX7, and an induction of GPX3 and GPX8 (Table S1) [29].

Similarly, POD activities did not change in the two genotypes under control conditions and increased only in wild type seedlings grown in presence of Lin (Fig. 6B).

3.3. Hydrophilic antioxidants decreased and were more oxidized only in wild type seedlings grown in presence of Lin

The different redox environment of wild type and *gun1* mutants grown in presence of Lin was confirmed through the analyses of the two major hydrophilic antioxidants, ASC and GSH (Fig. 7). Under control conditions, total contents, and redox state of the two antioxidants did not vary significantly between Col-0 and *gun1*. However, Lin triggered a reduction in total ascorbate content in both the genotypes, although this decrease was significantly greater in Col-0 than in *gun1* seedlings (Fig. 7A). On the other hand, total glutathione levels were lowered only in Col-0 grown in presence of Lin (Fig. 7C). Furthermore, the presence of Lin affected the oxidation of both antioxidants only in wild type seedlings (Figs. 7B, 7C).

To clarify the different redox state of ascorbate and glutathione in the two genotypes, the activity of the enzymes involved in the reduction of the oxidized forms of the two metabolites was determined. The activities of the three enzymes, namely MDHAR, DHAR and GR did not show significant differences between the two genotypes grown under control conditions (Fig. 8). Lin treatment was responsible, instend, for the increase in the activities of MDHAR and GR in *gun1* seedlings (Fig. 8A and C). On the contrary, Lin led to an induction of DHAR activity only in Col-0 seedlings (Fig. 8B).

4. Discussion

GUN1-dependent signaling has been proposed as one of the main retrograde signaling pathways active during plastid biogenesis. Our results indicate that during the GUN1-dependent biogenic retrograde communication $O_2^{\cdot-}$ and H_2O_2 might contribute differently to the chloroplast-to-nucleus retrograde communication.

Under optimal physiological conditions, except for a small percentage of chlorophyll-deficient variegated cotyledons [50], *gun1* mutants are mostly phenotypically indistinguishable from wild type (Fig. 1A). However, *gun1* mutants, grown in control conditions, accumulate a higher $O_2^{\cdot-}$ amount and a greater level of lipid peroxidation than Col-0

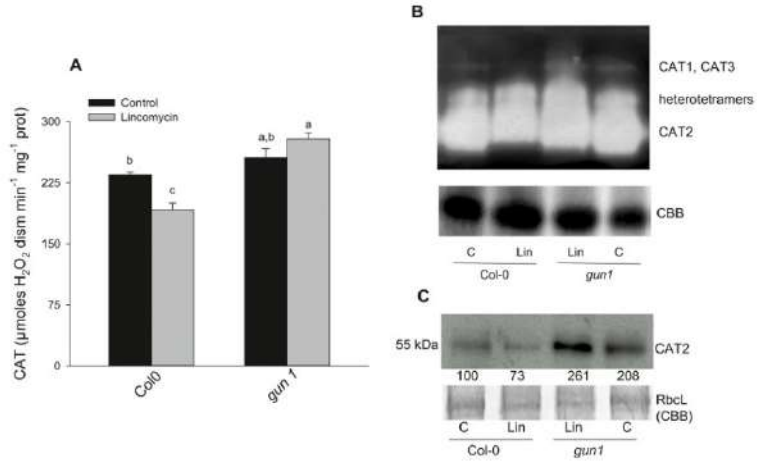

Fig. 4. Catalase (CAT) behaviour in response to lincomycin (Lin) in wild type (Col-0) and *gun1* seedlings. **(A)** Total CAT activity of Arabidopsis seedlings (Col-0 and *gun1*), grown in the absence (control) or presence of Lin. The values are the means ± standard errors of five independent experiments. Different letters indicate significant differences obtained by one-way ANOVA test ($P < 0.05$). **(B)** Representative image from three independent experiments of Native polyacrylamide gel electrophoresis of CAT. Each well was loaded with 50 µg of proteins. To control for loading, gel was stained with Coomassie Brilliant Blue (CBB). **(C)** Representative image of western blotting of CAT2. Each well was loaded with 10 µg of proteins; RcbL band, stained with Coomassie Brilliant Blue (CBB), was used as a loading control between genotypes. The decrease in RcbL in the "Lin" lanes confirmed the action of the treatment. Quantification of signals (by ImageJ) relative to the Col-0 without Lin (100%) is provided below the panel.

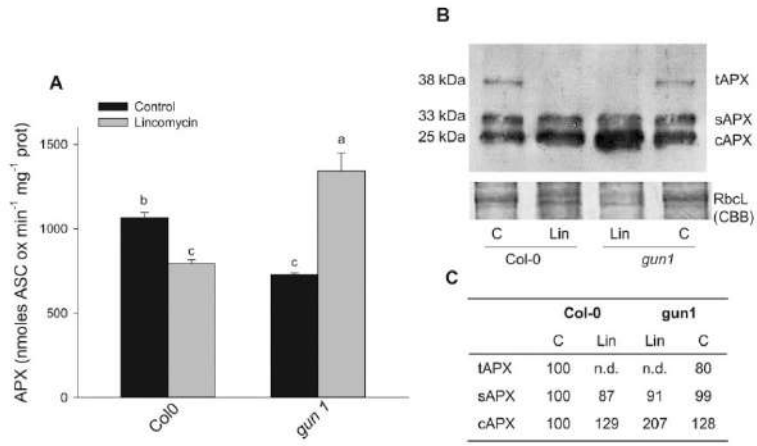

C

	Col-0		gun1	
	C	Lin	Lin	C
tAPX	100	n.d.	n.d.	80
sAPX	100	87	91	99
cAPX	100	129	207	128

Fig. 5. Ascorbate peroxidase (APX) in wild type (Col-0) and *gun1* seedlings after six days of growth in the absence (control) or presence of lincomycin (Lin). **(A)** Total APX activity of Arabidopsis seedlings (Col-0 and *gun1*), grown in presence or absence of Lin. The values are the means ± standard errors of five independent experiments. Different letters indicate significant differences obtained by one-way ANOVA test ($P < 0.05$). **(B)** Representative image of western blotting of CAT2; each well was loaded with 10 µg of proteins. RcbL band, stained with Coomassie Brilliant Blue (CBB), was used as a loading control between genotypes. The decrease in RcbL in the "Lin" lanes confirmed the action of the treatment. tAPX, sAPX and cAPX are thylacoidal, stromal and cytosolic APX, respectively. **(C)** Quantification of tAPX, sAPX and cAPX immunoblot signals (by ImageJ) relative to Col-0 without Lin (100%).

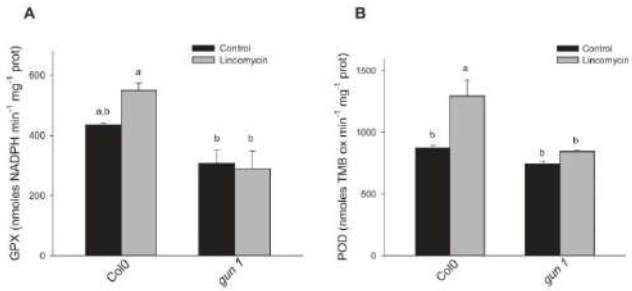

Fig. 6. Lincomycin increases glutathione peroxidase (GPX) and class III peroxidases (POD) activities only in wild type (Col-0) Arabidopsis seedlings. (**A**) GPX and (**B**) POD activity of *Arabidopsis* seedlings (Col-0 and *gun1*), grown in the absence (control) or presence of lincomycin. The values are the means ± standard errors of five independent experiments. Different letters indicate significant differences obtained by one-way ANOVA test ($P < 0.05$).

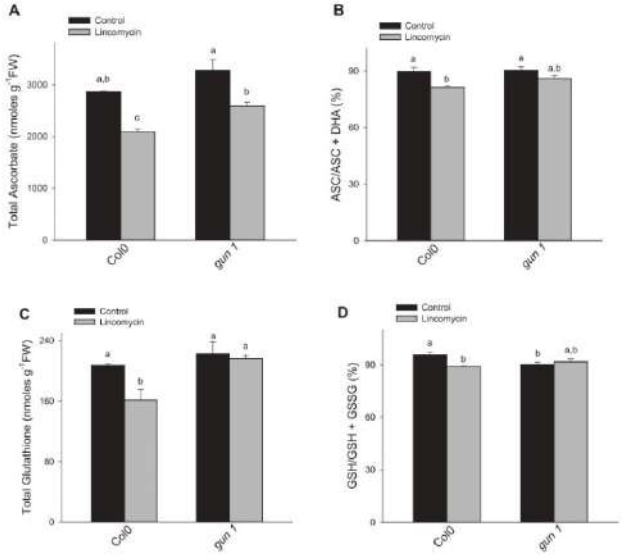

Fig. 7. Lincomycin induces a decrease of total content and redox state of ascorbate (ASC) and glutathione (GSH) only in wild type (Col-0) Arabidopsis seedlings. (**A**) Total content (ASC + dehydroascorbate-DHA) and (**B**) redox state (ASC/ASC + DHA) of ascorbate and (**C**) total content (GSH + glutathione disulfide -GSSG) and (**D**) redox state (GSH/GSH+GSSG) of glutathione in *Arabidopsis* seedlings (Col-0 and *gun1*), grown in the absence (control) or presence of lincomycin. The values are the means ± standard errors of five independent experiments. Different letters indicate significant differences obtained by one-way ANOVA test ($P < 0.05$).

seedlings (Figs. 1B, 2A). O_2^- accumulation in *gun1* mutants may contribute to cellular injuries oxidizing the iron-sulfur centers of proteins; moreover, O_2^- can lead to the formation of hydroxyl radicals, which promptly react with lipids, causing peroxidation [51,52]. The accumulation of O_2^- in *gun1* occurs in parallel with a significant decline in the activities of SOD and APX, two main players of ROS removal (Figs. 3, 5). SOD, catalyzing the dismutation of O_2^- to H_2O_2, represents the primary line of resistance against ROS [53]. In different plant species, high activities of SOD contribute to improve resistance to high light intensities [54,55]. Moreover, in Arabidopsis chloroplastic APX has been shown to play a significant role for photoprotection [55,56]. Thus, the more sensitive phenotype to photo-oxidative stress observed in *gun1* mutants compared with Col-0 plants [50,57], could be related to the high O_2^- accumulation and the low activity of SOD and APX (Figs. 1, 3, 5), suggesting that *gun1* plastids are more inclined to suffer ROS-mediated damage. Accordingly, the modest percentage of *gun1* cotyledons that fail the greening process [50] could be related to the photo-protective functions provided by GUN1 during chloroplast biogenesis. Our data support the idea that GUN1 optimizes chloroplast biogenesis minimizing the consequences of failures in developing chloroplasts, mainly preventing, or at least reducing, photo-oxidative damage [58,59]. The higher O_2^- level in *gun1* control conditions could also explain the enhanced sensitivity to low concentrations of Lin and norflurazon,when plastid functions are only mild impaired [59,60].

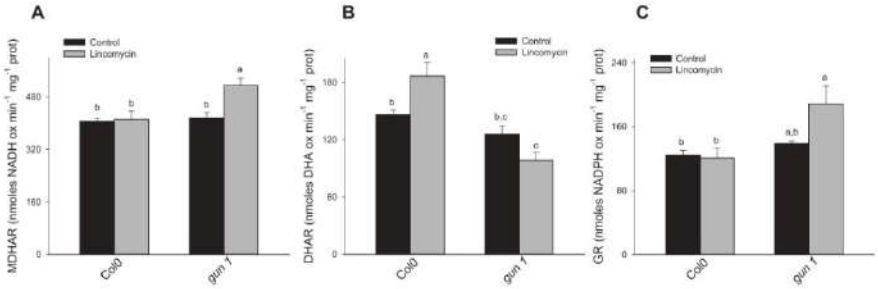

Fig. 8. Effects of lincomycin on ascorbate-glutathione recycling enzymes of Col-0 and *gun1* Arabidopsis seedlings. (**A**) Monodehydroascorbate reductase (MDHAR), (**B**) dehydroascorbate reductase (DHAR) and (**C**) glutathione reductase (GR) of *Arabidopsis* seedlings (Col-0 and *gun1*) grown in the absence (control) or presence of lincomycin. The values are the means ± standard errors of five independent experiments. Different letters indicate significant differences obtained by one-way ANOVA test ($P < 0.05$).

The block of translation in the chloroplast of wild type Arabidopsis seedlings by 550 μM Lin suppresses chloroplast development and impacts retrograde signaling, causing a strong downregulation of PhANGs [61]. Our results show that Lin treatment of Arabidopsis Col-0 seedlings causes an increase in the level of H_2O_2 (Fig. 1C). Due to its quite long half-life, its capability to move across the plasma membrane and to oxidize proteins, among ROS, H_2O_2 is considered the crucial signaling molecule [62]. Hence, H_2O_2 can trigger retrograde signaling from chloroplasts to the nucleus reprogramming NGE [63,64]. Intracellular H_2O_2 levels can influence cellular redox regulation leading to the oxidation of protein thiols [65]. By using roGFP2, an *in vivo* reporter of redox changes, it has been shown that the treatment of Arabidopsis plants with Lin increases the oxidation of cytosol and nuclei, suggesting that this oxidation can work as a redox signal that permits communication between chloroplasts and the nucleus [25]. Consistently, our results indicate that high H_2O_2 levels in Arabidopsis Lin-treated Col-0 seedlings correlate with a higher protein oxidation, measured as increase in carbonylated proteins as well as oxidation of protein sulfhydryl groups (Fig. 3B, C). The effect of Lin in increasing the oxidation of cellular environment of wild type seedlings has been confirmed by the decrease of redox sate of the two major hydrophilic antioxidants, ASC and GSH (Fig. 7B, D). Crosstalk between redox pools of different cellular compartments, possibly transferred by a redox shift in cellular components, has also been considered critical for controlling NGE [66,67]. Thus, our results indicate that the H_2O_2-dependent oxidation of cellular environment caused by Lin treatment could act as a redox signaling communicating to the nucleus the impairment of chloroplast development.

It has been previously proposed that plastid redox state and GUN1-dependent signaling can be interconnected [32,64]. Our data show that contrary to what happens in wild type plants, *gun1* mutants grown in presence of Lin do not accumulate H_2O_2 and do not have an oxidized cellular environment, as shown by the unchanged levels of oxidized proteins and the maintenance of redox state of ASC and GSH pools (Figs. 1C, 2B, C, 7B, D). The preservation of the reduced forms of ASC and GSH in Lin-treated *gun1* mutants is justified by the increase in the activities of MDAR and GR (Fig. 8). Thus, the redox-dependent communication from plastids to nucleus occurring in wild type seedlings fails in *gun1* mutants. The data emphasize the idea of an involvement of GUN1 in the control of the H_2O_2-dependent redox changes occurring during biogenic retrograde signaling.

Consistently, also the decrease in the content of GSH and ASC occurring in Lin-treated Col-0 seedlings is GUN1-dependent (Fig. 7). Our data are in accordance with literature data showing that GUN1 is required for the PGE-dependent suppression of ASC biosynthesis; indeed, Lin markedly decreases the transcript levels of many genes involved in ASC biosynthesis in the wild-type plants but does not significantly affect the expression of these genes in the *gun1* mutants [68]. A lowered ASC synthesis and therefore a lowered ROS buffering capacity in Lin-treated seedlings might be part of the cause for the oxidized environment. It is interesting to point out that cellular ASC homeostasis may affect NGE, particularly the expression of defense genes [69,70].

In wild type plants, Lin also induces a decrease in the activities of CAT and APX, which may contribute to the overaccumulation of H_2O_2 (Figs. 4, 5). Western blotting analysis (Figs. 5B, 5C), as well transcriptomic data (Table S1), highlight that the decrease in APX activity is particularly due to the thylakoidal isoform. Remarkably, it has been shown that when the expression of tAPX was silenced in leaves, levels of oxidized protein in chloroplasts increased in the absence of stress [12]. Moreover, in Lin-treated Col-0 seedlings, also the chloroplastic GPX, namely GPX1 and GPX7, are downregulated (Table S1), demonstrating a severe impairment of the chloroplastic H_2O_2-removal enzymes. On the other hand, the non-chloroplastic GPX3 and GPX8 increase, explaining the higher GPX activity (Fig. 6A) and suggesting their involvement in maintaining the thiol/disulfide balance [20]. Finally, the increase in POD activity observed in Lin-treated Col-0 plants (Fig. 6B) highlight the different behavior of class III peroxidases, which are closely connected with ROS dynamics, working in both H_2O_2 detoxification and production, mainly in the apoplast and vacuole [71]. The rise in POD activity may indicate a contribution of these enzymes to H_2O_2 accumulation caused by Lin. In Lin-treated Col-0 seedlings, the differential responses of CAT and APX on one side and POD on the other indicate that perturbation of chloroplast development triggers specific GUN1-dependent redox processing and signaling pathways.

The behavior of *gun1* mutants grown in presence of Lin is very different from that of wild type plants, which show a significant increase in SOD, CAT and cytosolic APX (Figs. 3–5). It has been recently reported that in Lin-treated *gun1* mutants, an altered chloroplast protein import causes an overaccumulation of unimported precursor with a subsequent cytosolic proteotoxic stress [33,59]. Thus, it is plausible to assume that the increase in the ROS removal enzymes, observed in *gun1* mutants, may represent an indirect response to the cytosolic proteotoxic stress, resembling what occurs in response to heat stress [46]. The increase in SOD activity can explain the decrease in $O_2^{\cdot-}$ accumulation observed in the *gun1* mutants after the Lin treatment. Moreover, in Lin-treated *gun1* mutants, the induction of APX2 and the failure in CAT2 downregulation (Table S1), followed by the increase in the activity of both the enzymes

(Figs. 4, 5), significantly contribute to the maintenance of low H_2O_2 levels, inhibiting the oxidative signaling to the nucleus.

5. Conclusions

This study revealed that during the GUN1-dependent biogenic retrograde signaling O_2^- and H_2O_2 might play a different role. During plastid biogenesis, occurring under optimal physiological conditions, GUN1 appears to influence the O_2^- accumulation, through the regulation of SOD and APX enzyme activities, playing a role in protecting the organelles from potential oxidative damage. On the other hand, in response to Lin treatment, GUN1 mediates the formation of an H_2O_2-dependent oxidized environment, which can represent a redox signal communicating to the nucleus the perturbation of chloroplast development [25].

Further investigation will be aimed at understanding whether the oxidation of the cellular environment is a common event when PGE is altered and to explore the molecular mechanisms through which GUN1 mediates cellular oxidation.

Funding

This research was funded by MUR–Ministero dell'Università e della Ricerca, Italy, Grant numbers PRIN-2017, 2017FBS8YN.

Author contributions

S.F., P.P., L.T., MCdP. conceived and designed research. S.F., C.L. N. J. F.V. performed the experiments. M.C.dP. advised on the experiments. All authors contributed drafting the manuscript. S.F., M.C.dP. coordinated the study and took care of the final version of the manuscript. All authors have read and agreed to the published version of the manuscript.

Declaration of Competing Interest

The authors declare that they have no known competing financial interests or personal relationships that could have appeared to influence the work reported in this paper.

Appendix A. Supporting information

Supplementary data associated with this article can be found in the online version at doi:10.1016/j.plantsci.2022.111265.

References

[1] B.J. Pogson, N.S. Woo, B. Forster, I.D. Small, Plastid signalling to the nucleus and beyond, Trends Plant Sci. 13 (2008) 602–609.
[2] R. Singh, S. Singh, P. Parihar, V.P. Singh, S.M. Prasad, Retrograde signaling between plastid and nucleus: A review, J. Plant Physiol. 181 (2015) 55–66.
[3] F. Ramel, S. Birtic, C. Ginies, L. Soubigou-Taconnat, C. Triantaphylides, M. Havaux, Carotenoid oxidation products are stress signals that mediate gene responses to singlet oxygen in plants, P. Natl. Acad. Sci. USA 109 (2012) 5535–5540.
[4] L. Shumbe, R. Bott, M. Havaux, Dihydroactinidiolide, a high light-induced beta-carotene derivative that can regulate gene expression and photoacclimation in Arabidopsis, Mol. Plant 7 (2014) 1248–1251.
[5] A. Strand, T. Asami, J. Alonso, J.R. Ecker, J. Chory, Chloroplast to nucleus communication triggered by accumulation of Mg-protoporphyrinIX, Nature 421 (2003) 79–83.
[6] J.D. Woodson, J.M. Perez-Ruiz, J. Chory, Heme synthesis by plastid Ferrochelatase I regulates nuclear gene expression in plants, Curr. Biol. 21 (2011) 897–903.
[7] L. Heinrichs, J. Schmitz, U.I. Flugge, R.E. Hausler, The mysterious rescue of adg1-1/tpt-2 - an *Arabidopsis thaliana* double mutant impaired in acclimation to high light - by exogenously supplied sugars, Front. Plant Sci. 3 (2012) 265.
[8] M.O. Vogel, M. Moore, K. Konig, P. Pecher, K. Alsharafa, J. Lee, K.J. Dietz, Fast retrograde signaling in response to high light involves metabolite export, MITOGEN-ACTIVATED PROTEIN KINASE6, and AP2/ERF transcription factors in Arabidopsis, Plant Cell 26 (2014) 1151–1165.
[9] Y.M. Xiao, T. Savchenko, E.E.K. Baidoo, W.E. Chehab, D.M. Hayden, V. Tolstikov, J.A. Corwin, D.J. Kliebenstein, J.D. Keasling, K. Dehesh, Retrograde signaling by the plastidial metabolite MEcPP regulates expression of nuclear stress-response genes, Cell 149 (2012) 1525–1535.
[10] G.M. Estavillo, P.A. Crisp, W. Pornsiriwong, M. Wirtz, D. Collinge, C. Carrie, E. Giraud, J. Whelan, P. David, H. Javot, C. Brearley, R. Hell, E. Marin, B.J. Pogson, Evidence for a SAL1-PAP chloroplast retrograde pathway that functions in drought and high light signaling in Arabidopsis, Plant Cell 23 (2011) 3992–4012.
[11] S. Bolazadeh, N. Jaspert, M. Arif, B. Mueller-Roeber, V.G. Maurino, Expression of ROS-responsive genes and transcription factors after metabolic formation of H_2O_2 in chloroplasts, Front Plant Sci. 3 (2012) 234.
[12] T. Maruta, M. Noshi, A. Tanouchi, M. Tamoi, Y. Yabuta, K. Yoshimura, T. Ishikawa, S. Shigeoka, H_2O_2-triggered retrograde signaling from chloroplasts to nucleus plays specific role in response to stress, J. Biol. Chem. 287 (2012) 11717–11729.
[13] K.X. Chan, S.Y. Phua, P. Crisp, R. McQuinn, B.J. Pogson, Learning the languages of the chloroplast: Retrograde signaling and beyond, Annu. Rev. Plant Biol. Vol 67 (67) (2016) 25 (+).
[14] R. Mittler, ROS are good, Trends Plant Sci. 22 (2017) 11–19.
[15] G. Noctor, C.H. Foyer, Intracellular redox compartmentation and ROS-related communication in regulation and signaling, Plant Physiol. 171 (2016) 1581–1592.
[16] C. Pucciella, A. Paradiso, M.C. de Pinto, Cellular redox homeostasis as central modulator in plant stress response, in: D.K. Gupta, J.M. Palma, F.J. Corpas (Eds.), Redox State as a Central Regulator of Plant-Cell Stress Responses, Springer International Publishing, Cham, 2016, pp. 1–23.
[17] K. Asada, Production and scavenging of reactive oxygen species in chloroplasts and their functions, Plant Physiol. 141 (2006) 391–396.
[18] C.H. Foyer, G. Noctor, Redox Signaling in Plants, Antioxid. Redox Sign. 18 (2013) 2087–2090.
[19] K.J. Dietz, Peroxiredoxins in plants and cyanobacteria, Antioxid. Redox Sign. 15 (2011) 1129–1159.
[20] K. Bela, E. Horvath, A. Galle, L. Szabados, I. Tari, J. Csiszar, Plant glutathione peroxidases: Emerging role of the antioxidant enzymes in plant development and stress responses, J. Plant Physiol. 176 (2015) 192–201.
[21] P. Pesaresi, A. Schneider, T. Kleine, D. Leister, Interorganellar communication, Curr. Opin. Plant Biol. 10 (2007) 600–606.
[22] V. Locato, S. Cimini, L. De Gara, ROS and redox balance as multifaceted players of cross-tolerance: Epigenetic and retrograde control of gene expression, J. Exp. Bot. 69 (2018) 3373–3391.
[23] C. Kim, ROS-driven oxidative modification: Its impact on chloroplasts-nucleus communication, Front. Plant Sci. 10 (2020) 1729.
[24] J. Mielecki, P. Gawronski, S. Karpinski, Retrograde signaling: Understanding the communication between organelles, Int. J. Mol. Sci. 21 (2020) 6173.
[25] B. Karpinska, S.O. Alomrani, C.H. Foyer, Inhibitor-induced oxidation of the nucleus and cytosol in *Arabidopsis thaliana*: implications for organelle to nucleus retrograde signalling, Philos. T. R. Soc. B 372 (2017), 20160392.
[26] R.E. Susek, F.M. Ausubel, J. Chory, Signal-transduction mutants of Arabidopsis uncouple nuclear cab and rbcs gene-expression from chloroplast development, Cell 74 (1993) 787–799.
[27] N. Mochizuki, J.A. Brusslan, R. Larkin, A. Nagatani, J. Chory, Arabidopsis Genomes Uncoupled 5 (GUN5) mutant reveals the involvement of Mg-chelatase H subunit in plastid-to-nucleus signal transduction, P. Natl. Acad. Sci. USA 98 (2001) 2053–2058.
[28] R.M. Larkin, J.M. Alonso, J.R. Ecker, J. Chory, GUN4, a regulator of chlorophyll synthesis and intracellular signaling, Science 299 (2003) 902–906.
[29] S. Koussevitzky, A. Nott, T.C. Mockler, F. Hong, G. Sachetto-Martins, M. Surpin, J. Lim, R. Mittler, J. Chory, Signals from chloroplasts converge to regulate nuclear gene expression, Science 316 (2007) 715–719.
[30] D. Moreira, H. Philippe, Smc: A bacterial and eukaryotic homologue of the C-terminal region of the Mut52 family, Trends Biochem. Sci. 24 (1999) 298–300.
[31] E. Kotera, M. Tasaka, T. Shikanai, A pentatricopeptide repeat protein is essential for RNA editing in chloroplasts, Nature 433 (2005) 326–330.
[32] L. Tadini, P. Pesaresi, T. Kleine, F. Rossi, A. Guljamow, F. Sommer, T. Muhlhaus, M. Schroda, S. Masiero, M. Pribil, M. Rothbart, B. Hedtke, B. Grimm, D. Leister, GUN1 controls accumulation of the plastid ribosomal protein S1 at the protein level and interacts with proteins involved in plastid protein homeostasis, Plant Physiol. 170 (2016) 1817–1830.
[33] G.Z. Wu, E.H. Meyer, A.S. Richter, M. Schuster, Q.H. Ling, M.A. Schottler, D. Walther, R. Zoschke, B. Grimm, R.P. Jarvis, R. Bock, Control of retrograde signalling by protein import and cytosolic folding stress, Nat. Plants 5 (2019) 525–538.
[34] L. Tadini, N. Jeran, P. Pesaresi, GUN1 and Plastid RNA metabolism: Learning from genetics, Cells 9 (2020) 2307.
[35] T. Shimizu, T. Masuda, The role of tetrapyrrole- and GUN1-dependent signaling on chloroplast biogenesis, Plants-Basel 10 (2021) 196.
[36] G.Z. Wu, R. Bock, GUN control in retrograde signaling: How GENOMES UNCOUPLED proteins adjust nuclear gene expression to plastid biogenesis, Plant Cell 33 (2021) 457–474.
[37] G.Z. Wu, C. Chalvin, M. Hoelscher, E.H. Meyer, X.N. Wu, R. Bock, Control of retrograde signaling by rapid turnover of GENOMES UNCOUPLED1, Plant Physiol. 176 (2018) 2472–2495.
[38] E. Llamas, P. Pulido, M. Rodriguez-Concepcion, Interference with plastome gene expression and Clp protease activity in Arabidopsis triggers a chloroplast unfolded protein response to restore protein homeostasis, PLoS Genet. 13 (2017), e1007022.
[39] M. Colombo, L. Tadini, C. Peracchio, R. Ferrari, P. Pesaresi, GUN1, a Jack-of-all-trades in chloroplast protein homeostasis and signaling, Front Plant Sci. 7 (2016) 1427.
[40] N. Jambunathan, Determination and detection of reactive oxygen species (ROS), lipid peroxidation, and electrolyte leakage in plants, in: R. Sunkar (Ed.), Plant

Stress Tolerance: Methods and Protocols, Humana Press, Totowa, NJ, 2010, pp. 291–297.
[41] A. Paradiso, S. Berardino, M.C. de Pinto, L. Sanita di Toppi, M.M. Storelli, F. Tommasi, L. De Gara, Increase in ascorbate-glutathione metabolism as local and precocious systemic responses induced by cadmium in durum wheat plants, Plant Cell Physiol. 49 (2008) 362–374.
[42] M.C. Romero-Puertas, J.M. Palma, M. Gomez, L.A. Del Rio, L.M. Sandalio, Cadmium causes the oxidative modification of proteins in pea plants, Plant Cell Environ. 25 (2002) 677–686.
[43] L. De Gara, M.C. de Pinto, V.M.C. Moliterni, M.G. D'Egidio, Redox regulation and storage processes during maturation in kernels of *Triticum durum*, J. Exp. Bot. 54 (2003) 249–258.
[44] M.C. de Pinto, D. Francis, L. De Gara, The redox state of the ascorbate-dehydroascorbate pair as a specific sensor of cell division in tobacco BY-2 cells, Protoplasma 209 (1999) 90–97.
[45] M.M. Bradford, A rapid and sensitive method for the quantitation of microgram quantities of protein utilizing the principle of protein-dye binding, Anal. Biochem. 72 (1976) 248–254.
[46] A. Paradiso, G. Domingo, E. Blanco, A. Buscaglia, S. Fortunato, M. Marzoni, P. Scarcia, S. Caretto, C. Vannini, M.C. de Pinto, Cyclic AMP mediates heat stress response by the control of redox homeostasis and ubiquitin-proteasome system, Plant Cell Environ. 43 (2020) 2727–2742.
[47] A. Villani, F. Tommasi, C. Paciolla, The arbuscular mycorrhizal fungus *Glomus viscosum* improves the tolerance to verticillium wilt in artichoke by modulating the antioxidant defense systems, Cells 10 (2021) 1944.
[48] M.C. de Pinto, F. Tommasi, L. De Gara, Enzymes of the ascorbate biosynthesis and ascorbate-glutathione cycle in cultured cells of tobacco Bright Yellow 2, Plant Physiol. Biochem. 38 (2000) 541–550.
[49] D. Nigro, S. Fortunato, S.L. Giove, A. Paradiso, V.Q. Gu, A. Blanco, M.C. de Pinto, A. Gadaleta, Glutamine synthetase in durum wheat: genotypic variation and relationship with grain protein content, Front. Plant Sci. 7 (2016) 971.
[50] M.E. Ruckle, S.M. DeMarco, R.M. Larkin, Plastid signals remodel light signaling networks and are essential for efficient chloroplast biogenesis in Arabidopsis, Plant Cell 19 (2007) 3944–3960.
[51] P. Sharma, A.B. Jha, R.S. Dubey, M. Pessarakli, Reactive oxygen species, oxidative damage, and antioxidative defense mechanism in plants under stressful conditions, J. Bot. 2012 (2012), 217037.
[52] E.E. Farmer, M.J. Mueller, ROS-mediated lipid peroxidation and RES-activated signaling, Annu. Rev. Plant Biol. 64 (2013) 429–450.
[53] L.A. del Rio, F.J. Corpas, E. Lopez-Huertas, J.M. Palma, Plant superoxide dismutases: function under abiotic stress conditions, in: D.K. Gupta, J.M. Palma, F. J. Corpas (Eds.), Antioxidants and Antioxidant Enzymes in Higher Plants, Springer International Publishing, Cham, 2018, pp. 1–26.
[54] W. Wang, M.X. Xia, J. Chen, R. Yuan, F.N. Deng, F.F. Shen, Gene Expression Characteristics and Regulation Mechanisms of Superoxide Dismutase and Its Physiological Roles in Plants under Stress, in: Biochemistry, Springer Nature Switzerland AG, Moscow, 2016, pp. 465–480 ( ).
[55] E. Szymanska, I. Slesak, A. Orzechowska, J. Kruk, Physiological and biochemical responses to high light and temperature stress in plants, Environ. Exp. Bot. 139 (2017) 165–177.
[56] T. Maruta, A. Tanouchi, M. Tamoi, Y. Yabuta, K. Yoshimura, T. Ishikawa, S. Shigeoka, Arabidopsis chloroplastic ascorbate peroxidase isoenzymes play a dual role in photoprotection and gene regulation under photooxidative stress, Plant Cell Physiol. 51 (2010) 190–200.
[57] N. Mochizuki, R. Susek, J. Chory, An intracellular signal transduction pathway between the chloroplast and nucleus is involved in de-etiolation, Plant Physiol. 112 (1996) 1465–1469.
[58] N. Jeran, L. Rotaperti, G. Frabetti, A. Calabritto, P. Pesaresi, L. Tadini, The PUB4 E3 ubiquitin ligase is responsible for the variegated phenotype observed upon alteration of chloroplast protein homeostasis in Arabidopsis cotyledons, Genes-Basel 12 (2021) 1387.
[59] L. Tadini, C. Peracchio, A. Trotta, M. Colombo, I. Mancini, N. Jeran, A. Costa, F. Faoro, M. Marzoni, C. Vannini, E.M. Aro, P. Pesaresi, GUN1 influences the accumulation of NEP-dependent transcripts and chloroplast protein import in Arabidopsis cotyledons upon perturbation of chloroplast protein homeostasis, Plant J. 101 (2020) 1198–1220.
[60] X. Zhao, J. Huang, J. Chory, Genome Uncoupled1 mutants are hypersensitive to norflurazon and lincomycin, Plant Physiol. 178 (2018) 960–964.
[61] P. Mulo, S. Pursiheimo, C.X. Hou, T. Tyystjarvi, E.M. Aro, Multiple effects of antibiotics on chloroplast and nuclear gene expression, Funct. Plant Biol. 30 (2003) 1097–1103.
[62] N. Smirnoff, D. Arnaud, Hydrogen peroxide metabolism and functions in plants, N. Phytol. 221 (2019) 1197–1214.
[63] J.D. Woodson, J. Chory, Coordination of gene expression between organellar and nuclear genomes, Nat. Rev. Genet. 9 (2008) 383–395.
[64] D. Leister, Piecing the puzzle together: The central role of reactive oxygen species and redox hubs in chloroplast retrograde signaling, Antioxid. Redox Sign. 30 (2019) 1206–1219.
[65] K.J. Dietz, I. Turkan, A. Krieger-Liszkay, Redox and reactive oxygen species-dependent signaling into and out of the photosynthesizing chloroplast, Plant Physiol. 171 (2016) 1541–1550.
[66] M. Baier, K.J. Dietz, Chloroplasts as source and target of cellular redox regulation: A discussion on chloroplast redox signals in the context of plant physiology, J. Exp. Bot. 56 (2005) 1449–1462.
[67] D. Leister, Genomics-based dissection of the cross-talk of chloroplasts with the nucleus and mitochondria in Arabidopsis, Gene 354 (2005) 110–116.
[68] H. Tanaka, T. Maruta, M. Tamoi, Y. Yabuta, K. Yoshimura, T. Ishikawa, S. Shigeoka, Transcriptional control of vitamin C defective 2 and tocopherol cyclase genes by light and plastid-derived signals: The partial involvement of GENOMES UNCOUPLED 1, Plant Sci. 231 (2015) 29–29.
[69] F. Horling, P. Lamkemeyer, J. Konig, I. Finkemeier, A. Kandlbinder, M. Baier, K. J. Dietz, Divergent light-, ascorbate-, and oxidative stress-dependent regulation of expression of the peroxiredoxin gene family in Arabidopsis, Plant Physiol. 131 (2003) 317–325.
[70] G.M. Pastori, G. Kiddle, J. Antoniw, S. Bernard, S. Veljovic-Jovanovic, P.J. Verrier, G. Noctor, C.H. Foyer, Leaf vitamin C contents modulate plant defense transcripts and regulate genes that control development through hormone signaling, Plant Cell 15 (2003) 939–951.
[71] S. Veljović Jovanović, B. Kukavica, M. Vidović, F. Morina, L. Menckhoff, Class III peroxidases: Functions, localization and redox regulation of isoenzymes, in: D. K. Gupta, J.M. Palma, F.J. Corpas (Eds.), Antioxidants and Antioxidant Enzymes in Higher Plants, Springer International Publishing, Cham, 2018, pp. 269–300.

genes

MDPI

Article

The PUB4 E3 Ubiquitin Ligase Is Responsible for the Variegated Phenotype Observed upon Alteration of Chloroplast Protein Homeostasis in Arabidopsis Cotyledons

Nicolaj Jeran †, Lisa Rotasperti †, Giorgia Frabetti, Anna Calabritto, Paolo Pesaresi and Luca Tadini *

Dipartimento di Bioscienze, Università degli Studi di Milano, 20133 Milano, Italy; nicolaj.jeran@unimi.it (N.J.); lisa.rotasperti@unimi.it (L.R.); giorgia.frabetti@studenti.unimi.it (G.F.); anna.calabritto@studenti.unimi.it (A.C.); paolo.pesaresi@unimi.it (P.P.)

* Correspondence: luca.tadini@unimi.it

† These authors equally contributed to the article.

Abstract: During a plant's life cycle, plastids undergo several modifications, from undifferentiated pro-plastids to either photosynthetically-active chloroplasts, ezioplasts, chromoplasts or storage organelles, such as amyloplasts, elaioplasts and proteinoplasts. Plastid proteome rearrangements and protein homeostasis, together with intracellular communication pathways, are key factors for correct plastid differentiation and functioning. When plastid development is affected, aberrant organelles are degraded and recycled in a process that involves plastid protein ubiquitination. In this study, we have analysed the Arabidopsis *gun1-102 ftsh5-3* double mutant, lacking both the plastid-located protein GUN1 (Genomes Uncoupled 1), involved in plastid-to-nucleus communication, and the chloroplast-located *FTSH5* (Filamentous temperature-sensitive H5), a metalloprotease with a role in photosystem repair and chloroplast biogenesis. *gun1-102 ftsh5-3* seedlings show variegated cotyledons and true leaves that we attempted to suppress by introgressing second-site mutations in genes involved in: (i) plastid translation, (ii) plastid folding/import and (iii) cytosolic protein ubiquitination. Different phenotypic effects, ranging from seedling-lethality to partial or complete suppression of the variegated phenotype, were observed in the corresponding triple mutants. Our findings indicate that Plant U-Box 4 (PUB4) E3 ubiquitin ligase plays a major role in the target degradation of damaged chloroplasts and is the main contributor to the variegated phenotype observed in *gun1-102 ftsh5-3* seedlings.

Keywords: chloroplast; ubiquitination; variegated phenotype; protein homeostasis

Citation: Jeran, N.; Rotasperti, L.; Frabetti, G.; Calabritto, A.; Pesaresi, P.; Tadini, L. The PUB4 E3 Ubiquitin Ligase Is Responsible for the Variegated Phenotype Observed upon Alteration of Chloroplast Protein Homeostasis in Arabidopsis Cotyledons. *Genes* **2021**, *12*, 1387. https://doi.org/10.3390/genes12091387

Academic Editors: Paola Vittorioso, Ignacio Ezquer and Stefan de Folter

Received: 13 August 2021
Accepted: 3 September 2021
Published: 6 September 2021

1. Introduction

Albinotic and variegated mutants have been widely used to investigate chloroplast biogenesis and the communication pathways between the nuclear-cytosolic compartment and chloroplasts [1–3]. Among these, Arabidopsis *ftsh5* (*var1*) and *ftsh2* (*var2*) mutants, devoid of two subunits of the thylakoid transmembrane metalloprotease complex *FTSH* (Filamentation Temperature Sensitive protein H), responsible for photosystem II (PSII) biogenesis and repair, and characterized by a leaf variegated phenotype, contributed greatly in revealing the strict link between chloroplast protein homeostasis and proper chloroplast biogenesis [4–8]. Transmission electron microscopy analyses of *ftsh2* and *ftsh5* leaves revealed, indeed, correctly-shaped chloroplasts in the green sectors, while the white sectors showed miss-shaped plastids with highly vacuolated organelle structures [6,9]. Furthermore, second-site suppressor screens aimed to identify mutations able to suppress the *ftsh* leaf variegated phenotype, so-called Suppressors of Variegation (SVR), allowed the identification of several nuclear genes encoding plastid-located proteins mostly involved in rRNA maturation, translation, protein folding and protein degradation [3,10–14]. Overall, these findings indicated that the differentiation of functional chloroplasts requires an

optimal balance between the rate of plastid protein synthesis and the activity of the plastid protein quality control machinery [15].

Recently, the variegated phenotype was also observed in cotyledons of *ftsh2* and *ftsh5* seedlings upon introgression of the *gun1* knock-out mutation (for further details see Tadini et al. [16]). GUN1 is a chloroplast-localized pentatricopeptide repeat (PPR) protein required during the early stages of chloroplast biogenesis and upon alterations of plastid gene expression and chloroplast protein homeostasis [16–21]. In particular, *gun1 ftsh2* cotyledons are characterized by the presence of highly vacuolated plastids, without any traces of thylakoid membranes, while *gun1 ftsh5* cotyledons show a less severe albino-variegated phenotype and possess cells with either functional chloroplasts or plastids with budding vesicles, an evidence of the ongoing plastid degradation process [16].

Recent studies have highlighted that the ubiquitin-dependent modification of proteins located on the chloroplast outer membrane is a pivotal event, at the basis of chloroplast adaptation to stress conditions, involving either targeted protein removal through the ubiquitin–proteasome system, or selective, whole-chloroplast degradation, based on the severity of the chloroplast damages [22–24]. Suppressor of PPI1 locus1 (SP1) and Plant U-Box 4 (PUB4) are the two main E3 ubiquitin ligases reported to be involved in chloroplast ubiquitination, so far [22,24,25]. SP1 is embedded in the outer envelope of the chloroplast and, by ubiquitination of Translocon of Outer membrane of Chloroplast (TOC) components, confers the ability to isolate the chloroplasts from the bulk of plastid precursor proteins in the cytoplasm, thus modulating the quantity and the quality of the imported pre-proteins [22,23,26]. On the other hand, PUB4 is soluble in the cytoplasm and acts on still unidentified proteins located on the chloroplast outer envelope, serving to target damaged chloroplasts for degradation in response to ROS stress. This would provide a chloroplast quality control mechanism to reduce the risk of further ROS accumulation [24,27].

In this work we attempted to suppress the variegated phenotype of *gun1-102 ftsh5-3* cotyledons through the introgression of additional mutations in nuclear genes, encoding proteins with roles in: (i) plastid translation, (ii) plastid folding/import and (iii) cytosolic protein ubiquitination. We demonstrated that the introgression of *pub4-7* mutation into the *gun1-102 ftsh5-3* genetic background suppresses the variegated phenotype of *gun1-102 ftsh5-3* cotyledons. In particular, the degenerating *gun1-102 ftsh5-3* plastids are replaced by functional chloroplasts in *gun1-102 ftsh5-3 pub4-7* cotyledons, indicating that the PUB4-dependendent chloroplast quality control mechanism is active in *gun1-102 ftsh5-3* cotyledons and is at the basis of the variegated phenotype.

2. Materials and Methods

2.1. Plant Material and Growth Conditions

Arabidopsis (*Arabidopsis thaliana*, genetic background Col-0) wild-type and mutant seeds were grown on soil in a climate chamber under long-day conditions (16 h at 100 µmol photons m^{-2} s^{-1} light and 8 h dark, at 22 °C temperature). Genetic loci and T-DNA flanking regions of insertional mutant lines used in this work are described in Figure S1. Primer sequences for genotype determination are listed in Table S1. Multiple mutants were generated by manual crossing and identified by PCR-based segregation analyses of F2 populations, with the only exception being the *gun1-102 ftsh5-3 pub4-7* mutant, where the *pub4-7* mutant allele was generated using the CRISPR-Cas9 genome editing strategy. In particular, the *gun1-102 ftsh5-3 pub4-7* triple mutant was generated by targeting the fourth exon of the *PUB4* locus in the *gun1-102 ftsh5-3* mutant background using the pHEE401E vector described by Xing et al. [28]. Mutant plants carrying the mutation of interest and devoid of the Cas9 endonuclease were selected in the T3 generation. Primer sequences used for guide RNA design are listed in Table S1. Cotyledon and leaf area were determined by the ImageJ software (http://imagej.nih.gov/ij/index.html, accessed on 15 August 2021). The Variegation Index (V.I.) was calculated as the ratio of green area over the total area of the organ.

2.2. Chlorophyll Fluorescence Measurements and Chlorophyll Quantification

The imaging Chl fluorometer (Walz Imaging PAM; https://walz.com/, accessed on 15 August 2021) was used to measure in vivo Chl a fluorescence. Six plants of each genotype were analyzed at 6 and 12 days after sowing (DAS) and average values plus-minus standard deviations were calculated. Dark-adapted plants were exposed to blue measuring beam (intensity 4) and a saturating light flash (intensity 4) to obtain the maximum quantum yield of PSII, *Fv/Fm*. A 5-min exposure to actinic light (36 µmol photons m^{-2} s^{-1}) allowed for the calculation of the effective quantum yield of PSII, Y_{II}. For Chl quantification, 100 mg (fresh weight) of 6 DAS seedlings were ground in liquid nitrogen and extracted in 90% acetone. Chlorophyll (Chl) a and b concentrations were measured according to Porra et al. [29]. Measurements were performed in triplicate.

2.3. Transmission Electron Microscopy (TEM) Analyses

For TEM observations, tissue samples from fully expanded cotyledons of Col-0, *ftsh5-3*, *pub4-2* and *gun1-102 ftsh5-3 pub4-7* seedlings were prepared according to Tadini et al. [16]. In particular, 6 DAS seedlings were fixed in 3.3% (*v/v*) paraformaldehyde and 1.2% (*v/v*) glutaraldehyde in 0.1 M phosphate buffer (pH 7.4) at 4 °C for 2 h and post-fixed in 1% OsO_4 in the same buffer for 2 h. Samples were then dehydrated in an ethanol series and embedded in Spurr's resin. Ultrathin sections were stained with 2% uranyl acetate and lead citrate and observed with a Jeol 100SX TEM (Jeol; https://www.jeol.co.jp/, accessed on 15 August 2021) operating at 80 KV.

2.4. Quantitative Real-Time PCR (qRT-PCR) Analyses

Total RNA was isolated from 6 DAS Col-0 and mutant seedlings. For qRT-PCR analyses, 1 µg of total RNA was treated with iScript™ gDNA Clear cDNA Synthesis Kit (Bio-Rad; https://www.bio-rad.com/, accessed on 15 August 2021) for genomic DNA digestion and first-strand cDNA synthesis. qRT-PCR analyses were performed on a CFX96 Real-Time system (Bio-Rad; https://www.bio-rad.com/, accessed on 15 August 2021) using primer pairs listed in Table S1. *PP2AA3* (*AT1G13320*) transcripts were used as internal reference, as described [30]. Data obtained from three biological and three technical replicates for each sample were analyzed with the Bio-Rad CFX Maestro 1.1 (v 4.1) (Bio-Rad; https://www.bio-rad.com/, accessed on 15 August 2021).

2.5. Protein Sample Preparation and Immunoblot Analyses

For immunoblot analyses, cotyledons from 6 DAS seedlings were homogenized in Laemmli sample buffer (20% [*v/v*] glycerol, 4% [*w/v*] SDS, 160 mM Tris-HCl pH 6.8, 10% [*v/v*] 2-mercaptoethanol) to a final concentration of 0.1 mg μL^{-1} (fresh weight/Laemmli sample buffer). Samples were incubated at 65 °C for 15 min and, after a centrifugation step at 16,000× *g* for 10 min, the supernatant was incubated at 95 °C for 5 min. Protein extracts corresponding to 4 mg (fresh-weight) seedlings were loaded onto SDS–PAGE (10% [*w/v*] acrylamide) gels and transferred to polyvinylidene-difluoride (PVDF) filters (0.20 µm pore size). Replicate membranes were immuno-decorated with specific antibodies.

Intact chloroplasts were isolated from 100 mg (fresh weight) 6 DAS seedlings according to Kunst [31], with a few changes. Samples were homogenized in 1 mL of 45 mM sorbitol, 20 mM Tricine-KOH pH 8.4, 10 mM EDTA, 10 mM $NaHCO_3$ and 0.1% (*w/v*) BSA fraction V, supplemented with proteinase inhibitor cocktail (cOmplete™, COEDTAF-RO, Roche; https://www.roche.com/, accessed on 15 August 2021), and centrifuged for 7 min at 700× *g*. The supernatant was discarded, while the pellet was washed twice with 1 mL of homogenization buffer. After a centrifugation step (7 min at 700× *g*), the pellet was collected as the intact chloroplast fraction. The level of signals was quantified by the ImageJ software (http://imagej.nih.gov/ij/index.html, accessed on 15 August 2021).

Antibodies specific for LHCB5 (AS01 009), VIPP1 (AS06 145), CLPB3 (AS09 459), cpHSC70-1 (AS08 348), CPN60 (AS12 2613), HSP90-1 (AS08 346) and UBQ11 (AS08 307A) were obtained from Agrisera (https://www.agrisera.com/, accessed on 15 August 2021).

The HSC70-4 antibody was purchased from Antibodies-online (https://www.antibodies-online.com/, accessed on 15 August 2021).

2.6. Accession Numbers

The Arabidopsis Genome Initiative accession numbers for the genes mentioned in this work can be found at TAIR (https://www.arabidopsis.org/, accessed on 15 August 2021): *GUN1* (*AT2G31400*), *FTSH5* (*AT5G42270*), *FUG1* (*AT1G17220*), *PRPS21* (*AT3G27160*), *cpHSC70-1* (*AT4G24280*), *SP1* (*AT1G63900*), *PUB4* (*AT2G23140*), *PP2AA3* (*AT1G13320*) and *HSFA2* (*AT2G26150*).

3. Results

3.1. The Cytosolic E3 Ubiquitin Ligase PUB4 Is Responsible for the Variegated Phenotype Observed in Cotyledons and Leaves of gun1-102 ftsh5-3 Seedlings

To dissect the molecular mechanisms responsible for the variegated phenotype observed in *gun1-102 ftsh5-3* cotyledons and true leaves, as a consequence of chloroplast protein homeostasis perturbation ([16]; Figures 1a and 2a), we introgressed mutations in genes involved in: (i) plastid translation, *fug1-3* and *prps21-1* [32,33]; (ii) plastid protein folding/import, *cphsc70-1* [34,35]; (iii) cytosolic protein ubiquitination, *sp1-3* and *pub4-7* [22,24] (see Figure S1 and Table 1), with the aim of identifying Arabidopsis triple mutants able to suppress the *gun1-102 ftsh5-3* double mutant phenotype. The large majority of the mutations investigated are caused by T-DNA insertions in the transcribed regions of the genes of interest, resulting in knock-out alleles. The only exception is represented by *fug1-3* knock-down allele caused by a T-DNA insertion in the promoter region of *At1g17220* locus (see Figure S1). Moreover, since the *PUB4* and *GUN1* loci are located on adjacent regions of chromosome 2, the *PUB4* gene was silenced in the *gun1-102 ftsh5-3* genetic background by using the CRISPR-Cas9 gene editing strategy. In particular, the *pub4-7* allele is due to a frameshift mutation caused by the insertion of a Thymine in the fourth exon of the *At2g23140* gene, in position +1804 from the transcription starting site (see Figure S1).

Table 1. List of mutant lines analysed in this study. Gene names, AGI accession numbers, subcellular localization of the gene products, functions and references where mutant alleles have been described are included.

Gene Name	AGI Code	Subcellular Localization	Allele	Function
GUN1	At2g31400	chloroplast stroma	*gun1-102* [19]	PPR protein involved in chloroplast-to-nucleus communication and maintenance of plastid protein homeostasis [16–18,20].
FTSH5	At5g42270	chloroplast thylakoids	*ftsh5-3* [19]	Transmembrane protease involved in thylakoid biogenesis and PSII maintenance by removal of damaged D1 subunit [6].
FUG1	At1g17220	chloroplast stroma	*fug1-3* [32]	Initiation factor essential for plastid protein translation [32].
PRPS21	At3g27160	chloroplast stroma	*prps21-1* [19]	Structural component of the 30S plastid ribosome subunit [36].
cpHSC70-1	At4g24280	chloroplast stroma	*cphsc70-1* [34]	Plastid chaperone involved in protein import and folding processes [34].
SP1	At1g63900	cytosolic side of the plastid outer envelope	*sp1-3* [22]	E3 ubiquitin ligase involved in the regulation of plastid protein import and component of CHLORAD, i.e., ubiquitination and retro-translocation of outer membrane proteins for proteasome-dependent degradation [22].
PUB4	At2g23140	cytosol	*pub4-2* [24] *pub4-7* [This work]	E3 ubiquitin ligase associated with the selective degradation of ROS-damaged chloroplasts [24].

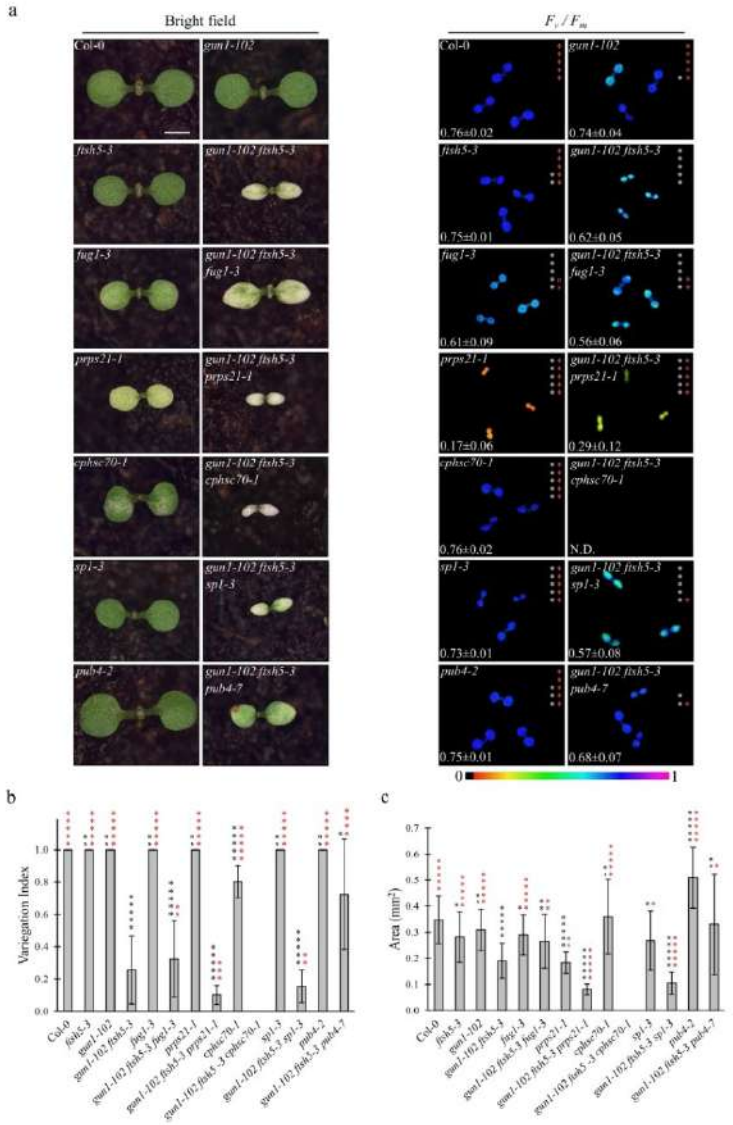

Figure 1. Visible phenotypic characteristics and photosynthetic performance of Arabidopsis Col-0 and mutant seedlings at

cotyledon stage. (**a**) Visible phenotypes and maximum quantum yield of PSII (F_v/F_m) of Col-0, *gun1-102*, *ftsh5-3*, *gun1-102 ftsh5-3*, *fug1-3*, *gun1-102 ftsh5-3 fug1-3*, *prps21-1*, *gun1-102 ftsh5-3 prps21-1*, *cphsc70-1*, *gun1-102 ftsh5-3 cphsc70-1*, *sp1-3*, *gun1-102 ftsh5-3 sp1-3*, *pub4-2*, *gun1-102 ftsh5-3 pub4-7* cotyledons at six days after sowing (DAS) grown on soil. Scale bar corresponds to 1 mm. F_v/F_m parameter was measured through the IMAGING PAM Fluorimeter (Walz) and reported both in false colour (black equals to 0, violet to 1) and as average ± standard deviation of six independent measurements; N.D.: not detected. Asterisks indicate statistical significance with respect to Col-0 (white) or *gun1-102 ftsh5-3* (red) as evaluated by Student's *t*-test and Welch correction (* $p < 0.05$; ** $p < 0.01$; *** $p < 0.001$; **** $p < 0.0001$; ***** $p < 0.00001$; ns: not significant). (**b**) Average Variegation Index (V.I.) calculated as ratio between the green area over the total area of the cotyledon of Col-0 and mutant seedlings grown on soil at 6 DAS. Error bars indicate standard deviations of at least six independent measurements. Asterisks indicate statistical significance with respect to Col-0 (black) or gun1-102 ftsh5-3 (red) as evaluated by Student's t-test and Welch correction (* $p < 0.05$; ** $p < 0.01$; *** $p < 0.001$; **** $p < 0.0001$; ***** $p < 0.00001$; ns: not significant). (**c**) Average area in mm^2 of single cotyledons of the indicated genotypes grown on soil at 6 DAS. Error bars indicate standard deviations of at least six independent measurements. Asterisks indicate statistical significance with respect to Col-0 (black) or *gun1-102 ftsh5-3* (red) as evaluated by Student's *t*-test and Welch correction (* $p < 0.05$; ** $p < 0.01$; *** $p < 0.001$; **** $p < 0.0001$; ***** $p < 0.00001$; ns: not significant).

The obtained triple mutants were analysed at 6 DAS (Figure 1) and 12 DAS (Figure 2) to evaluate the Variegation Index (V.I.; see also Materials and Methods) and the total organ area in cotyledons and the first true leaves (Figures 1b,c and 2b,c). Furthermore, the functionality of chloroplasts was also assessed by determining their photosynthetic performance through the measurement of F_v/F_m (Maximum quantum yield of PSII) and Y_{II} (Effective quantum yield of PSII) parameters (Figures 1a, 2a and S2a), (b). Strikingly, the *gun1-102 ftsh5-3 pub4-7* triple mutant was the only one showing a marked improvement of all the considered parameters at 6 and 12 DAS.

The significant increase in V.I. in both cotyledons and leaves, as well as the higher values of both F_v/F_m and Y_{II} parameters, together with the increased total area of both cotyledons and first true leaves (see Figures 1c and 2c), indicated that the *pub4-7* allele in *gun1-102 ftsh5-3 pub4-7* seedlings was the only second-site mutation able to suppress the variegated phenotype of *gun1-102 ftsh5-3* cotyledons and leaves. Indeed, *gun1-102 ftsh5-3 prps21-1* seedlings showed an even exacerbated phenotype in terms of V.I. and photosynthetic performance at the cotyledon stage, while the *gun1-102 ftsh5-3 cphsc70-1* triple mutant exhibited seedling lethality. In the latter case, the few seedlings able to germinate showed reduced white cotyledons virtually devoid of chloroplasts, as their photosynthetic parameters were undetectable. Only in the case of *gun1-102 ftsh5-3 sp1-3* and *gun1-102 ftsh5-3 fug1-3* cotyledons was the non-additive effect observed in terms of variegation and photosynthetic parameters. However, the total area of cotyledons slightly increased in *gun1-102 ftsh5-3 fug1-3*. Conversely, introgression of *sp1-3* led to a small but significant reduction in cotyledon size while, at 12 DAS, the first true leaves of *gun1-102 ftsh5-3 sp1-3* plants were notably smaller than those of *gun1-102 ftsh5-3*. Interestingly, *gun1-102 ftsh5-3 prps21-1* and *gun1-102 ftsh5-3 fug1-3* true leaves showed a statistically significant increase in V.I. in comparison with the leaves of *gun1-102 ftsh5-3* double mutant, indicating that both the plastid protein synthesis rate and cytosolic protein ubiquitination could contribute to the onset of leaf variegation, upon perturbation of chloroplast protein homeostasis.

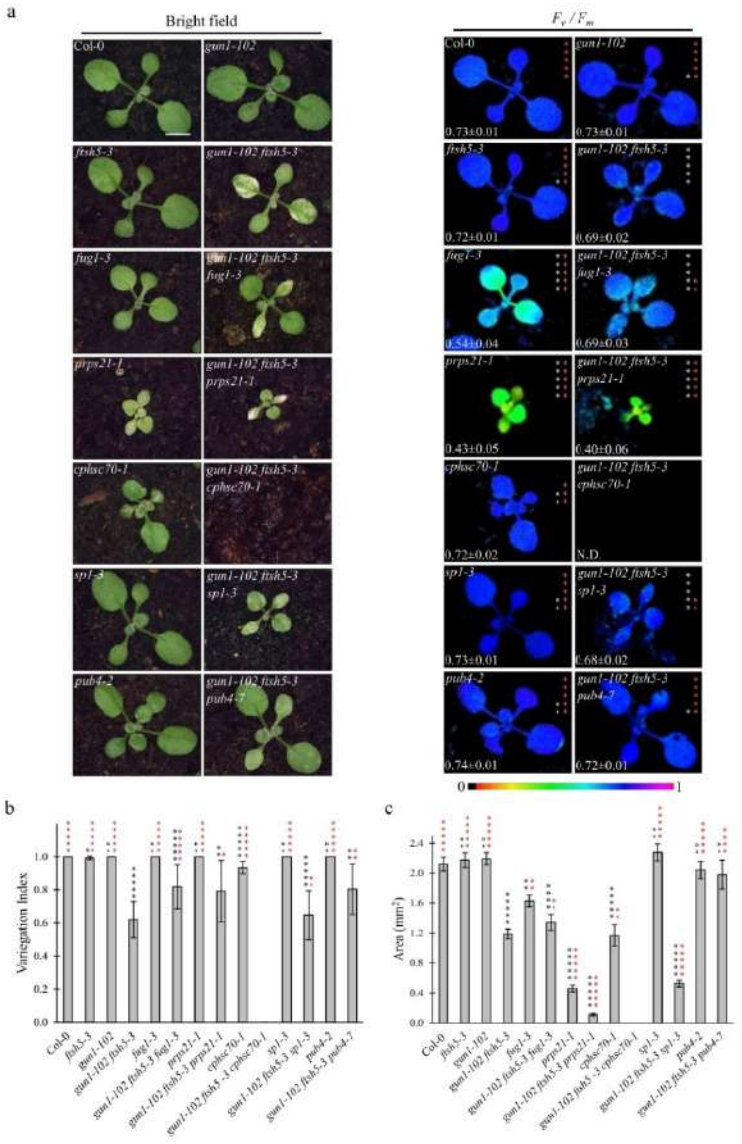

Figure 2. Visible phenotypic characteristics and photosynthetic performance of Arabidopsis Col-0 and mutant seedlings at

two-leaves stage. (**a**) Visible phenotypes and maximum quantum yield of PSII (F_v/F_m) of Col-0, *gun1-102*, *ftsh5-3*, *gun1-102 ftsh5-3*, *fug1-3*, *gun1-102 ftsh5-3 fug1-3*, *prps21-1*, *gun1-102 ftsh5-3 prps21-1*, *cphsc70-1*, *gun1-102 ftsh5-3 cphsc70-1*, *sp1-3*, *gun1-102 ftsh5-3 sp1-3*, *pub4-2* and *gun1-102 ftsh5-3 pub4-7* true leaves at 12 days after sowing (DAS) grown on soil. Scale bar corresponds to 1 cm. F_v/F_m parameter was measured through the IMAGING PAM Fluorimeter (Walz) and reported in false colour (black equals to 0, violet to 1) and as average ± standard deviation of at least six independent measurements; N.D.: not detected. Asterisks indicate statistical significance with respect to Col-0 (white) or *gun1-102 ftsh5-3* (red) as evaluated by Student's *t*-test and Welch correction (* $p < 0.05$; ** $p < 0.01$; *** $p < 0.001$; **** $p < 0.0001$; ***** $p < 0.00001$; ns, not significant). (**b**) Average Variegation Index (V.I.) calculated as ratio between green area and total area of the leaf of Col-0 and mutants grown on soil at 12 DAS. Error bars indicate standard deviations of at least six independent measurements. Asterisks indicate statistical significance with respect to Col-0 (black) or *gun1-102 ftsh5-3* (red) as evaluated by Student's *t*-test and Welch correction (* $p < 0.05$; ** $p < 0.01$; *** $p < 0.001$; **** $p < 0.0001$; ns: not significant). (**c**) Average area in mm^2 of single first leaves of the indicated genotypes grown on soil at 12 DAS. Error bars indicate standard deviations of at least six independent measurements. Asterisks indicate statistical significance with respect to Col-0 (black) or *gun1-102 ftsh5-3* (red) as evaluated by Student's *t*-test and Welch correction (* $p < 0.05$; ** $p < 0.01$; *** $p < 0.001$; **** $p < 0.0001$; ***** $p < 0.00001$; ns: not significant).

3.2. PUB4 E3 Ubiquitin Ligase Plays a Major Role in Chloroplast Degradation upon Alteration of Plastid Protein Homeostasis

To further investigate the role of PUB4 as a component of the chloroplast quality control machinery (see also [16]), thin sections of cotyledons from the Col-0, *gun1-102 ftsh5-3* double mutant, *pub4-2* T-DNA insertional mutant (Figure S1) and *gun1-102 ftsh5-3 pub4-7* triple mutant were analysed by Transmission Electron Microscope (TEM) (Figure 3a). Chloroplasts of Col-0 and *pub4-2* cotyledons appeared to be correctly shaped, with the proper thylakoid ultrastructure organization in grana stacks and stroma lamellae and abundant starch granules in the stroma, as in the case of *gun1-102* and *ftsh5-3* chloroplasts (Figure 3a; see also Tadini et al. [16]). In agreement with the V.I. values, several plastids devoid of thylakoid membranes and with large vesicles either inside the stroma (Figure 3a) or budding from the envelope, as also reported in Tadini et al. [16], were observed in *gun1-102 ftsh5-3* cotyledon cells, indicating advanced chloroplast degradation.

On the contrary, *gun1-102 ftsh5-3 pub4-7* cotyledons contained functional chloroplasts with severely altered shape, but that were still able to accumulate thylakoid membranes organized in grana and stroma lamellae and that were capable of performing photosynthesis, as proven by the accumulation of starch granules (Figure 3a). The suppression of *gun1-102 ftsh5-3* variegated phenotype, achieved by the introgression of *pub4-7* mutation, was also investigated by measuring the cotyledon chlorophyll content through a spectrophotometer-based assay (Figure 3b). Chlorophyll content was similar in Col-0, *gun1-102*, *ftsh5-3* and *pub4-2* cotyledons, while it was reduced to about 60% of control levels in *gun1-102 ftsh5-3* seedlings. In agreement with previous observations (Figures 1 and 3a), *gun1-102 ftsh5-3 pub4-7* cotyledons showed almost double the amount of chlorophyll compared to the variegated *gun1-102 ftsh5-3* cotyledons.

3.3. The Absence of PUB4 E3 Ubiquitin Ligase Activity Increases Cytosolic Protein Folding Stress

Immunoblot analyses of total protein extracts from Col-0, *gun1-102*, *ftsh5-3*, *pub4-2*, *gun1-102 ftsh5-3* and *gun1-102 ftsh5-3 pub4-7* cotyledons were performed to monitor the accumulation of components of the thylakoid electron transport chain, i.e., LHCB5, of thylakoid membrane biogenesis/maintenance, such as VIPP1 [37,38], of the plastid protein homeostasis machinery, such as CLPB3, cpHSC70-1 and CPN60 [34,39,40] and of the plastid pre-protein guidance complex and molecular markers of the cytosolic folding stress, as in the case of HSC70-4 and HSP90-1 cytosolic chaperones [17,26,41] (Figure 4a).

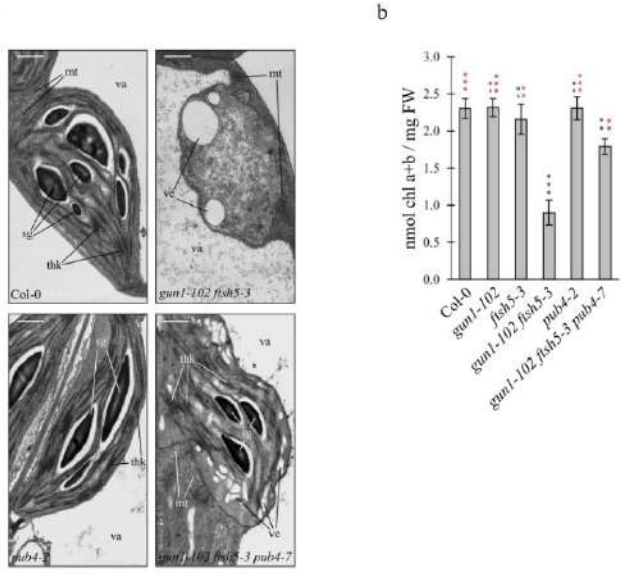

Figure 3. Chloroplast ultrastructure and chlorophyll content of Arabidopsis Col-0 and mutant cotyledons. (**a**) TEM micrographs of chloroplasts in mesophyll cells of Col-0, *gun1-102 ftsh5-3*, *pub4-2* and *gun1-102 ftsh5-3 pub4-7* cotyledons at 6 DAS. Ultrathin sections of cotyledons from Col-0 and mutant seedlings were stained with 2% uranyl acetate and lead citrate and examined by TEM. Scale bars correspond to 1 µm. The main cellular structures are indicated (sg: starch granule; thk: thylakoid membranes; ve: budding vesicles; mt: mitochondrion; va: vacuole). (**b**) Cotyledon chlorophyll content of the indicated Arabidopsis genotypes grown on soil at 6 DAS. The total chlorophyll content is normalised on the cotyledon fresh weight (nmol Chl a + b/mg FW). Asterisks indicate statistical significance with respect to Col-0 (black) or *gun1-102 ftsh5-3* (red) as evaluated by Student's *t*-test and Welch correction (** $p < 0.01$; *** $p < 0.001$; ns: not significant).

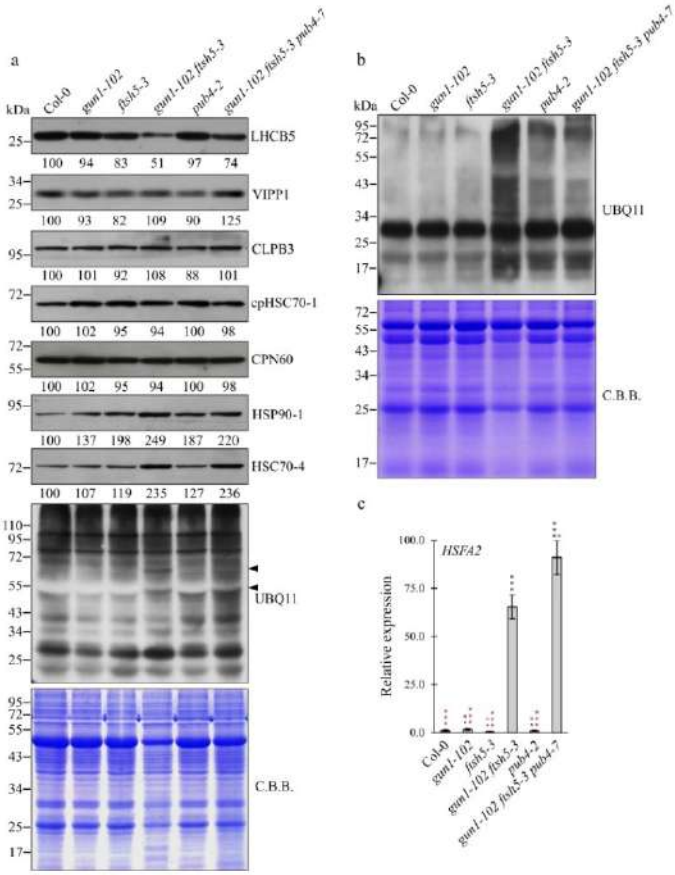

Figure 4. Protein and transcript accumulation in Arabidopsis Col-0 and mutant cotyledons. (**a**) Immuno-blot analyses of total protein extracts from cotyledons of Col-0, *gun1-102*, *ftsh5-3*, *gun1-102 ftsh5-3*, *pub4-2* and *gun1-102 ftsh5-3 pub4-7* grown on soil at 6 DAS. PVDF filters bearing fractionated total proteins were incubated with antibodies raised against LHCB5 antenna protein, VIPP1 plastid membrane chaperone, CLPB3 plastid unfoldase, cpHSC70-1 plastid chaperone, CPN60 plastid chaperonin, HSP90-1 cytosolic chaperone, HSC70-4 cytosolic chaperone and UBQ11 ubiquitin protein. Coomassie Brilliant Blue (CBB) stained SDS-PAGE is included as loading control. (**b**) Immunoblot analyses of chloroplast protein extracts from Col-0, *gun1-102*, *ftsh5-3*, *gun1-102 ftsh5-3*, *pub4-2* and *gun1-102 ftsh5-3 pub4-7* grown on soil at 6 DAS. PVDF filters bearing fractionated proteins were incubated with antibodies raised against UBQ11 ubiquitin protein. CBB-stained SDS-PAGE is included as loading control. (**c**) Relative expression level of *HSFA2* gene determined by qRT-PCR analyses of total RNA extracted from cotyledons of Col-0, *gun1-102*, *ftsh5-3*, *gun1-102 ftsh5-3*, *pub4-2* and *gun1-102 ftsh5-3 pub4-7* grown on soil at 6 DAS. Error bars indicate standard deviations of three replicates. Asterisks indicate statistical significance with respect to Col-0 (black) or *gun1-102 ftsh5-3* (red) as evaluated by Student's *t*-test and Welch correction (* $p < 0.05$; *** $p < 0.001$; ns: not significant).

In agreement with previous observations, the higher level of LHCB5 in *gun1-102 ftsh5-3 pub4-7* cotyledons with respect to *gun1-102 ftsh5-3* further supported the ability of *pub4-7* mutation to suppress the variegated phenotype of *gun1-102 ftsh5-3* cotyledons. Furthermore, the accumulation of VIPP1 appeared comparable among all the genotypes except for *gun1-102 ftsh5-3 pub4-7*, which showed a slight increase in VIPP1 levels, while CLPB3, cpHSC70-1 and CPN60 resulted unchanged in all the genotypes. Interestingly, the accumulation of HSC70-4 and HSP90-1 cytosolic chaperones increased markedly in both the *gun1-102 ftsh5-3* double mutant and *gun1-102 ftsh5-3 pub4-7* triple mutant (Figure 4a) in line with what observed in *gun1* single mutant upon Lincomycin treatment [16,17], pointing to a relatively high cytosolic protein folding stress in both mutant backgrounds. Finally, the total protein ubiquitination level was assessed by a UBQ11 specific antibody. Overall, no evident difference in total signal intensity was observed between wild-type and the different mutant samples. However, the protein ubiquitination pattern in *gun1-102 ftsh5-3* cotyledons showed two relatively strong bands at around 70 and 55 kDa (see arrow heads in Figure 4a), not detectable in Col-0 and in the single mutant cotyledons. Strikingly, the band at 55 kDa was also visible in *gun1-102 ftsh5-3 pub4-7* cotyledons, while the signal at 70 kDa disappeared in the triple mutant genetic background (Figure 4a). The lack of important discrepancies in the ubiquitination levels among all of the genotypes, even in the absence of PUB4 E3 ubiquitin ligase enzyme, prompted us to investigate whether major differences could be observed at the chloroplast level, given the ability of PUB4 to promote chloroplast degradation upon alteration of plastid protein homeostasis (see above). To this aim, intact purified chloroplasts were isolated from cotyledons of Col-0 and mutant seedlings and chloroplast proteins probed with the UBQ11 specific antibody (see Figure 4b). While chloroplast ubiquitination levels of Col-0, *gun1-102* and *ftsh5-3* chloroplasts were rather similar and most of the ubiquitination signal was concentrated in a single band migrating at around 30 kDa, the plastid ubiquitination levels increased largely in the *gun1-102 ftsh5-3* genetic background, where signals of ubiquitinated proteins could be also detected at molecular weights different from the 30 kDa main band (Figure 4b). Intriguingly, a large part of the increased ubiquitination signals disappeared upon depletion of PUB4 activity in *gun1-102 ftsh5-3 pub4-7* chloroplasts (Figure 4b). In addition, the relative expression of *HSFA2* transcription factor, a key regulator of the chloroplast-related nuclear stress response [42,43], was assessed via qRT-PCR (Figure 4c). Consistently with the increase in cytosolic chaperone accumulation (see Figure 4a), *HSFA2* transcripts were strongly up-regulated in *gun1-102 ftsh5-3* and, to an even larger extent, in *gun1-102 ftsh5-3 pub4-7* seedlings.

4. Discussion

Variegated mutants represent an important genetic tool to investigate chloroplast biogenesis and to dissect the functional interactions of different pathways involved in plastid differentiation, chloroplast protein homeostasis, chloroplast quality control and degradation. In this manuscript, we studied the GUN1-mediated plastid development and degradation, in the context of altered plastid protein homeostasis, as shown by the variegated phenotype of *gun1-102 ftsh5-3* seedlings.

As the *gun1-102 ftsh5-3* double mutant possesses chloroplasts prone to suffer terminal damages, the recovery of *gun1-102 ftsh5-3 pub4-7* phenotype observed in cotyledons and true leaves (Figures 1 and 2) suggests that PUB4-mediated ubiquitination is the preferential pathway for degrading and recycling damaged chloroplasts upon alteration of plastid protein homeostasis (Figure 5). These observations are in agreement with previous studies, in which ROS-damaged chloroplasts in Arabidopsis plants lacking the plastid ferrochelatase 2 (*fc2-1*) exhibited a PUB4-dependent increase in poly-ubiquitinated proteins [24]. The altered shape of chloroplasts observed in *gun1-102 ftsh5-3 pub4-7* cotyledons (Figure 3a) is compatible with the early steps of the degradation process, not effectively achieved or delayed due to the absence of PUB4 protein activity, as previously reported [24]. In line with this, the up-regulation of the stress-responsive gene *HSFA2*, here used as molecular

marker of damaged chloroplasts and the related nuclear stress response [42,43], observed in *gun1-102 ftsh5-3*, was comparable or even higher in *gun1-102 ftsh5-3 pub4-7*, proving that *pub4* mutation does not suppress the damage itself (Figure 4). It is tempting to explain the higher *HSFA2* expression as a consequence of the increased number of chloroplasts in cells that, although defective, are still performing photosynthesis and, consequently, generating ROS and other stress-related signals. Worth noticing, *HSFA2* expression is triggered by a GUN1-indepentent retrograde signalling pathway, as previously observed [43]. Furthermore, the introgression of *pub4-7* mutation does not suppress the increased cytosolic folding stress observed in *gun1-102 ftsh5-3* cotyledons (Figure 4), and previously described in *gun1* seedlings upon lincomycin treatment [16,17] as proven by the over-accumulation of the cytosolic chaperones HSC70-4 and HSP90-1 and the increased total protein ubiquitination level. Noteworthy is that the comparison between *gun1-102 ftsh5-3* and *gun1-102 ftsh5-3 pub4-7* ubiquitination profiles, performed, for example, by mass spectrometry analyses of ubiquitin-enriched protein extracts, seems to be an optimal strategy to identify those chloroplast outer envelope proteins that are modified by the PUB4 ubiquitin ligase.

On the contrary, the *sp1-3* mutation, which abolishes the activity of a transmembrane ubiquitin ligase responsible for controlling TOC protein complex composition and activity, does not suppress variegation in *gun1-102 ftsh5-3* cotyledons and leaves (Figures 1 and 2). SP1 activity has been recognized as essential for chloroplast biogenesis in etiolated seedlings and to play a role in the tolerance of abiotic stresses, by modulating the import rate of photosynthetic proteins, and, therefore, to prevent ROS accumulation [22,25,26]. In light of this, the *gun1-102 ftsh5-3 sp1-3* triple mutant is devoid of an additional level of chloroplast quality control mechanism that results in an overall decrease in plant growth with respect to *gun1-102 ftsh5-3* (Figures 1 and 2). Taken together, these observations corroborate the model in which ubiquitination of specific chloroplast proteins triggers different mechanisms of stress tolerance, in cotyledons and leaves, not only in response to abiotic stresses but also as adaptation to genetic defects.

The introgression of *cphsc70-1* mutation, impaired in plastid protein import and protein folding [34,35], into the *gun1-102 ftsh5-3* genetic background led to a complete seedling lethal phenotype. This is in agreement with previous results, as *GUN1* was shown to have functional interactions with *FTSH5* and *cpHSC70-1* loci [16,17]. The fact that *ftsh5-3 cphsc70-1* double mutant displays no additive phenotype compared to *cphsc70-1* (Figure S3), while the *gun1-102 ftsh5-3 cphsc70-1* shows seedling-lethality (Figure 1), suggests that plastid protein import, protein folding and plastid proteolysis act synergistically for achieving the correct chloroplast development and GUN1 is essential for such orchestration.

At last, in line with previous observations [10,32,33], the suppression of variegated phenotype was effectively achieved in *gun1-102 ftsh5-3* true leaves by reducing the plastid translation rate, driven by the introgression of either *fug1-3* or *prps21-1* mutated alleles. Strikingly, this compensatory effect failed to occur in cotyledons, proving further that the pathways that underlie chloroplast biogenesis in cotyledons and leaves are characterized by substantial differences.

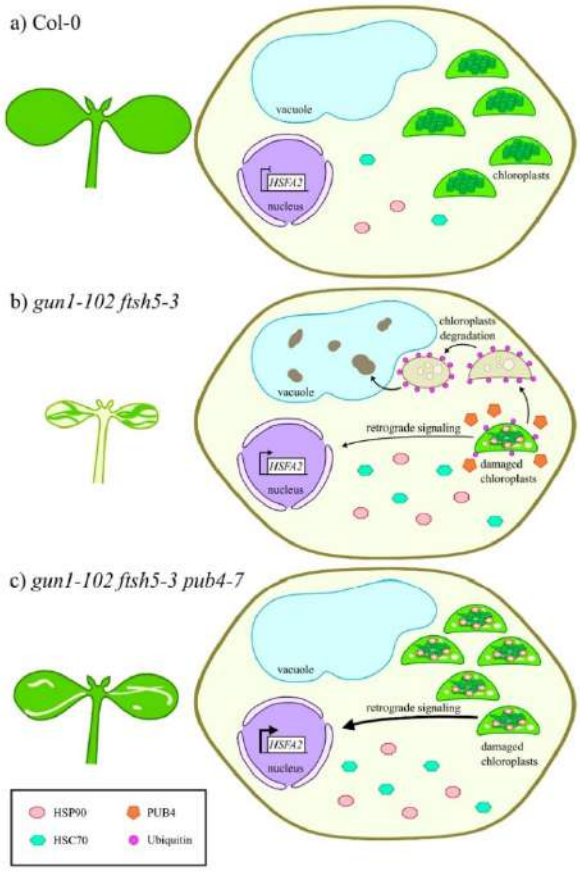

Figure 5. Schematic overview representing the *pub4*-mediated suppression of variegation. (**a**) In Col-0 seedlings, cells display functional chloroplasts, physiological cytosolic folding stress and clear vacuoles. (**b**) On the contrary, chloroplasts in advanced degradation stages and vacuoles filled with electron-dense material are visible in *gun1-102 fish5-3* variegated cotyledons. The electron dense material inside the vacuole might derive from plastid degradation. The expression of the stress-responsive *HSFA2* nuclear gene is strongly up-regulated, in response to signals from chloroplasts with altered protein homeostasis. Furthermore, the accumulation of cytosolic chaperones, namely HSP90 and HSC70, is increased, while the removal of damaged chloroplasts is favoured by PUB4 ubiquitin ligase. (**c**) The absence of PUB4 in the *gun1-102 fish5-3 pub4-7* genetic background largely prevents the degradation of damaged chloroplasts, resulting in the suppression of variegation in both cotyledons and true leaves. Nevertheless, damaged chloroplasts, still functioning, trigger stress-related retrograde signals and lead to even higher *HSFA2* expression levels.

Supplementary Materials: The following are available online at https://www.mdpi.com/article/10.3390/genes12091387/s1, Figure S1: Graphical representations of the loci mentioned in this study, Figure S2: Photosynthetic performance of Arabidopsis Col-0 and mutant seedlings, Figure S3: Visible phenotypic characteristics and Variegation Index of Arabidopsis Col-0 and mutant seedlings at cotyledon stage, Table S1: Sequences of oligonucleotides employed for the molecular characterization of mutant lines.

Author Contributions: P.P. and L.T. designed the study. N.J., L.R., A.C. and L.T. took care of isolation of single and higher-order mutants. N.J., L.R. and G.F. took care of the phenotypical description of the mutants. N.J., L.R. and L.T. performed the molecular biology and biochemical characterization of mutants. N.J., L.R., P.P. and L.T. helped drafting the manuscript. L.T. and P.P. coordinated the study and took care of the final version of the manuscript. All authors have read and agreed to the published version of the manuscript.

Funding: This research was funded by MIUR—Ministero dell'Università e della Ricerca, grant number PRIN-2017 2017FBS8YN. The authors acknowledge support from the University of Milan through the APC initiative.

Acknowledgments: We are grateful to Francesca Lopez for critical reading of the manuscript and English editing. We are also grateful to Franco Faoro, Dario Maffi, Valerio Paravicini and Mario Beretta for excellent technical assistance.

Conflicts of Interest: The authors declare no conflict of interest.

References

1. Sakamoto, W. Leaf-variegated mutations and their responsible genes in Arabidopsis thaliana. *Genes Genet. Syst.* **2003**, *78*, 1–9. [CrossRef] [PubMed]
2. Yu, F.; Fu, A.; Aluru, M.; Park, S.; Xu, Y.; Liu, H.; Liu, X.; Foudree, A.; Nambogga, M.; Rodermel, S. Variegation mutants and mechanisms of chloroplast biogenesis. *Plant Cell Environ.* **2007**, *30*, 350–365. [CrossRef]
3. Putarjunan, A.; Liu, X.; Nolan, T.; Yu, F.; Rodermel, S. Understanding chloroplast biogenesis using second-site suppressors of immutans and var2. *Photosynth. Res.* **2013**, *116*, 437–453. [CrossRef] [PubMed]
4. Chen, M.; Choi, Y.D.; Voytas, D.F.; Rodermel, S. Mutations in the Arabidopsis VAR2 locus cause leaf variegation due to the loss of a chloroplast *Ftsh* protease. *Plant J.* **2000**, *22*, 303–313. [CrossRef]
5. Takechi, K.; Sodmergen; Murata, M.; Motoyoshi, F.; Sakamoto, W. The YELLOW VARIEGATED (VAR2) locus encodes a homologue of *Ftsh*, an ATP-dependent protease in arabidopsis. *Plant Cell Physiol.* **2000**, *41*, 1334–1346. [CrossRef]
6. Sakamoto, W.; Tamura, T.; Hanba-Tomita, Y.; Sodmergen; Murata, M. The VAR1 locus of Arabidopis encodes a choloroplastic *Ftsh* and is responsible for leaf variegation in the mutant alleles. *Genes Cells* **2002**, *7*, 769–780. [CrossRef] [PubMed]
7. Van Wijk, K.J. Protein maturation and proteolysis in plant plastids, mitochondria, and peroxisomes. *Annu. Rev. Plant Biol.* **2015**, *66*, 75–111. [CrossRef]
8. Nishimura, K.; Kato, Y.; Sakamoto, W. Chloroplast proteases: Updates on proteolysis within and across suborganellar compartments. *Plant Physiol.* **2016**, *171*, 2280–2293. [CrossRef]
9. Chen, M.; Jensen, M.; Rodermel, S. The yellow variegated mutant of Arabidopsis is plastid autonomous and delayed in chloroplast biogenesis. *J. Hered.* **1999**, *90*, 207–214. [CrossRef]
10. Liu, X.; Yu, F.; Rodermel, S. Arabidopsis Chloroplast *Ftsh*, var2 and Suppressors of var2 Leaf Variegation: A Review. *J. Integr. Plant Biol.* **2010**, *52*, 750–761. [CrossRef]
11. Wagner, R.; Aigner, H.; Funk, C. *Ftsh* proteases located in the plant chloroplast. *Physiol. Plant* **2012**, *145*, 203–214. [CrossRef]
12. Zheng, M.; Liu, X.; Liang, S.; Fu, S.; Qi, Y.; Zhao, J.; Shao, J.; An, L.; Yu, F. Chloroplast translation initiation factors regulate leaf variegation and development. *Plant Physiol.* **2016**, *172*, 1117–1130. [CrossRef] [PubMed]
13. Qi, Y.; Zhao, J.; An, R.; Zhang, J.; Liang, S.; Shao, J.; Liu, X.; An, L.; Yu, F. Mutations in circularly permuted GTPase family genes AtNOA1/RIF1/SVR10 and BPG2 suppress var2-mediated leaf variegation in Arabidopsis thaliana. *Photosynth. Res.* **2016**, *127*, 355–367. [CrossRef]
14. Liu, S.; Zheng, L.; Jia, J.; Guo, J.; Zheng, M.; Zhao, J.; Shao, J.; Liu, X.; An, L.; Yu, F.; et al. Chloroplast translation elongation factor EF-Tu/SVR11 is involved in Var2-mediated leaf variegation and leaf development in Arabidopsis. *Front. Plant Sci.* **2019**, *10*, 8–18. [CrossRef]
15. Sun, J.L.; Li, J.Y.; Wang, M.J.; Song, Z.T.; Liu, J.X. Protein Quality Control in Plant Organelles: Current Progress and Future Perspectives. *Mol. Plant* **2021**, *14*, 95–114. [CrossRef]
16. Tadini, L.; Peracchio, C.; Trotta, A.; Colombo, M.; Mancini, I.; Jeran, N.; Costa, A.; Faoro, F.; Marsoni, M.; Vannini, C.; et al. GUN1 influences the accumulation of NEP-dependent transcripts and chloroplast protein import in Arabidopsis cotyledons upon perturbation of chloroplast protein homeostasis. *Plant J.* **2020**, *101*, 1198–1220. [CrossRef]
17. Wu, G.Z.; Meyer, E.H.; Richter, A.S.; Schuster, M.; Ling, Q.; Schöttler, M.A.; Walther, D.; Zoschke, R.; Grimm, B.; Jarvis, R.P.; et al. Control of retrograde signalling by protein import and cytosolic folding stress. *Nat. Plants* **2019**, *5*, 525–538. [CrossRef]

18. Koussevitzky, S.; Nott, A.; Mockler, T.C.; Hong, F.; Sachetto-Martins, G.; Surpin, M.; Lim, J.; Mittler, R.; Chory, J. Signals from Chloroplasts Converge to Regulate Nuclear Gene Expression. *Science* **2007**, *316*, 715–719. [CrossRef]
19. Tadini, L.; Pesaresi, P.; Kleine, T.; Rossi, F.; Guljamow, A.; Sommer, F.; Mühlhaus, T.; Schroda, M.; Masiero, S.; Pribil, M.; et al. GUN1 controls accumulation of the plastid ribosomal protein S1 at the protein level and interacts with proteins involved in plastid protein homeostasis. *Plant Physiol.* **2016**, *170*, 1817–1830. [CrossRef]
20. Zhao, X.; Huang, J.; Chory, J. GUN1 interacts with MORF2 to regulate plastid RNA editing during retrograde signaling. *Proc. Natl. Acad. Sci. USA* **2019**, *116*, 10162–10167. [CrossRef]
21. Tadini, L.; Jeran, N.; Pesaresi, P. GUN1 and Plastid RNA Metabolism: Learning from Genetics. *Cells* **2020**, *9*, 2307. [CrossRef]
22. Ling, Q.; Huang, W.; Baldwin, A.; Jarvis, P. Chloroplast Biogenesis Is Regulated by Direct Action of the Ubiquitin-Proteasome System. *Science* **2012**, *338*, 655–659. [CrossRef]
23. Ling, Q.; Jarvis, P. Regulation of chloroplast protein import by the ubiquitin E3 ligase SP1 is important for stress tolerance in plants. *Curr. Biol.* **2015**, *25*, 2527–2534. [CrossRef] [PubMed]
24. Woodson, J.D.; Joens, M.S.; Sinson, A.B.; Gilkerson, J.; Salomé, P.A.; Weigel, D.; Fitzpatrick, J.A.; Chory, J. Ubiquitin facilitates a quality-control pathway that removes damaged chloroplasts. *Science* **2015**, *350*, 450–454. [CrossRef] [PubMed]
25. Ling, Q.; Jarvis, P. Plant Signaling: Ubiquitin Pulls the Trigger on Chloroplast Degradation. *Curr. Biol.* **2016**, *26*, 38–40. [CrossRef]
26. Thomson, S.M.; Pulido, P.; Jarvis, R.P. Protein import into chloroplasts and its regulation by the ubiquitin-proteasome system. *Biochem. Soc. Trans.* **2020**, *48*, 71–82. [CrossRef]
27. Woodson, J.D. Chloroplast stress signals: Regulation of cellular degradation and chloroplast turnover. *Curr. Opin. Plant Biol.* **2019**, *52*, 30–37. [CrossRef]
28. Xing, H.-L.; Dong, L.; Wang, Z.-P.; Hai-Yan, Z.; Chun-Yan, H.; Bing, L.; Xue-Chen, W.; Chen, Q.-J. A CRISPR/Cas9 toolkit for multiplex genome editing in plants. *BMC Plant Biol.* **2014**, *14*, 1–12. [CrossRef]
29. Porra, R.J.; Thompson, W.A.; Kriedemann, P.E. Determination of accurate extinction coefficients and simultaneous equations for assaying chlorophylls a and b extracted with four different solvents: Verification of the concentration of chlorophyll standards by atomic absorption spectroscopy. *Biochim. Biophys. Acta* **1989**, *975*, 384–394. [CrossRef]
30. Czechowski, T.; Stitt, M.; Altmann, T.; Udvardi, M.K.; Wolf-Rüdiger, S. Genome-Wide Identification and Testing of Superior Reference Genes for Transcript Normalization in Arabidopsis. *Genome Anal.* **2005**, *139*, 5–17. [CrossRef] [PubMed]
31. Kunst, L. Preparation of physiologically active chloroplasts from Arabidopsis. *Methods Mol. Biol.* **1998**, *82*, 43–48. [CrossRef]
32. Miura, E.; Kato, Y.; Matsushima, R.; Albrecht, V.; Laalami, S.; Sakamoto, W. The balance between protein synthesis and degradation in chloroplasts determines leaf variegation in Arabidopsis yellow variegated mutants. *Plant Cell* **2007**, *19*, 1313–1328. [CrossRef]
33. Liu, X.; Zheng, M.; Wang, R.; Wang, R.; An, L.; Rodermel, S.R.; Yu, F. Genetic interactions reveal that specific defects of chloroplast translation are associated with the suppression of var2-mediated leaf variegation. *J. Integr. Plant Biol.* **2013**, *55*, 979–993. [CrossRef]
34. Latijnhouwers, M.; Xu, X.M.; Møller, S.G. Arabidopsis stromal 70-kDa heat shock proteins are essential for chloroplast development. *Planta* **2010**, *232*, 567–578. [CrossRef] [PubMed]
35. Su, P.H.; Li, H.M. Stromal Hsp70 is important for protein translocation into pea and Arabidopsis chloroplasts. *Plant Cell* **2010**, *22*, 1516–1531. [CrossRef]
36. Morita-Yamamuro, C.; Tsutsui, T.; Tanaka, A.; Yamaguchi, J. Knock-out of the plastid ribosomal protein S21 causes impaired photosynthesis and sugar-response during germination and seedling development in Arabidopsis thaliana. *Plant Cell Physiol.* **2004**, *45*, 781–788. [CrossRef]
37. Zhang, L.; Kato, Y.; Otters, S.; Vothknecht, U.C.; Sakamoto, W. Essential role of VIPP1 in chloroplast envelope maintenance in Arabidopsisw. *Plant Cell* **2012**, *24*, 3695–3707. [CrossRef]
38. Zhang, L.; Sakamoto, W. Possible function of VIPP1 in thylakoids: Protection but not formation? *Plant Signal. Behav.* **2013**, *8*. [CrossRef]
39. Myouga, F.; Motohashi, R.; Kuromori, T.; Nagata, N.; Shinozaki, K. An Arabidopsis chloroplast-targeted Hsp101 homologue, APG6, has an essential role in chloroplast development as well as heat-stress response. *Plant J.* **2006**, *48*, 249–260. [CrossRef]
40. Vitlin Gruber, A.; Nisemblat, S.; Azem, A.; Weiss, C. The complexity of chloroplast chaperonins. *Trends Plant Sci.* **2013**, *18*, 688–694. [CrossRef] [PubMed]
41. Paila, Y.D.; Richardson, L.G.L.; Inoue, H.; Parks, E.S.; McMahon, J.; Inoue, K.; Schnell, D.J. Multi-functional roles for the polypeptide transport associated domains of Toc75 in chloroplast protein import. *Elife* **2016**, *5*, 1–29. [CrossRef] [PubMed]
42. Nishizawa, A.; Yabuta, Y.; Yoshida, E.; Maruta, T.; Yoshimura, K.; Shigeoka, S. Arabidopsis heat shock transcription factor A2 as a key regulator in response to several types of environmental stress. *Plant J.* **2006**, *48*, 535–547. [CrossRef] [PubMed]
43. Llamas, E.; Pulido, P.; Rodriguez-Concepcion, M. Interference with plastome gene expression and Clp protease activity in Arabidopsis triggers a chloroplast unfolded protein response to restore protein homeostasis. *PLoS Genet.* **2017**, *13*, 1–27. [CrossRef] [PubMed]

SCIENTIFIC REPORTS
nature research

OPEN

Higher order photoprotection mutants reveal the importance of ΔpH-dependent photosynthesis-control in preventing light induced damage to both photosystem II and photosystem I

Roberto Barbato[1] ✉, Luca Tadini[2], Romina Cannata[1], Carlotta Peracchio[2], Nicolaj Jeran[2], Alessandro Alboresi[3], Tomas Morosinotto[3], Azfar Ali Bajwa[4], Virpi Paakkarinen[4], Marjaana Suorsa[4], Eva-Mari Aro[4] & Paolo Pesaresi[2]

Although light is essential for photosynthesis, when in excess, it may damage the photosynthetic apparatus, leading to a phenomenon known as photoinhibition. Photoinhibition was thought as a light-induced damage to photosystem II; however, it is now clear that even photosystem I may become very vulnerable to light. One main characteristic of light induced damage to photosystem II (PSII) is the increased turnover of the reaction center protein, D1: when rate of degradation exceeds the rate of synthesis, loss of PSII activity is observed. With respect to photosystem I (PSI), an excess of electrons, instead of an excess of light, may be very dangerous. Plants possess a number of mechanisms able to prevent, or limit, such damages by safe thermal dissipation of light energy (non-photochemical quenching, NPQ), slowing-down of electron transfer through the intersystem transport chain (photosynthesis-control, PSC) in co-operation with the Proton Gradient Regulation (PGR) proteins, PGR5 and PGRL1, collectively called as short-term photoprotection mechanisms, and the redistribution of light between photosystems, called state transitions (responsible of fluorescence quenching at PSII, qT), is superimposed to these short term photoprotective mechanisms. In this manuscript we have generated a number of higher order mutants by crossing genotypes carrying defects in each of the short-term photoprotection mechanisms, with the final aim to obtain a direct comparison of their role and efficiency in photoprotection. We found that mutants carrying a defect in the ΔpH-dependent photosynthesis-control are characterized by photoinhibition of both photosystems, irrespectively of whether PSBS-dependent NPQ or state transitions defects were present or not in the same individual, demonstrating the primary role of PSC in photoprotection. Moreover, mutants with a limited capability to develop a strong PSBS-dependent NPQ, were characterized by a high turnover of the D1 protein and high values of Y(NO), which might reflect energy quenching processes occurring within the PSII reaction center.

Photoinhibition of photosynthesis is a long-known phenomenon[1]. Due to the discovery of the high turnover D1-protein[2] and its subsequent recognition as a main component of PSII reaction center harboring most of PSII redox cofactors[3,4], photoinhibition was thought as the increase of degradation rate for the D1 over its synthesis or, more in general, as an unbalance between damage and repair of PSII[5,6]. The repair cycle of PSII is now a

[1]Department of Sciences and Innovation Technology, University of Eastern Piedmont Amadeo Avogadro, I-15121, Alessandria, Italy. [2]Department of Biosciences, University of Milan, I-20133, Milan, Italy. [3]Department of Biology, University of Padua, 35121, Padova, Italy. [4]Molecular Plant Biology, Department of Biochemistry, University of Turku, SF-20520, Turku, Finland. ✉e-mail: roberto.barbato@uniupo.it

well-established phenomenon in which damaged PSII centers, localized in the grana domain, undergo monomerization, partial dismantling and lateral migration to the stroma-exposed regions, where newly synthesized D1-proteins, co-translationally inserted in the thylakoid membrane, substitute the damaged ones; reassembly of repaired centers, back migration to grana membranes and dimerization close the cycle[6–8]. Post-translational modifications of some subunits, such as reversible phosphorylation of D1, D2, CP43 and PSBH subunits, may have a regulative role in the process[9].

Although photoinhibition has since long been considered as a process dealing with PSII, it is now clear that, under some conditions, also PSI may be highly vulnerable to light. Among them, irradiation with high light in the cold (at least in chilling-sensitive species), was first described as a condition affecting PSI. Electrons from PSI could generate superoxide radicals which, once reduced to hydrogen peroxide, could react with iron-sulfur centers on the acceptor side of the PSI, producing irreversible damages[10]. In addition, mutations such as *pgr5*, in which the ability to develop a full ΔpH trans-thylakoidal gradient is impaired, make PSI very sensitive to light, both in growth chamber[11,12] and field conditions[12], because of over-reduction of electron acceptors[13]. Owing to the absence of high turnover rates for PSI subunits, damages to this photosystem is very dangerous for plants. In this kind of mutants, PSII was also found to be highly vulnerable to light[14], to the extent that PSII damage/repair cycle has been proposed as a photoprotection mechanism for PSI[15].

Plants possess a number of different mechanisms able to regulate the use of light[14]. Excess of absorbed light is thermally dissipated in a process defined as non-photochemical quenching (NPQ) which, in turn, comprises a number of different processes. Among them, the principal, fastest and more investigated is qE (energy-dependent quenching), whose formation depends on low luminal pH, synthesis of zeaxanthin through the xanthophyll cycle, protonation of PSBS protein and participation of Lhcb proteins[16,17]. Depending on the redox state of Q_A, LHCII may be phosphorylated by the STN7 kinase and act as an antenna also for PSI, re-equilibrating the distribution of light between the two photosystems[18,19], resulting in a quenching of fluorescence known as qT[20]. In addition, inactivated PSII centers could act as quenchers, the extent of which is defined as qI[21].

The trans-thylakoidal pH gradient is formed by the action of the linear electron transport (LET) and the cyclic electron transport (CET). In LET, electrons released from water in PSII are transferred to NADP/Ferrodoxin *via* PSI, with cytochrome b_6/f connecting the two photosystems and generating ΔpH used for ATP synthesis. In CET, electrons may be recycled from NADPH or ferredoxin to plastoquinone and then to cytochrome b_6/f, producing ΔpH which can be used to synthesize ATP without accumulation of reduced species. As stated above, ΔpH is essential for the activation of NPQ; it is also essential for photosynthesis-control, *i.e.* the slowing down of electron transfer from cytochrome b_6/f to PSI, which limits the amount of electrons reaching PSI. In mutants with defects in ΔpH formation, such as *pgr5* (not able to photo-accumulate $P700^+$), not only PSI but also PSII is very sensitive to high light[22]. As a consequence, the PGR5 protein should be regarded also as a component of the photoprotective machinery. Whether CET itself has a role in photoprotection is still a matter of discussion. Cyclic electron transport is composed of two pathways, the first one depending on the PGR5/PGRL1 complex sensitive to Antimycin A, the second depending on NADH-deyhydrogenase, insensitive to Antimycin A. While mutants impaired in the PGR5/PGRL1 pathway cannot accumulate $P700^+$ in the light, NDH mutants such as *crr2-2*, *crr-3*, *crr4-2*[23] and *crr4-3*[24] can, with the former being more light sensitive than the latter[25]. Moreover, it should also be reminded that PGR5/PGRL1 proteins could affect the ΔpH regulation also in a CET-independent pathways[26].

Although photoprotection is considered as a mechanism preventing PSII from photoinhibition, its relationship with D1 protein turnover is far from clear. Even less clear is the relative importance of the different described mechanisms in protecting PSII from photoinhibition, also through the high-turnover of the D1 protein.

In this paper, we analyzed light sensitivity of mutants carrying defects on the photoprotective PSBS-dependent NPQ (*npq4-1*), defects on trans-thylakoidal pH gradient formation (*pgr5*, *pgrl1ab*), and defects on the regulatory mechanism of state transitions (*stn7 stn8*) which was then compared with that of higher order mutants, in which PSBS-dependent NPQ, ΔpH formation and state transitions were depleted in different combinations. We found that light sensibility was higher when the ability to form ΔpH was impaired, irrespectively of whether PSBS-dependent NPQ or STN7-dependent state transitions were operative or not, indicating that the ΔpH, possibly by means of photosynthesis-control mechanism, is one main short-term photoprotective mechanism in leaves of higher plants. In addition, photoinhibition of PSII appears to be a further strategy to limit PSI damage and balance the activity of both photosystems.

Results

Arabidopsis plants devoid of short-term regulatory mechanisms highlight the primary importance of ΔpH-dependent photosynthesis-control for optimal PSI activity. In order to dissect the interconnections and the relative importance of short-term photoprotective mechanisms, mutations that abolish PSBS-dependent NPQ (*npq4-1*, lacking the PSBS subunit of photosystem II), ΔpH mutants (*pgr5* and *pgrl1a pgrl1b*, henceforth referred to as *pgrl1ab*, devoid of the PGR5-PGRL1 protein complex) and thylakoid protein phosphorylation (*stn7 stn8*, lacking the thylakoid-associated STN kinases) have been combined with the aim to obtain both higher order mutants (*npq4-1 pgrl1ab*, *npq4-1 pgr5*) and the sextuple mutant, lacking the entire set of short-term regulatory mechanisms, hereafter referred to as *ΔSTeM* (Fig. 1A). Worth to note that about 25% of PGRL1 protein is still detectable in *pgr5* and *npq4-1 pgr5* thylakoids (Fig. 1B), whereas no accumulation of PGR5 protein is observable in *pgrl1ab* and *npq4-1 pgrl1ab* (see also Dal Corso *et al.*[27]). As shown in Fig. 1A,C, a marked reduction in the growth rate is observed in the *stn7 stn8* and in the *ΔSTeM* mutants when grown under optimal conditions (growth light intensity of 100 μmol photons m^{-2} s^{-1}, over a photoperiod of 16 h light/8 h dark). In particular, *stn7 stn8* and *ΔSTeM* growth rates appear comparable to Col-0 until 14 days after sowing (DAS), whereas they diverge at 18 DAS resulting in rosettes with a decreased size at 24 DAS (Fig. 1A,C). No major differences are, instead, observed in the total chlorophyll content (Chl a + b) and Chl a/b ratio between the entire set of mutants and Col-0 (Fig. 1D), with the exception of *pgr5* leaves that accumulate less chlorophyll without changing the Chl

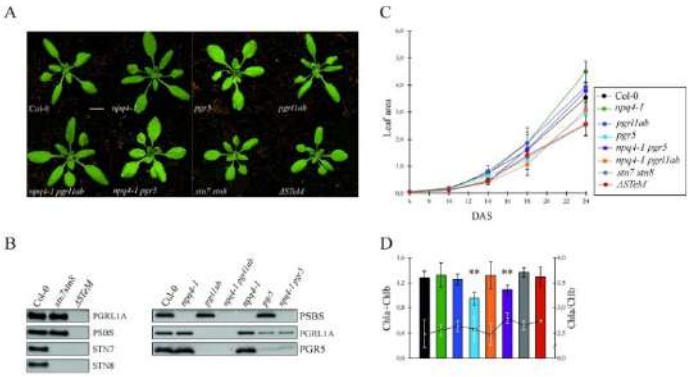

Figure 1. Phenotypes of Col-0 and mutant plants lacking short-term photoprotective mechanism, such as the *npq4-1* mutant lacking the PSBS subunit responsible of NPQ, the *pgrl1ab* and *pgr5* mutants devoid of the PGR5-PGRL1 protein complex that contributes to the formation of the ΔpH transthylakoidal gradient, the *stn7* and *stn8* mutants lacking the thylakoid STN kinases and the sextuple *ΔSTeM* mutant with no short-term regulatory mechanisms. (**A**) Images of Col-0 and mutant plants grown under long-day conditions in a growth chamber for 24 days. The size bar corresponds to 1 cm. (**B**) Immunoblots of fractionated total proteins from Col-0 and mutant leaves probed with antibodies specific for PSBS, PGRL1A, PGR5, STN7 and STN8 proteins. (**C**) Growth rate measurements of plants grown under long-day conditions in a growth chamber for 24 days. Leaf area is expressed as cm^2 (DAS, Days after sowing). (**D**) Chlorophyll content expressed as μg mg^{-1} leaf fresh weight (histogram) and ratio between Chl a and Chl b (curve). Pigments were extracted from adult plants grown under long-day conditions in a growth chamber for 24 days. Bars indicate the standard deviation and the asterisks represents the statistical significance (** *p-value* < 0,01), as evaluated by ANOVA test and Student t-test.

a/b ratio. To confirm the main role of PGR5-PGRL1 protein complex in the formation of the proton motive force (*pmf*), Col-0, *npq4-1*, *pgr5*, *npq4-1 pgr5*, *stn7 stn8* and *ΔSTeM* plant lines were subjected to the kinetic analysis of the electrochromic pigment absorbance shift (ECS) (Fig. 2). Leaf material adapted to moderate-light (50 μmol photons·m^{-2}·s^{-1}) was exposed for 5 min to red actinic light (LED, 500 μmol photons m^{-2} s^{-1}), then relaxed in the dark for 50 seconds (Fig. 2A), and the ECS relaxation kinetic was measured during the light-to-dark transition (Fig. 2B). As described in Fig. 2A,B, *npq4-1* and *stn7 stn8* mutants showed an ECS kinetic similar to Col-0 control, generating a comparable *pmf*. On the contrary, *pgr5*-containing plant lines showed a marked difference in ECS relaxation kinetics, revealing a significantly reduced (~30% drop) capability of *pgr5*, *npq4-1 pgr5* and *ΔSTeM* in generating *pmf*, when acclimated to moderate-light conditions (50 μmol photons m^{-2} s^{-1}). These findings are in line to what previously reported[22,23,28]. An identical analysis was performed after 4 h exposure to 500 μmol photons m^{-2} s^{-1} white light, and comparable differences between *pgr5*-containg plants and Col-0 were observed (Fig. S1A,B).

In addition, the effective quantum yield of PSII [Y(II), see Fig. 3A], measured after dark-adaptation and at increasing actinic light intensities (0 to 829 μmol-photons m^{-2}·s^{-1}) was generally comparable among the different genotypes, despite the PSBS-dependent NPQ [Y(NPQ)] resulted to be completely abolished in the *npq4-1*-containing genotypes and dramatically decreased in *pgrl1ab* and *pgr5* mutants, in which reached 40% of Col-0 level, after exposure to high light (Fig. 3B). In agreement with these observations, values of the Y(NO) parameter, indicating the energy quenching processes occurring within the PSII reaction center[29,30], rapidly raised as light intensity increased in the *npq4-1*-containing mutants, whereas ΔpH mutants, showed a peculiar kinetic, characterized by a *npq4*-like behavior, at moderate light intensities, and lower values at higher light intensity (>400 μmol·m^{-2}·s^{-1}), as the mutants succeeded to establish a proton gradient in the lumen and to induce the PsbS-dependent NPQ (Fig. 3C, see also Tikkanen *et al.*[31],). In agreement with that, the fraction of open PSII centers[29] (qL, Fig. 3D) resulted to be higher in Col-0 and *stn7 stn8* leaves than the rest of the genetic backgrounds, particularly at moderate light intensities (100–350 μmol·photons m^{-2}·s^{-1}).

An identical experimental set-up was used to assess PSI activity in the different genetic backgrounds (Fig. 3E–G). In particular, the quantum yield of PSI, Y(I), was relatively high in Col-0, *npq4-1* and *stn7 stn8* mutant plants even at high light intensities (till around 500 μmol·m^{-2}·s^{-1}), whereas single and multiple mutants devoid of the PGR5-PGRL1 protein complex showed a marked drop of PSI yield at moderate-to-high light intensities (>100 μmol·photons m^{-2}·s^{-1}), as a consequence of their inability to efficiently oxidize the P700 chlorophyll pair (Fig. 3E, Tikkanen *et al.*[31], Grieco *et al.*[32]). As a matter of fact, the kinetic of Y(NA) parameter, *i.e.* the quantum yield of non-photochemical energy dissipation in PSI due to acceptor side limitation (Fig. 3F), was similar in *npq4-1*, *stn7 stn8* and Col-0 leaves, reaching peaks at low light intensities (around 20–40 μmol photons·m^{-2}·s^{-1}) and showing

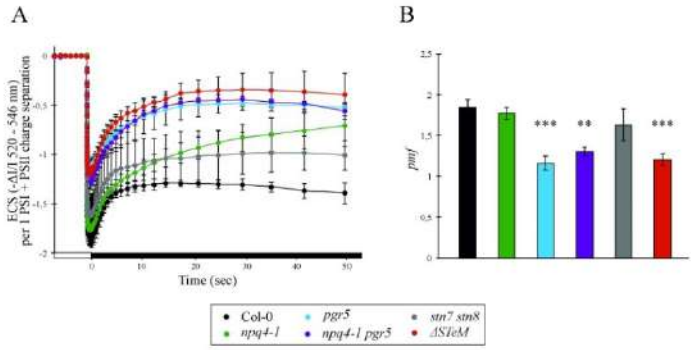

Figure 2. *In vivo* kinetic of ECS dark relaxation, measured in Col-0, *npq4-1*, *pgr5*, *npq4-1 pgr5*, *stn7 stn8* and *ΔSTeM* plants adapted to moderate-light (50 μmol photons·m^{-2}·s^{-1}). (**A**) Detached leaves were exposed to actinic light (500 μmol photons m^{-2} s^{-1}) for 5 min and ECS relaxation was measured during the light-to-dark transition (Time 0). White boxes indicate actinic light illumination, while black boxes indicate dark recovery. (**B**) The proton motive force (*pmf*) was calculated, accordingly. Measurements were performed in at least 3 biological replicates, average values and standard deviations are indicated. ECS signals were normalized on PSI + PSII charge separation signals (see Fig. S1C,D). Bars indicate the standard deviation and the asterisks represents the statistical significance (**p-value* < 0,01; ***p-value* < 0,001) as evaluated by ANOVA test and Student t-test. Note, that we preferred to report the *pmf* rather than ΔpH values, since the real partitioning of the *pmf* between its two components (Δψ and ΔpH) is still debated[58,59].

a strong decrease at higher light conditions, as soon as the photosynthetic control is engaged. On the other hand, PGR-devoid mutants showed a rapid increase of Y(NA) values, reaching a plateau at light intensity values higher than 300 μmol·photons m^{-2}·s^{-1}, as a consequence of the over-reduction of PSI acceptor side. Similarly, the Y(ND) values, *i.e.* the non-photochemical PSI quantum yield of donor-side limited heat dissipation (Fig. 3G), showed the incapability of PGR-devoid mutants to accumulate P700 in the oxidized form, as previously described[24,33,34]. Overall, our findings highlight the primary importance of proton gradient regulation (PGR)-dependent photosynthesis-control with respect to PSI yield, especially under moderate actinic light intensities.

Photoinhibition of PSII is phenomenologically linked to the lack of ΔpH-dependent photosynthesis-control and the consequent over-reduction of PSI reaction centers. Photoinhibition of Col-0 and mutant plants was evaluated via the maximum quantum yield of PSII (Fv/Fm), measured after 2 hours of exposure to 130, 500 or 1000 μmol·m^{-2}·s^{-1} of light (Fig. 4A). The results clearly show that mutants lacking either the STN kinases and, surprisingly, even the PSBS protein behaved very similarly to Col-0. On the contrary, single and higher order mutants devoid of the ability to form a full *pmf* (see also Fig. 2) were strongly photoinhibited, with no major differences between *ΔSTeM* and the *pgrl1ab* and *pgr5* mutants. Thus, it seems that the impairment of ΔpH-dependent photosynthesis-control confers enhanced light sensitivity, irrespectively of whether NPQ or state transitions are developed or not. In particular, when the negative slopes of trend lines obtained from Fig. 4A (used to estimate photoinhibition) were plotted as a function of State Transitions (Figs. 4B and S2; ST%, percentage of state transition with respect to Col-0 values), PSBS-dependent NPQ [Fig. 4C; Y(NPQ)] and Y(ND) (Fig. 4D) values, a clear association with photoinhibition was only displayed by the lines containing the *pgr* mutations. Indeed, *stn7 stn8* and *ΔSTeM* leaves, both devoid of the State Transitions mechanism, had very different slope values: much smaller, therefore indicating higher photoinhibition, in *ΔSTeM* with respect to *stn7 stn8* (Fig. 4B). Similarly, a higher slope value, *i.e.* less photoinhibition, was observed in *npq4-1* leaves with respect to *ΔSTeM* plants lacking both ΔpH-dependent photosynthesis-control and NPQ (Fig. 4C). Thus, taking these findings together, it appears clear that the ΔpH-dependent photosynthesis-control plays a major role in photoprotection.

To further characterize the functionality of PSII in the different genetic backgrounds, fluorescence decay measurements in the 10^{-4}–10^{2} sec time-range were performed on dark-adapted and HL-treated plants, irradiated with high-light (500 μmol·photons m^{-2}·s^{-1}) for either 2 or 4 hours (Fig. 5). A single-turnover saturating flash was used to trigger the reduction of Q_A with a single electron, extracted from the donor side of PSII, leading to increased fluorescence yield. The subsequent dark-induced re-oxidation of Q_A^- resulted in the relaxation of fluorescence yield and exhibited three main decay phases: fast, middle and slow[35]. For each phase, amplitude and decay time constant were determined, as reported in Table 1. In the case of dark-adapted Col-0 (Fig. 5A), the fast phase, raised from re-oxidation of Q_A^- by plastoquinone bound to Q_B site in the dark, contributed to 82% of total amplitude, with a time constant (T_1) of 309 μs. The middle phase, originated from re-oxidation of Q_A^- by

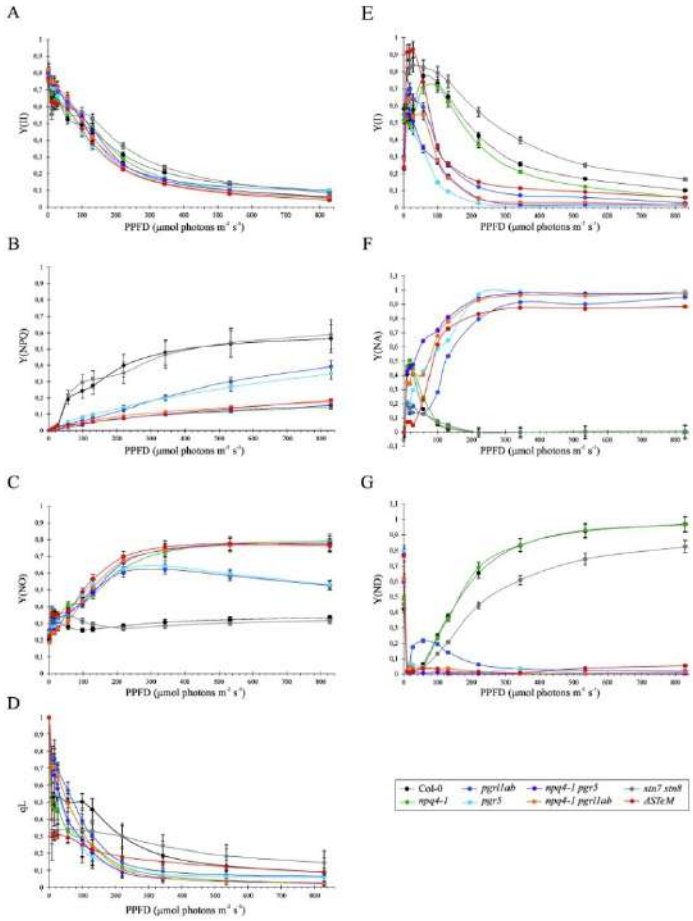

Figure 3. Photosynthetic performance of PSII and PSI complexes in Col-0 and mutant leaves. **(A–D)** Parameters of PSII functionality Y(II), Y(NPQ), Y(NO), and qL were measured after 30 min of dark adaptation and upon exposure to increasing light intensities. **(E–G)** PSI efficiency was also evaluated, through the quantification of Y(I), Y(ND) and Y(NA) parameters; (PPFD, photosynthetic photon flux density).

plastoquinone molecules in reaction centers with empty Q_B site at the time of the flash light, displayed 9,5% of total amplitude with a time constant (T_2) of 17 ms. Finally, the slow phase that arises from a back-reaction of the S_2 state of the water-oxidizing complex with Q_A^-, which is populated via the equilibrium between $Q_A^-Q_B$ and $Q_AQ_B^-$, had a 8,8% relative amplitude with a time constant (T_3) of 4.2 sec. Comparable amplitude values for the three phases could also be observed for all the dark-adapted mutant genotypes, although clear differences were present in the time constants of the middle phase, ranging from a minimum value of 13 ms, observed in *npq4-1 pgr5*, to 65 ms calculated for *ΔSTeM*, indicating that under standard growth conditions PSII is working in a similar way in Col-0 and mutant thylakoids. However, when plants were exposed to high light for 2 and 4 hours a totally different scenario appeared. In particular, Col-0 leaves irradiated with high light for 2 or 4 hours

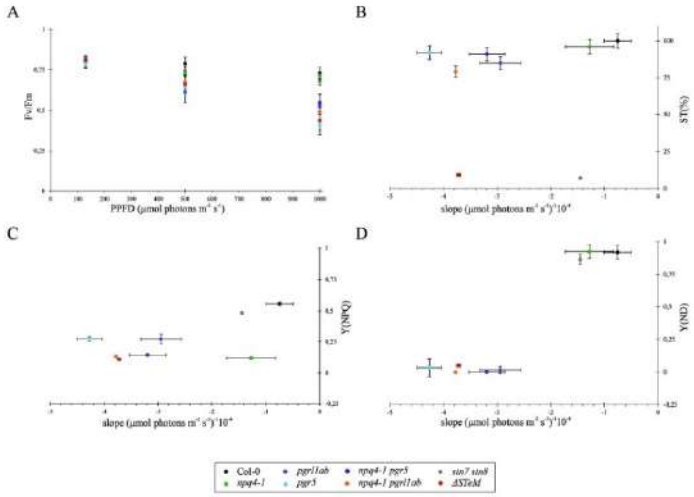

Figure 4. Levels of PSII photoinhibition with respect to the absence of State Transitions (ST), PSBS-dependent NPQ [Y(NPQ)] and ΔpH-dependent photosynthesis-control [Y(ND)]. (**A**) Photoinhibition was estimated by measuring the Y(II) parameter, after 2 h of exposure to 130, 500 and 1000 μmol-photons m^{-2}·s^{-1} of actinic light. The slopes of the trend lines in (**A**) were plotted *vs* either state transition percentage (ST%) with respect to Col-0 level (see also Fig. S2) (**B**), Non-Photochemical-Quencing [Y(NPQ)] (**C**), and PSI donor site limitation Y(ND) (**D**). Measurements are shown as average ± s.d. of three biological replicates. Note that NPQ and Y(ND) values refer to Fig. 3B,C, respectively, at 829 μmol-photons m^{-2}·s^{-1} of light.

decreased the total amplitude of 4 and 11%, respectively, as a result of a reduction of the fast phase and the concomitant increase of the middle and slow phase (Fig. 5A and Table 1). T_1 and T_2 remained in the order of 0,3 ms and 15–30 ms, irrespectively of the irradiation length, whereas a marked shortening of T_3 was observed upon high light exposure. A similar situation was observed in *npq4-1* (Fig. 5B) and *stn7 stn8* (Fig. 5C) leaves, but major differences were detected in mutants defective in ΔpH formation and, therefore, the photosynthesis-control regulatory mechanism (Fig. 5D–H). First of all, a loss of a total amplitude between 25% and 30% is observed in all genotypes after 4 hours of high light exposure, due to a marked loss of the fast phase and the increase of middle and slow phase (Table 1). In addition, while T_1 remained in the order of 0,3 ms both T_2 and T_3 values showed marked drops, further confirming the over-reduction of the electron transport chain in the absence of a normal ΔpH transthylakoidal gradient.

Thylakoid protein phosphorylation does not have a major impact on D1 protein turnover and PSII photoinhibition. The level of PSII photoinhibition was also measured as the maximum PSII quantum yield (Fv/Fm), in dark-adapted leaves and in leaves exposed to either optimal growth light (GL, 100 μmol photons m^{-2} s^{-1}) or stressful high light (HL, 500 μmol photons m^{-2} s^{-1}) for 60, 120 and 240 minutes, in absence or presence of Lincomycin (Lin) (Fig. 6). Under GL condition, where there is no effect of light on Fv/Fm, the addition of Lin leads to a partial loss of PSII activity, linked to the inhibition of the *de novo* synthesis of D1 and, more in general, of plastid-encoded proteins (not shown). Under HL conditions, in the absence of Lin, a general decrease of Fv/Fm values after 60 minutes of HL exposure could be appreciated, more obvious in *pgrl1ab* and *npq4-1 pgrl1ab* mutants (Fig. 6A). A similar trend was observed after 120 minutes of HL treatment, whereas the exposure to HL for 240 min indicated that photosynthesis-control devoid mutants are more susceptible to photoinhibition than Col-0, *stn7 stn8* and *npq4-1*, confirming the data reported in Fig. 4A. As expected, in presence of Lin, all genotypes displayed a similar trend as in GL but with a much larger susceptibility to the HL treatment, as revealed by the considerable decrease of Fv/Fm after 120 and 240 min of HL exposure (Fig. 6B). In particular, Col-0 Fv/Fm was reduced of about 40% after HL treatment for 240 min in presence of Lin, whereas *npq4-1 pgr5* and *ΔSTeM* mutants showed the largest PSII photoinhibition, with Fv/Fm values reduced by 80 and 75%, respectively, in comparison to dark-adapted samples.

In addition to PSII photoinhibition evaluated by fluorescence-based methods (PAM, single turnover flash), the same samples were also analyzed for the ability to accumulate D1 protein by immunoblot analyses under GL and HL conditions with and without Lin treatments (Fig. 7). In all tested genotypes, D1 accumulation was not

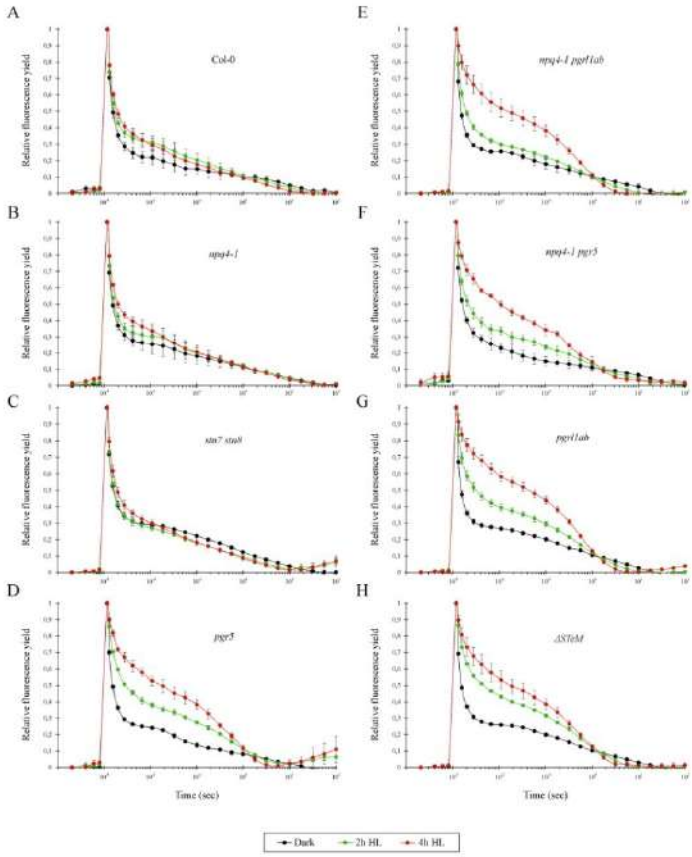

Figure 5. Chlorophyll fluorescence decay, measured in Col-0 (**A**), *npq4-1* (**B**), *stn7 stn8* (**C**), *pgr5* (**D**), *npq4-1 pgrl1ab* (**E**), *npq4-1 pgr5* (**F**), *pgrl1ab* (**G**) and *ΔSTeM* (**H**) leaves after dark adaptation and exposure to HL for 2 and 4 hours. Chlorophyll fluorescence values are reported in the y-axis, where maximum fluorescence was set to 1. The X-axis indicates the decay time scale, from 10^{-4} to 10^{2} sec. Measurements are shown as mean ± s.d., n = 3.

affected under GL conditions in the absence of Lin treatment, whereas leaves incubated overnight with 2,3 mM of Lin and then exposed to GL for 240 min, showed decreased D1 amount similar to the levels observed after HL exposure for 240 min in the absence of Lin. However, when the HL exposure was combined with the Lin treatment, differences became evident. In particular, D1 accumulation was markedly decrease in *npq4-1*, *pgr5*, *pgrl1ab*, *npq4-1 pgrl1ab*, *npq4-1 pgr5* and *ΔSTeM* with respect to Col-0 amount. Interestingly, no additive effects were observed when the accumulation of D1 protein in *npq4-1* thylakoids was compared with *npq4-1 pgrl1ab* and *npq4-1 pgr5* and the *ΔSTeM* sextuple mutant, in agreement with the Fv/Fm values reported in Figs. 4A and 6B. On the contrary, Col-0 and the *stn7 stn8* mutant suffered a comparable and marginal decrease of D1 amount after 240 min of HL.

The fact that Col-0 and the *stn7 stn8* double mutant do not show major differences with respect to PSII yield under HL stress conditions with and without Lin, points to a marginal role of thylakoid protein phosphorylation with respect to PSII photoprotection. To investigate further this aspect, the thylakoid phosphorylation pattern

	Total amplitude			Fast phase [$t_{1/2}$ (µs)/amp (%)]			Middle phase [$t_{1/2}$ (ms)/amp (%)]			Slow phase [$t_{1/2}$ (s)/amp (%)]		
	Dark	2 h HL	4 h HL	Dark	2 h HL	4 h HL	Dark	2 h HL	4 h HL	Dark	2 h HL	4 h HL
Col-0	100	96	89	309 ± 18^{a}/ $82 \pm 3,4^{a}$	307 ± 18^{a}/ $76 \pm 3,3^{a}$	353 ± 39^{a}/ $70 \pm 2,9^{a}$	17 ± 4^{a}/ $9,5 \pm 0,9^{a}$	29 ± 6^{a}/ $12 \pm 0,9^{a}$	14 ± 2^{a}/ $16 \pm 1,1^{a}$	$4,2 \pm 1,6^{a}$/ $8,8 \pm 0,8^{a}$	$1,2 \pm 0,3^{a}$/ $12 \pm 0,9^{a}$	$0,9 \pm 0,2^{a}$/ $14 \pm 0,7^{a}$
npq4-1	100	93	85	283 ± 18^{a}/ $81 \pm 4,9^{a}$	313 ± 19^{a}/ $77 \pm 3,4^{b}$	353 ± 21^{b}/ $69 \pm 2,5^{b}$	26 ± 8^{a}/ $8 \pm 0,1^{A}$	37 ± 9^{b}/ $11 \pm 1,0^{B}$	19 ± 3^{B}/ $16 \pm 0,9^{B}$	$2,1 \pm 0,7^{a}$/ $11 \pm 0,8^{c}$	$1,8 \pm 0,6^{b}$/ $12 \pm 0,9^{b}$	$1,1 \pm 0,2^{b}$/ $15 \pm 0,7^{b}$
pgrl1ab	100	81	70	258 ± 16^{a}/ $85 \pm 4,5^{a}$	312 ± 25^{b}/ $54 \pm 2,0^{b}$	316 ± 65^{b}/ $31 \pm 3,2^{c}$	51 ± 16^{A}/ $8 \pm 0,1^{A}$	$3,7 \pm 0,2^{B}$/ $17 \pm 1,4^{B}$	$6,6 \pm 0,3^{C}$/ $41 \pm 0,3$	$2,4 \pm 0,8^{a}$/ $12 \pm 0,9^{a}$	$0,43 \pm 0,03^{b}$/ $29 \pm 0,4^{b}$	$0,005 \pm 0,003^{c}$/ $28 \pm 1,9$
pgr5	100	78	71	301 ± 16^{a}/ $81 \pm 3,2^{a}$	362 ± 66^{b}/ $54 \pm 4,1^{b}$	387 ± 15^{c}/ $38 \pm 6,7^{c}$	36 ± 7^{A}/ $11 \pm 0,8^{A}$	$3,3 \pm 1,1^{B}$/ $20 \pm 4,0^{B}$	$5,3 \pm 0,8^{C}$/ $34 \pm 2,6^{C}$	$2,84 \pm 1,0^{a}$/ $8 \pm 0,7^{a}$	$0,28 \pm 0,04^{b}$/ $26 \pm 1,0^{b}$	$0,005 \pm 0,003^{c}$/ $32 \pm 5,4^{c}$
npq4-1 pgrl1ab	100	87	74	277 ± 16^{a}/ $82 \pm 3,8^{a}$	300 ± 25^{a}/ $65 \pm 2,6^{b}$	330 ± 54^{a}/ $37 \pm 2,8^{c}$	50 ± 15^{A}/ $8 \pm 1,3^{A}$	$3,4 \pm 0,7^{B}$/ $15 \pm 1,8^{B}$	$3,9 \pm 0,7^{B}$/ $20 \pm 2,0^{B}$	$2,97 \pm 1,06^{a}$/ $10 \pm 0,1^{a}$	$0,50 \pm 0,05^{b}$/ $20 \pm 0,1^{b}$	$0,33 \pm 0,02^{b}$/ $43 \pm 0,1^{c}$
npq4-1 pgr5	100	89	77	303 ± 23^{a}/ $78 \pm 4,0^{a}$	327 ± 36^{a}/ $64 \pm 3,5^{b}$	$363 \pm {}^{ns}$/ $41 \pm 2,8^{c}$	$13 \pm 2,8^{A}$/ $13 \pm 1,1^{A}$	$5,0 \pm 1,2^{B}$/ $16 \pm 2,0^{A}$	$6,6 \pm 1,0^{B}$/ $22 \pm 1,5^{B}$	$4,81 \pm 1,89^{a}$/ $9 \pm 0,1^{a}$	$0,62 \pm 0,01^{b}$/ $20 \pm 0,1^{b}$	$0,37 \pm 0,03^{c}$/ $37 \pm 0,1^{c}$
stn7 stn8	100	98	92	307 ± 20^{a}/ $78 \pm 3,6^{a}$	246 ± 27^{a}/ $73 \pm 4,7^{a}$	342 ± 40^{a}/ $68 \pm 3,9^{a}$	$27 \pm 2,8^{A}$/ $7 \pm 1,0^{A}$	$2,8 \pm 0,9^{B}$/ $13 \pm 2,5^{B}$	$5,4 \pm 1,9^{B}$/ $14 \pm 2,3^{B}$	$1,30 \pm 0,33^{a}$/ $15 \pm 3,2^{a}$	$0,24 \pm 0,05^{a}$/ $15 \pm 3,1^{a}$	$0,22 \pm 0,06^{b}$/ $18 \pm 1,3^{a}$
ΔSTeM	100	78	75	292 ± 18^{a}/ $81 \pm 4,1^{a}$	387 ± 31^{b}/ $51 \pm 1,8^{b}$	332 ± 64^{a}/ $37 \pm 3,5^{c}$	$65 \pm 2,6^{A}$/ $7 \pm 1,2^{A}$	$5,5 \pm 0,8^{B}$/ $17 \pm 1,3^{B}$	$5,0 \pm 0,1^{B}$/ $20 \pm 2,1^{B}$	$2,19 \pm 0,87^{a}$/ $12 \pm 1,2^{a}$	$0,44 \pm 0,03^{b}$/ $32 \pm 5,3^{b}$	$0,33 \pm 0,03^{b}$/ $43 \pm 0,1^{b}$

Table 1. Chlorophyll fluorescence decay parameters, i.e. amplitude and time constant, measured in Col-0 and mutants after dark adaptation and 2 and 4 hours of high-light (HL) exposure. The time constants of fluorescence decay, indicated as $t_{1/2}$, and related to fast, middle and slow phases, are reported. The total amplitude of the fluorescence decay, measured in dark-adapted samples, was set to 100. The amplitude of fluorescence decay kinetic for each phase is indicated as percentage of total amplitude. Measurements were performed in triplicates, average values ± s.d. are indicated. Data are grouped in three blocks (i.e. Fast phase, Middle phase, Slow phase). In each group, identical letters mean that there are not significant differences at the level of p-value < 0,05, as evaluated by ANOVA test.

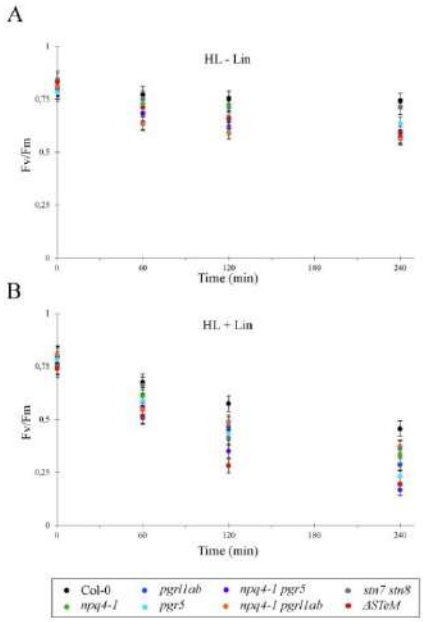

Figure 6. Photoinhibition of PSII estimated as Y(II) decrease, upon irradiation of dark-adapted leaves (values corresponding to 0 min) with high-light (60, 120 and 240 min of 500 µmol photons·m^{-2}·s^{-1}), in absence (**A**) or presence (**B**) of Lincomycin, measured in Col-0 and mutants. Measurements are shown as mean ± s.d., n = 3.

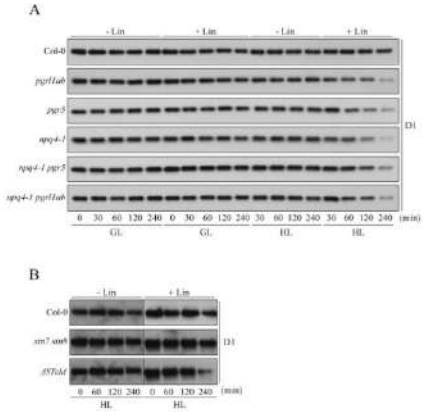

Figure 7. Immunoblot analyses of PSII integrity in Col-0 and mutants impaired in NPQ, ΔpH-dependent photosynthesis-control and State Transitions mechanisms. (**A**) Col-0, *npq4-1*, *pgrl1ab*, *pgr5*, *npq4-1 pgrl1ab* and *npq4-1 pgr5* mutants were dark-adapted in absence or presence of Lincomycin (0 min, +/− Lin) and then exposed to growth-light (GL) and high-light (HL) for 30, 60, 120 and 240 min. The accumulation of D1 subunit of PSII was investigated via immunoblot. (**B**) D1 accumulation was tested in Col-0, *stn7 stn8* and *ΔSTeM* mutants after dark-adaptation (0 min, +/− Lin) and upon 60, 120 and 240 min HL exposure, in absence or presence of Lincomycin.

was monitored in plants devoid of either NPQ or ΔpH-dependent photosynthesis-control and in the corresponding mutants where both mechanisms are inactivated (Fig. 8). In agreement with previous observations, the exposure of Col-0 leaves to GL led to a general increase in phosphorylation of all main phosphoproteins, *i.e.* LHCII, D1 and D2, over time (0-to-240 min), whereas CP43 was already strongly phosphorylated in our experimental conditions. The addition of Lin increased the phosphorylation level of PSII-core proteins even in the absence of light and a comparable accumulation of PSII-core phosphoproteins was maintained until 120 min of GL exposure. On the contrary, P-LHCII signal reached its peak at 60 min, markedly decreased at 120 min and disappear after 240 min of GL with Lin treatment. HL exposure in the absence of Lin maintained a relatively high accumulation of CP43, D1 and D2 phosphoproteins, comparable to what observed at 120–240 min of GL conditions, throughout the tested time points. However, LHCII phosphorylation was barely detectable after 30 min and disappeared after 60 min exposure to high light. The addition of Lin to HL conditions resulted in a gradual loss of phosphorylation levels. In general, the PSII-core phosphorylation pattern observed in mutant plants (see Fig. 8) was very similar to Col-0 under the different light regimes in presence or absence of Lin, although the accumulation of PSII core phosphoproteins was markedly higher in *npq4-1* thylakoids and clearly reduced in *pgrl1ab* in comparison to Col-0. Notably, the D1 phosphoprotein was barely detectable in *pgrl1ab* thylakoids even after 240 min of GL exposure. On the contrary, the LHCII phosphorylation pattern, upon HL illumination, was markedly different between Col-0 and mutant plants devoid PGR proteins. In particular, LHCII phosphorylation was retained in *pgr* mutants upon high light treatment, unlike Col-0 and *npq4-1* thylakoids where high light exposure suppressed LHCII phosphorylation. This phosphorylation pattern resembles the one of *tap38* mutant[36] and is certainly the consequence of the high reduction state of the thylakoid electron transport carriers, including Cyt b_6f, upon depletion of the ΔpH-dependent PSI photosynthesis control.

PSII photoinhibition guarantees PSI integrity. In order to evaluate the impact of PSII photoinhibition on PSI integrity, Fv/Fm and Pm (the maximal change of the P700 signal upon quantitative transformation of P700 from the fully reduced to the fully oxidized state) parameters were measured from dark-adapted and HL-treated (2 and 4 hours) plants, in either absence or presence of Lin (Fig. S3 and Table 2). In the dark, Fv/Fm did not shown any marked difference among genotypes ($p < 0,05$), whereas the Pm parameter was higher in Col-0, *npq4-1*, *stn7 stn8*, than all *pgr*-containing mutants ($p < 0,05$). The Fv/Fm values slightly decreased by increasing the length of exposure to HL, while addition of Lin led to a marked drop of Fv/Fm values (see Table 2). On the other hand, Pm values remained higher than 0,40 at the different HL regimes, irrespectively of the presence or absence of Lin. On the contrary, PGR-devoid mutants were highly sensitive to high light conditions, displaying Fv/Fm values in the range of 0,65–0,31, much lower than 0,78 observed in Col-0 (Fig. S3 and Table 2). In addition, PSI activity was found to be lower than 0,15 in *pgr5*, *npq4-1 pgrl1ab* and *npq4-1 pgr5* thylakoids under the same conditions. Interestingly, the addition of Lin to the high-light treatment restored PSI activity in PGR-devoid mutants, while PSII efficiency dropped to values even lower than 0,30, as in the case of *pgr5*, *npq4-1 pgr5* and *ΔSTeM* leaves.

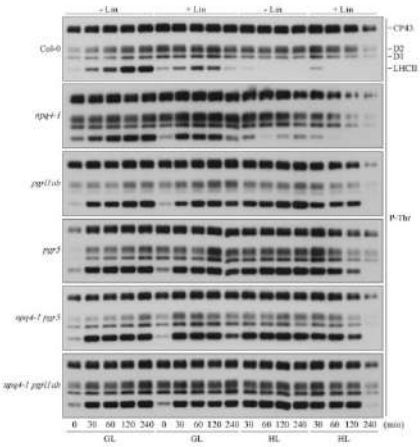

Figure 8. Thylakoid protein phosphorylation pattern. Thylakoid membranes were isolated from Col-0, single and multiple mutants, fractionated onto SDS-PAGE, transferred onto nitrocellulose membranes and probed with a polyclonal anti-phosphothreonine antibody. Levels of phosphorylation of CP43, D2, D1 and LHCII are shown over time (0-to-240 min) upon exposure to optimal growth light (GL) and high-light (HL) conditions. Lincomycin treatment was performed overnight in the dark where indicated (+Lin). One representative immunoblot (n = 3) for each genotype is shown.

Overall, these findings indicate that in the absence of the PGR-dependent photosynthesis control, a marked inhibition of PSII activity is beneficial to prevent PSI inactivation, highlighting further the primary importance of photosynthesis control in photoprotection of PSI.

Discussion

Light induced inactivation of PSII causes enhanced degradation of the D1 protein, while the PSII recovery relies on *de novo* synthesis of D1. Under PSII photoinhibitory conditions (high light), activity and stability of PSI is not affected, unless high light treatment is performed in cold environment[10] or in mutant backgrounds lacking the PGR5/PGRL1 complex, in which the ability to form a normal ΔpH and activate the photosynthesis-control is not working properly[11,12].

A large number of molecular processes have been suggested to function as protection mechanisms against an excess of light. Among those, the most relevant consists in the formation of the PSBS-dependent component of NPQ. Nevertheless, several authors argued that NPQ could have only a little role in the direct photoprotection of PSII, while could be important for the PSII recovery[14]. Our data from *PSBS*-depleted mutants are in line with these findings, as *npq4-1* plants show sensitivity to high light similar to wild type. Accordingly, in a very recent study is reported that *npq4-1* mutant, after 10 h irradiation with 1500 μmol photons m^{-2} s^{-1} showed a Fv/Fm ratio of about 0.48–0.50 whereas for the wild type the ratio was about 0.58–0.60[37]. However, the fact that high light irradiation, combined with Lincomycin treatment, led to the enhanced degradation of D1 in *npq4-1* mutant, indicated that, in mutant background devoid of PSBS, the turnover of D1 is constitutively higher. A similar effect on D1 turnover in PSBS-less mutant was previously reported[39]. Thus, the loss of PSII activity is not observed as long as the rate of damage does not exceed the rate of repair[5,6], indicating that the absence of PSBS-dependent NPQ is compensated by up-regulation of PSII repair. From these observations, we can suggest that the ability to engage a full NPQ might actually act as a signal aimed to regulate the D1 turnover, as well as a direct photoprotection mechanism meant to prevent D1 degradation. From a redox point of view, a reduced level of NPQ correlates with a higher accumulation of centers with a reduced Q_A. As $Q_A^- Q_B$ is in equilibrium with $Q_A Q_B^-$, it could be expected that in PSBS-less mutants a higher fraction of centers could accumulate a semi-reduced secondary quinone acceptor, which, according to previous works[39,40], could play a role as a photosensitizer for enhanced degradation of the D1 protein. This could be the mechanism by which the turnover of D1 protein in the *npq4-1* mutant is constitutively higher with respect to the wild-type, although it has to be taken into account that the high turnover rate of D1 and the accumulation of reduced Q_A is not usually associated with reduced NPQ in wild-type leaves under physiological conditions.

Furthermore, it should be noted that Y(NO) reflects the energy quenching processes occurring within PSII reaction center with Q_A in a reduced state, and that the reduction of Q_A has been suggested to be a major requirement and a prerequisite for an efficient PSII reaction centre quenching[41–43]. Therefore, the substantial increase of

	Dark		2h HL		4h HL		2h HL + Lin		4h HL + Lin	
	F_V/F_M	Pm	F_V/F_M	Pm	F_V/F_M	Pm	F_V/F_M	Pm	F_V/F_M	Pm
Col-0	0,814 ± 0,046^a	0,505 ± 0,024^A	0,799 ± 0,007^a	0,527 ± 0,011^B	0,785 ± 0,004^a	0,517 ± 0,011^A	0,561 ± 0,025^c	0,512 ± 0,037^A	0,490 ± 0,016^a	0,536 ± 0,004^A
npq4-1	0,802 ± 0,00697^a	0,87 ± 0,00697^A	0,758 ± 0,0194^{ab}	0,83 ± 0,05^A	0,722 ± 0,013^{ab}	0,83 ± 0,05^A	0,450 ± 0,021^c	0,87 ± 0,03^A	0,401 ± 0,019^a	0,83 ± 0,03^A
pgrl1ab	0,807 ± 0,006^a	0,285 ± 0,023^A	0,677 ± 0,020^b	0,197 ± 0,012^A	0,650 ± 0,016^b	0,151 ± 0,007^B	0, 496 ± 0,027^b	0,286 ± 0,053^A	0,293 ± 0,036^c	0,286 ± 0,023^A
pgr5	0,794 ± 0,005^a	0,259 ± 0,020^A	0,628 ± 0,022^b	0,107 ± 0,01^b	0,597 ± 0,033^c	0,037 ± 0,025^B	0,521 ± 0,018^d	0,241 ± 0,035^A	0,223 ± 0,005^c	0,215 ± 0,042^A
npq4-1 pgrl1ab	0,806 ± 0,002^a	0,234 ± 0,027^A	0,535 ± 0,048^b	0,187 ± 0,011^A	0,320 ± 0,038^c	0,063 ± 0,053^B	0,457 ± 0,022^b	0,287 ± 0,027^A	0,330 ± 0,050^b	0,266 ± 0,030^A
npq4-1 pgr5	0,811 ± 0,006^a	0,382 ± 0,022^A	0,625 ± 0,023^b	0,126 ± 0,006^B	0,467 ± 0,023^c	0,025 ± 0,017^C	0,451 ± 0,020^c	0,197 ± 0,008^B	0,226 ± 0,035^c	0,117 ± 0,034^B
stn7 stn8	0,807 ± 0,008^a	0,410 ± 0,014^A	0,724 ± 0,005^a	0,437 ± 0,055^A	0,685 ± 0,065^a	0,438 ± 0,019^A	0,561 ± 0,060^b	0,468 ± 0,044^A	0,525 ± 0,013^b	0,406 ± 0,041^A
ΔSTeM	0,811 ± 0,004^a	0,268 ± 0,011^A	0,444 ± 0,063^b	0,084 ± 0,021^B	0,314 ± 0,015^b	0,031 ± 0,011^B	0,408 ± 0,023^b	0,261 ± 0,040^A	0,294 ± 0,013^b	0,217 ± 0,018^A

Table 2. Photosynthetic efficiency of PSII and PSI measured in Col-0 and mutants after dark adaptation and exposure for 2 and 4 hours to high-light (HL) in either absence or presence of Lincomycin. Chl fluorescence emission and $P700^+$ absorbance were recorded to monitor PSII and PSI activity, respectively. Photosynthetic efficiency related to PSII and PSI (F_V/F_M and Pm), respectively, were calculated as reported in Materials and Methods. Measurements were performed at least in triplicates, average values ± s.d. are indicated. Lower case letters are referred to Fv/Fm, whereas upper case letters are referred to Pm. Same letter mean no significant differences at the level of *p-value* < 0,05, as detected by ANOVA test.

Y(NO) observed in the *npq4-1*-containing mutants, and in *pgr* mutants at moderate light intensities (see Fig. 3), also suggest the activation of PSII reaction center quenching, as a compensatory mechanism for an effective photoprotection, although this aspect is still debated.

In addition to that, mutants with defect in building up proper trans-thylakoidal pH gradient, such as *pgr5* and *pgrl1ab*, show enhanced degradation of D1, similarly to PSBS-less mutant. In particular, in PGR-devoid mutants, the treatment with high light caused a strong inactivation of PSII, even in the absence of lincomycin. As they are able to engage about 40% of the NPQ observed in wild type and are much more sensitive to light than PSBS-less plants (where the extent of NPQ is near zero), we conclude that, at least in our experimental conditions, the PGR-dependent photosynthesis-control act as an efficient photoprotection mechanism.

Furthermore, unlike wild type and *npq4-1* plants, the photosynthesis-control depleted mutants are not able to photo-accumulate $P700^+$, as their Y(ND) is near zero at any light intensity due to the low values of both thylakoid proton gradient (ΔpH) and proton motive force (*pmf*) they can develop[44]. At the same time, they are characterized by the overreduction of PSI acceptors, observed as an increase of Y(NA). Thus besides PSII, PSI is also photodamaged in these mutants, likely because of impairment of iron-sulfur clusters[13]. As no additive phenotypic effects are observed between the photosynthetic characteristics of ΔpH mutants (*pgr5* and *pgrl1ab*) and the ones of higher order mutants (*npq4-1 pgr5*, *npq4-1 pgrl1ab*, *ΔSTeM*), it can be concluded that the short-term light adaptation is highly depending on the photosynthesis-control regulatory mechanism. Accordingly, mutants lacking of NDH-dependent CET such as *crr2-2*, *crr-3*, *crr4-2*[23] but still able to photo-accumulate $P700^+$, are more light resistant than the *pgr5* mutant, deficient in CET and unable to photoaccumulate P700 in the oxidized form[25].

It is noteworthy that PSI photodamage in PGR-depleted mutants can be markedly reduced through the inhibition of PSII activity, as a consequence of the fact that the amount of electrons injected in the intersystem transport chain is decreased. This indicates that the photosynthesis-control is the main regulator of photosynthetic electron transport and that PSII photoinhibition is the very last option to reduce PSI photodamage[15]. On the other hand, damages to PSI are relevant in inducing inactivation of PSII: the acceptor side of PSII becomes over-reduced and this, in turn, increases the rate of charge recombination with formation of $^3P680$[35] and PSII inactivation. In addition, the absence of ΔpH-dependent photosynthesis-control affects the value of pmf[34], and this could alter the electron transfer between Q_A and Q_B, promoting PSII inactivation.

Overall, it appears clear that the ΔpH-dependent photosynthesis control is essential for safeguarding the entire photosynthetic electron transport chain in the thylakoid membrane, and its failure induces a rapid and coordinated inactivation of both PSII and PSI. ΔpH-dependent photosynthesis-control thus maintains the optimal balance between the two main power-units of the photosynthetic apparatus.

Methods

Plant material and growth conditions. *Arabidopsis thaliana* single mutant lines were obtained from the Arabidopsis Stock Center (http://arabidopsis.info/). The *npq4-1* mutant was described in Li *et al.*[17], the *pgrl1a pgrl1b* (also referred as *pgrl1ab*) double mutant in Dal Corso *et al.*[27], *pgr5* in Munekage *et al.*[22] and the *stn7 stn8* double mutant in Bonardi *et al.*[19]. All mutant lines are in the Columbia-0 (Col-0) genetic background, except for *pgr5* that has been isolated in Columbia *gl1*. The multiple mutants were obtained by manual crossing and PCR-based segregation analyses. Arabidopsis plants were grown under controlled growth-chamber conditions as described previously[45], with a growth light intensity of 100 μmol photons m^{-2} s^{-1}, over a photoperiod of 16 h light/8 h dark. High light treatment, otherwise stated, was performed with a light intensity of 500 μmol photons m^{-2} s^{-1} for the indicated duration. Lincomycin treatment was performed by floating detached leaves overnight in a solution of lincomycin (1 mg ml^{-1} corresponding to a concentration of 2, 3 mM) in water.

Chlorophyll quantification and growth rate measurements. For chlorophyll quantification, 50 mg of leaves from 4-week-old Arabidopsis plants were ground in liquid nitrogen. Ground material was resuspended in

90% acetone and centrifuged ay 16.000 *g* for 5 min. Chl a and b concentrations were measured according to Porra *et al.*[46]. Chlorophyll measurements were performed in triplicate. Growth rate was determined by evaluating the leaf area with ImageJ 1.43u (http://imagej.nih.gov/ij/index.html) software. 12 plants per genotype were measured.

Immunoblot analyses. Thylakoid isolation was performed as reported[47] from 4-week-old plants. For immunoblot analyses, thylakoid proteins, corresponding to 3 µg of chlorophyll, were prepared as described[48] and fractionated by SDS–PAGE (12% w/v acrylamide[49]). Proteins were then transferred onto polyvinylidene difluoride membranes[50], and replicate filters were immunodecorated using specific antibodies. The PGR5-specific antibody was obtained from Toshiharu Shikanai, Phospho-Threonine Antibody from Cell Signaling Technology, PsbS from Agrisera whereas D1[51], PGRL1A[27], STN7 and STN8[52] antibodies were produced in our laboratory.

Chlorophyll a fluorescence. *In vivo* chlorophyll a fluorescence and P700 absorbance were measured at different light intensities using the Dual-PAM 100 (Walz, http://www.walz.com/) as previously described[45]. The PSII Fv/Fm, Y(II), Y(NO), Y(NPQ) parameters, together with PSI yield [Y(I)], Pm, donor side Y(ND) and acceptor side Y(NA) limitations, were calculated as reported[53,54]. In the case of Fv/Fm parameter, measurements were performed after 20 min of dark adaptation. State transitions measurements were performed as previously described[55]. In particular, state transitions were monitored on detached leaves with the DualPAM-100 fluorometer. Leaves were exposed to a 800 ms flash of saturating white light to determine F_m, and subsequently illuminated for 15 min with 25 µmol photons $m^{-2} s^{-1}$ red light (PSII light) directly in the PAM fluorometer. Far-red (PSI) light (intensity step 15) was turned on, and after 15 min the maximum fluorescence yield in state 1 (F_{m1}) was determined. The far-red light was then switched off and the fluorescence recorded for 15 min, after which the maximum fluorescence yield in state 2 (F_{m2}) was determined. The relative change in fluorescence was calculated as $F_r = [(F_{i'} - F_i) - (F_{ii'} - F_{ii})]/(F_{i'} - F_i)$, where F_i and F_{ii} designate fluorescence in the presence of PSI light in state 1 and state 2, respectively, while $F_{i'}$ and $F_{ii'}$ designate fluorescence in the absence of PSI light in state 1 and state 2, respectively. Decay of flash-induced chlorophyll fluorescence was measured by the double modulation fluorometer FL-3500 (PSI, Brno, Czech Republic) and data were analyzed as described[55]. Multicomponent deconvolution of the measured curves was performed by using a fitting function with two exponential components and one hyperbolic component: $F_{(t)} - F_0 = A_1 \exp(-t/T_1) + A2\exp(-t/T_2) + A_3/(1 + t/T_3) + A_0$. $F_{(t)}$ is the variable fluorescence yield, F_0 is the basic fluorescence before the flash, A_0 to A_3 are the amplitudes and T_1 to T_3 are the time constants. Very slowly decaying fluorescence is described by a constant A_0 amplitude. All measurements were performed after 20 min dark adaptation.

Electrochromic pigment absorbance shift measurements. *In vivo* electrochromic pigment absorbance shift (ECS) analyses were performed with a JTS-10 spectrophotometer (Biologic, France) on detached leaves, adapted to moderate-light (50 µmol photons·m^{-2}·s^{-1}) or treated with high-light (500 µmol photons·m^{-2}·s^{-1}) for 240 min. Leaf material was exposed to red actinic light (500 µmol photons $m^{-2} s^{-1}$) for 5 min and ECS relaxation was measured during the light-to-dark transition. Data were collected as the difference between the signals at 520 and 546 nm as described by Cruz *et al.*[56] and Avenson *et al.*[57]. The amplitude of the ECS signal was normalized to the signal corresponding to one PSI + PSII charge separation, calculated after the application of xenon-induced ECS signals. The *pmf* was evaluated following ECS relaxation kinetics after actinic light switch off.

Data analysis. Data (statistics analysis, data fitting) were analysed by using the software package OriginPro 9.0 (Microcal SR2; Northampton MA01060 USA).

Received: 8 October 2019; Accepted: 12 March 2020;
Published online: 21 April 2020

References

1. Powles, S. B. Photoinhibition of Photosynthesis Induced by Visible Light. *Annu. Rev. Plant Physiol.* **35**, 15–44 (1984).
2. Reisfeld, A., Gressel, J., Jakob, K. M. & Edelman, M. Characterization of the 32,000 dalton membrane protein—i. Early synthesis during photoinduced plastid development of spirodela. *Annu. Eur. Symp. Photomorphogenes.* 161–165, https://doi.org/10.1016/B978-0-08-022677-4.50011-3 (1978).
3. Nanba, O. & Satoh, K. Isolation of a photosystem II reaction center consisting of D-1 and D-2 polypeptides and cytochrome b-559. *Proc. Natl. Acad. Sci. USA* **84**, 109–12 (1987).
4. Barber, J., Chapman, D. J. & Telfer, A. Characterisation of a PS II reaction centre isolated from the chloroplasts of Pisum sativum. *FEBS Lett.* **220**, 67–73 (1987).
5. Aro, E.-M., Virgin, I. & Andersson, B. Photoinhibition of Photosystem II. Inactivation, protein damage and turnover. *Biochim. Biophys. Acta - Bioenerg.* **1143**, 113–134 (1993).
6. Li, L., Aro, E.-M. & Millar, A. H. Mechanisms of Photodamage and Protein Turnover in Photoinhibition. *Trends Plant Sci.* **23**, 667–676 (2018).
7. Järvi, S., Suorsa, M. & Aro, E.-M. Photosystem II repair in plant chloroplasts — Regulation, assisting proteins and shared components with photosystem II biogenesis. *Biochim. Biophys. Acta - Bioenerg.* **1847**, 900–909 (2015).
8. Gururani, M. A., Venkatesh, J. & Tran, L. S. P. Regulation of Photosynthesis during Abiotic Stress-Induced Photoinhibition. *Mol. Plant* **8**, 1304–1320 (2015).
9. Baena-González, E., Barbato, R. & Aro, E.-M. Role of phosphorylation in the repair cycle and oligomeric structure of photosystem II. *Planta* **208**, 196–204 (1999).
10. Sonoike, K. Photoinhibition of photosystem I. *Physiol. Plant.* **142**, 56–64 (2011).
11. Munekage, Y. N., Genty, B. & Peltier, G. Effect of PGR5 Impairment on Photosynthesis and Growth in Arabidopsis thaliana. *Plant Cell Physiol.* **49**, 1688–1698 (2008).
12. Suorsa, M. *et al.* Proton Gradient Regulation5 is essential for proper acclimation of Arabidopsis photosystem I to naturally and artificially fluctuating light conditions. *Plant Cell* **24**, 2934–48 (2012).
13. Tiwari, A. *et al.* Photodamage of iron–sulphur clusters in photosystem I induces non-photochemical energy dissipation. *Nat. Plants* **2**, 16035 (2016).

14. Takahashi, S. & Badger, M. R. Photoprotection in plants: a new light on photosystem II damage. *Trends Plant Sci.* **16**, 53–60 (2011).
15. Tikkanen, M., Mekala, N. R. & Aro, E.-M. Photosystem II photoinhibition-repair cycle protects Photosystem I from irreversible damage. *Biochim. Biophys. Acta - Bioenerg.* **1837**, 210–215 (2014).
16. Ruban, A. V., Johnson, M. P. & Duffy, C. D. P. The photoprotective molecular switch in the photosystem II antenna. *Biochim. Biophys. Acta - Bioenerg.* **1817**, 167–181 (2012).
17. Li, X.-P. *et al.* A pigment-binding protein essential for regulation of photosynthetic light harvesting. *Nature* **403**, 391–395 (2000).
18. Bellafiore, S., Barneche, F., Peltier, G. & Rochaix, J.-D. State transitions and light adaptation require chloroplast thylakoid protein kinase STN7. *Nature* **433**, 892–895 (2005).
19. Bonardi, V. *et al.* Photosystem II core phosphorylation and photosynthetic acclimation require two different protein kinases. *Nature* **437**, 1179–1182 (2005).
20. Walters, R. G. & Horton, P. Resolution of components of non-photochemical chlorophyll fluorescence quenching in barley leaves. *Photosynth. Res.* **27**, 121–133 (1991).
21. Osmond, C. B. What is photoinhibition? Some insights from comparisons of shade and sun plants. In *Photoinhibition of Photosynthesis from molecular mechanisms to the field* 1–19 (BIOS, 1994).
22. Munekage, Y. *et al.* PGR5 Is Involved in Cyclic Electron Flow around Photosystem I and Is Essential for Photoprotection in Arabidopsis. *Cell* **110**, 361–371 (2002).
23. Munekage, Y. *et al.* Cyclic electron flow around photosystem I is essential for photosynthesis. *Nature* **429**, 579–582 (2004).
24. Suorsa, M. *et al.* PGR5-PGRL1-Dependent Cyclic Electron Transport Modulates Linear Electron Transport Rate in Arabidopsis thaliana. *Mol. Plant* **9**, 271–288 (2016).
25. Kono, M. & Terashima, I. Elucidation of photoprotective mechanisms of PSI against fluctuating light photoinhibition. *Plant Cell Physiol.* **57**, 1405–1414 (2016).
26. Kanazawa, A. *et al.* Chloroplast ATP Synthase Modulation of the Thylakoid Proton Motive Force: Implications for Photosystem I and Photosystem II Photoprotection. *Front. Plant Sci.* **8**, 719 (2017).
27. Dal Corso, G. *et al.* A Complex Containing PGRL1 and PGR5 Is Involved in the Switch between Linear and Cyclic Electron Flow in Arabidopsis. *Cell* **132**, 273–285 (2008).
28. Kawashima, R., Sato, R., Harada, K. & Masuda, S. Relative contributions of PGR5- and NDH-dependent photosystem I cyclic electron flow in the generation of a proton gradient in Arabidopsis chloroplasts. *Planta* **246**, 1045–1050 (2017).
29. Kramer, D. M., Johnson, G., Kiirats, O. & Edwards, G. E. New fluorescence parameters for the determination of QA redox state and excitation energy fluxes. *Photosynth. Res.* **79**, 209–218 (2004).
30. Hendrickson, L., Furbank, R. T. & Chow, W. S. A simple alternative approach to assessing the fate of absorbed light energy using chlorophyll fluorescence. *Photosynth. Res.* **82**, 73–81 (2004).
31. Tikkanen, M., Rantala, S. & Aro, E.-M. Electron flow from PSII to PSI under high light is controlled by PGR5 but not by PSBS. *Front. Plant Sci.* **6**, 521 (2015).
32. Grieco, M., Tikkanen, M., Paakkarinen, V., Kangasjärvi, S. & Aro, E.-M. Steady-State Phosphorylation of Light-Harvesting Complex II Proteins Preserves Photosystem I under Fluctuating White Light. *Plant Physiol.* **160**, 1896–1910 (2012).
33. Yamamoto, H. & Shikanai, T. PGR5-Dependent Cyclic Electron Flow Protects Photosystem I under Fluctuating Light at Donor and Acceptor Sides. *Plant Physiol.* **179**, 588–600 (2019).
34. Chaux, F., Peltier, G. & Johnson, X. A security network in PSI photoprotection: regulation of photosynthetic control, NPQ and O2 photoreduction by cyclic electron flow. *Front. Plant Sci.* **6**, 875 (2015).
35. Vass, I. & Styring, S. Spectroscopic characterization of triplet forming states in photosystem II. *Biochemistry* **31**, 5957–5963 (1992).
36. Pribil, M., Pesaresi, P., Hertle, A., Barbato, R. & Leister, D. Role of plastid protein phosphatase TAP38 in LHCII dephosphorylation and thylakoid electron flow. *PLoS Biol.* **8**, e1000288 (2010).
37. Khuong, T. T. H., Robaglia, C. & Caffarri, S. Photoprotection and growth under different lights of Arabidopsis single and double mutants for energy dissipation (npq4) and state transitions (pph1). *Plant Cell Rep.* **38**, 741–753 (2019).
38. Roach, T. & Krieger-Liszkay, A. The role of the PsbS protein in the protection of photosystems I and II against high light in Arabidopsis thaliana. *Biochim. Biophys. Acta - Bioenerg.* **1817**, 2158–2165 (2012).
39. Keren, N., Berg, A., van Kan PJ, P. J. M., Levanon, H. & Ohad, I. Mechanism of photosystem II photoinactivation and D1 protein degradation at low light: the role of back electron flow. *Proc. Natl. Acad. Sci. USA* **94**, 1579–84 (1997).
40. Greenberg, B. M. *et al.* Separate photosensitizers mediate degradation of the 32-kDa photosystem II reaction center protein in the visible and UV spectral regions. *Proc. Natl. Acad. Sci. USA* **86**, 6617–20 (1989).
41. Bukhov, N. G., Heber, U., Wiese, C. & Shuvalov, V. A. Energy dissipation in photosynthesis: Does the quenching of chlorophyll fluorescence originate from antenna complexes of photosystem II or from the reaction center? *Planta* **212**, 749–758 (2001).
42. Ivanov, A. G. *et al.* Low-temperature modulation of the redox properties of the acceptor side of photosystem II: Photoprotection through reaction centre quenching of excess energy. *Physiologia Plantarum* **119**, 376–383 (2003).
43. Ivanov, A. G., Sane, P. V., Hurry, V., Öquist, G. & Huner, N. P. A. Photosystem II reaction centre quenching: Mechanisms and physiological role. *Photosynthesis Research* **98**, 565–574 (2008).
44. Sato, R. *et al.* Significance of PGR5-dependent cyclic electron flow for optimizing the rate of ATP synthesis and consumption in Arabidopsis chloroplasts. *Photosynth. Res.* **139**, 359–365 (2019).
45. Pesaresi, P. *et al.* Arabidopsis STN7 kinase provides a link between short- and long-term photosynthetic acclimation. *Plant Cell* **21**, 2402–23 (2009).
46. Porra, R. J., Thompson, W. A. & Kriedemann, P. E. Determination of accurate extinction coefficients and simultaneous equations for assaying chlorophylls a and b extracted with four different solvents: verification of the concentration of chlorophyll standards by atomic absorption spectroscopy. *BBA - Bioenerg.* **975**, 384–394 (1989).
47. Järvi, S., Suorsa, M., Paakkarinen, V. & Aro, E.-M. Optimized native gel systems for separation of thylakoid protein complexes: novel super- and mega-complexes. *Biochem. J.* **439**, 207–214 (2011).
48. Martínez-García, J. F., Monte, E. & Quail, P. H. A simple, rapid and quantitative method for preparing Arabidopsis protein extracts for immunoblot analysis. *Plant J.* **20**, 251–257 (1999).
49. Schägger, H. & von Jagow, G. Tricine-sodium dodecyl sulfate-polyacrylamide gel electrophoresis for the separation of proteins in the range from 1 to 100 kDa. *Anal. Biochem.* **166**, 368–379 (1987).
50. Ihnatowicz, A. *et al.* Mutants for photosystem I subunit D of *Arabidopsis thaliana*: effects on photosynthesis, photosystem I stability and expression of nuclear genes for chloroplast functions. *Plant J.* **37**, 839–852 (2004).
51. Barbato, R. *et al.* Breakdown of the Photosystem II Reaction Center D1 Protein under Photoinhibitory Conditions: Identification and Localization of the C-Terminal Degradation Products. *Biochemistry* **30**, 10220–10226 (1991).
52. Trotta, A., Suorsa, M., Rantala, M., Lundin, B. & Aro, E. M. Serine and threonine residues of plant STN7 kinase are differentially phosphorylated upon changing light conditions and specifically influence the activity and stability of the kinase. *Plant J.* **87**, 484–494 (2016).
53. Klughammer, C. & Schreiber, U. Complementary PS II quantum yields calculated from simple fluorescence parameters measured by PAM fluorometry and the Saturation Pulse method. *PAM Appl. Notes* **1**, 27–35 (2008).
54. Schreiber, U. Saturation pulse method for assessment of energy conversion in PSI. *PAM Appl. Notes* **1**, 11–14 (2008).
55. Lunde, C., Jensen, P. E., Haldrup, A., Knoetzel, J. & Scheller, H. V. The PSI-H subunit of photosystem I is essential for state transitions in plant photosynthesis. *Nature* **408**, 613–615 (2000).

56. Cruz, J. A., Sacksteder, C. A., Kanazawa, A. & Kramer, D. M. Contribution of electric field ($\Delta\psi$) to steady-state transthylakoid proton motive force (pmf) *in vitro* and *in vivo*. Control of pmf parsing into $\Delta\psi$ and ΔpH by ionic strength. *Biochemistry* **40**, 1226–1237 (2001).
57. Avenson, T. J., Cruz, J. A. & Kramer, D. M. Modulation of energy-dependent quenching of excitons in antennae of higher plants. *Proc. Natl. Acad. Sci. USA* **101**, 5530–5535 (2004).
58. Johnson, M. P. & Ruban, A. V. Rethinking the existence of a steady-state $\Delta\psi$ component of the proton motive force across plant thylakoid membranes. *Photosynth. Res.* **119**, 233–242 (2014).
59. Davis, G. A., Rutherford, A. W. & Kramer, D. M. Hacking the thylakoid proton motive force for improved photosynthesis: Modulating ion flux rates that control proton motive force partitioning into $\Delta\Psi$ and ΔpH. *Philos. Trans. R. Soc. B Biol. Sci.* **372** (2017).

Acknowledgements
We would like to thank Eveliina Pakula for growing plants. This research is original and has a financial support of the Università del Piemonte Orientale" (FAR 2018).

Author contributions
R.B., E.-M.A., T.M. and P.P. conceived experiments; R.B., L.T., R.C., C.P., N.J., A.A.B., A.A., V.P. and M.S. carried out the experimental work; R.B., E.-M.A. and P.P. wrote the paper.

Competing interests
The authors declare no competing interests.

Additional information
Supplementary information is available for this paper at https://doi.org/10.1038/s41598-020-62717-1.

Correspondence and requests for materials should be addressed to R.B.

Reprints and permissions information is available at www.nature.com/reprints.

Publisher's note Springer Nature remains neutral with regard to jurisdictional claims in published maps and institutional affiliations.

cells

MDPI

Opinion

GUN1 and Plastid RNA Metabolism: Learning from Genetics

Luca Tadini †, Nicolaj Jeran † and Paolo Pesaresi *

Department of Biosciences, University of Milan, 20133 Milan, Italy; luca.tadini@unimi.it (L.T.); nicolaj.jeran@unimi.it (N.J.)

* Correspondence: paolo.pesaresi@unimi.it; Tel.: +39-02503-15057

† These authors contributed equally to the manuscript.

Received: 29 September 2020; Accepted: 14 October 2020; Published: 16 October 2020

check for updates

Abstract: GUN1 (genomes uncoupled 1), a chloroplast-localized pentatricopeptide repeat (PPR) protein with a C-terminal small mutS-related (SMR) domain, plays a central role in the retrograde communication of chloroplasts with the nucleus. This flow of information is required for the coordinated expression of plastid and nuclear genes, and it is essential for the correct development and functioning of chloroplasts. Multiple genetic and biochemical findings indicate that GUN1 is important for protein homeostasis in the chloroplast; however, a clear and unified view of GUN1's role in the chloroplast is still missing. Recently, GUN1 has been reported to modulate the activity of the nucleus-encoded plastid RNA polymerase (NEP) and modulate editing of plastid RNAs upon activation of retrograde communication, revealing a major role of GUN1 in plastid RNA metabolism. In this opinion article, we discuss the recently identified links between plastid RNA metabolism and retrograde signaling by providing a new and extended concept of GUN1 activity, which integrates the multitude of functional genetic interactions reported over the last decade with its primary role in plastid transcription and transcript editing.

Keywords: GUN1; RNA polymerase; transcript accumulation; transcript editing; retrograde signaling

1. Introduction

The GUN1 (genomes uncoupled 1) protein is a pentatricopeptide repeat (PPR)-containing protein that localizes to plastids and relays signals to the nucleus after exposure to either norflurazon (NF) or lincomycin (Lin) treatment [1,2]. Although these inhibitors block distinctly different processes—NF inhibits carotenoid biosynthesis by non-competitively binding to phytoene desaturase [3], while Lin is a plastid-specific inhibitor of 70S ribosomes and plastid translation [4]—both drug treatments have been shown to reduce levels of plastid transcripts, indicating that a GUN1-dependent pathway is triggered by perturbation of transcription in the plastids [5]. The involvement of plastid transcription in signaling to the nucleus was initially deduced from the observation that treatment of barley seedlings with tagetitoxin, an inhibitor of the plastid-encoded RNA polymerase (PEP; [6]), decreased transcription of members of the nuclear *RbcS* and *Lhcb1* gene families, without altering plastid DNA replication [7]. Later studies have shown that loss of sigma factor 2 (SIG2) or 6 (SIG6)—each of which is utilized by the PEP to transcribe specific sets of plastid genes [8–10]—also activates retrograde signaling [11]. The fact that nuclear gene expression is restored in *sig2 gun1* and *sig6 gun1* double mutants has provided further support for the key role of plastid transcription in triggering a GUN1-dependent retrograde response [11].

Here, we propose a new model for GUN1 function in plastids and GUN1-mediated retrograde communication, which integrates the interactions observed between GUN1 and the machinery that controls plastid protein homeostasis with the recently discovered role of GUN1 in plastid RNA metabolism [12–16]. The many additive phenotypic effects and the very few suppressor phenotypes

observed in higher-order (compound) mutants containing *gun1* together with mutations affecting various aspects of plastid protein homeostasis, sugar sensing, and plastid osmosis can all be interpreted as pleiotropic phenotypic effects of a primary alteration in plastid transcription and plastid transcript editing attributable to the lack of the GUN1 protein under conditions that would otherwise trigger plastid-to-nucleus retrograde communication.

2. GUN1 and the "Δ-*rpo* Phenotype"

GUN1 does not appear to bind directly to RNAs [17], unlike typical PPR proteins [17]. But it is targeted to an organelle, the chloroplast, and has recently been reported by two independent laboratories to influence plastid transcript accumulation [13–15]. In particular, following perturbation of PEP activity, a peculiar pattern of plastid transcription, designated as the "Δ-*rpo* phenotype", is typically observed in different plant species [14,18–20]. For example, Arabidopsis seedlings lacking proteins required for PEP-mediated transcription and regulation, such as sigma factors (*sig6*; [21]), PEP-associated proteins (*pap2* and *pap8*; [22]), and the plastid redox insensitive 2 (*prin2*) protein [23,24], show a decrease in the expression of genes, coding for subunits of the photosynthetic apparatus (*petB*, *psaB*, *psbA*, *psbB*, *psbC*, *psbD*, *rbcL*), which are normally transcribed by PEP (see Figure 1). Conversely, the expression levels of nucleus-encoded RNA polymerase (NEP)-dependent transcripts of genes, encoding the core subunits of the PEP enzymes (*rpoA*, *rpoB*, *rpoC1*), ribosomal subunits (*rps2* and *rps15*), *ycf1* (translocon at inner envelope membrane of chloroplasts 214), and *clpP1* (a subunit of the 350-kDa chloroplast Clp complex), increase significantly (Figure 1). A similar plastid gene expression pattern is observed in seedlings impaired in plastid transcript maturation (*pdm1*; [25]) and in seedlings grown in the presence of Lin (Col-0 + Lin) or altered in plastid protein synthesis by depletion of plastid ribosomal proteins [14]. Strikingly, *gun1* cotyledons have shown a limited increase in the accumulation of NEP-dependent transcripts when grown in the presence of Lin (*gun1* + Lin, [14]; see also Figure 1) and when the *gun1* mutation is introgressed into genetic backgrounds lacking plastid ribosomal subunits [14]. Furthermore, the same set of NEP-dependent transcripts is highly downregulated after treatment of *gun1* seedlings with NF (*gun1* + NF), but their levels do not exhibit major changes in Col-0 + NF and *gun5* + NF seedlings, implying a specific role for GUN1 in NEP-dependent transcript accumulation (Figure 1). Recently, a similar observation has been reported based on a comparison of the plastid gene expression profiles of *cue8* (chlorophyll a/b-binding protein-underexpressed 8) and *cue8 gun1* mutants: i.e., the "Δ-*rpo* phenotype" characteristic of *cue8* seedlings is almost completely abolished in *cue8 gun1* cotyledons [13].

The "Δ-*rpo* phenotype" is thought to be part of the regulatory mechanisms that serve to modulate the activities of NEP and PEP enzymes during plastid differentiation and in the course of responses of mature chloroplasts to environmental cues [27,29–31]. The physical interaction of GUN1 with NEP, as revealed by co-immunoprecipitation studies and bimolecular fluorescence complementation (BiFC) assays [14], seems to lie at the basis of the GUN1-mediated accumulation of NEP-dependent plastid transcripts following activation of retrograde communication, possibly favored by decreased competition for template binding and/or increased availability of dNTPs. As an alternative explanation, Loudya et al. proposed that GUN1 sustained chloroplast DNA (cpDNA) replication under specific conditions, as demonstrated by copy numbers of cpDNA, which were reduced by half in *cue8 gun1* chloroplasts with respect to the single mutants and wild-type plants [13].

Figure 1. Expression analyses of a subset of PEP- and NEP-dependent plastid genes in different genetic backgrounds and after treatments that alter PEP activity. Values are expressed as the logarithm of the fold-change (log_2-FC) relative to wild-type seedlings grown under optimal conditions. Data are retrieved from the literature in the case of *sig6* [26], *pap2* and *pap8* [27], *prin2* [23], and *pdm1* (*pigment-deficient mutant 1*) [28] and from the GEO public repository in the case of *gun1*, Col-0 + Lin, *gun1* + Lin (GEO accession GSE5770; [2]), Col-0 + NF, *gun1* + NF, and *gun5* + NF (GEO accession GSE12887;[2]). Lincomycin treatment of wild-type Arabidopsis seedlings (Col-0 + Lin) leads to a drop in PEP-dependent transcript accumulation. As an adaptive response, NEP-dependent transcript levels are increased in plastids, giving rise to what is known as the "Δ-*rpo* phenotype". Similar behavior is observed in mutants, such as *sig6*, *pap2*, *pap8*, *prin2*, and *pdm1*, which lack either nucleus-encoded plastid proteins required for PEP activity (SIG6, PAP2, PAP8, PRIN2) or mRNA maturation factors (PDM1). However, *gun1* seedlings grown in the presence of lincomycin (*gun1* + Lin) show an impaired "Δ-*rpo* phenotype": i.e., NEP-dependent transcripts show a very limited degree of upregulation. Similarly to lincomycin, *gun1* seedlings grown on norflurazon-containing medium (*gun1* + NF) undergo severe repression of PEP-dependent genes, and repression is even more pronounced if NEP-dependent transcripts are considered. On the contrary, Col-0 and *gun5* (*genomes uncoupled 5*) seedlings in the presence of norflurazon (Col-0 + NF and *gun5* + NF) show a wild-type-like plastid gene expression, indicating that the drastically reduced accumulation of PEP- and NEP-dependent transcripts upon NF treatment is a characteristic of the *gun1* genetic background.

3. GUN1 and Plastid RNA Editing

Like several other PPR proteins (for a review, see [32]), GUN1 has also been reported to influence plastid RNA editing [12], i.e., the enzymatic conversion of specific cytidines (Cs) to uridines (Us) in mRNAs, such that the information in mature RNAs deviates from that encoded in the plastid genome. The link between plastid retrograde signaling and plastid RNA editing was initially reported by Kakizaki et al. [33]. The authors demonstrated that RNA editing in plastids was indeed affected under conditions, such as Lin and NF treatments, that triggered plastid-to-nucleus signaling. In particular, reduced RNA editing levels were observed in *rps14* transcripts and RNAs encoding NAD(P) dehydrogenase (NDH) subunits when Arabidopsis seedlings were treated with either of these drugs. However, direct evidence for a causal relationship between altered RNA editing and plastid signaling was lacking, and the proteins involved remained unknown. This issue has now been clarified by the recent demonstration that GUN1 interacts with an essential component of the plant RNA editosome—multiple organellar RNA editing factor 2 (MORF2)—and affects the editing of multiple plastid RNA sites during retrograde signaling. In particular, *gun1* seedlings treated with NF affect the RNA editing levels at 11 sites in plastids, indicating the high specificity of GUN1 for target RNAs. Intriguingly, all the edited sites are in NEP-dependent transcripts encoding subunits of the ATP-dependent Clp protease, the NDH

complex, the ribosomes, photosystem II, and core subunits of PEP. Furthermore, treatment of *gun1* mutants with either NF or Lin leads to similarly increased RNA editing levels only at the *rps12-i-58* site, while comparable decreases are observed for *rpoC1-488*, *psbZ-50*, and *rpoB-551* editing sites [12]. RNA editing is usually associated with amino-acid substitutions in protein-coding sequences or is used to create start/stop codons, thus serving as a correction mechanism for otherwise defective transcripts. As a matter of fact, mutants with altered RNA editing in plant organelles exhibit defects in development and growth, including pale and albino phenotypes [34–37]. In this specific case, GUN1 is responsible for the exchange of three highly conserved amino-acid residues in the β subunit of the PEP core, known to be the catalytic site of the enzyme, and one in the *rpoC1*-encoded β′ subunit, also part of the PEP core but with unknown function. Therefore, it is tempting to hypothesize that changes in RNA editing levels for *rpoB* and *rpoC1* ultimately affect the activity of PEP. This, together with the impairment of GUN1-dependent regulation of NEP activity, might be the primary cause of the altered plastid transcript accumulation patterns observed in *gun1* cotyledons upon NF- or Lin-based stimulation of plastid communication with the nucleus ([14]; see also Figure 1).

4. Genetic Evidence for GUN1's Interactions with the Plastid Protein Homeostasis Machinery

Genetic evidence indicates that GUN1 plays an essential role during the early stages of chloroplast development in response to functional impairment of plastid gene expression, plastid protein import, plastid protein degradation, sugar sensing, or maintenance of plastid osmosis (see Tables 1 and 2 for details). This notion is based on the additive phenotypic effects observed when the *gun1* mutation is introgressed by manual crosses into genetic backgrounds, exhibiting defects in plastid transcription, transcript maturation and editing, plastid protein synthesis, import or degradation, or sugar sensing. Among the 31 *gun1*-containing higher-order mutants listed in Tables 1 and 2, 20 are characterized by additive phenotypic effects with respect to the single mutants (see also Figure 2). These include viable pale-green plants with reduced growth and photosynthetic performance, albino seedlings unable to grow autotrophically, and one embryo-lethal combination. These enhanced phenotypes, leading in some cases to non-viable double mutants, reveal the importance of GUN1 function in the plastid. They confirm that GUN1 activity indeed supports plant development by optimizing chloroplast biogenesis—and hence photosynthetic efficiency—even when plastid gene expression is impaired by genetic modifications.

Table 1. Visible phenotypic characteristics of Arabidopsis mutants altered in plastid protein homeostasis and crossed with *gun1*. Arabidopsis mutants affected in plastid transcription, plastid transcript maturation and editing, plastid translation, plastid protein import, and plastid protein degradation have been crossed manually with different *gun1* alleles, including *gun1-1*[a], *gun1-9*[b], *gun1-101*[c], *gun1-102*[d], *gun1-103*[e]. The phenotypic characteristics of single and higher-order mutants, together with the existence of physical interactions between the corresponding proteins with GUN1, are reported. Superscript a–e letters specify the *gun1* alleles introgressed in the different mutant backgrounds reported in the Table.

Locus	Function	Single Mutant Name and Phenotype	Double Mutant Phenotype	Additive (A) or Suppressor (S) Effect	Physical Interaction	Ref.
Plastid Transcription						
At2g24120	NEP: Nucleus- encoded RNA polymerase	*sca3-1*[d]: pale cotyledons; reduced growth	albino-seedling lethal	A	Yes	[14]
At1g08540	SIG2: determines PEP promoter specificity	*sig2-2*[b]: pale cotyledons; reduced growth	paler green/yellow cotyledons and young leaves	A	No	[11]
At2g36990	SIG6: determines PEP promoter specificity	*sig6-1*[b]: identical to WT	yellow/white cotyledons	A	No	[11]
At3g18420	SG1: chloroplast-localized, tetratricopeptide repeat-containing protein required for chloroplast development; involved in the regulation of plastid gene expression	*sgl1*[a]: slow green1—newly formed albino leaves gradually turn pale-green and are fully green at 3 weeks after germination; reduced growth	the delayed-greening phenotype of the *sgl1* single mutant is alleviated; leaves of *sgl1 gun1* are of similar green color to the leaves of WT plants	S	No	[38]
At1g10522	PRIN2: regulates PEP activity	*prin2-1*[a]: yellow/white cotyledons; reduced growth	identical to *prin2-1* single mutant	No effect	No	[23]

Table 1. *Cont.*

Locus	Function	Single Mutant Name and Phenotype	Double Mutant Phenotype	Additive (A) or Suppressor (S) Effect	Physical Interaction	Ref.
Plastid Transcript Maturation/Editing						
Unknown	Cab-underexpressed 8 (Cue8): chloroplast development	*cue8*[a]: virescent-delayed greening; reduced growth; altered RNA editing	albino-seedling lethal	A	Unknown	[13]
At3g03710	RIF10: exoribonuclease—processing of plastid RNA	*rif10-2*[c]: green cotyledons and pale true leaves; reduced growth	albino-seedling lethal	A	No	[38]
At3g57180	BPG2: regulates ribosomal RNA maturation	*bpg2-2*[c]: pale green/yellow cotyledons	identical to *bpg2-2* single mutant	No effect	No	[40]
At3g06980	RH50: modulates RNA secondary structure	*rh50-1*[d]: identical to WT	marked reduction of growth rate	A	No	[41]
At4g02990	mTERF4: processing of plastid transcripts	*ocl/mterf4*[a]: pale-yellow cotyledons and leaves; reduced growth	more severe pale-yellow phenotype; reduced growth	A	No	[42]
Plastid Translation						
At1g17220	FUG1: chloroplast translation initiation factor	*fug1-3*[b]: pale-green cotyledons and leaves; reduced growth	yellow cotyledons and leaves; enhanced reduction of growth rate and photosynthesis performance	A	Yes	[17,43]
At1g32990	PRPL11: plastid ribosomal protein L11	*prpl11-1*[d]: pale-green cotyledons and leaves; reduced growth	albino-seedling lethal	A	No	[17]
At5g30510	PRPS1: plastid ribosomal protein S1	*prps1-1*[d]: pale green cotyledons and leaves; reduced growth	less severe pale cotyledons and leaves; increased growth	S	Yes	[17]
At3g27160	PRPS21: plastid ribosomal protein S21	*prps21-1*[d]: pale green cotyledons and leaves; reduced growth	identical to *prps21-1* single mutant	No effect	No	[17]
At5g54600	PRPL24: plastid ribosomal protein L24	*prpl24-1*[d]: pale green cotyledons and leaves; reduced growth	albino-seedling lethal	A	No	[41]
At1g79850	PRPS17: plastid ribosomal protein S17	*prps17-1*[d]: pale green cotyledons and leaves; reduced growth	albino-seedling lethal	A	No	[41]
Plastid Protein Import						
At5g16620	Tic40: subunit of the plastid protein import apparatus	*tic40-4*[c]: pale-green cotyledons and leaves; reduced growth	embryo-lethal	A	No	[44]
At4g02510	Toc159: plastid protein import receptor	*ppi2-2*[c]: albino-seedling lethal	embryo-lethal	A	No	[33]
At4g24280	cpHSC70-1: plastid protein import and folding	*cphsc70-1*[cd]: altered cotyledon and leaf shape; slight variegation	much smaller cotyledons; larger variegation; reduced growth	A	Yes	[14,44]
At5g50920	CLPC1: protein import into chloroplast stroma	*clpc1-1*[c]: pale-green cotyledons and leaves; reduced growth	reduced photosynthetic performance; reduced growth	A	Yes	[44]
Plastid Protein Degradation						
At1g50250	FTSH1: subunit of the thylakoid-associated heteromeric FTSH protease	*fsh1-1*[d]: cotyledons identical to WT	identical to *fsh1-1* single mutant	No effect	No	[14]
At2g30950	FTSH2: subunit of the thylakoid-associated heteromeric FTSH protease	*fsh2-3*[b]: pale-green and small cotyledons; reduced growth	albino-seedling lethal	A	No	[14]
At5g42270	FTSH5: subunit of the thylakoid-associated heteromeric FTSH protease	*fsh5-3*[d]: cotyledons identical to WT	severely variegated cotyledons	A	No	[14]
At1g06430	FTSH8: subunit of the thylakoid-associated heteromeric FTSH protease	*fsh8-1*[d]: cotyledons identical to WT	identical to *fsh8-1* single mutant	No effect	No	[14]
At1g49970	CLPR1: subunit of the chloroplastic endopeptidase Clp complex	*clpr1*[c]: pale-green and small cotyledons; reduced growth	albino-seedling lethal	A	No	[39]

RIF10, resistant to inhibition with fosmidomycin 10; mTERF4, mitochondrial transcription termination factor 4; FUG1, fu-gaeri1; Tic40, translocon at the inner envelope membrane of chloroplasts; Toc159, translocon at the outer envelope membrane of chloroplasts; cpHSC70-1, chloroplast heat shock protein 70-1; CLPC1, caseinolytic protease complex component C1; CLPR1, caseinolytic protease complex component R1; FTSH, filamentation temperature sensitive metalloprotease.

In eight genetic backgrounds, the *gun1* mutation does not exacerbate the original mutant phenotype. The lack of any additive effect in *gun1 ftsh1-1* and *gun1 ftsh8-1* cotyledons and leaves can be ascribed to the fact that defective FtsH1 can be complemented by the major FtsH5 (type A) subunit, while FtsH8 can be replaced by the major FtsH2 (type B) subunit of the heteromeric filamentation temperature-sensitive (FtsH) metalloprotease associated with thylakoids (for a review, see [45]). Indeed, unlike *ftsh2* and *ftsh5*, single *ftsh1-1* and *ftsh8-1* mutants do not display any visible phenotype [14], indicating that lack of either product does not perturb the activity of the FtsH metalloprotease. This can explain why GUN1-mediated retrograde signaling is not required in *ftsh1-1* or *ftsh8-1*. Moreover, no additive effects are observed when the *gun1* mutation is combined with *gun2*, *gun4*, and *gun5* single mutants [46,47]. Indeed, the double mutants *gun1 gun2*, *gun1 gun4*, and *gun1 gun5* accumulate chlorophylls to very similar levels and display growth rates comparable to those of *gun2*, *gun4*, and *gun5* single mutants (see Table 2). Conversely, *gun2 gun4* and *gun4 gun5* double mutants are characterized by a more extreme chlorophyll phenotype than that of the corresponding single mutants. The exacerbation of the single mutant phenotype is even more prominent in *gun2 gun5*, in which chlorophyll is undetectable [46,47]. Overall, these functional interactions allow us to exclude a major role for GUN1 in the tetrapyrrole biosynthetic pathway, which provides chlorophylls and other tetrapyrrole end-products, such as heme, siroheme, and phytochromobilin.

On the other hand, *gun1 prin2-1*, *gun1 bpg2-2*, and *gun1 prps21-1* double mutants are also indistinguishable from the visible phenotypes of *plastid redox insensitive 2-1* (*prin2-1*; [23]), *brassinazole insensitive pale green 2-2* (*bpg2-2*; [40]), and *plastid ribosomal protein s21-1* (*prps21-1*; [17]), respectively. In particular, comparison of *prps21-1* with *gun1 prps21-1* mutants seems to support the existence of an 'impairment threshold' in plastid gene expression, below which the activity of GUN1 is not required, or at the least, GUN1 activity is so low that its complete loss does not exacerbate the corresponding double mutant phenotypes. As a matter of fact, the *prps21-1* single mutant accumulates more PEP-dependent (*rbcL* and *psbA*) and NEP-dependent (*rpoA* and *rpl12-3'*) transcripts than the *prpl11-1* single mutant [14], possibly explaining the marked difference between the albino-lethal phenotype of *gun1 prpl11-1* seedlings and the pale-green phenotype of *gun1 prps21-1* plants.

Only in three cases, *gun1*-containing higher-order mutants display an attenuated (suppressor) phenotype with respect to single mutants. For instance, the callus tissue formation observed in the shoot apex of the *msl2 msl3* double mutant is suppressed in the *gun1 msl2 msl3* triple mutant, which results in the formation of green and normally shaped true leaves. Clearly, this genetic interaction highlights a major role of GUN1 protein in chloroplast biogenesis during the switch from leaf cell proliferation to expansion and differentiation [48]. The direct involvement of GUN1 in chloroplast biogenesis and, as a consequence, in cotyledon and leaf greening is further supported by the suppression in the *gun1 sg1* double mutant of the delayed-greening phenotype seen in *sg1* plants, which is itself characterized by newly formed albino leaves that gradually turn green and become fully green by 3 weeks after germination ([38]; see also Table 1). Similarly, the *gun1 prps1-1* double mutant shows less severe bleaching of cotyledons and leaves and increased photosynthetic performance and growth with respect to the *prps1-1* single mutant due to GUN1-dependent control of the accumulation of the plastid ribosomal protein S1 (PRPS1; [17]).

Table 2. Visible phenotypic characteristics of Arabidopsis mutants altered in tetrapyrrole biosynthesis and other functions and crossed with *gun1*. Arabidopsis mutants affected in tetrapyrrole biosynthesis, plastid osmosis, sugar metabolism, and plastid gene expression are crossed manually with different *gun1* alleles, including *gun1-1*[a], *gun1-9*[b], *gun1-101*[c]. The phenotypic characteristics of single and higher-order mutants, together with the existence of physical interactions between the corresponding proteins with GUN1, are reported. Superscript a–c letters specify the *gun1* alleles introgressed in the different mutant backgrounds reported in the Table.

Locus	Function	Single Mutant Name and Phenotype	Double Mutant Phenotype	Additive (A), Suppressor (S) Effect	Physical Interaction	Ref.
Tetrapyrrole Biosynthesis						
At2g26670	GUN2: heme oxygenase	*gun2*[a]: long hypocotyl; pale green cotyledons; reduced growth	identical to *gun2*	No effect	No	[46]
At3g59400	GUN4: regulates Mg-chelatase	*gun4*[a]: pale green cotyeldons and leves; reduced growth	identical to *gun4*	No effect	No	[47]
At5g13630	GUN5: ChlH subunit of Mg-chelatase	*gun5*[a]: pale green cotyledons and leaves; reduced growth	identical to *gun5*	No effect	No	[47]
Other Plastid Functions						
At5g10490; At1g58200	MSL2 and MSL3: two members of the MscS-like family of mechanosensitive ion channels. They are localized in the plastid envelope and are required for normal plastid size and shape	*msl2 msl3*[b]: enlarged and deformed plastids in the shoot apical meristem; develop a mass of callus tissue at the shoot apex	abolished callus formation at the shoot apex; larger, greener, and more normally shaped true leaves	S	No	[48]
At5g22510	INV-E: a chloroplast-targeted alkaline/neutral invertase that is implicated in the development of the photosynthetic apparatus	*sicy-192*[c]: *sugar-inducible cotyledon yellow-192 mutant*: yellow cotyledons upon treatment with sucrose; gain of function mutant of plastid invertase	enhanced cotyledon phenotype due to a further decrease of chlorophyll content	A	No	[49]
At1g31410	ENF2: a chloroplast-targeted protein similar to bacterial polyamine transporters; important for plastid gene expression	*enf2-1*[a]: *enlarged fil expression domain2 mutant*—mature leaves are pale green, more serrated, and narrower than WT; in less than 1% of cases, *enf2-1* forms needle-like leaves; chloroplast development is delayed	albino-seedling lethal	A	No	[50]

5. GUN1: A Major Checkpoint for the Control of Developmental Defects during Chloroplast Biogenesis and Mitigation of the Deleterious Effects of Stress

GUN1 is a very low-abundance protein with a very short half-life and has never been detected in analyses of the plastid proteome. However, its stability and amount increase upon activation of retrograde signaling, as a consequence of the reduction/inhibition of Clp protease activity [51]. Nevertheless, it is reasonable to assume that even under conditions that activate the retrograde signaling pathway(s), GUN1 is unlikely to have a direct regulatory effect on the many highly abundant proteins that make up the plastid protein homeostasis machinery. A more realistic view suggests that most of the genetic interactions observed in the last decade and reported in Tables 1 and 2 can be ascribed to pleiotropic effects.

The recent findings that point to a primary and direct role of GUN1 in plastid RNA metabolism imply that the protein stimulates NEP activity and alters editing levels of a few NEP-dependent transcripts [12–16] and offer a novel perspective on GUN1 activity. In particular,

the decreased accumulation of NEP-dependent transcripts, i.e., transcripts encoding mainly rRNA, tRNA, and housekeeping proteins, and the reduced editing levels of some of them observed in *gun1* seedlings upon either NF or Lin treatments, straightforwardly explain the additive effects observed in *gun1*-containing double mutants with defects in (i) plastid transcription, (ii) plastid transcript maturation and editing, and (iii) plastid translation. Moreover, the reduced accumulation of NEP-dependent *ycf1* transcripts [14], which code for the Tic214 subunit of the 1-MDa TIC (translocon at the inner envelope membrane of chloroplasts) complex involved in protein import into the stroma [52], could explain the enhanced/altered phenotypes of the double mutants *gun1 tic40-4*, *gun1 ppi2*, *gun1 cphsc70-1*, and *gun1 clpc1-1*, all of which are defective in plastid protein import. Similarly, the albino-seedling lethal phenotype of *gun1 ftsh2-3* and the severely variegated cotyledons typical of *gun1 ftsh5-3* could be due to the concomitant alteration of the thylakoid-associated heteromeric metalloprotease FtsH and the stromal Clp protease.

With respect to suppressor phenotypes, gene expression analysis has revealed that the introduction of *gun1* into plants carrying the *sg1* genetic background partially rectifies the imbalance in the expression of chloroplast-related genes caused by the *sg1* mutation [38]. For example, the *gun1 sg1* double mutant shows increased expression of *RbcL* and *accD* (both of which are expressed at very low levels in *sg1*) and much reduced expression of *rpoB*, relative to that in *sg1*. Therefore, it seems that *gun1* can partially correct the imbalance in levels of chloroplast-related genes in *sg1*, thereby suppressing the deleterious phenotypes. Similarly, the increased accumulation of PRPS1 protein observed in the leaky *prps1-1* mutant in the absence of the GUN1 protein (*gun1 prps1-1*; [17]) could be related to the lack of upregulation and editing of *ClpP1* transcripts encoding a subunit of the major plastid stromal protease. As a consequence, PRPS1 may be degraded less efficiently [17,51]. The suppression of the *msl2 msl3* double mutant phenotype seen in *gun1 msl2 msl3* seedlings is more difficult to explain [48]. Certainly, GUN1-mediated retrograde communication is only one of the many regulatory pathways and feedback loops that govern dynamic cell identity decision-making at the plant shoot apex. It may be speculated that the absence of this communication still permits proper leaf differentiation, even in the presence of plastid dysfunctions in the shoot apex.

This large collection of genetic and molecular data related to GUN1 function can now be integrated into a model, which is based on the following lines of evidence (Figure 2):

a. GUN1 is present in very low amounts as long as chloroplast biogenesis proceeds normally, i.e., in the absence of stresses/dysfunction of developing plastids. As a matter of fact, the *gun1* mutant is hardly distinguishable from wild-type plants under optimal chloroplast biogenesis conditions (Figure 2a).

b. GUN1 protein levels increase when stresses and/or alterations of plastid functions occur during chloroplast biogenesis. Under these conditions, NEP activity is favored relative to PEP in the developing chloroplasts. This, together with the ensuing retrograde inhibition of photosynthesis-associated nuclear gene (*PhANGs*) expression, results in pale cotyledons and/or leaves in the best-case scenario. Therefore, the prevention of photo-oxidative damage seems to prevail over the optimal organization of the photosynthetic apparatus and its capacity for light absorption (Figure 2b).

c. Lack of GUN1 disables, at least partially, retrograde signaling and its repressive influence on *PhANGs* and causes major alterations in plastid RNA metabolism, including reduced NEP activity and changes in editing levels of RNAs encoding subunits of the ATP-dependent Clp protease, the NDH complex, the ribosomes, photosystem II, and the core of the PEP enzyme (Figure 2c). When the *gun1* mutation is introgressed into genetic backgrounds with defects in either the plastid protein homeostasis machinery (see as examples *sca3-1*, *sg1*, *prpl11-1*, *prps1-1*, *ftsh5-3*, *prin2-1*, *bpg2-2*, *ftsh1-1*; for further details, refer to Table 1), sugar sensing (*sicy-192*; for further details, refer to Table 2), or plastid osmosis (*msl2 msl3*; for further details, refer to Table 2), the corresponding higher-order mutants show a range of phenotypes. (i) In most cases, an exacerbated phenotype is observed, as a consequence of the fact that *gun1*-associated alterations

are added to the impairments caused by the original mutant backgrounds as, for instance, in the case of *sca3-1 gun1-102*, *prpl11-1 gun1-102*, *ftsh5-3 gun1-102* (for further details, see Table 1). (ii) In a few cases, no additive phenotype is detected, either because GUN1 activity is not required under that specific plastid perturbation, or is rather limited, as in the case of *prin2-1 gun1-1*, *hpg2-2 gun1-101*, *ftsh1-1 gun1-102* (for further details, see Table 1). (iii) In a small minority of cases, a suppressor phenotype is observed as a consequence of the ability of *gun1*-associated alterations to mitigate the imbalances caused by the initial mutant backgrounds. This is the case of *sg1 gun1-1* and *prps1-1 gun1-102* double mutants and *msl2 msl3 gun1-9* triple mutant.

Overall, GUN1 seems to modulate photosynthetic efficiency in cotyledons and leaves to minimize the consequences of malfunctions in developing chloroplasts, primarily with a view to preventing, or at least reducing, photo-oxidative damage.

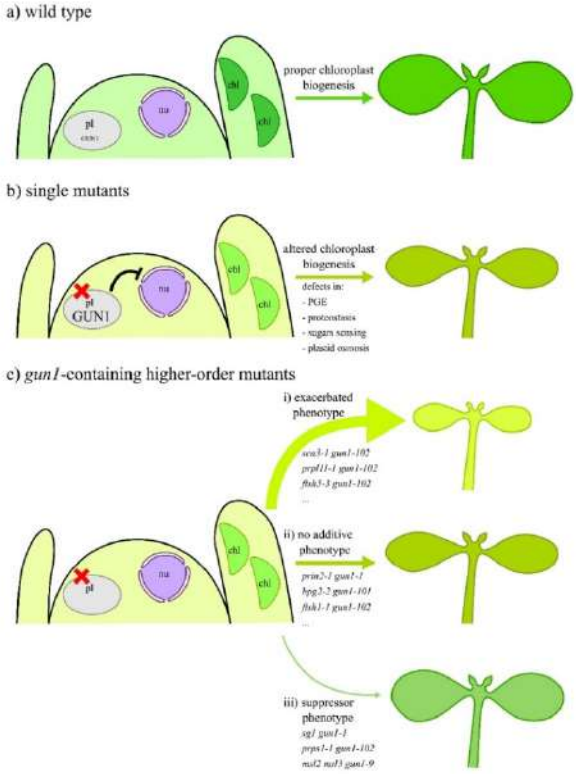

Figure 2. Schematic overview of the role of GUN1 protein during the early stages of chloroplast biogenesis. (**a**) Under optimal conditions, i.e., environmental and genetic conditions, the abundance of the GUN1 protein is rather low, and no GUN1-dependent negative retrograde signal is sent from the

developing chloroplasts to the nucleus to downregulate the expression of *PhANGs*. As a result, proper chloroplast biogenesis occurs in cotyledons and leaves. (b) Under conditions that alter plastid activity, i.e., genetic defects that impair plastid gene expression (PGE), plastid protein homeostasis (proteostasis), sugar sensing, and plastid osmosis, the abundance of GUN1 protein increases in developing chloroplasts. As a consequence, NEP activity is favored over PEP, changes in plastid RNA editing levels take place, and a GUN1-dependent negative signal reaches the nucleus and reduces expression of *PhANGs*. In this scenario, seedlings show defects in chloroplast development, photosynthetic performance, and growth. (c) The importance of the GUN1 protein in chloroplast biogenesis becomes evident when the *gun1* mutation is introgressed into Arabidopsis mutants with defects in PGE, proteostasis, sugar sensing, and maintenance of plastid osmosis. Under these conditions, chloroplast biogenesis is altered, and the GUN1-dependent negative retrograde signal is absent. These conditions, in most of the analyzed cases (20 out of 31, 64.5%), result in exacerbated phenotypes, characterized by a marked reduction in leaf pigmentation and reduced photosynthetic performance and growth. Only in few cases (25.8%), the lack of GUN1 protein fails to cause additive phenotypic effects, while in the remaining three cases (9.7%), lack of GUN1 suppresses the mutant phenotypes. pl, proplastid; nu, nucleus; chl, chloroplast.

6. Conclusions and Open Questions

Over the past decade, several labs worldwide have collected important pieces of genetic and molecular information concerning the role of GUN1 during the early stages of chloroplast biogenesis. The very recent data on the involvement of GUN1 in plastid RNA metabolism obtained in our lab, almost concomitantly with the labs of Joanne Chory and Enrique Lopez-Juez, allow us to integrate all the information now available into a unified model, which is schematically depicted in Figure 2 [12–16]. As yet, little can be said about how GUN1 is recruited to modulate transcript accumulation and editing under conditions that trigger retrograde communication. Furthermore, the molecular mechanism(s) that link(s) plastid RNA metabolism to retrograde signaling deserve(s) further study. The changes in editing levels of transcripts encoding subunits of the NDH complex prompt the speculation that alteration of NDH activity could affect the redox state of plastids, thereby triggering retrograde communication. In addition, modification of Clp protease activity, as a consequence of a GUN1-dependent influence on *clpP* RNA metabolism, could be at the basis of the unfolded protein response signaling pathway [39,53–55]. Similarly, altered expression of the plastid gene *ycf1* could provide the connection between plastid protein import, cytosolic folding stress, and plastid precursor protein-mediated retrograde communication [14,44]. Further analyses of GUN1 and its involvement in plastid RNA metabolism will provide important clues to the molecular mechanisms at the root of the coordination of plastid-nucleus gene expression. In this context, we suggest the use of GUN1 chimeras expressed under the control of the wild-type GUN1 promoter—which can be obtained by the recently developed CRISPR/Cas9-mediated gene targeting approach [56]—to resolve remaining ambiguities in GUN1 function—introduced, most probably, by the use of *GUN1* over-expressing lines for molecular studies. This strategy, designed in several labs to boost the very low abundance of the GUN1, might have led to the identification of interacting partners that are not essential for its function, as a consequence of the rather sticky nature of the protein, as highlighted by the identification of several protein interactors [57]. In the end, GUN1 may turn out to an "almost" typical plastid PPR protein, as indicated by its involvement in RNA metabolism.

Author Contributions: L.T. and N.J. have drafted the manuscript. L.T. organized Tables 1 and 2 while N.J. took care of Figures 1 and 2. P.P. supervised the entire work and finalized the manuscript. All authors have read and agreed to the published version of the manuscript.

Funding: This research was funded by MUR—Ministero dell'Università e della Ricerca, grant number PRIN-2017 2017FBS8YN.

Acknowledgments: We apologize to the authors who did not get their work discussed in this manuscript due to space limitations. We are grateful to Paul Hardy for critical reading of the manuscript.

Conflicts of Interest: The authors declare no conflict of interest.

References

1. Susek, R.E.; Ausubel, F.M.; Chory, J. Signal transduction mutants of arabidopsis uncouple nuclear CAB and RBCS gene expression from chloroplast development. *Cell* **1993**, *74*, 787–799. [CrossRef]
2. Koussevitzky, S.; Nott, A.; Mockler, T.C.; Hong, F.; Sachetto-Martins, G.; Surpin, M.; Lim, J.; Mittler, R.; Chory, J. Signals from Chloroplasts Converge to Regulate Nuclear Gene Expression. *Science* **2007**, *316*, 715–719. [CrossRef]
3. Bramley, P.M. Inhibition of carotenoid biosynthesis. In *Carotenoids in Photosynthesis*; Springer: Berlin/Heidelberg, Germany, 1993; pp. 127–159.
4. Mulo, P.; Pursiheimo, S.; Hou, C.X.; Tyystjärvi, T.; Aro, E.M. Multiple effects of antibiotics on chloroplast and nuclear gene expression. *Funct. Plant Biol.* **2003**, *30*, 1097–1103. [CrossRef] [PubMed]
5. Gray, J.C.; Sullivan, J.A.; Wang, J.H.; Jerome, C.A.; MacLean, D.; Allen, J.F.; Horner, D.S.; Howe, C.J.; Lopez-Juez, E.; Herrmann, R.G.; et al. Coordination of plastid and nuclear gene expression. *Philos. Trans. R. Soc. B Biol. Sci.* **2003**, *358*, 135–145. [CrossRef]
6. Mathews, D.E.; Durbin, R.D. Tagetitoxin inhibits RNA synthesis directed by RNA polymerases from chloroplasts and Escherichia coli. *J. Biol. Chem.* **1990**, *265*, 493–498.
7. Rapp, J.C.; Mullet, J.E. Chloroplast transcription is required to express the nuclear genes rbcS and cab. Plastid DNA copy number is regulated independently. *Plant Mol. Biol.* **1991**, *17*, 813–823. [CrossRef] [PubMed]
8. Allison, L.A. The role of sigma factors in plastid transcription. *Biochimie* **2000**, *82*, 537–548. [CrossRef]
9. Lysenko, E.A. Plant sigma factors and their role in plastid transcription. *Plant Cell Rep.* **2007**, *26*, 845–859. [CrossRef] [PubMed]
10. Chi, W.; He, B.; Mao, J.; Jiang, J.; Zhang, L. Plastid sigma factors: Their individual functions and regulation in transcription. *Biochim. Biophys. Acta Bioenerg.* **2015**, *1847*, 770–778. [CrossRef] [PubMed]
11. Woodson, J.D.; Perez-Ruiz, J.M.; Schmitz, R.J.; Ecker, J.R.; Chory, J. Sigma factor-mediated plastid retrograde signals control nuclear gene expression. *Plant J.* **2013**, *73*, 1–13. [CrossRef]
12. Zhao, X.; Huang, J.; Chory, J. GUN1 interacts with MORF2 to regulate plastid RNA editing during retrograde signaling. *Proc. Natl. Acad. Sci. USA* **2019**, *116*, 10162–10167. [CrossRef] [PubMed]
13. Loudya, N.; Okunola, T.; He, J.; Jarvis, P.; López-Juez, E. Retrograde signalling in a virescent mutant triggers an anterograde delay of chloroplast biogenesis that requires GUN1 and is essential for survival. *Philos. Trans. R. Soc. B Biol. Sci.* **2020**, *375*, 20190400. [CrossRef] [PubMed]
14. Tadini, L.; Peracchio, C.; Trotta, A.; Colombo, M.; Mancini, I.; Jeran, N.; Costa, A.; Faoro, F.; Marsoni, M.; Vannini, C.; et al. GUN1 influences the accumulation of NEP-dependent transcripts and chloroplast protein import in Arabidopsis cotyledons upon perturbation of chloroplast protein homeostasis. *Plant J.* **2020**, *101*, 1198–1220. [CrossRef] [PubMed]
15. Tadini, L.; Jeran, N.; Peracchio, C.; Masiero, S.; Colombo, M.; Pesaresi, P. The plastid transcription machinery and its coordination with the expression of nuclear genome: Plastid-Encoded Polymerase, Nuclear-Encoded Polymerase and the Genomes Uncoupled 1-mediated retrograde communication. *Philos. Trans. R. Soc. B Biol. Sci.* **2020**, *375*, 20190399. [CrossRef] [PubMed]
16. Zhao, X.; Huang, J.; Chory, J. Unraveling the Linkage between Retrograde Signaling and RNA Metabolism in Plants. *Trends Plant Sci.* **2020**, *25*, 141–147. [CrossRef] [PubMed]
17. Tadini, L.; Pesaresi, P.; Kleine, T.; Rossi, F.; Guljamow, A.; Sommer, F.; Mühlhaus, T.; Schroda, M.; Masiero, S.; Pribil, M.; et al. GUN1 Controls Accumulation of the Plastid Ribosomal Protein S1 at the Protein Level and Interacts with Proteins Involved in Plastid Protein Homeostasis. *Plant Physiol.* **2016**, *170*, 1817–1830. [CrossRef] [PubMed]
18. Allison, L.A.; Simon, L.D.; Maliga, P. Deletion of rpoB reveals a second distinct transcription system in plastids of higher plants. *EMBO J.* **1996**, *15*, 2802–2809. [CrossRef]
19. Hajdukiewicz, P.T.J.; Allison, L.A.; Maliga, P. The two RNA polymerases encoded by the nuclear and the plastid compartments transcribe distinct groups of genes in tobacco plastids. *EMBO J.* **1997**, *16*, 4041–4048. [CrossRef]
20. De Santis-Maciossek, G.; Kofer, W.; Bock, A.; Schoch, S.; Maier, R.M.; Wanner, G.; Rüdiger, W.; Koop, H.U.; Herrmann, R.G. Targeted disruption of the plastid RNA polymerase genes rpoA, B and C1: Molecular biology, biochemistry and ultrastructure. *Plant J.* **1999**, *18*, 477–489. [CrossRef]
21. Lerbs-Mache, S. Function of plastid sigma factors in higher plants: Regulation of gene expression or just preservation of constitutive transcription? *Plant Mol. Biol.* **2011**, *76*, 235–249. [CrossRef]

22. Steiner, S.; Schroter, Y.; Pfalz, J.; Pfannschmidt, T. Identification of Essential Subunits in the Plastid-Encoded RNA Polymerase Complex Reveals Building Blocks for Proper Plastid Development. *Plant Physiol.* **2011**, *157*, 1043–1055. [CrossRef] [PubMed]
23. Kindgren, P.; Kremnev, D.; Blanco, N.E.; de Dios Barajas López, J.; Fernández, A.P.; Tellgren-Roth, C.; Small, I.; Strand, Å. The plastid redox insensitive 2 mutant of Arabidopsis is impaired in PEP activity and high light-dependent plastid redox signalling to the nucleus. *Plant J.* **2012**, *70*, 279–291. [CrossRef] [PubMed]
24. Díaz, M.G.; Hernández-Verdeja, T.; Kremnev, D.; Crawford, T.; Dubreuil, C.; Strand, Å. Redox regulation of PEP activity during seedling establishment in Arabidopsis thaliana. *Nat. Commun.* **2018**, *9*. [CrossRef]
25. Wu, H.; Zhang, L. The PPR protein PDM1 is involved in the processing of rpoA pre-mRNA in Arabidopsis thaliana. *Chin. Sci. Bull.* **2010**, *55*, 3485–3489. [CrossRef]
26. Schweer, J.; Geimer, S.; Meurer, J.; Link, G. Arabidopsis mutants carrying chimeric sigma factor genes reveal regulatory determinants for plastid gene expression. *Plant Cell Physiol.* **2009**, *50*, 1382–1386. [CrossRef]
27. Pfalz, J.; Liere, K.; Kandlbinder, A.; Dietz, K.J.; Oelmüller, R. pTAC2, -6, and -12 are components of the transcriptionally active plastid chromosome that are required for plastid gene expression. *Plant Cell* **2006**, *18*, 176–197. [CrossRef]
28. Pyo, Y.J.; Kwon, K.C.; Kim, A.; Cho, M.H. Seedling lethal1, a pentatricopeptide repeat protein lacking an E/E+ or DYW domain in Arabidopsis, is involved in plastid gene expression and early chloroplast development. *Plant Physiol.* **2013**, *163*, 1844–1858. [CrossRef]
29. Myouga, F.; Hosoda, C.; Umezawa, T.; Iizumi, H.; Kuromori, T.; Motohashi, R.; Shono, Y.; Nagata, N.; Ikeuchi, M.; Shinozaki, K. A heterocomplex of iron superoxide dismutases defends chloroplast nucleoids against oxidative stress and is essential for chloroplast development in arabidopsis. *Plant Cell* **2008**, *20*, 3148–3162. [CrossRef]
30. Zhou, W.; Cheng, Y.; Yap, A.; Chateigner-Boutin, A.L.; Delannoy, E.; Hammani, K.; Small, I.; Huang, J. The Arabidopsis gene YS1 encoding a DYW protein is required for editing of rpoB transcripts and the rapid development of chloroplasts during early growth. *Plant J.* **2009**, *58*, 82–96. [CrossRef]
31. Ramos-Vega, M.; Guevara-García, A.; Llamas, E.; Sánchez-León, N.; Olmedo-Monfil, V.; Vielle-Calzada, J.P.; León, P. Functional analysis of the Arabidopsis thaliana CHLOROPLAST BIOGENESIS 19 pentatricopeptide repeat editing protein. *New Phytol.* **2015**, *208*, 430–441. [CrossRef]
32. Small, I.D.; Schallenberg-Rüdinger, M.; Takenaka, M.; Mireau, H.; Ostersetzer-Biran, O. Plant organellar RNA editing: What 30 years of research has revealed. *Plant J.* **2020**, *101*, 1040–1056. [CrossRef]
33. Kakizaki, T.; Yazu, F.; Nakayama, K.; Ito-Inaba, Y.; Inaba, T. Plastid signalling under multiple conditions is accompanied by a common defect in RNA editing in plastids. *J. Exp. Bot.* **2012**, *63*, 251–260. [CrossRef] [PubMed]
34. Yu, Q.B.; Jiang, Y.; Chong, K.; Yang, Z.N. AtECB2, a pentatricopeptide repeat protein, is required for chloroplast transcript accd rna editing and early chloroplast biogenesis in arabidopsis thaliana. *Plant J.* **2009**, *59*, 1011–1023. [CrossRef] [PubMed]
35. Tseng, C.C.; Sung, T.Y.; Li, Y.C.; Hsu, S.J.; Lin, C.L.; Hsieh, M.H. Editing of accD and ndhF chloroplast transcripts is partially affected in the Arabidopsis vanilla cream1 mutant. *Plant Mol. Biol.* **2010**, *73*, 309–323. [CrossRef] [PubMed]
36. Takenaka, M.; Zehrmann, A.; Verbitskiy, D.; Kugelmann, M.; Härtel, B.; Brennicke, A. Multiple organellar RNA editing factor (MORF) family proteins are required for RNA editing in mitochondria and plastids of plants. *Proc. Natl. Acad. Sci. USA* **2012**, *109*, 5104–5109. [CrossRef] [PubMed]
37. Chateigner-Boutin, A.L.; Ramos-Vega, M.; Guevara-García, A.; Andrés, C.; Gutiérrez-Nava, M.D.L.L.; Cantero, A.; Delannoy, E.; Jiménez, L.F.; Lurin, C.; Small, I.; et al. CLB19, a pentatricopeptide repeat protein required for editing of rpoA and clpP chloroplast transcripts. *Plant J.* **2008**, *56*, 590–602. [CrossRef] [PubMed]
38. Hu, Z.; Xu, F.; Guan, L.; Qian, P.; Liu, Y.; Zhang, H.; Huang, Y.; Hou, S. The tetratricopeptide repeat-containing protein slow green1 is required for chloroplast development in Arabidopsis. *J. Exp. Bot.* **2014**, *65*, 1111–1123. [CrossRef]
39. Llamas, E.; Pulido, P.; Rodriguez-Concepcion, M. Interference with plastome gene expression and Clp protease activity in Arabidopsis triggers a chloroplast unfolded protein response to restore protein homeostasis. *PLoS Genet.* **2017**, *13*, e1007022. [CrossRef]
40. Wang, J.; Xia, H.; Zhao, S.Z.; Hou, L.; Zhao, C.Z.; Ma, C.L.E.; Wang, X.J.; Li, P.C. A role of GUNs-Involved retrograde signaling in regulating Acetyl-CoA carboxylase 2 in Arabidopsis. *Biochem. Biophys. Res. Commun.* **2018**, *505*, 712–719. [CrossRef]

41. Paieri, F.; Tadini, L.; Manavski, N.; Kleine, T.; Ferrari, R.; Morandini, P.; Pesaresi, P.; Meurer, J.; Leister, D. The DEAD-box RNA helicase RH50 is a 23S-4.5S rRNA maturation factor that functionally overlaps with the plastid signaling factor GUN1. *Plant Physiol.* **2018**, *176*, 634–648. [CrossRef]
42. Sun, X.; Xu, D.; Liu, Z.; Kleine, T.; Leister, D. Functional relationship between mTERF4 and GUN1 in retrograde signaling. *J. Exp. Bot.* **2016**, *67*, 3909–3924. [CrossRef] [PubMed]
43. Marino, G.; Naranjo, B.; Wang, J.; Penzler, J.F.; Kleine, T.; Leister, D. Relationship of GUN1 to FUG1 in chloroplast protein homeostasis. *Plant J.* **2019**, *99*, 521–535. [CrossRef] [PubMed]
44. Wu, G.Z.; Meyer, E.H.; Richter, A.S.; Schuster, M.; Ling, Q.; Schöttler, M.A.; Walther, D.; Zoschke, R.; Grimm, B.; Jarvis, R.P.; et al. Control of retrograde signalling by protein import and cytosolic folding stress. *Nat. Plants* **2019**, *5*, 525–538. [CrossRef] [PubMed]
45. Kato, Y.; Sakamoto, W. FtsH protease in the thylakoid membrane: Physiological functions and the regulation of protease activity. *Front. Plant Sci.* **2018**, *9*, 855. [CrossRef] [PubMed]
46. Vinti, G.; Hills, A.; Campbell, S.; Bowyer, J.R.; Mochizuki, N.; Chory, J.; López-Juez, E. Interactions between hy1 and gun mutants of Arabidopsis, and their implications for plastid/nuclear signalling. *Plant J.* **2008**, *24*, 883–894. [CrossRef]
47. Mochizuki, N.; Brusslan, J.A.; Larkin, R.; Nagatani, A.; Chory, J. Arabidopsis genomes uncoupled 5 (GUN5) mutant reveals the involvement of Mg-chelatase H subunit in plastid-to-nucleus signal transduction. *Proc. Natl. Acad. Sci. USA* **2001**, *98*, 2053–2058. [CrossRef]
48. Wilson, M.E.; Mixdorf, M.; Berg, R.H.; Haswell, E.S. Plastid osmotic stress influences cell differentiation at the plant shoot apex. *Development* **2016**, *143*, 3382–3393. [CrossRef]
49. Maruta, T.; Miyazaki, N.; Nosaka, R.; Tanaka, H.; Padilla-Chacon, D.; Otori, K.; Kimura, A.; Tanabe, N.; Yoshimura, K.; Tamoi, M.; et al. A gain-of-function mutation of plastidic invertase alters nuclear gene expression with sucrose treatment partially via GENOMES UNCOUPLED1-mediated signaling. *New Phytol.* **2015**, *206*, 1013–1023. [CrossRef]
50. Tameshige, T.; Fujita, H.; Watanabe, K.; Toyokura, K.; Kondo, M.; Tatematsu, K.; Matsumoto, N.; Tsugeki, R.; Kawaguchi, M.; Nishimura, M.; et al. Pattern Dynamics in Adaxial-Abaxial Specific Gene Expression Are Modulated by a Plastid Retrograde Signal during Arabidopsis thaliana Leaf Development. *PLoS Genet.* **2013**, *9*, e1003655. [CrossRef]
51. Wu, G.Z.; Chalvin, C.; Hoelscher, M.; Meyer, E.H.; Wu, X.N.; Bock, R. Control of retrograde signaling by rapid turnover of GENOMES UNCOUPLED1. *Plant Physiol.* **2018**, *176*, 2472–2495. [CrossRef]
52. Kikuchi, S.; Bédard, J.; Hirano, M.; Hirabayashi, Y.; Oishi, M.; Imai, M.; Takase, M.; Ide, T.; Nakai, M. Uncovering the protein translocon at the chloroplast inner envelope membrane. *Science* **2013**, *339*, 571–574. [CrossRef]
53. Ramundo, S.; Rochaix, J.D. Chloroplast unfolded protein response, a new plastid stress signaling pathway? *Plant Signal. Behav.* **2014**, *9*, 1–3. [CrossRef]
54. Ramundo, S.; Casero, D.; Muhlhaus, T.; Hemme, D.; Sommer, F.; Crevecoeur, M.; Rahire, M.; Schroda, M.; Rusch, J.; Goodenough, U.; et al. Conditional Depletion of the Chlamydomonas Chloroplast ClpP Protease Activates Nuclear Genes Involved in Autophagy and Plastid Protein Quality Control. *Plant Cell* **2014**, *26*, 2201–2222. [CrossRef] [PubMed]
55. Perlaza, K.; Toutkoushian, H.; Boone, M.; Lam, M.; Iwai, M.; Jonikas, M.C.; Walter, P.; Ramundo, S. The mars1 kinase confers photoprotection through signaling in the chloroplast unfolded protein response. *eLife* **2019**, *8*. [CrossRef]
56. Miki, D.; Zhang, W.; Zeng, W.; Feng, Z.; Zhu, J.K. CRISPR/Cas9-mediated gene targeting in Arabidopsis using sequential transformation. *Nat. Commun.* **2018**, *9*. [CrossRef]
57. Colombo, M.; Tadini, L.; Peracchio, C.; Ferrari, R.; Pesaresi, P. GUN1, a Jack-Of-All-Trades in Chloroplast Protein Homeostasis and Signaling. *Front. Plant. Sci.* **2016**, *7*. [CrossRef] [PubMed]

PHILOSOPHICAL TRANSACTIONS B

royalsocietypublishing.org/journal/rstb

Review

Cite this article: Tadini L, Jeran N, Peracchio C, Masiero S, Colombo M, Pesaresi P. 2020 The plastid transcription machinery and its coordination with the expression of nuclear genome: Plastid-Encoded Polymerase, Nuclear-Encoded Polymerase and the Genomes Uncoupled 1-mediated retrograde communication. *Phil. Trans. R. Soc. B* **375**: 20190399.
http://dx.doi.org/10.1098/rstb.2019.0399

Accepted: 24 October 2019

One contribution of 20 to a theme issue 'Retrograde signalling from endosymbiotic organelles'.

Subject Areas:
plant science

Keywords:
plastid, RNA polymerases, retrograde communication, photosynthesis, cotyledons, *Arabidopsis thaliana*

Author for correspondence:
Paolo Pesaresi
e-mail: paolo.pesaresi@unimi.it

†Present address: Istituto per la Protezione Sostenibile delle Piante, Consiglio Nazionale delle Ricerche, Strada delle Cacce 73, I-10135 Torino, Italy.

THE ROYAL SOCIETY PUBLISHING

The plastid transcription machinery and its coordination with the expression of nuclear genome: Plastid-Encoded Polymerase, Nuclear-Encoded Polymerase and the Genomes Uncoupled 1-mediated retrograde communication

Luca Tadini[1], Nicolaj Jeran[1], Carlotta Peracchio[1,†], Simona Masiero[1], Monica Colombo[2] and Paolo Pesaresi[1]

[1]Dipartimento di Bioscienze, Università degli studi di Milano, 20133 Milano, Italy
[2]Centro Ricerca e Innovazione, Fondazione Edmund Mach, 38010 San Michele all'Adige, Italy

PP, 0000-0002-3236-7005

Plastid genes in higher plants are transcribed by at least two different RNA polymerases, the plastid-encoded RNA polymerase (PEP), a bacteria-like core enzyme whose subunits are encoded by plastid genes (*rpoA*, *rpoB*, *rpoC1* and *rpoC2*), and the nuclear-encoded plastid RNA polymerase (NEP), a monomeric bacteriophage-type RNA polymerase. Both PEP and NEP enzymes are active in non-green plastids and in chloroplasts at all developmental stages. Their transcriptional activity is affected by endogenous and exogenous factors and requires a strict coordination within the plastid and with the nuclear gene expression machinery. This review focuses on the different molecular mechanisms underlying chloroplast transcription regulation and its coordination with the photosynthesis-associated nuclear genes (*PhANGs*) expression. Particular attention is given to the link between NEP and PEP activity and the GUN1- (Genomes Uncoupled 1) mediated chloroplast-to-nucleus retrograde communication with respect to the *Δrpo* adaptive response, i.e. the increased accumulation of NEP-dependent transcripts upon depletion of PEP activity, and the editing-level changes observed in NEP-dependent transcripts, including *rpoB* and *rpoC1*, in *gun1* cotyledons after norflurazon or lincomycin treatment. The role of cytosolic preproteins and HSP90 chaperone as components of the GUN1-retrograde signalling pathway, when chloroplast biogenesis is inhibited in *Arabidopsis* cotyledons, is also discussed.

This article is part of the theme issue 'Retrograde signalling from endosymbiotic organelles'.

1. Introduction

Compared to its cyanobacterial ancestor, the transcriptional apparatus of the land plant chloroplast is more complex and reflects the evolutionary integration of a prokaryotic gene expression system into a eukaryotic host cell. Unlike bacteria, chloroplasts of angiosperms and the moss *Physcomitrella patens* require at least two different RNA polymerases to ensure transcription of plastid genes: the plastid-encoded polymerase (PEP), a multimeric bacterial-type enzyme [1], and, in addition, the nuclear-encoded polymerase (NEP), a monomeric T3-T7 bacteriophage-type enzyme [2,3]. Correct plastid development and functionality necessitate the interplay of both PEP and NEP enzymes, together with nuclear-encoded factors, such as sigma-like factors (Sig) and PEP-associated proteins (PAPs) [4–8]. These are just a few examples of nuclear factors that exert control

over the plastid gene expression (PGE), since the nuclear genome encodes most of the plastid proteins [9]. On the other hand, chloroplast biogenesis and functionality also require tight coordination of the transcription of thousands of nuclear genes with the expression of the relatively few plastid genes. This coordination is achieved through an extensive flow of information from developing plastids to the nucleus, via biogenic retrograde signalling, and from mature chloroplasts to the nucleus, via operational retrograde signalling [10–12]. The GUN1 (genomes uncoupled 1) protein, a pentatricopetide repeat protein that localizes to plastids, was proposed as the central node relaying information from multiple retrograde signalling pathways that regulate photosynthesis-associated nuclear genes (*PhANGs*) expression [13]. Interestingly, the involvement of GUN1 in relaying signals after norfluorazon (NF) and lincomycin (Lin) treatments [13], and after impairment of protein import [14] and PGE [15–17] raises the possibility that each of the treatments or mutant genetic backgrounds may affect a similar process, thereby using GUN1 as a common signalling component [18]. Intriguingly, GUN1 and NEP proteins have some features in common including the fact that (i) NEP, as GUN1, should be found in plastid nucleoids, since plastid DNA is exclusively located in these domains; (ii) the NEP polymerase and the GUN1 protein have never been detected in plastid proteomics analysis [6,19,20], most probably as a consequence of their very low abundance; and (iii) they are highly active during early stages of chloroplast biogenesis [2,21]. This review focuses on the recently discovered molecular mechanisms at the basis of the regulation of chloroplast transcription and its coordination with *PhANGs* expression during early stages of chloroplast development and upon alteration of plastid protein homeostasis in *Arabidopsis* cotyledons. Particular emphasis is given to the link between NEP and PEP activity and the GUN1-mediated chloroplast-to-nucleus retrograde communication in *Arabidopsis* cotyledons [22–24].

2. The plastid-encoded RNA polymerase

The PEP catalytic core is made of α_2 (it occurs as a dimer and serves as a stabilizing agent of the PEP core), β (the catalytic subunit), β' (unknown function) and β'' (DNA binding function) subunits, encoded by the plastid *rpoA*, *rpoB*, *rpoC1* and *rpoC2* genes, respectively, and inherited from the cyanobacterial ancestor [25]. Studies performed in barley, tobacco and *Arabidopsis* showed that *rpo* genes are essential for proper chloroplast biogenesis, as mutants lacking any PEP subunit exhibit an albino or yellowish phenotype [26]. As in any other bacterial RNA polymerase, the PEP enzyme needs sigma factors (σ) for promoter recognition and initiation of transcription [27]. Genes coding for plastid sigma factors are located in the nuclear genome, thus, PGE is strictly controlled by the nucleus. In *Arabidopsis thaliana*, six different sigma factors, SIG1–SIG6, have been identified. Their specific functions in chloroplast physiology have not been fully understood yet, however, the investigation of knockout mutants has provided the first insights [5]. The PEP enzyme is located in the nucleoids and the Rpo core subunits jointly with one of the sigma factors form the holoenzyme that, upon light exposure, recruits additional subunits driving chloroplasts biogenesis. Different nucleus-encoded proteins, unrelated to bacterial transcription factors, are consistently co-purified with PEP and collectively are named PEP-associated proteins (PAPs) [6]. PAPs are an evolutionary conquest of solely land plants, as no PAP orthologues were found in *Chlamydomonas reinhardtii* [6,28]. Intriguingly, functional studies on PAP knockout mutants indicate that PAP proteins are required for PEP-mediated transcription and regulation [29–36], contributing to establish a subdomain in the plastid nucleoid where PEP-mediated transcription takes place [6].

3. Origin and evolution of nuclear-encoded polymerase

In the early 1990s, researchers postulated the existence of a nuclear-encoded and plastid-located RNA polymerase, NEP. The first evidence came from the obligate parasitic angiosperm *Epifagus virginiana* that possesses plastids with a reduced genome (just nine genes are retained), deprived of all *rpo* genes [37], and from the barley mutant *albostrians* deficient in plastid ribosomes [38] and therefore unable to synthesize the PEP core subunits. Despite the absence of PEP, plastid transcripts were detectable both in *Epifagus virginiana* and in *albostrians* barley mutant, suggesting the existence of a nuclear-encoded plastid RNA polymerase. In the same period, a 110 kDa polypeptide was purified from spinach chloroplasts via sodium dodecyl sulfate-polyacrylamide gel electrophoresis. The purified polypeptide actively synthesized RNA in the presence of supercoiled DNA template and nucleoside triphosphates, showing features of a single-subunit RNA polymerase of the T3-T7 bacteriophage type [39]. The plant genome era, inaugurated by the release of the *Arabidopsis thaliana* genome, allowed the identification of three nuclear genes, called *RPOT*, coding for phage-like RNA polymerases, targeted to mitochondria (*RPOT1*/RpoTm), chloroplasts (*RPOT3*/RpoTp) and to both organelles (*RPOT2*/RpoTmp) [40,41]. In general, the three *RPOT* genes are present in eudicotyledon plants, while *RPOT2*, encoding the dual-located RpoTmp, is absent in monocots and early-diverging angiosperms [42,43]. The basal angiosperm *Nuphar advena*, for instance, has two mitochondrial RNA polymerases and a proper NEP, which could be considered the phylogenetically earliest RpoTp enzyme in higher plants [44]. Unicellular green algae, such as *C. reinhardtii*, *Ostreococcus tauri* and *Thalassiosira pseudonana*, also have a single gene for the RpoTm and no RpoTmp enzyme [43,45]. This feature is in common with fungi and mammals, as well as the spike-moss *Selaginella moellendorffii* [43,46]. However, the nuclear genome of the moss *P. patens* bears three *RPOT* gene as in *Arabidopsis*. However, one gene codes for an exclusively mitochondrial polymerase, while the other two produce two dual-located RpoTmp enzymes [3]. In the light of these phylogenetic data, the NEP enzyme appeared to originate from duplication of the *RPOT1* gene, which could have occurred multiple times in the evolution of land plants, as three copies of *RPOT* genes are present in mosses and dicot plants but not in spike-mosses and monocots. Alternatively, the extra dual-located enzyme could have been lost during evolution [43,44].

NEP, like PEP, is essential for chloroplast transcription. Knocking out the *RPOT2* or *RPOT3* genes in *Arabidopsis* yields plants with delayed chloroplast biogenesis, while the *rpot2 rpot3* double mutant is characterized by chlorophyll deficiency and a complete arrest of growth early in development [47], indicating partially overlapping functions of RpoTp and RpoTmp in chloroplast gene transcription.

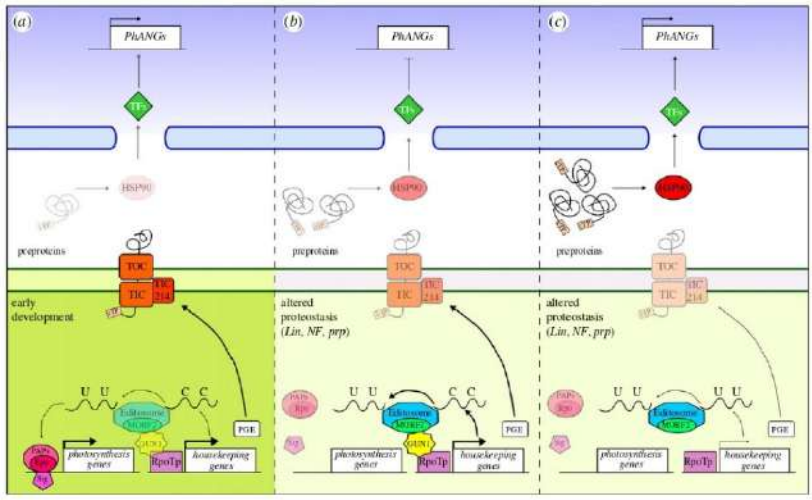

Figure 1. Schematic overview of the GUN1-dependent coordination of plastid and nuclear transcriptional machinery in three different scenarios: early stages of chloroplast development (*a*), altered protein homeostasis (*b*) and altered protein homeostasis in the absence of GUN1 protein (*c*). The role of GUN1 becomes evident when chloroplast biogenesis is altered either by chemical treatments (lincomycin of norflurazon) or genetic defects that impair plastid protein homeostasis (see panels indicated as altered proteostasis) [15,16,24]. Under these conditions, GUN1 has been reported to (i) interact with NEP and favour accumulation of NEP-dependent transcripts, including *ycf1* that encodes the Tic214 subunit of the protein translocon at the inner envelope membrane of chloroplasts [24]; (ii) interact with MORF2, a component of the Editosome protein complex, and edit NEP-dependent transcripts, including *rpoB* and *rpoC1*, but also *rps12*, *rps14*, *ndhB* and *ndhD* mRNAs [22]; (iii) interact with cpHSC70-1 and regulate plastid protein import (this detail is not shown) [23]. Overaccumulation of preproteins in the cytosol of *gun1* cotyledon cells induces the accumulation of cytosolic HSP90 proteins that favour *PhANGs* transcription [23,24]. This could be obtained by either 26S proteasome-dependent degradation of negative transcriptional regulators or activation, through HSP90-promoting folding, of positive ones (transcription factors, TFs). It is conceivable that a similar mechanism could be active even at early stages of chloroplast development [21], to fine-tune the chloroplast and nuclear transcription machineries with respect to the developmental needs. However, under these conditions the accumulation of preproteins and downstream components of the signalling pathway have not been described yet. Note that the thickness and brightness of lines and shapes is directly proportional to the activity of the specific process. cTP, chloroplast transite peptide; TOC, translocon at the outer chloroplast membrane; TIC, translocon at the inner chloroplast membrane; Lin, lincomycin; NF, norflurazon; *prp*, plastid ribosomal protein mutants; PGE, plastid gene expression, defined as transcription and translation rate of plastid-encoded genes.

4. Nuclear-encoded polymerase and plastid-encoded polymerase and their role in plastid gene expression

Data obtained during the last two decades indicate that both PEP and NEP polymerases are active in all green and non-green tissues, but with different degrees of activity according to the developmental stages and physiological conditions (figure 1). As a matter of fact, *Arabidopsis* dry seeds already contain several transcripts of the plastid transcription machinery, such as the NEP *RPOT2* and *RPOT3*, the PEP core *rpoA*, *rpoB*, *rpoC1*, *rpoC2*, and the nuclear-encoded PEP-associated sigma factors *SIG2* and *SIG5* [48,49]. These PEP core transcripts derive from chloroplasts present in photosynthetically active *Arabidopsis* embryos, before dedifferentiation to small non-green plastids, termed eoplasts, occurs during late embryo and seed maturation. In addition, during stratification (72 h at 4°C in the dark) several plastid house keeping genes, including *rpoA*, *rpoB*, *rpoC1* and *rpoC2*, and many nuclear genes encoding SIG1–6 factors and the RpoTp, RpoTmp enzymes are actively transcribed [48,50].

At the protein level, rpoB, RpoTp and RpoTmp are also present in dry seeds. Furthermore, a dramatic accumulation of RpoTp protein occurs shortly after imbibition, and its increased activity leads to a higher accumulation of PEP core proteins as well. Upon seed germination, NEP activities and transcripts increase and peak at 2–3 days after germination, leading to increased accumulation of NEP-dependent transcripts, followed by a severe drop as *RPOT3* gene expression decreases [51,52]. Moreover, gene expression studies revealed that *RPOT3* is mainly active in green photosynthetic tissues while *RPOT2* plays its role in dividing and non-green cells [53].

When seed germination takes place in darkness, the eoplasts turn into etioplasts, where a soluble inactive form of the PEP holoenzyme, termed PEP-B and made of core proteins only, is present. Upon illumination, the PEP complex starts interacting with several PAP proteins and becomes part of the membrane-bound plastid transcription active chromosome (pTAC) megadalton complex. This more complex enzyme, named PEP-A, increases the PEP activity and leads to the transcription of *Photosynthesis-Associated Plastid-Encoded Genes (PhAPGs)* and cotyledon greening [34,54,55].

NUCLEAR CONTROL OF PEP ACTIVITY (NCP), a dual-targeted nuclear/plastidial protein, also known as MRL7-L (Mesophyll-cell RNAi Library line 7-like) [56] and SVR4-like (Suppressor of Variegation 4-like) [57] because of its essential role in chloroplast biogenesis [56,57], is required for both the nuclear and plastidial signalling steps of *PhAPGs* activation, promoting the assembly of the PEP complex upon illumination [58]. In particular, NCP mediates the degradation of two repressors of chloroplast biogenesis in the nucleus, PIF1 and PIF3, thus participating in the phytochrome-mediated signalling at the basis of chloroplast biogenesis. NCP also has a paralog in *Arabidopsis*, At4g28590 also known as ECB1 (Early Chloroplast Biogenesis 1) [59], SVR4 (Suppressor of Variegation 4) [57] and MRL7 (Mesophyll-cell RNAi Library line 7), which was renamed Regulator of Chloroplast Biogenesis (RCB) [60]. Like NCP, RCB is also a dual-targeted nuclear/plastidial protein required for the degradation of the nuclear transcriptional regulators PIF1 and PIF3 and for PEP assembly and *PhAPGs* expression in the plastids. These data support a model in which phytochromes control *PhAPGs* expression through light-dependent double nuclear and plastidial switches that are linked by evolutionarily conserved and dual-localized regulatory proteins.

Following PEP-A assembly, the enzyme takes over most of the transcription activity, including mRNAs, rRNAs and most of the tRNAs [61–65], while the NEP enzyme remains active to perform the transcription of *rpoB* (forming an operon with *rpoC1* and *rpoC2*), *accD* (in dicots), *clpP*, *atpB*, *atp1*, genes coding for ribosomal proteins and a few tRNAs, and, in dicots, *ycf1* and *ycf2* until senescence.

5. Plastid-encoded polymerase regulation

PEP promoter recognition and transcription initiation are mediated by σ^{70}-like factors, as occurs in prokaryotes [27]. *Arabidopsis* has six different sigma factors, SIG1-SIG6. All *Arabidopsis sig* knockout mutants fail to accumulate wild-type levels of plastid transcripts; nevertheless, only *sig2* and *sig6* displayed a pale-green phenotype, suggesting a more relevant role in plastid transcription and chloroplast development [66]. Furthermore, only a partial functional redundancy among *Arabidopsis* SIG factors during early steps of seedling development has been revealed, indicating gene-specific functions [4,5].

Unlike their bacterial counterparts, the plastid sigma factors SIG1, SIG2 and SIG6 can be modified post-translationally by phosphorylation at the N-terminal variable region in fully mature chloroplasts [4,67]. SIG2 and SIG6 phosphorylation have been related to alterations in the promoter binding efficiency of PEP [68]. Similarly, SIG1 phosphorylation is regulated in a redox-dependent manner and serves to adapt PSII/PSI stoichiometry to light changes by modulating the relative transcription of the photosynthesis reaction centre genes *psbA* (photosystem II, PSII) and *psaA/B* (photosystem I, PSI), indicating that phosphorylation is also needed to adapt the PEP-dependent transcription to the redox state of the thylakoid electron transport chain [67]. Lastly, a role for SIG6 in the operational retrograde signalling during singlet oxygen stress has been reported [69]. In particular, a genetic screen uncovered a *sig6* mutant (*soldat8*) that was able to survive the high levels of singlet oxygen in the *Arabidopsis flu* mutant that has uncontrolled tetrapyrrole synthesis. This regulatory mechanism originated after the endosymbiosis event, since the N-terminal of plastid SIG factors is not conserved among bacteria and chloroplasts, and makes plastid SIG factors incompatible with the transcription machinery of bacteria [70,71].

SIG factors also contribute to the construction of PEP-A holoenzyme, together with the 12 true PAP proteins, identified through genetic and biochemical studies, and shown to be essential for chloroplast biogenesis in *Arabidopsis* [6]. Indeed, all *pap* mutants display an albinotic/chlorotic phenotype, corroborating the hypothesis that PAP proteins are fundamental for PEP activity, as Rpo-core subunits. In particular, PAPs are involved in different regulatory functions [34], including:

(i) DNA/RNA metabolism-related gene expression regulation, as in the case of PAP1, 2, 3, 5, 7 and 12. For instance, PAP1 and PAP2 display pentatricopeptide repeat (PPR) motifs, known to be involved in RNA metabolism [72] and PAP3 is predicted to interact with RNAs through its S1-like domain [35].

(ii) Redox-dependent gene regulation and protection against oxidative stresses, as in PAP4, 6, 9 and 10. As an example, PAP10/TrxZ physically interacts with the PLASTID REDOX INSENSITIVE 2 (PRIN2) protein, a key regulator of PEP activity, capable of transducing the redox state of thylakoid membranes into regulation of PEP-dependent transcription [73,74]. In particular, PAP10 interacts with the PRIN2 dimer and through its thioredoxin domain causes the reduction of inter-molecular disulfide bridges and the release of PRIN2 monomers, that are then able to boost the transcription of PEP-dependent genes, providing a mechanistic link between photosynthetic electron transport and activation of photosynthetic gene expression.

Chloroplast transcription has also been reported to be under the control of phytohormones during the greening of etioplasts [75] and in fully developed chloroplasts of barley (*Hordeum vulgare* L.). In particular, stimulatory effects of cytokinin (6-benzyladenine BA) and repressive effects of methyl jasmonate (MeJA), auxin (indole-3-acetic acid, IAA) and gibberellic acid (GA3) on chloroplast gene expression at the levels of transcription and transcript accumulation of both NEP- and PEP-transcribed genes have been reported [76,77]. More detailed information is available for abscisic acid (ABA). In particular, it has been shown that exogenously supplied ABA represses the transcription of plastid genes during greening and in fully mature chloroplasts in barley leaves, with the exception of *psbA*, *psbD* and a few other genes that remain as active as in untreated leaves [78]. Based on these findings, ABA seems to coordinate the repression of photosynthesis genes in the nuclear and chloroplast genomes while leaving active those chloroplast genes that are needed for the protection of the PSII reaction centres from damage by reactive oxygen species (ROS) [78]. This adaptive response involves the ABA-activated expression of *RSH2* and *RSH3* nuclear genes, coding for enzymes in the chloroplast that synthesize guanosine-3′, 5′-bisdiphosphate (ppGpp), an inhibitor of chloroplast transcription. In particular, ppGpp was shown to inhibit transcriptional activities of purified PEP preparations *in vitro* [79]. In addition, an assay based on the *in planta* incorporation of the base analogue 4-thiouridine into nascent chloroplast RNA demonstrated that the accumulation of ppGpp inhibits the transcription of PEP-dependent and, to a lesser extent, of NEP-dependent genes in developing seedlings [80], resembling the ancient bacterial stress-signalling pathway

known as the stringent response (for a review see [81]). Furthermore, relatively high ABA levels increase the amount of SIG5 by activating the expression of its gene in the nucleus leading to a subpopulation of SIG5–PEP. The SIG5–PEP transcribes chloroplast genes from specific promoters, resulting in the observed escape of a few plastid genes (*psbA*, *psbD*) from the otherwise general downregulation of transcription of chloroplast genes [78].

6. Nuclear-encoded polymerase regulation

Although PEP regulation has been widely characterized and several regulatory factors identified, only a few pieces of information on NEP activity regulation are currently available. Firstly, the tRNA-Glu is able to bind and inhibit the activity of NEP *in vitro*, displaying specificity compared to tRNA-Val, tRNA-Gly and tRNA-Trp, used as control [51]. The tRNA-Glu is different from the other plastid-encoded tRNAs, since it is not only involved in plastid protein synthesis but is the substrate for the synthesis of 5-aminolevulinic acid, an early step of the tetrapyrrole biosynthesis pathway that leads to chlorophyll, heme and phytochrome production. In particular, the tRNA-Glu, massively transcribed by PEP during the greening process, has a pivotal role in the switch between NEP and PEP activity, by inhibiting the NEP-dependent transcription in a threshold manner, once the greening has occurred [51]. A second regulatory mechanism of NEP activity was initially observed in tobacco leaves through the impairment of the plastid *rpoB* gene, encoding the β-subunit of the PEP enzyme. In particular, an entire class of plastid transcripts was found to accumulate at high level upon the complete loss of PEP activity [62,82]. Such an adaptation mechanism, termed as '*Δrpo* phenotype', was then reproduced in tobacco leaves upon depletion of the *rpoA*, *rpoB*, *rpoC1* and *rpoC2* genes [83], encoding the core complex of the PEP enzyme. Later, the *Δrpo* adaptive response was described in nearly every mutant identified as PEP regulator and impaired in PEP-dependent gene expression in *Arabidopsis*, including mutants with *PAP* gene expression defects (for further details, see table 1), together with many other mutants affected in the accumulation of key players of chloroplast protein homeostasis, such as PPR proteins involved in mRNA metabolism (CRP1 and PPR4), plastid ribosomal proteins (PRPL11 and PRPS21), chaperones (CLPR1 and cpHSP70–1), and the iron superoxide dismutase FSD2 and FSD3 (table 1). Moreover, impairment of chloroplast translation upon lincomycin treatment activates the *Δrpo* adaptive response in *Arabidopsis* seedlings [13,24]. More generally, it appears that every genetic- or chemical-induced impairment of plastid protein homeostasis leads to the upregulation of NEP-dependent transcripts, as an attempt by the PGE machinery to maintain non-photosynthetic plastid functions by expressing housekeeping genes. Strikingly, we have recently reported that GUN1 protein is able to physically interact with NEP in chloroplasts of *Arabidopsis* cotyledons and is required for the *Δrpo* adaptive response, providing an important link between plastid transcription and the GUN1-mediated plastid-to-nucleus retrograde communication [24].

7. Interplay between plastid transcription regulation and retrograde signalling

Due to the chimeric nature of PEP enzyme, made of subunits encoded by both the plastid and the nuclear genome, and the nuclear localization of NEP encoding genes, it is clear that the coordinated transcription of plastid and nuclear genes is essential for proper development of all plastid types. This coordination takes place through the nuclear control of PGE and the retrograde signalling pathways [10].

In the case of chloroplast biogenesis, multiple pieces of evidence on the coordination of plastid transcription and *PhANGs* expression have been reported. In particular, the status of plastid transcription and translation as a trigger for retrograde signalling has been demonstrated by repression of *PhANGs* expression upon chemical treatments, for instance with the plastid translation inhibitor lincomycin or by rifampicin, which selectively inhibit the PEP enzyme [12,66]. More specifically related to PEP-dependent transcription, increasing evidence indicates that several factors involved in the coordination of plastid and nuclear transcriptional machineries are characterized by the presence of both the chloroplast transit peptide (cTP) and the nuclear localization signal (NLS) in their peptide sequence, implying a plastid and nuclear dual localization [20]. These proteins have potential access to plastid and nuclear DNA and, therefore, they can be directly involved in the coordination of gene expression in both compartments. Among them are NCP and RCB, described above, and PAP1, –5, –7, –8, –9 and –12. Currently, only in the case of PAP5/pTAC12 has the dual localization been experimentally confirmed [88,100]. Indeed, PAP5 seems to be involved in the red light-mediated skotomorphogenesis-to-photomorphogenesis transition, through the physical interaction and degradation of phytochrome-interacting-factors PIF1 and PIF3, thereby affecting gene expression in the nucleus [101–103], similarly to NCP and RCB. Interestingly, genes coding for PAPs were found to be expressed in non-green tissues before the assembly of the PEP-A complex, which is induced in the light. It is, therefore, possible to speculate that the NLS-containing PAP proteins can form two different complexes, one in the nucleus and one in the chloroplast, and modulate gene expression in both compartments by interacting with different kinds of RNA polymerases [26]. In this scenario, a nuclear PAP complex could assemble in the dark at first, mediating the early steps of plastid development by interacting with RNA polymerase II, and upon illumination migrate to the chloroplast to form PEP-A, in a sort of NLS-cTP competition which could determine the PAP protein intracellular localization.

In addition to dual-located proteins, proteins specifically located in plastids are also able to coordinate plastid and nuclear gene expression. For instance, PRIN2 has been reported to be able to trigger retrograde signalling in response to light, besides its direct regulation of PEP activity, [73,74].

Furthermore, depletion of SIG2 and SIG6 in *Arabidopsis* allowed demonstration that the activity of both sigma factors is the source of retrograde signals that promote *PhANGs* expression [66]. The addition of the *gun1* mutation in *sig6* mutant led to a global reduction of 72 plastid transcripts, both PEP- and NEP-dependent, suggesting a possible involvement of GUN1 in the regulation of the plastid and nuclear transcriptional machineries. The physical interaction between PAP8/pTAC6 and GUN1 observed by Tadini *et al.* [15] points further to a direct link between PEP activity modulation and retrograde signalling.

More recently, Tadini and co-workers demonstrated that GUN1 plays a central role in the regulation of NEP activity, thus creating a direct link between retrograde signalling and

Table 1. List of genes/proteins whose impairments result in the activation of the *Δrpo* adaptive response, i.e. increase accumulation of NEP-dependent transcripts upon depletion of PEP activity.

gene	accession	phenotype	molecular defect	refs
plastid transcription regulation				
SIG2	AT1G08540	pale	reduced PEP activity	[66]
SIG6	AT2G36990	pale	reduced PEP activity	[66,84]
DG1	AT5G67570	delayed greening	reduced PEP activity	[84,85]
PAP2/pTAC2	AT1G74850	pale	reduced PEP activity; RNA maturation	[29]
PAP3/pTAC10	AT3G48500	albino	reduced PEP activity	[86]
PAP4/FSD3	AT5G23310	pale	reduced ROS scavenging; reduced PEP activity	[87]
PAP5/pTAC12/HMR	AT2G34640	pale	reduced PEP activity; altered phytochrome signalling	[88,89]
PAP6/FLN1	AT3G54090	albino	reduced PEP activity	[89]
FLN2	AT1G69200	virescent	reduced PEP activity	[89,90]
PAP7/pTAC14	AT4G20130	albino	reduced PEP activity	[90]
PAP8/pTAC6	AT1G21600	albino	reduced PEP activity	[29]
PAP9/FSD2	AT5G51100	pale	reduced ROS scavenging; reduced PEP activity	[87]
PAP10/TrxZ	AT3G06730	albino	reduced PEP activity	[34]
PAP12/pTAC7	AT5G24314	albino	reduced PEP activity	[91]
pTAC5	AT4G13670	pale	reduced PEP activity	[92]
PRIN2	AT1G10522	albino	reduced PEP activity; impaired redox-mediated retrograde signalling	[73,74]
ECB1/MRL7/SVR4/RCB	AT4G28590	tall/albino	reduced PEP activity; altered phytochrome signalling	[56,57,60]
MRL7-L/SVR4-L/NCP	AT2G31840	tall/albino	reduced PEP activity; altered phytochrome signalling	[57,58]
plastid transcripts maturation				
CRP1	AT5G42310	albino	impaired plastid mRNA maturation	[93]
PPR4	AT5G04810	embryo-lethal	impaired plastid mRNA maturation	[94]
PDM1	AT4G18520	albino	impaired plastid mRNA maturation	[95]
plastid translation				
PRPS21	AT3G27160	pale	reduced plastid ribosome activity	[24,96]
PRPL11	AT1G32990	pale	reduced plastid ribosome activity	[15,24,97]
plastid proteostasis maintenance				
HSP21	AT4G27670	none (22°C); albino (30°C)	reduced PEP activity under heat stress	[92]
cpHSC70-1	AT4G24280	variegated	reduced plastid import capacity; impaired protein quality control	[24,98]
CLPR1	AT1G49970	virescent	impaired protein quality control	[99]

PEP/NEP-dependent transcription (figure 1). In particular, GUN1 was shown to interact physically with RpoTp and to have a direct role in the upregulation of NEP-dependent transcripts upon perturbation of plastid protein homeostasis, i.e. during the *Δrpo* adaptive response [24]. Concomitantly, GUN1 has been reported to have a direct role in RNA editing by physically interacting with the MULTIPLE ORGANELLAR RNA EDITING FACTOR 2 (MORF2), a member of the so-called plastid RNA Editosome, which is involved in editing nearly all sites of plastid RNA [22], in agreement with previous studies where a link between plastid signalling and RNA editing was shown [18,104]. Consistent with this, *gun1* mutant cotyledons have differential efficiency of RNA editing (C->U) levels of 11 sites in the plastid transcriptome, after norflurazon or lincomycin treatment, compared to wild type. Intriguingly, the target genes were NEP-dependent, including transcripts of PEP core subunits β and β' [22]. The *rpoB* and *rpoC1* editing sites have been observed in previous studies and lead to amino acid

changes in the protein sequence [105]. However, the biological meaning of such editing events and the impact on the transcripts is not always clear. RNA editing is usually associated with the restoration of conserved codons or aims to recreate start/stop codons serving as a correction for otherwise defective transcripts [106]. In this specific case, GUN1 is responsible for three amino acid changes in *rpoB* sequence (S113F, S184 L and S811 L) and one in *rpoC1* (S163 L) [22]. The edited residues are highly conserved in several species, suggesting that the lack of GUN1 leads to the production of altered forms of PEP core proteins. In this scenario (figure 1), GUN1 appears to be part of a protein complex that act as a positive regulator of both NEP- and PEP-dependent transcription, and that could contribute to the increase of cellular RNA amount observed during germination or even to the doubling of plant cell RNA detected within 48 h under stress conditions, i.e. in response to herbicide-induced Mg-protoporphyrin and heme accumulation or a high level of sugar treatment, as previously reported [107]. According to this model, GUN1-dependent closure of the photosynthetic apparatus, by repressing photosynthesis-associated nuclear gene expression, would contribute further to protection from oxidative stress [107]. Alternatively, the GUN1-dependent increased accumulation of NEP-dependent transcripts upon depletion of PEP activity would serve to maintain the house keeping functions of plastids, reducing to a minimum the photosynthesis-dependent oxidative damage.

Interestingly, the over-accumulation of unimported precursor proteins (preproteins) observed in the cytosol of *gun1* cotyledon cells upon growth in the presence of lincomycin (figure 1) induces upregulation of cytosolic Heat Shock Protein 90 (HSP90) and in turn sustains the expression of *PhANGs*, indicating that this pathway might play a key role in the coordination of plastid and nuclear gene transcription [23,24]. In particular, HSP90 could mediate retrograde communication by either repressing negative regulators of transcription (for example, through delivery to the 26S proteasome for degradation) such as abscisic acid insensitive 4 (ABI4) [13], although its role in retrograde signalling has been questioned recently [108], or by activating a positive regulator of transcription (for example, through promoting folding or refolding of a transcription factor) such as Elongated Hypocotyl 5 (HY5) [109] and Golden-Like 1/2 (GLK1/2) [110], reported to be involved in retrograde communication and required for coordinated expression of key genes in chloroplast biogenesis [111,112].

8. Concluding remarks and future perspectives

The field of plastid-to-nucleus signalling has been very dynamic over the last few years, and there have been several major breakthroughs leading to a much more advanced understanding of the mechanisms involved in plastid and nuclear genome cross-talk. Three recent studies have identified GUN1-interacting proteins in *Arabidopsis* cotyledons, contributing to unravelling the mechanism by which the activity of plastid transcription machinery is coordinated with the nuclear gene expression apparatus [22–24]. A direct connection between GUN1 and the NEP-PEP plastid RNA polymerases has been provided by both the physical interaction of GUN1 with RpoTp and its role in favouring the NEP-dependent transcript accumulation upon alteration of plastid protein homeostasis [24], and by the editing-level changes observed in *rpoB* and *rpoC1* transcripts, which encode subunits of plastid-encoded RNA polymerase [22]. In agreement with previous studies [66,74], it is conceivable that the alteration of the activity of the plastid RNA polymerases results in abnormal transcription of a specific set of plastid genes and, possibly, in the source of the GUN1-dependent retrograde signalling. Furthermore, the altered transcription of the NEP-dependent *ycf1* gene, which encodes the Tic214 subunit of the 1 MDa TIC complex [24], together with the GUN1-cpHSC70-1 (chloroplast heat shock protein 70-1) interaction [23], have provided the connection between cytosolic folding stress and the GUN1-dependent retrograde signalling. HSP90, induced by cytosolic preproteins, has been verified to sustain the expression of nuclear photosynthesis-related genes [23], pointing to a possible connection of GUN1-retrograde signalling and the chloroplast unfolded protein response (cpUPR) [113,114].

These recent findings offer a novel point of view to elucidate the mechanisms by which the plastid transcriptional machinery and, more generally, the PGE apparatus communicates with the nucleus; however, several questions still remain. Critical future directions for the research field include efforts to understand whether cytosolic folding stress only occurs in the *gun1* mutant. Also, the identity of the downstream signal components of HSP90 require further exploration. Another question is whether plastid RNA editing and cytosolic folding stress are also connected with each other. Finally, the intriguing dual localization of a few PAP proteins and their role in the coordination of plastid and nuclear transcription deserves further investigation. Nuclear proteomics analyses, and the in-depth biochemical analyses of the main players identified, could provide important clues on the molecular mechanisms at the root of plastid-nucleus transcription machinery coordination, essential during early stages of chloroplast biogenesis and upon alteration of plastid protein homeostasis.

Data accessibility. This article has no additional data.

Authors' contributions. L.T. and P.P. designed the study. N.J. and M.C. took care of table 1 and figure 1. All authors helped draft the manuscript. P.P. coordinated the study and took care of the final version of the manuscript. All authors gave final approval for publication and agree to be held accountable for the work performed therein.

Competing interests. We declare we have no competing interests.

Funding. This work was supported by Ministero dell'Istruzione dell'Università e della Ricerca – MIUR, grant no. PRIN-2017FBS8YN to P.P.

Acknowledgements. We apologize to the authors who did not get their work discussed in this review due to space limitation.

References

1. Lgloi GL, Kössel H. 1992 The transcriptional apparatus of chloroplasts. *CRC. Crit. Rev. Plant Sci.* **10**, 525–558. (doi:10.1080/07352689209382326)
2. Börner T, Aleynikova AYU, Zubo YO, Kusnetsov VV. 2015 Chloroplast RNA polymerases: role in chloroplast biogenesis. *Biochim. Biophys. Acta* **1847**, 761–769. (doi:10.1016/j.bbabio.2015.02.004)
3. Richter U, Kiessling J, Hedtke B, Decker E, Reski R, Börner T, Weihe A. 2002 Two *RpoT* genes of *Physcomitrella patens* encode phage-type RNA polymerases with dual targeting to mitochondria

and plastids. *Gene* **290**, 95–105. (doi:10.1016/S0378-1119(02)00583-8)

4. Schweer J, Türkeri H, Kolpack A, Link G. 2010 Role and regulation of plastid sigma factors and their functional interactors during chloroplast transcription—recent lessons from *Arabidopsis thaliana*. *Eur. J. Cell Biol.* **89**, 940–946. (doi:10.1016/j.ejcb.2010.06.016)
5. Lerbs-Mache S. 2011 Function of plastid sigma factors in higher plants: regulation of gene expression or just preservation of constitutive transcription? *Plant Mol. Biol.* **76**, 235–249. (doi:10.1007/s11103-010-9714-4)
6. Pfalz J, Pfannschmidt T. 2013 Essential nucleoid proteins in early chloroplast development. *Trends Plant Sci.* **18**, 186–194. (doi:10.1016/j.tplants.2012.11.003)
7. Yu Q-B, Huang C, Yang Z-N. 2014 Nuclear-encoded factors associated with the chloroplast transcription machinery of higher plants. *Front. Plant Sci.* **5**, 316. (doi:10.3389/fpls.2014.00316)
8. Chi W, He B, Mao J, Jiang J, Zhang L. 2015 Plastid sigma factors: their individual functions and regulation in transcription. *Biochim. Biophys. Acta Bioenerg.* **1847**, 770–778. (doi:10.1016/j.bbabio.2015.01.001)
9. Kleine T, Maier UG, Leister D. 2009 DNA transfer from organelles to the nucleus: the idiosyncratic genetics of endosymbiosis. *Annu. Rev. Plant Biol.* **60**, 115–138. (doi:10.1146/annurev.arplant.043008.092119)
10. Pogson BJ, Albrecht V. 2011 Genetic dissection of chloroplast biogenesis and development: an overview. *Plant Physiol.* **155**, 1545–1551. (doi:10.1104/pp.110.170365)
11. Woodson JD, Chory J. 2008 Coordination of gene expression between organellar and nuclear genomes. *Nat. Rev. Genet.* **9**, 383–395. (doi:10.1038/nrg2348)
12. Chan KX, Phua SY, Crisp P, McQuinn R, Pogson BJ. 2016 Learning the languages of the chloroplast: retrograde signaling and beyond. *Annu. Rev. Plant Biol.* **67**, 25–53. (doi:10.1146/annurev-arplant-043015-111854)
13. Koussevitzky S, Nott A, Mockler TC, Hong F, Sachetto-Martins G, Surpin M, Lim J, Mittler R, Chory J. 2007 Signals from chloroplasts converge to regulate nuclear gene expression. *Science* **316**, 715–719. (doi:10.1126/science.1140516)
14. Kakizaki T, Matsumura H, Nakayama K, Che F-S, Terauchi R, Inaba T. 2009 Coordination of plastid protein import and nuclear gene expression by plastid-to-nucleus retrograde signaling. *Plant Physiol.* **151**, 1339–1353. (doi:10.1104/pp.109.145987)
15. Tadini L *et al.* 2016 GUN1 controls accumulation of the plastid ribosomal protein s1 at the protein level and interacts with proteins involved in plastid protein homeostasis. *Plant Physiol.* **170**, 1817–1830. (doi:10.1104/pp.15.02033)
16. Paieri F, Tadini L, Manavski N, Kleine T, Ferrari R, Morandini P, Pesaresi P, Meurer J, Leister D. 2018 The DEAD-box RNA helicase RH50 is a 23S-4.5S rRNA maturation factor that functionally overlaps with the plastid signaling factor GUN1. *Plant Physiol.* **176**, 634–648. (doi:10.1104/pp.17.01545)
17. Colombo M, Tadini L, Peracchio C, Ferrari R, Pesaresi P. 2016 GUN1, a jack-of-all-trades in chloroplast protein homeostasis and signaling. *Front. Plant Sci.* **7**, 1427. (doi:10.3389/fpls.2016.01427)
18. Kakizaki T, Yazu F, Nakayama K, Ito-Inaba Y, Inaba T. 2012 Plastid signalling under multiple conditions is accompanied by a common defect in RNA editing in plastids. *J. Exp. Bot.* **63**, 251–260. (doi:10.1093/jxb/err257)
19. Majeran W, Friso G, Asakura Y, Qu X, Huang M, Ponnala L, Watkins KP, Barkan A, van Wijk KJ. 2012 Nucleoid-enriched proteomes in developing plastids and chloroplasts from maize leaves: a new conceptual framework for nucleoid functions. *Plant Physiol.* **158**, 156–189. (doi:10.1104/pp.111.188474)
20. Krupinska K, Melonek J, Krause K. 2013 New insights into plastid nucleoid structure and functionality. *Planta* **237**, 653–664. (doi:10.1007/s00425-012-1817-5)
21. Wu GZ, Chalvin C, Hoelscher M, Meyer EH, Wu XN, Bock R. 2018 Control of retrograde signaling by rapid turnover of GENOMES UNCOUPLED1. *Plant Physiol.* **176**, 2472–2495. (doi:10.1104/pp.18.00009)
22. Zhao X, Huang J, Chory J. 2019 GUN1 interacts with MORF2 to regulate plastid RNA editing during retrograde signaling. *Proc. Natl Acad. Sci. USA* **116**, 10 162–10 167. (doi:10.1073/pnas.1820426116)
23. Wu GZ *et al.* 2019 Control of retrograde signalling by protein import and cytosolic folding stress. *Nat. Plants* **5**, 525–538. (doi:10.1038/s41477-019-0415-y)
24. Tadini L *et al.* 2019 GUN1 influences the accumulation of NEP-dependent transcripts and chloroplast protein import in *Arabidopsis* cotyledons upon perturbation of chloroplast protein homeostasis. *Plant J.* **101**, 1198–1220. (doi:10.1111/tpj.14585)
25. Hu J, Bogorad L. 1990 Maize chloroplast RNA polymerase: the 180-, 120-, and 38-kilodalton polypeptides are encoded in chloroplast genes. *Proc. Natl Acad. Sci. USA* **87**, 1531–1535. (doi:10.1073/pnas.87.4.1531)
26. Pfannschmidt T, Blanvillain R, Merendino L, Courtois F, Chevalier F, Liebers M, Grübler B, Hommel E, Lerbs-Mache S. 2015 Plastid RNA polymerases: orchestration of enzymes with different evolutionary origins controls chloroplast biogenesis during the plant life cycle. *J. Exp. Bot.* **66**, 6957–6973. (doi:10.1093/jxb/erv415)
27. Tiller K, Link G. 1995 σ-like plastid transcription factors. *Methods Mol. Biol.* **37**, 337–348. (doi:10.1385/0-89603-288-4:337)
28. Surzycki SJ. 1969 Genetic functions of the chloroplast of *Chlamydomonas reinhardi*: effect of rifampin on chloroplast DNA-dependent RNA polymerase. *Proc. Natl Acad. Sci. USA* **63**, 1327–1334. (doi:10.1073/pnas.63.4.1327)
29. Pfalz J, Liere K, Kandlbinder A, Dietz K-J, Oelmüller R. 2006 pTAC2, -6, and -12 are components of the transcriptionally active plastid chromosome that are required for plastid gene expression. *Plant Cell* **18**, 176–197. (doi:10.1105/tpc.105.036392)
30. García M, Myouga F, Takechi K, Sato H, Nabeshima K, Nagata N, Takio S, Shinozaki K, Takano H. 2008 An *Arabidopsis* homolog of the bacterial peptidoglycan synthesis enzyme MurE has an essential role in chloroplast development. *Plant J.* **53**, 924–934. (doi:10.1111/j.1365-313X.2007.03379.x)
31. Myouga F *et al.* 2008 A heterocomplex of iron superoxide dismutases defends chloroplast nucleoids against oxidative stress and is essential for chloroplast development in *Arabidopsis*. *Plant Cell Online* **20**, 3148–3162. (doi:10.1105/tpc.108.061341)
32. Arsova B, Hoja U, Wimmelbacher M, Greiner E, Üstün Ş, Melzer M, Petersen K, Lein W, Börnke F. 2010 Plastidial thioredoxin *z* interacts with two fructokinase-like proteins in a thiol-dependent manner: evidence for an essential role in chloroplast development in *Arabidopsis* and *Nicotiana benthamiana*. *Plant Cell* **22**, 1498–1515. (doi:10.1105/tpc.109.071001)
33. Gao Z-P, Yu Q-B, Zhao T-T, Ma Q, Chen G-X, Yang Z-N. 2011 A functional component of the transcriptionally active chromosome complex, *Arabidopsis* pTAC14, interacts with pTAC12/HEMERA and regulates plastid gene expression. *Plant Physiol.* **157**, 1733–1745. (doi:10.1104/pp.111.184762)
34. Steiner S, Schröter Y, Pfalz J, Pfannschmidt T. 2011 Identification of essential subunits in the plastid-encoded RNA polymerase complex reveals building blocks for proper plastid development. *Plant Physiol.* **157**, 1043–1055. (doi:10.1104/pp.111.184515)
35. Jeon Y, Jung HJ, Kang H, Park Y-I, Lee SH, Pai H-S. 2012 S1 domain-containing STF modulates plastid transcription and chloroplast biogenesis in *Nicotiana benthamiana*. *New Phytol.* **193**, 349–363. (doi:10.1111/j.1469-8137.2011.03941.x)
36. Yagi Y, Ishizaki Y, Nakahira Y, Tozawa Y, Shiina T. 2012 Eukaryotic-type plastid nucleoid protein pTAC3 is essential for transcription by the bacterial-type plastid RNA polymerase. *Proc. Natl Acad. Sci. USA* **109**, 7541–7546. (doi:10.1073/pnas.1119403109)
37. Morden CW, Wolfe KH, DePamphilis CW, Palmer JD. 1991 Plastid translation and transcription genes in a non-photosynthetic plant: intact, missing and pseudo genes. *EMBO J.* **10**, 3281–3288. (doi:10.1002/j.1460-2075.1991.tb04892.x)
38. Hess WR, Prombona A, Fieder B, Subramanian AR, Börner T. 1993 Chloroplast rps15 and the rpoB/C1/C2 gene cluster are strongly transcribed in ribosome-deficient plastids: evidence for a functioning non-chloroplast-encoded RNA polymerase. *EMBO J.* **12**, 563–571. (doi:10.1002/j.1460-2075.1993.tb05688.x)
39. Lerbs-Mache S. 1993 The 110-kDa polypeptide of spinach plastid DNA-dependent RNA polymerase: single-subunit enzyme or catalytic core of multimeric enzyme complexes? *Proc. Natl Acad. Sci. USA* **90**, 5509–5513. (doi:10.1073/pnas.90.12.5509)
40. Hedtke B, Börner T, Weihe A. 1997 Mitochondrial and chloroplast phage-type RNA polymerases in *Arabidopsis*. *Science* **277**, 809–811. (doi:10.1126/science.277.5327.809)
41. Hedtke B, Börner T, Weihe A. 2000 One RNA polymerase serving two genomes. *EMBO Rep.* **1**, 435–440. (doi:10.1093/embo-reports/kvd086)

42. Emanuel C, Weihe A, Graner A, Hess WR, Börner T. 2004 Chloroplast development affects expression of phage-type RNA polymerases in barley leaves. *Plant J.* **38**, 460–472. (doi:10.1111/j.0960-7412.2004.02060.x)
43. Liere K, Weihe A, Börner T. 2011 The transcription machineries of plant mitochondria and chloroplasts: composition, function, and regulation. *J. Plant Physiol.* **168**, 1345–1360. (doi:10.1016/j.jplph.2011.01.005)
44. Yin C, Richter U, Börner T, Weihe A. 2010 Evolution of plant phage-type RNA polymerases: the genome of the basal angiosperm *Nuphar advena* encodes two mitochondrial and one plastid phage-type RNA polymerases. *BMC Evol. Biol.* **10**, 379. (doi:10.1186/1471-2148-10-379)
45. Maier UG, Bozarth A, Funk HT, Zauner S, Rensing SA, Schmitz-Linneweber C, Börner T, Tillich M. 2008 Complex chloroplast RNA metabolism: just debugging the genetic programme? *BMC Biol.* **6**, 36. (doi:10.1186/1741-7007-6-36)
46. Tracy RL, Stern DB. 1995 Mitochondrial transcription initiation: promoter structures and RNA polymerases. *Curr. Genet.* **28**, 205–216. (doi:10.1007/bf00309779)
47. Hricová A, Quesada V, Micol JL. 2006 The *SCABRA3* nuclear gene encodes the plastid RpoTp RNA polymerase, which is required for chloroplast biogenesis and mesophyll cell proliferation in *Arabidopsis*. *Plant Physiol.* **141**, 942–956. (doi:10.1104/pp.106.080069)
48. Demarsy E, Courtois F, Azevedo J, Buhot L, Lerbs-Mache S. 2006 Building up of the plastid transcriptional machinery during germination and early plant development. *Plant Physiol.* **142**, 993–1003. (doi:10.1104/pp.106.085043)
49. Allorent G, Courtois F, Chevalier F, Lerbs-Mache S. 2013 Plastid gene expression during chloroplast differentiation and dedifferentiation into non-photosynthetic plastids during seed formation. *Plant Mol. Biol.* **82**, 59–70. (doi:10.1007/s11103-013-0037-0)
50. Demarsy E, Buhr F, Lambert E, Lerbs-Mache S. 2012 Characterization of the plastid-specific germination and seedling establishment transcriptional programme. *J. Exp. Bot.* **63**, 925–939. (doi:10.1093/jxb/err322)
51. Hanaoka M, Kanamaru K, Fujiwara M, Takahashi H, Tanaka K. 2005 Glutamyl-tRNA mediates a switch in RNA polymerase use during chloroplast biogenesis. *EMBO Rep.* **6**, 545–550. (doi:10.1038/sj.embor.7400411)
52. Kusumi K, Chono Y, Shimada H, Gotoh E, Tsuyama M, Iba K. 2010 Chloroplast biogenesis during the early stage of leaf development in rice. *Plant Biotechnol.* **27**, 85–90. (doi:10.5511/plantbiotechnology.27.85)
53. Emanuel C, von Groll U, Müller M, Börner T, Weihe A. 2006 Development- and tissue-specific expression of the *RpoT* gene family of *Arabidopsis* encoding mitochondrial and plastid RNA polymerases. *Planta* **223**, 998–1009. (doi:10.1007/s00425-005-0159-y)
54. Pfannschmidt T, Link G. 1994 Separation of two classes of plastid DNA-dependent RNA polymerases that are differentially expressed in mustard (*Sinapis alba* L.) seedlings. *Plant Mol. Biol.* **25**, 69–81. (doi:10.1007/BF00024199)
55. Pfannschmidt T, Ogrzewalla K, Baginsky S, Sickmann A, Meyer HE, Link G. 2000 The multisubunit chloroplast RNA polymerase A from mustard (*Sinapis alba* L.). Integration of a prokaryotic core into a larger complex with organelle specific functions. *Eur. J. Biochem.* **267**, 253–261. (doi:10.1046/j.1432-1327.2000.00991.x)
56. Qiao J, Ma C, Wimmelbacher M, Bömke F, Luo M. 2011 Two novel proteins, MRL7 and its paralog MRL7-l, have essential but functionally distinct roles in chloroplast development and are involved in plastid gene expression regulation in *Arabidopsis*. *Plant Cell Physiol.* **52**, 1017–1030. (doi:10.1093/pcp/pcr054)
57. Powikrowska M, Khrouchtchova A, Martens HJ, Zygadlo-Nielsen A, Melonek J, Schulz A, Krupinska K, Rodermel S, Jensen PE. 2014 SVR4 (suppressor of variegation 4) and SVR4-like: two proteins with a role in proper organization of the chloroplast genetic machinery. *Physiol. Plant.* **150**, 477–492. (doi:10.1111/ppl.12108)
58. Yang EJ *et al.* 2019 NCP activates chloroplast transcription by controlling phytochrome-dependent dual nuclear and plastidial switches. *Nat. Commun.* **10**, 1–13. (doi:10.1038/s41467-019-10517-1)
59. Yua Q-B, Ma Q, Kong M-M, Zhao T-T, Zhang X-L, Zhou Q, Huang C, Chong K, Yang Z-N. 2014 AtECB1/MRL7, a thioredoxin-like fold protein with disulfide reductase activity, regulates chloroplast gene expression and chloroplast biogenesis in *Arabidopsis thaliana*. *Mol. Plant* **7**, 206–217. (doi:10.1093/mp/sst092)
60. Yoo CY, Pasoreck EK, Wang H, Cao J, Blaha GM, Weigel D, Chen M. 2019 Phytochrome activates the plastid-encoded RNA polymerase for chloroplast biogenesis via nucleus-to-plastid signaling. *Nat. Commun.* **10**, 1–16. (doi:10.1038/s41467-019-10518-0)
61. Zhelyazkova P, Sharma CM, Förstner KU, Liere K, Vogel J, Börner T. 2012 The primary transcriptome of barley chloroplasts: numerous noncoding RNAs and the dominating role of the plastid-encoded RNA polymerase. *Plant Cell* **24**, 123–136. (doi:10.1105/tpc.111.089441)
62. Hajdukiewicz PTJ, Allison LA, Maliga P. 1997 The two RNA polymerases encoded by the nuclear and the plastid compartments transcribe distinct groups of genes in tobacco plastids. *EMBO J.* **16**, 4041–4048. (doi:10.1093/emboj/16.13.4041)
63. Williams-Carrier R, Zoschke R, Belcher S, Pfalz J, Barkan A. 2014 A major role for the plastid-encoded RNA polymerase complex in the expression of plastid transfer RNAs. *Plant Physiol.* **164**, 239–248. (doi:10.1104/pp.113.228726)
64. Liere K, Kaden D, Maliga P, Börner T. 2004 Overexpression of phage-type RNA polymerase RpoTp in tobacco demonstrates its role in chloroplast transcription by recognizing a distinct promoter type. *Nucleic Acids Res.* **32**, 1159–1165. (doi:10.1093/nar/gkh285)
65. Zoschke R, Liere K, Börner T. 2007 From seedling to mature plant: *Arabidopsis* plastidial genome copy number, RNA accumulation and transcription are differentially regulated during leaf development. *Plant J.* **50**, 710–722. (doi:10.1111/j.1365-313X.2007.03084.x)
66. Woodson JD, Perez-Ruiz JM, Schmitz RJ, Ecker JR, Chory J. 2013 Sigma factor-mediated plastid retrograde signals control nuclear gene expression. *Plant J.* **73**, 1–13. (doi:10.1111/tpj.12011)
67. Shimizu M, Kato H, Ogawa T, Kurachi A, Nakagawa Y, Kobayashi H. 2010 Sigma factor phosphorylation in the photosynthetic control of photosystem stoichiometry. *Proc. Natl Acad. Sci. USA* **107**, 10 760–10 764. (doi:10.1073/pnas.0911692107)
68. Türkeri H, Schweer J, Link G. 2012 Phylogenetic and functional features of the plastid transcription kinase cpCK2 from *Arabidopsis* signify a role of cysteinyl SH-groups in regulatory phosphorylation of plastid sigma factors. *FEBS J.* **279**, 395–409. (doi:10.1111/j.1742-4658.2011.08433.x)
69. Coll NS, Danon A, Meurer J, Cho WK, Apel K. 2009 Characterization of *soldat8*, a suppressor of singlet oxygen-induced cell death in *Arabidopsis* seedlings. *Plant Cell Physiol.* **50**, 707–718. (doi:10.1093/pcp/pcp036)
70. Hakimi MA, Privat I, Valay JG, Lerbs-Mache S. 2000 Evolutionary conservation of C-terminal domains of primary sigma(70)-type transcription factors between plants and bacteria. *J. Biol. Chem.* **275**, 9215–9221. (doi:10.1074/jbc.275.13.9215)
71. Mache R, Cottet A, Imberty A, Hakimi AM, Lerbs-Mache S. 2002 The plant sigma factors: structure and phylogenetic origin. *Genome Lett.* **1**, 71–76. (doi:10.1166/gl.2002.007)
72. Schmitz-Linneweber C, Small I. 2008 Pentatricopeptide repeat proteins: a socket set for organelle gene expression. *Trends Plant Sci.* **13**, 663–670. (doi:10.1016/j.tplants.2008.10.001)
73. Kindgren P, Kremnev D, Blanco NE, de Dios Barajas López J, Fernández AP, Tellgren-Roth C, Small I, Strand Å. 2012 The plastid redox insensitive 2 mutant of *Arabidopsis* is impaired in PEP activity and high light-dependent plastid redox signalling to the nucleus. *Plant J.* **70**, 279–291. (doi:10.1111/j.1365-313X.2011.04865.x)
74. Díaz MG, Hernández-Verdeja T, Kremnev D, Crawford T, Dubreuil C, Strand Å. 2018 Redox regulation of PEP activity during seedling establishment in *Arabidopsis thaliana*. *Nat. Commun.* **9**, 1–12. (doi:10.1038/s41467-017-02468-2)
75. Kravtsov AK, Zubo YO, Yamburenko MV, Kulaeva ON, Kusnetsov VV. 2011 Cytokinin and abscisic acid control plastid gene transcription during barley seedling de-etiolation. *Plant Growth Regul.* **64**, 173–183. (doi:10.1007/s10725-010-9553-y)
76. Zubo YO, Yamburenko MV, Kusnetsov VV, Börner T. 2011 Methyl jasmonate, gibberellic acid, and auxin affect transcription and transcript accumulation of chloroplast genes in barley. *J. Plant Physiol.* **168**, 1335–1344. (doi:10.1016/j.jplph.2011.01.009)
77. Zubo YO *et al.* 2008 Cytokinin stimulates chloroplast transcription in detached barley leaves. *Plant Physiol.* **148**, 1082–1093. (doi:10.1104/pp.108.122275)
78. Yamburenko MV, Zubo YO, Börner T. 2015 Abscisic acid affects transcription of chloroplast genes via

protein phosphatase 2C-dependent activation of nuclear genes: repression by guanosine-3′-5′-bisdiphosphate and activation by sigma factor 5. *Plant J.* **82**, 1030–1041. (doi:10.1111/tpj.12876)

79. Sato M, Takahashi K, Ochiai Y, Hosada T, Ochi K, Nabeta K. 2009 Bacterial alarmone, guanosine 5′-diphosphate 3′-diphosphate (ppGpp), predominantly binds the β' subunit of plastid-encoded plastid RNA polymerase in chloroplasts. *Chembiochem* **10**, 1227–1233. (doi:10.1002/cbic.200800737)
80. Sugliani M, Abdelkefi H, Ke H, Bouveret E, Robaglia C, Caffarri S, Field B. 2016 An ancient bacterial signaling pathway regulates chloroplast function to influence growth and development in *Arabidopsis*. *Plant Cell* **28**, 661–679. (doi:10.1105/tpc.16.00045)
81. Field B. 2018 Green magic: regulation of the chloroplast stress response by (p)ppGpp in plants and algae. *J. Exp. Bot.* **69**, 2797–2807. (doi:10.1093/jxb/erx485)
82. Allison LA, Simon LD, Maliga P. 1996 Deletion of rpoB reveals a second distinct transcription system in plastids of higher plants. *EMBO J.* **15**, 2802–2809. (doi:10.1002/j.1460-2075.1996.tb00640.x)
83. Serino G, Maliga P. 1998 RNA polymerase subunits encoded by the plastid *rpo* genes are not shared with the nucleus-encoded plastid enzyme. *Plant Physiol.* **117**, 1165–1170. (doi:10.1104/pp.117.4.1165)
84. Chi W, Mao J, Li Q, Ji D, Zou M, Lu C, Zhang L. 2010 Interaction of the pentatricopeptide-repeat protein DELAYED GREENING 1 with sigma factor SIG6 in the regulation of chloroplast gene expression in *Arabidopsis* cotyledons. *Plant J.* **64**, 14–25. (doi:10.1111/j.1365-313X.2010.04304.x)
85. Chi W, Ma J, Zhang D, Guo J, Chen F, Lu C, Zhang L. 2008 The pentratricopeptide repeat protein DELAYED GREENING1 is involved in the regulation of early chloroplast development and chloroplast gene expression in *Arabidopsis*. *Plant Physiol.* **147**, 573–584. (doi:10.1104/pp.108.116194)
86. Yu Q-B, Zhao T-T, Ye L-S, Cheng L, Wu Y-Q, Huang C, Yang Z-N. 2018 pTAC10, an S1-domain-containing component of the transcriptionally active chromosome complex, is essential for plastid gene expression in *Arabidopsis thaliana* and is phosphorylated by chloroplast-targeted casein kinase II. *Photosynth. Res.* **137**, 69–83. (doi:10.1007/s11120-018-0479-y)
87. Kuo WY, Huang CH, Liu AC, Cheng CP, Li SH, Chang WC, Weiss C, Azem A, Jinn TL. 2013 CHAPERONIN 20 mediates iron superoxide dismutase (FeSOD) activity independent of its co-chaperonin role in *Arabidopsis* chloroplasts. *New Phytol.* **197**, 99–110. (doi:10.1111/j.1469-8137.2012.04369.x)
88. Chen M, Galvão RM, Li M, Burger B, Bugea J, Bolado J, Chory J. 2010 *Arabidopsis* HEMERA/pTAC12 initiates photomorphogenesis by phytochromes. *Cell* **141**, 1230–1240. (doi:10.1016/j.cell.2010.05.007)
89. Gilkerson J, Perez-Ruiz J, Chory J, Callis J. 2012 The plastid-localized pfkB-type carbohydrate kinases FRUCTOKINASE-LIKE 1 and 2 are essential for growth and development of *Arabidopsis thaliana*. *BMC Plant Biol.* **12**, 102. (doi:10.1186/1471-2229-12-102)
90. Huang C, Yu QB, Lv RH, Yin QQ, Chen GY, Xu L, Yang ZN. 2013 The reduced plastid-encoded polymerase-dependent plastid gene expression leads to the delayed greening of the *Arabidopsis fln2* mutant. *PLoS ONE* **8**, e73092. (doi:10.1371/journal.pone.0073092)
91. Yu QB, Lu Y, Ma Q, Zhao TT, Huang C, Zhao HF, Zhang XL, Lv RH, Yang ZN. 2012 TAC7, an essential component of the plastid transcriptionally active chromosome complex, interacts with FLN1, TAC10, TAC12 and TAC14 to regulate chloroplast gene expression in *Arabidopsis thaliana*. *Physiol. Plant.* **148**, 408–421. (doi:10.1111/j.1399-3054.2012.01718.x)
92. Zhong L, Zhou W, Wang H, Ding S, Lu Q, Wen X, Peng L, Zhang L, Lu C. 2013 Chloroplast small heat shock protein HSP21 interacts with plastid nucleoid protein pTAC5 and is essential for chloroplast development in *Arabidopsis* under heat stress. *Plant Cell* **25**, 2925–2943. (doi:10.1105/tpc.113.111229)
93. Ferrari R *et al.* 2017 CRP1 Protein: (dis)similarities between *Arabidopsis thaliana* and *Zea mays*. *Front. Plant Sci.* **8**, 1–18. (doi:10.3389/fpls.2017.00163)
94. Tadini L *et al.* 2018 Trans-splicing of plastid *rps12* transcripts, mediated by AtPPR4, is essential for embryo patterning in *Arabidopsis thaliana*. *Planta* **248**, 257–265. (doi:10.1007/s00425-018-2896-8)
95. Wu H, Zhang L. 2010 The PPR protein PDM1 is involved in the processing of rpoA pre-mRNA in *Arabidopsis thaliana*. *Chinese Sci. Bull.* **55**, 3485–3489. (doi:10.1007/s11434-010-4040-4)
96. Morita-Yamamuro C, Tsutsui T, Tanaka A, Yamaguchi J. 2004 Knock-out of the plastid ribosomal protein S21 causes impaired photosynthesis and sugar-response during germination and seedling development in *Arabidopsis thaliana*. *Plant Cell Physiol.* **45**, 781–788. (doi:10.1093/pcp/pch093)
97. Pesaresi P, Varotto C, Meurer J, Jahns P, Salamini F, Leister D. 2001 Knock-out of the plastid ribosomal protein L11 in *Arabidopsis*: effects on mRNA translation and photosynthesis. *Plant J.* **27**, 179–189. (doi:10.1046/j.1365-313x.2001.01076.x)
98. Su PH, Li HM. 2010 Stromal Hsp70 is important for protein translocation into pea and *Arabidopsis* chloroplasts. *Plant Cell* **22**, 1516–1531. (doi:10.1105/tpc.109.071415)
99. Koussevitzky S, Stanne TM, Peto CA, Giap T, Sjögren LLE, Zhao Y, Clarke AK, Chory J. 2007 An *Arabidopsis thaliana* virescent mutant reveals a role for ClpR1 in plastid development. *Plant Mol. Biol.* **63**, 85–96. (doi:10.1007/s11103-006-9074-2)
100. Pfalz J, Holtzegel U, Barkan A, Weisheit W, Mittag M, Pfannschmidt T. 2015 ZmpTAC12 binds single-stranded nucleic acids and is essential for accumulation of the plastid-encoded polymerase complex in maize. *New Phytol.* **206**, 1024–1037. (doi:10.1111/nph.13248)
101. Chen M, Chory J. 2011 Phytochrome signaling mechanisms and the control of plant development. *Trends Cell Biol.* **21**, 664–671. (doi:10.1016/j.tcb.2011.07.002)
102. Galvão RM, Li M, Kothadia SM, Haskel JD, Decker PV, Van Buskirk EK, Chen M. 2012 Photoactivated phytochromes interact with HEMERA and promote its accumulation to establish photomorphogenesis in *Arabidopsis*. *Genes Dev.* **26**, 1851–1863. (doi:10.1101/gad.193219.112)
103. Qiu Y *et al.* 2015 HEMERA couples the proteolysis and transcriptional activity of PHYTOCHROME INTERACTING FACTORs in *Arabidopsis* photomorphogenesis. *Plant Cell* **27**, 1409–1427. (doi:10.1105/tpc.114.136093)
104. Tseng CC, Lee CJ, Chung YT, Sung TY, Hsieh MH. 2013 Differential regulation of *Arabidopsis* plastid gene expression and RNA editing in non-photosynthetic tissues. *Plant Mol. Biol.* **82**, 375–392. (doi:10.1007/s11103-013-0069-5)
105. Zeltz P, Hess WR, Neckermann K, Börner T, Kössel H. 1993 Editing of the chloroplast rpoB transcript is independent of chloroplast translation and shows different patterns in barley and maize. *EMBO J.* **12**, 4291–4296. (doi:10.1002/j.1460-2075.1993.tb06113.x)
106. Stern DB, Goldschmidt-Clermont M, Hanson MR. 2010 Chloroplast RNA metabolism. *Annu. Rev. Plant Biol.* **61**, 125–155. (doi:10.1146/annurev-arplant-042809-112242)
107. Zhang Z-W *et al.* 2011 Mg-protoporphyrin, haem and sugar signals double cellular total RNA against herbicide and high-light-derived oxidative stress. *Plant. Cell Environ.* **34**, 1031–1042. (doi:10.1111/j.1365-3040.2011.02302.x)
108. Kacprzak SM, Mochizuki N, Naranjo B, Xu D, Leister D, Kleine T, Okamoto H, Terry MJ. 2019 Plastid-to-nucleus retrograde signalling during chloroplast biogenesis does not require ABI4. *Plant Physiol.* **179**, 18–23. (doi:10.1104/pp.18.01047)
109. Ruckle ME, DeMarco SM, Larkin RM. 2007 Plastid signals remodel light signaling networks and are essential for efficient chloroplast biogenesis in *Arabidopsis*. *Plant Cell* **19**, 3944–3960. (doi:10.1105/tpc.107.054312)
110. Waters MT, Wang P, Korkaric M, Capper RG, Saunders NJ, Langdale JA. 2009 GLK transcription factors coordinate expression of the photosynthetic apparatus in *Arabidopsis*. *Plant Cell* **21**, 1109–1128. (doi:10.1105/tpc.108.065250)
111. Kobayashi K *et al.* 2012 Regulation of root greening by light and auxin/cytokinin signaling in *Arabidopsis*. *Plant Cell* **24**, 1081–1095. (doi:10.1105/tpc.111.092254)
112. Kobayashi K *et al.* 2013 Photosynthesis of root chloroplasts developed in *Arabidopsis* lines overexpressing GOLDEN2-LIKE transcription factors. *Plant Cell Physiol.* **54**, 1365–1377. (doi:10.1093/pcp/pct086)
113. Ramundo S *et al.* 2014 Conditional depletion of the *Chlamydomonas* chloroplast ClpP protease activates nuclear genes involved in autophagy and plastid protein quality control. *Plant Cell* **26**, 2201–2222. (doi:10.1105/tpc.114.124842)
114. Dogra V, Li M, Singh S, Li M, Kim C. 2019 Oxidative post-translational modification of EXECUTER1 is required for singlet oxygen sensing in plastids. *Nat. Commun.* **10**, 2834. (doi:10.1038/s41467-019-10760-6)

Submitted article

⌘ Tadini L, Jeran N, Domingo G, Zambelli F, Masiero S, Costantini E, Forlani S, Marsoni M, Briani F, Pesaresi P (2022) Perturbation of protein homeostasis brings plastids at the crossroad between repair and Luca Tadini 1a. bioRxiv 1: 790

https://doi.org/10.1101/2022.07.19.500576

(Submitted article currently under revision, the submitted manuscript, available also on bioRxiv, is attached.)

In this work, we studied the complex regulatory chloroplast-quality-control mechanisms by modulating the expression of two nuclear genes encoding plastid ribosomal proteins PRPS1 and PRPL4. My direct contribution was: the physiological and biochemical characterization of Arabidopsis transgenic lines, the analyses of the bacterial strains, the preparation of the samples for the RNA-seq and the bioinformatic analysis, the generation of the double mutants and their characterization, the studies of the flowering time, the preparation of the figures and the drafting of the manuscript.

Perturbation of protein homeostasis brings plastids at the crossroad between repair and dismantling

Luca Tadini[1a], Nicolaj Jeran[1a], Guido Domingo[2], Federico Zambelli[1], Simona Masiero[1], Anna Calabritto[1b], Elena Costantini[2], Sara Forlani[1c], Milena Marsoni[2], Federica Briani[1], Candida Vannini[2], Paolo Pesaresi1*

[1] Dipartimento di Bioscienze, Università degli Studi di Milano, 20133 Milano, Italy

[2] Dipartimento di Biotecnologie e Scienze della Vita, Università degli Studi dell'Insubria, via J.H. Dunant 3, 21100 Varese, Italy

[a] These authors contributed equally to the manuscript

[b] Current address: Department of Physics and Astronomy, Faculty of Science, Vrije Universiteit Amsterdam, Amsterdam, the Netherlands

[c] Current address: Faculty of Biological and Environmental Sciences, Organismal and Evolutionary Biology Research Programme, University of Helsinki, Viikinkari 1, 00790 Helsinki (Finland).

* Correspondence to: paolo.pesaresi@unimi.it

Abstract

The chloroplast proteome is a dynamic mosaic of plastid- and nuclear-encoded proteins. Plastid protein homeostasis is maintained through the balance between *de novo* synthesis and proteolysis. Intracellular communication pathways, including the plastid-to-nucleus signalling and the protein homeostasis machinery, made of stromal chaperones and proteases, shape chloroplast proteome based on developmental and physiological needs. However, the maintenance of fully functional chloroplasts is costly and under specific stress conditions the degradation of damaged chloroplasts is essential to the maintenance of a healthy population of photosynthesising organelles while promoting nutrient redistribution to sink tissues. In this work, we have addressed this complex regulatory chloroplast-quality-control pathway by modulating the expression of two nuclear genes encoding plastid ribosomal proteins PRPS1 and PRPL4. By transcriptomics, proteomics and transmission electron microscopy analyses, we show that the increased expression of *PRPS1* gene leads to chloroplast degradation and early flowering, as an escape strategy from stress. On the contrary, the overaccumulation of PRPL4 protein is kept under control by increasing the amount of plastid chaperones and components of the unfolded protein response (cpUPR) regulatory mechanism. This study advances our understanding of molecular mechanisms underlying chloroplast retrograde communication and provides new insight into cellular responses to impaired plastid protein homeostasis.

Introduction

Chloroplasts are plant cell organelles of cyanobacterial origin that perform essential metabolic and biosynthetic functions including photosynthesis and fatty acid biosynthesis. The Arabidopsis chloroplast proteome is estimated to consist of several thousand proteins, most of which are encoded by the nuclear genome and post-translationally imported into the organelle (Kmiec *et al.*, 2014). The plastid genome, encoding about a hundred proteins, is expressed by transcriptional and translational machineries that conserve many bacteria-like elements. For instance, the chloroplast ribosome shares several features with that of the model organism *E. coli*, used as the reference in early investigations (Mache, 1990). Almost all the chloroplast ribosomal proteins have an orthologue in *E. coli*, however, few differences in ribosome composition, protein domain organisation and function have been described (Bubunenko *et al.*, 1994; Yamaguchi *et al.*, 2000; Yamaguchi & Subramanian, 2003; Tiller & Bock, 2014; Ahmed *et al.*, 2016; Graf *et al.*, 2017; Bieri *et al.*, 2017; Zoschke & Bock, 2018).

This is the case, for instance, of the S1 protein, encoded by *rpsA* gene, the largest ribosomal protein present in *E. coli* 30S subunit essential for cell viability (Kitakawa & Isono, 1982). S1 promotes the translation initiation step by recognising diverse mRNA leaders and mediating their interaction with the ribosome (Sørensen *et al.*, 1998; Hajnsdorf & Boni, 2012). Furthermore, S1 is found in *E. coli* cells both as ribosome-associated- and as free-subunit in cytoplasm (Subramanian, 1983; Kalapos *et al.*, 1997; Delvillani *et al.*, 2011), and it is responsible for its own post-transcriptional regulation (Skouv *et al.*, 1990). S1 bears six homologous non-identical repeats known as S1 domains, members of an ancient RNA binding OB-fold family (Subramanian, 1983; Bycroft *et al.*, 1997). It has been proposed that the six S1 domains have a partial functional specialisation, which correlates with their relative position (Salah *et al.*, 2009). In particular, domains 1 and 2 mediate the interaction with the ribosome (Giorginis & Subramanian, 1980; Byrgazov *et al.*, 2015), domains 3, 4, 5 and 6 are responsible for RNA binding and unfolding (Subramanian, 1983; Duval *et al.*, 2013; Cifuentes-Goches *et al.*, 2019), with domains 5 and 6 also involved in transcription stimulation and autoregulation (Boni *et al.*, 2000; Sukhodolets *et al.*, 2006). Recently, domains 4 and 6 have been shown to be implicated in ribosome dimerization and hibernation under stress (Beckert *et al.*, 2018).

Unlike S1, the *Arabidopsis thaliana* Plastid Ribosomal Protein Small subunit 1 (PRPS1) is characterised by three S1 domains. Its function was characterised by exploiting the knock-down allele *prps1-1*, which produces about one-tenth of wild-type PRPS1 transcripts resulting in one-third of wild-type PRPS1 protein levels in adult plants. Such impairment in *prps1-1* mutants affects the overall plant growth rate and results in pale leaves due to decreased translation in chloroplasts (Romani *et al.*, 2012). *A. thaliana* PRPS1 has been found to genetically and physically interact with

the nuclear-encoded plastid protein GUN1 (Tadini *et al.*, 2016). As a consequence, the depletion of GUN1 in the *prps1-1* genetic background leads to the partial rescue of the mutant phenotype, restoring to wild-type-like levels both PRPS1 abundance and the chloroplast translation capacity (Tadini *et al.*, 2016). These results indicate a direct negative regulation of PRPS1, and therefore of chloroplast translation, by GUN1, possibly due to its relations with the chloroplast protein homeostasis machinery (Colombo *et al.*, 2016; Tadini *et al.*, 2016). Further investigations revealed the involvement of PRPS1 and plastid translation in retrograde signalling upon heat-stress. Under such conditions, the diminished chloroplast translational capacity of *prps1-1* prevents the up-regulation of the *HSFA2* gene, a master regulator of the chloroplast Unfolded Protein Response (Nishizawa *et al.*, 2006; Yu *et al.*, 2012). Accordingly, seedlings and adult *prps1-1* plants are unable to cope with high temperature showing low survival rates with respect to the wild-type (Yu *et al.*, 2012). Interestingly, the introgression of *gun1* mutation in *prps1-1* genetic background rescues its low survival rate in such conditions (Tadini *et al.*, 2016). In addition, attempts to constitutively overexpress *PRPS1* gene resulted in a virescent phenotype and in the decrement of PRPS1 protein levels (Yu *et al.*, 2012).

Taken together, these observations indicate that chloroplast gene expression is largely controlled at the translational and post-translational level and set the chloroplast translation as a crucial step for the genesis of chloroplast-to-nucleus retrograde signalling pathways (Zoschke & Bock, 2018; Wu *et al.*, 2019). Furthermore, the peculiar features of ribosomal protein S1 identified during studies on *E. coli* and *Arabidopsis thaliana*, make it an interesting subject for deeper investigations regarding its role in chloroplast biogenesis, translational regulation and the interconnection with the protein homeostasis maintenance and retrograde communication.

These aspects have been investigated in the present manuscript, where we demonstrate that the knock-out of *PRPS1* gene is incompatible with chloroplast biogenesis and embryo development. Further, we assessed that PRPS1 is unable to functionally replace S1 in *E. coli* cells, and its overexpression inhibits cell growth, as in the case of the endogenous S1 protein (Briani *et al.*, 2008; Delvillani *et al.*, 2011). We also show that PRPS1 protein accumulation in chloroplasts is prevented post-translationally by the plastid CLP protease complex, while its constitutive over-expression promotes chloroplast degradation via micro- and macro-autophagy (Woodson, 2022), and induces early flowering. This adaptive response is organised at the very beginning of *PRPS1* transcript over-accumulation, as revealed by the transcriptome profile of short-term induced *PRPS1* expression lines. On the contrary, the over-accumulation of Plastid Ribosomal Protein Large subunit 4 (PRPL4) (Bryant *et al.*, 2011; Romani *et al.*, 2012), here used as control, is tolerated by chloroplasts and leads to the accumulation of transcripts and proteins, such as chaperons and proteases, that are part of the

116 chloroplast-derived Unfolded Protein Response mechanism (cpUPR; Ramundo & Rochaix, 2014;
117 Ramundo *et al.*, 2014; Pérez-Martín *et al.*, 2014; Llamas *et al.*, 2017).

118

Materials and methods

Bioinformatic analyses

S1 domain sequences have been identified using InterPro online tool (https://www.ebi.ac.uk/interpro/). Multiple sequence alignment was performed with MUSCLE online tool (https://www.ebi.ac.uk/Tools/msa/muscle/) and represented as phylogenetic tree employing PhyML (https://toolkit.tuebingen.mpg.de/tools/phyml) and iTOL (https://itol.embl.de/).

Plant material and growth conditions

The *PRPS1/prps1-2* heterozygous mutant lines were generated by targeting the first exon of *PRPS1* locus in *Arabidopsis thaliana* wild-type (Col-0) genetic background, using the pDe-CAS9 vector described by Fauser et al. (2014) (guide RNA sequence is listed in Table S1). *PRPS1/prps1-2* heterozygous plants, devoid of CAS9 T-DNA, were selected based on the mutation in *PRPS1* sequence. *prps1-2 pPRPS1::PRPS1* complemented lines were obtained by introgressing *PRPS1* genomic locus, including the *pPRPS1* promoter region, in *PRPS1/prps1-2* heterozygous plants and by selecting *prps1-2* viable plants carrying the *pPRPS1::PRPS1* construct. *oePRPS1* and *oePRPL4* lines were obtained by Agrobacterium-mediated transformation of Arabidopsis Col-0 genetic background with the coding sequences of *PRPS1* and *PRPL4* genes, under the control of CaMV35S promoter (pB2GW7 plasmid; https://gatewayvectors.vib.be/). *indPRPS1* and *indPRPL4* lines were obtained by cloning the *PRPS1* and *PRPL4* coding sequences in the Dexamethasone (DEX)-inducible *pOp/LhG4* system (Samalova *et al.*, 2005) and by Agrobacterium transformation of Arabidopsis Col-0 plants. *prps1-1* (SAIL_560_B02), *prpl11-1* (GABI_380H05), *clpc1-1* (SALK_014058C) and *clpd-1* (SALK_110649C) T-DNA lines were described in previous works (Pesaresi *et al.*, 2001; Sjögren *et al.*, 2004; Romani *et al.*, 2012; Pulido *et al.*, 2016) and manually crossed for obtaining *prps1-1 prpl11-1, prps1-1 clpc1-1, prps1-1 clpd-1* double mutants. Primers required for gene cloning and mutant line isolation are listed in Table S1. Wild-type and mutant seeds were grown on soil in climate chambers under long-day (150 µmol m^{-2} sec^{-1} 16 h/8 h light/dark cycles) and short-day (150 µmol m^{-2} sec^{-1} 8 h/16 h light/dark cycles) conditions. For growth experiments on Dexamethasone, seeds were surface-sterilised and grown for 16 days (80 µmol m^{-2} sec^{-1} on a 16 h/8 h light/dark cycle) on Murashige and Skoog medium (Duchefa) supplemented with 1% (w/v) sucrose and 1.5% Phyto-Agar (Duchefa), Dexamethasone was added at the final concentration of 2 µM. Growth rate was determined by ImageJ software (https://imagej.nih.gov/).

151 **Whole-mount preparation and optical microscopy**

152 To analyse defects in embryo development, siliques of Col-0 and heterozygous *PRPS1/prps1-2* plants
153 were manually dissected and cleared as reported in Tadini *et al.*, 2018. Developing seeds were
154 observed using a Zeiss Axiophot D1 microscope equipped with differential interface contrast optics.
155 Images were documented with an Axiocam MRc5 camera (Zeiss).

156 ***E. coli* strains**

157 *PRPS1* coding sequence was cloned into pQE31-pREP4 plasmid system (primers are listed in Table
158 S1), under the control of bacteriophage T5 promoter fused upstream to *lacO* operator sequences.
159 *PRPS1-pQE31-pREP4* and *rpsA-pQE31-pREP4* plasmids (Briani *et al.*, 2008) were then transferred
160 into *araBp-rpsA* conditional expression strain C-5699, in which the *rpsA* gene is expressed in
161 presence of 1% (w/v) arabinose and repressed in presence of 0.4% (w/v) glucose. To obtain the
162 *PRPS1* overexpressing strain, *PRPS1-pQE31-pREP4* plasmids were introduced into the *E. coli* C-1a
163 strain (Sasaki & Bertani, 1965), while *rpsA-pQE31-pREP4* strain C-5691 was used as control (Briani
164 *et al.*, 2008; Delvillani *et al.*, 2011).

165 **Chlorophyll a fluorescence measurements**

166 The Imaging Chl a fluorometer (Walz Imaging PAM; https://www.walz.com/) was used to determine
167 Chl fluorescence *in vivo*. Eight plants for each genotype and condition were analysed at 18 days after
168 sowing (DAS). Average values plus-minus standard deviations were then calculated. 20 min dark-
169 adapted plants were exposed to blue measuring light (intensity 4) and a saturating light flash (intensity
170 4) was used to calculate the maximum quantum yield of PSII, *Fv/Fm*.

171 **Nucleic acid analyses**

172 For qRT-PCR analyses, 1 µg of total RNA were treated with iScript™ gDNA Clear cDNA Synthesis
173 Kit (Bio-Rad; https://www.bio-rad.com/) for genomic DNA digestion and first-strand cDNA
174 synthesis. qRT-PCR analyses were performed on a CFX96 Real-Time system (Bio-Rad;
175 https://www.bio-rad.com/), using primer pairs listed in Table S1. *PP2AA3* (*AT1G13320*) transcripts
176 were used as internal reference, as described in Czechowski et al. (2005). Data obtained from three
177 biological and three technical replicates for each sample were analysed with the Bio-Rad CFX
178 Maestro 1.1 (v 4.1) (Bio-Rad; https://www.bio-rad.com/).

179 ***In vivo* Translation Assay**

180 The *in vivo* translation assay was performed essentially as previously described (Tadini *et al.*, 2012).
181 *indPRPS1* leaf discs (6 mm in diameter) were vacuum-infiltrated in liquid MS medium supplemented

with 1% (w/v) sucrose and, where indicated, 2 µM Dexamethasone. After 6-hours exposure to 80 µmol photons m^{-2} s^{-1} white light, leaf discs were incubated with a buffer containing 1 mM K_2HPO_4–KH_2PO_4 (pH 6.3) and 0.05% (v/v) Tween-20, supplemented with 20 µg/ml cycloheximide, to inhibit cytosolic translation. [^{35}S]methionine was then added (0.1 mCi/ml) and leaf discs were vacuum-infiltrated and exposed to light (80 µmol photons m^{-2} s^{-1}). 5 leaf discs were collected at each time point (15 and 30 min). Total proteins extraction and Tris-glycine SDS-PAGE fractionation is described below. Signals were detected using the Phosphorimager GE Healthcare Life Sciences (https://www.gehealthcare.com/).

Isolation of PRPS1-containing protein complexes

The isolation of PRPS1-containing complexes was performed according to previous works (Barkan, 1998; Merendino *et al.*, 2003). 100 mg of leaf fresh weight were ground in liquid nitrogen and resuspended in 1 ml 0.2 M Tris-HCl, pH 9, 0.2 M KC1, 35 mM $MgC1_2$, 25 mM EGTA, 0.2 M sucrose, 1% Triton X-100, 2% polyoxyethylene-10-tridecyl ether, supplemented with 500 µg/ml heparin, 100 µg/ml chloramphenicol and 25 µg/ml cycloheximide. The extract was then solubilised with 0.5% (w/v) sodium deoxycholate for 5 min on ice. After centrifugation (15 min at 10000g), 800 µl of supernatant was loaded onto 3.6 ml 15-55% (w/v) sucrose gradients in polysome gradient buffer (40 mM TrisHCl pH 8, 20 mM KCl, 10 mM $MgCl_2$, 100 µg/ml chloramphenicol and 500 µg/ml heparin). Sucrose gradients were centrifuged in SW60 rotors (Beckman) for 18 h at 180000 g at 4 °C. 9 fractions of 400 µl each were collected from the top of the tube and subjected to SDS-PAGE fractionation. *E. coli* ribosome fractionation was performed accordingly to Delvillani et al. (2011).

Transmission electron microscopy (TEM)

TEM analyses were performed as described previously (Jeran *et al.*, 2021). Plants were grown for 16 days on MS synthetic medium supplemented with 1% (w/v) sucrose and, where indicated, 4 µM Dexamethasone. Plant material was vacuum-infiltrated with 2.5% glutaraldehyde, in 100 mM sodium cacodylate buffer, for 4 h at room temperature and incubated overnight at 4 °C. Samples were rinsed twice with 100 mM sodium cacodylate buffer for 10 min each, and post-fixed in 1% (w/v) osmium tetroxide in 100 mM cacodylate buffer for 2 h at 4 °C. After washings, samples were counterstained with 0.5% (w/v) uranyl acetate overnight at 4 °C, in the dark. The tissues were then dehydrated by increasing concentrations of ethanol (70%, 80%, 90%; v/v), 10 min each. Samples were then dehydrated with 100% ethanol for 15 min and permeated twice with 100% propylene oxide for 15 min. Epon-Araldite resin was prepared mixing properly Embed-812, Araldite 502, dodecenylsuccinic anhydride (DDSA) and Epon Accelerator DMP-30. Samples were infiltrated first with a 1:2 mixture of Epon-Araldite and propylene oxide for 2 h, then with Epon-Araldite and propylene oxide (1:1) for

1 h and left in a 2:1 mixture of Epon-Araldite and propylene oxide overnight at room temperature. Samples were then incubated in pure resin before polymerisation at 60 °C for 48 h. Ultra-thin sections of 70 nm were then cut with a diamond knife (Ultra 45°, DIATOME) and collected on copper grids (G300-Cu, Electron Microscopy Sciences). Samples were observed by transmission electron microscopy (Talos L120C, Thermo Fisher Scientific) at 120 kV. Images were acquired with a digital camera (Ceta CMOS Camera, Thermo Fisher Scientific).

Protein sample preparation and immunoblot analyses

For immunoblot analyses, total proteins were prepared as described (Tadini *et al.*, 2020c). Plant material was homogenised in Laemmli sample buffer [20% (v/v) glycerol, 4% (w/v) SDS, 160 mm Tris–HCl pH 6.8, 10% (v/v) 2-mercaptoethanol] to a concentration of 0.1 mg μl^{-1} (leaf fresh weight/Laemmli sample buffer). Samples were incubated for 15 min at 65°C and, after a centrifugation step (10 min at 16 000 g), the supernatant was incubated for 5 min at 95 °C. Protein samples corresponding to 4 mg (fresh weight) of seedlings were fractionated by SDS–PAGE 10% (w/v) acrylamide (Schägger & von Jagow, 1987) and then transferred to polyvinylidene difluoride (PVDF) membranes (0.45 µm pore size). Replicate filters were immunodecorated with specific antibodies. Antibodies directed against AtHsp90-1 (AS08 346) and ClpB3 (AS09 459) were obtained from Agrisera (https://www.agrisera.com/), AtHsc70-4 antibody was obtained from Antibodies-online (https://www.antibodies-online.com/), antibodies directed against plastid ribosomal proteins (PRPS1, PRPL4 and PRPS5) were obtained from Uniplastomic, while polyclonal S1 antibody was kindly donated by U. Bläsi (University of Vienna).

Transcriptome analysis

Total RNA was extracted from leaf discs harvested from *indPRPS1* and *indPRPL4* plants and vacuum infiltrated in either the absence or presence of DEX for 6 hours for a total of 5 biological replicates for each group. Total RNA extraction was performed using RNeasy Mini Kit (Qiagen), according to the manufacturer's instructions. RNA concentrations and integrity were determined via NanoDrop One C (ThermoFisher Scientific) and agarose-gel electrophoresis. Extracted RNA samples were sent to Novogene for sequencing via high throughput Illumina NovaSeq platform which employ a paired-end 150 bp sequencing strategy. Raw data were processed and mapped to the Arabidopsis genome TAIR10 using STAR-RSEM software (Li & Dewey, 2011). Differentially Expressed Genes (DEGs) were identified through the R package EdgeR (v 3.15; Robinson *et al.*, 2009). Called DEGs were statistically filtered via Benjamini-Hochberg False Discovery Rate method (FDR < 0.05). GO enrichment analyses were performed using agriGO v2.0 online tool and further processed by REVIGO

(Supek *et al.*, 2011; Tian *et al.*, 2017). The RNA-seq data were deposited in the Gene Expression Omnibus data repository under the dataset identifier GSE205271.

Proteome analysis

Proteins were extracted from 1 g of plantlets following SDS/phenol method as described in Vannini et al. (2021). Proteins were then digested with trypsin via Filter Aided Sample Preparation (FASP) (Wiśniewski, 2019). Peptides were analysed by LC-MS/MS as described by Paradiso et al. (2020). Briefly, after LC separation peptides were sprayed into the mass spectrometer and eluting ions were measured in an Orbitrap mass analyser set at a resolution of 35000 and scanned between m/z 380 and 1500. Data dependent scans (top 20) were employed to automatically isolate and generate fragment ions by higher energy collisional dissociation (HCD); Normalised collision energy (NCE): 25% in the HCD collision cell and measurement of the resulting fragment ions was performed in the Orbitrap analyser, set at a resolution of 17500. Peptide ions with charge states of 2^+ and above were selected for fragmentation. Raw data were searched against the *Arabidopsis thaliana* TAIR protein database (2010 version) with MaxQuant program (v.1.5.3.3), using default parameters. For the quantitative analysis, the "ProteinGroups" output files were filtered to retain only protein groups detected with at least two peptides in at least three of the four biological replicates, and in at least one analytical group. The mass spectrometry proteomics data have been deposited in the ProteomeXchange Consortium via the PRIDE (Perez-Riverol *et al.*, 2019) partner repository under the dataset identifier PXD034479. Missing values were replaced with the R package imputeLCMD (v.2.1) using Hybrid imputation method: imputation of left-censored missing data (missing values $\geq$ 50% of number of replicas) was done using QRILC method, instead missed at random data (< 50% of replicas) were imputed using KNN method. Log2 transformed LFQ intensities were centred by Zscore normalisation method of Perseus (https://www.maxquant.org/perseus/) and then subjected to Student's Tests (S0=0.1, FDR<0.05) in order to discover Differentially Abundant Proteins (DAPs). Hierarchical clustering analysis was carried out using Perseus software and default parameters. DAPs categorisation was achieved using TAIR GO annotation tool (https://www.arabidopsis.org/tools/bulk/go/index.jsp). GO term enrichment analysis was performed using the PANTHER classification system (Mi et al., 2021; http://geneontology.org).

Results

Depletion of *PRPS1* gene leads to embryo lethality

Previous studies reported on the Arabidopsis *prps1-1* knock-down mutant phenotype, characterised by pale-green leaves, reduced growth rate and photosynthetic performance, as result of hampered plastid protein synthesis (Romani *et al.*, 2012; Yu *et al.*, 2012). However, the consequences of the complete inhibition of PRPS1 protein accumulation in Arabidopsis plastids has not yet been investigated. To fill this gap, the nuclear *PRPS1* gene was edited by targeting the first exon of *PRPS1* coding sequence using the CRISPR/Cas9 technology. Plant lines devoid of the Cas9 gene were obtained in T2 generation and the DNA region complementary to the designed guide RNA was sequenced (primers and guide RNA sequences are listed in Table S1). Only *PRPS1/prps1* heterozygous plants, with wild-type-like plant size, leaf pigmentation and photosynthetic performance, could be isolated and the resulting *prps1-2* allele showed the deletion of a Cytosine in the first exon (+80 bp from the transcription starting site), right downstream the ATG translation start codon (+ 4 bp from ATG, Fig.1 A, B). This event disrupts the *PRPS1* reading frame and introduces a premature Umber STOP codon in place of Leu-11 (+108 bp from the transcription starting site) (Fig. 1A). Furthermore, only *PRPS1/prps1-2* heterozygous and *PRPS1/PRPS1* homozygous plants could be identified within the progeny of the self-fertilised *PRPS1/prps1-2* heterozygous line, showing the 2-to-1 mendelian segregation ratio typical of mutations causing embryo lethality, as in the case of other plastid ribosomal protein knock-out mutants (Bryant *et al.*, 2011; Romani *et al.*, 2012; Yin *et al.*, 2012). Accordingly, the observation of *PRPS1/prps1-2* developing siliques at 10 Days After Fertilisation (DAF) revealed one-quarter of the seeds to be albino (Fig.1 C), indicating that *PRPS1* is essential during early stages of embryogenesis and seed development. In particular, optical section of cleared, whole-mount seeds from *PRPS1/prps1-2* siliques at 3 DAF showed that around 25% of the embryos were arrested at the globular development stage, displaying a disorganised cell division pattern similar to the ones previously described for other knock-out mutants in essential plastid ribosomal proteins (Romani et al., 2012; Fig. 1 D). Furthermore, the defect in embryo development was fully rescued in *prps1-2 pPRPS1::PRPS1* plants, obtained by introducing the *PRPS1* genomic DNA into the *PRPS1/prps1-2* genetic background and isolating wild-type homozygous *prps1-2* plants carrying the *pPRPS1::PRPS1* construct (Fig. 1 C, D).

***PRPS1* over-expression impairs chloroplast activity and biogenesis**

Besides the embryo lethal phenotype caused by the *prps1-2* allele and the slightly pale cotyledons and true leaves, together with hampered photosynthetic efficiency (F_V/F_M), typical of plants carrying the knock-down *prps1-1* allele (Fig. 2 A; see also Romani et al., 2012; Yu et al., 2012), the *CaMV35S*-mediated over-expression of *PRPS1* gene in the Arabidopsis Col-0 background (*oePRPS1*), also resulted in a visible phenotype, characterised by virescent young leaves with a marked drop in F_V/F_M values (Fig. 2 A). Interestingly, *oePRPS1* seedlings were incapable of over-accumulating the PRPS1 protein (Fig. 2 B), showing an accumulation level lower than the one observed in *prps1-1* leaves, despite the *PRPS1* transcript level having been about two-fold the Col-0 control leaves (Fig. 2 C, see also Tadini et al. 2016). On the contrary, Col-0 plants carrying the *CaMV35S::PRPL4* construct (*oePRPL4*), here used as the control, were able to accumulate up to 25-30 fold more *PRPL4* transcripts and almost double the amount of PRPL4 protein without affecting chloroplast biogenesis and activity, as shown by *oePRPL4* lines indistinguishable from Col-0 (Fig. 2 A, B, C).

In order to investigate this aspect further, *PRPS1* and *PRPL4* coding sequences were cloned into the *pOp/LhG4* vector, which allows the inducible over-expression of the two genes once the glucocorticoid analogue dexamethasone (DEX) is provided. The two constructs were introduced into Arabidopsis Col-0 genetic background, via Agrobacterium-mediated transformation, resulting in the dexamethasone-inducible lines *indPRPS1* and *indPRPL4*. In the absence of DEX, the *indPRPS1* line was virtually indistinguishable from Col-0 when grown on MS medium under sterile conditions for 16 days (Fig 2 A). Conversely, when the growth medium was supplemented with 2µM DEX, *indPRPS1* seedlings showed a leaf virescent phenotype and a drop in photosynthetic performance, together with a reduced accumulation of PRPS1 protein resembling the phenotype of *prps1-1* and *oePRPS1* lines (Fig 2 A, B). This was despite *PRPS1* transcripts accumulation to levels higher than Col-0 control leaves (Fig. 2 C). On the other hand, the inducible overexpression of *PRPL4* resulted in an increased accumulation of *PRPL4* transcripts and protein, similar to *oePRPL4* seedlings (Fig. 2 B, C), without any impact on chloroplast activity and leaf greening (Fig. 2 A).

To understand how chloroplasts ultrastructure organization is affected by the increased expression of *PRPS1* gene, thin sections of emerging young leaves from 16 DAS seedlings were observed under Transmission Electron Microscopy (TEM; Fig. 3). As expected, Col-0, *prps1-1*, *indPRPS1* - DEX, *indPRPL4* ± DEX, and *oePRPL4* mesophyll cells displayed properly developed chloroplasts with the typical organization in grana stacks and stroma lamellae (Fig. 3). However, both the induction (*indPRPS1* + DEX) and the constitutive increased expression of *PRPS1* caused the formation of miss-shaped and swollen chloroplasts containing enlarged plastoglobuli in the stroma

(Fig. 3). Furthermore, large budding vesicles with electron dense material were detectable, suggesting ongoing chloroplast degradation, resembling the fission-type ATG-independent micro-autophagy (Woodson, 2016, 2022; Tadini *et al.*, 2020c; Jeran *et al.*, 2021). In some cases, entire round-shaped chloroplasts, detached from the plasma membranes and with still recognizable grana stacks, were observed inside the vacuole, compatible with the ATG-dependent micro-autophagy process (Fig. 3J; Zhuang and Jiang, 2019; Woodson, 2022). To further prove that chloroplasts are indeed undergoing vacuole-mediated degradation, we investigated the relative expression of genes associated with either the chloroplast ATG-dependent or ATG-independent chloroplast quality-check and degradation pathways (Fig. S1). Strikingly, both *ATI1* (Michaeli *et al.*, 2014) and *ATG8f* (Liu *et al.*, 2021) transcripts were highly enriched in plantlets with increased *PRPS1* transcript accumulation, driven by either *CaMV35S*- or DEX-induced promoters (Fig. S1 A), whereas *NPC1* and *VPS15* (Lemke *et al.*, 2021) were the only genes of the ATG-independent pathway significantly up-regulated in *oePRPS1* plantlets (Fig. S1 B).

***PRPS1* short-term increased expression inhibits plastid protein translation**

To gain a dynamic view on PRPS1 function, the kinetics of *PRPS1* transcript and protein accumulation was monitored in leaf discs (6 mm in diameter) from young leaves of *indPRPS1* plantlets infiltrated with 2 μM DEX. Leaf discs were sampled at 0, 3, 6 and 24 hours after infiltration (HAI) and transcript and protein accumulation were monitored by RT-qPCR (Fig. 4 A) and immunoblotting (Fig. 4 B), respectively. As control, the same experimental set-up was used to monitor the induction of *PRPL4* expression (Fig. 4 A, C). The accumulation of *PRPL4* and *PRPS1* mRNAs indicated that both inducible lines were able to specifically express the related genes with comparable kinetics and transcript amounts (Fig. 4 A). Both lines reacted to the presence of DEX showing a high expression level of the related transcripts at 3 HAI, reaching the peak at 6 HAI and a significant decrease at 24 HAI. Nevertheless, the induction of *PRPS1* expression failed to yield the over-accumulation of PRPS1 protein. Indeed, PRPS1 protein level remained stable until 3 HAI, while diminished to almost undetectable levels from 6 to 24 HAI (Fig. 4 B). Interestingly, other plastid ribosomal proteins, such as PRPL4 and PRPS5, showed a marked decreased over time, indicating a general alteration of plastid ribosome accumulation, and possibly of plastid translation. On the contrary, the 24-hour induction of *PRPL4* resulted in more than two-fold accumulation of PRPL4 protein with respect to time 0 (Fig. 4 C). In particular, the increase in PRPL4 protein accumulation was observed over time, starting from 3 HAI and reaching the largest amount at 6 HAI, while the accumulation of PRPS1 and PRPS5 plastid ribosomal proteins remained unaltered.

To investigate the possible negative effect of *PRPS1* inducible expression on plastid protein translation, *indPRPS1* leaf discs were incubated in MS medium (± DEX) for 6 hours and then infiltrated with ^{35}S-Methionine and cycloheximide, allowing for the detection of *de novo* synthesized plastid-encoded proteins, while blocking the cytosolic translation. As shown by the pulse-labelling experiment, the synthesis rate of RbcL and D1/D2 proteins were markedly reduced in *indPRPS1* + DEX, over 15 and 30 minutes, when compared to *indPRPS1* leaf discs in the absence of dexamethasone (- DEX; Fig. 4 D), proving that *PRPS1* inducible over-expression leads to plastid translation inhibition. This aspect was investigated further by isolating the PRPS1-containing complexes and monitoring the PRPS1-to-ribosome stoichiometry and the accumulation of "free" PRPS1 fraction, as previously reported in *E. coli* (Delvillani *et al.*, 2011). To do so, *indPRPS1* leaf material (6 hours ± DEX) was subjected to sucrose gradient fractionation and probed with the PRPS1 antibody (Fig. 4 E). As observed in Chlamydomonas (Merendino *et al.*, 2003), PRPS1 protein was found in two distinct populations, as "Low Molecular Weight (LMW, free PRPS1 fraction)", bound solely to the mRNA, and as "High Molecular Weight (HMW)", corresponding to the S1 fraction bound to the ribosome core. The increase of PRPS1 presence in the LMW fractions of *indPRPS1* + DEX line, compared to the - DEX counterpart (Fig. 4 E, F), supports further the inhibition of plastid translation observed in Fig. 4 D. Consistent with these data, we observed that PRSP1 was almost absent in HMW fraction in *oePRPS1* samples (Fig. S2).

The over-accumulation of Arabidopsis PRPS1 protein inhibits *Escherichia coli* cell growth

Similarly to Arabidopsis, the depletion of the ribosomal protein S1 (Rps1) in *E. coli* cells leads to lethality (Kitakawa & Isono, 1982). Moreover, the down-regulation as well as the over-accumulation of Rps1 impairs protein translation by altering the stoichiometry between Rps1 and the ribosome core, leading to bacteriostatic effects (Briani et al., 2008; Delvillani et al., 2011; see also Fig. 5). The *E. coli* S1 protein is 557 aa long with a molecular weight of 61.2 kDa and possesses six S1 domains (Bycroft et al., 1997; Fig. 5 A) that are typical of several RNA binding proteins (Murzin, 1993; Arcus, 2002; Theobald *et al.*, 2003). In *A. thaliana*, the S1 homologous PRPS1 is markedly smaller, with 373 aa and a molecular weight of 40.5 kDa, as mature form. The *in silico* analysis of PRPS1 amino acid sequence identified three S1 domains (Fig. 5 A), in agreement with early analyses of spinach S1 protein (Franzetti *et al.*, 1992). In addition, PRPS1 protein shows a high degree of identity (*i.e.* about 50%) with the S1 ribosomal proteins from cyanobacteria, which possess three S1 domains as well (Sugita *et al.*, 1995; Salah *et al.*, 2009). In order to investigate the possible relationships between the three S1 domains identified in PRPS1 and the six S1 domains in *E. coli* S1, the amino acidic sequences

of each S1 domain were aligned and clustered in a phylogenetic tree (Fig. S3). The resulting tree showed that domains 1 and 2 of PRPS1 are more similar to the corresponding domains of S1, while the PRPS1 domain 3 clusters together with the domains 3, 4 and 5 of S1.

The possible functional homology between the two proteins was then investigated by introducing the *PRPS1* gene in *E. coli* cells, for over-expression and complementation assays. To experimentally test the ability of PRPS1 to complement S1 functions and to repress cell growth when over-accumulated in bacterial cells, both *rpsA* (encoding the S1 protein) and *PRPS1* coding sequences were cloned into pQE31-pREP4 plasmid system under the control of *pT5-lacO* promoter in pQE31. The plasmids were then introduced into the arabinose-dependent strain C-5699 (Briani *et al.*, 2008), in which the chromosomal *rpsA* gene is transcribed from the *araBp* promoter, generating *indrpsA* and *indPRPS1* strains. Such systems provide a mechanism to deplete cells of the endogenous S1 protein in absence of arabinose and presence of glucose (Briani *et al.*, 2008; Delvillani *et al.*, 2011) and to modulate the expression of either *rpsA* or *PRPS1* genes cloned in pQE31 depending on IPTG concentration.

Both *indrpsA* and *indPRPS1* strains were cultured in three different conditions: Depletion (0.4% glucose and no IPTG), Complementation (0.4% glucose and 0.01 mM IPTG) and Overexpression (1% arabinose and 1 mM IPTG). The growth conditions for the complementation assay were experimentally optimized based on the growth of *indrpsA E. coli* strain. Cell growth was measured every 45 minutes up to 225 minutes after the induction (MAI, Fig. 5 B). At each time point cells were sampled, normalized on the optical density (OD_{600}) value, and the total protein extract was used to detect the accumulation of S1 and PRPS1 proteins in both strains (Fig. 5 C). Under Depletion conditions, both strains showed almost completely impaired growth rate, due to the limited accumulation/absence of S1 protein. When grown in Complementation conditions, *indrpsA* cells were able to actively replicate and showed comparable amounts of S1 protein at each time point, indicating that the experimental conditions were properly set up to induce a wild-type-like S1 protein accumulation. On the other hand, *indPRPS1* cells failed to sustain growth in such conditions despite the gradual accumulation of PRPS1 protein, proving the inability of PRPS1 to complement the S1 function in *E. coli*. As expected, under Overexpression conditions, *indrpsA* strain growth was inhibited due to the excessive amount of S1 protein (Fig 5 B, C). Strikingly, the over-accumulation of PRPS1 protein was effectively repressing the bacterial growth and led to S1 protein depletion, too (Fig. 5 B, C). It is worth noting, that the overaccumulation of PRPS1 Arabidopsis protein was able to repress the growth of *E. coli* cells, comparably to S1 overaccumulation, even when the overexpression of either *rpsA* or *PRPS1* genes was achieved in the C-1a *E. coli* strain, devoid of the conditional depletion system of the endogenous S1 protein (Fig. S4 A). To better understand whether PRPS1

protein is capable of interacting with *E. coli* ribosomes under overexpression conditions, we sampled both *indrpsA* and *indPRPS1* cells at 90 MAI. Cell lysates were then fractionated into ribosome-unbound (supernatant, SN) and ribosome-bound (pellet, P) fractions and analysed via immunoblotting to detect either S1 or PRPS1 protein localisation. Interestingly, PRPS1 was retrieved in both ribosome-bound and -unbound fractions, similarly to S1 from *E. coli*, suggesting that the Arabidopsis PRPS1 can compete for the ribosome core with *E. coli* S1 protein (Fig. S4 B). Taken together, these data indicate that PRPS1 protein is able to inhibit *E. coli* growth when over-expressed in addition to the endogenous S1, whereas it is unable to functionally replace the *E. coli* endogenous S1 protein.

PRPS1 accumulation is negatively regulated by chloroplast CLP protease complex

The phenotypes observed in Arabidopsis plants upon *PRPS1* overexpression indicate that the abundance of PRPS1 protein must be kept under a strict post-transcriptional control to prevent inhibition of protein synthesis and chloroplast damage (see Fig. 2-4). This notion is supported further by the inhibitory role of PRPS1 protein over-accumulation on *E. coli* cell growth (Fig. 5 and Fig. S4). In order to investigate the molecular mechanism responsible for controlling PRPS1 protein abundance, leaf discs were infiltrated with DEX supplemented with lincomycin (LIN), a specific inhibitor of plastid 70S ribosomes. Strikingly, a large accumulation of PRPS1 protein, most probably as result of PRPS1 degradation suppression, could be observed even after 24 hours from DEX infiltration, unlike the control sample (Fig. 6 A). Intriguingly, the most relevant chloroplast stromal protease is represented by the CLP complex, which is composed by several nuclear-encoded subunits and one plastid-encoded component, ClpP1, that is part of central proteolytic core (van Wijk, 2015; Llamas *et al.*, 2017). To investigate whether the CLP complex could indeed be responsible for maintaining PRPS1 protein below levels that would otherwise cause damages to the chloroplast, we crossed *prps1-1* with mutants altered either in chloroplast protein translation, *prpl11-1*, or lacking two plastid chaperones required to feed CLP protease with protein substrates, *clpc1-1* and *clpd-1* (Pulido et al., 2016; Fig. 6 B). *prps1-1 prpl11-1* double mutant showed reduced growth rate (Fig. S5) and a slight decrease in photosynthetic efficiency (Fv/F_M) with respect to *prpl11-1* parental line. Similar genetic interactions were observed in *prps1-1 clpc1-1* double mutant, which showed a severe reduction in growth rate with respect to *prps1-1* and *clpc1-1* single mutants. Interestingly, *prps1-1 clpd-1* double mutant showed partially restored growth rate, close to wild-type-like levels, and a slight recovery of Fv/F_M parameter. Strikingly, the accumulation of PRPS1 protein increased about two-fold in all the double mutants tested (Fig. 6 C) with respect to *prps1-1*, further supporting the notion that plastid translation and the CLP protease complex play an important role in controlling PRPS1 abundance in the stroma of chloroplasts.

Short-term induction of *PRPS1* and *PRPL4* gene expression induces different nuclear gene expression responses

The opposite behaviour of *indPRPS1* and *indPRPL4* plants in terms of protein pattern accumulation upon DEX-mediated induction of gene expression make them the ideal genetic material to investigate the primary nuclear gene expression response to changes in plastid ribosomal protein content. To this aim, a transcriptome analysis was performed on leaf discs harvested from *indPRPS1* and *indPRPL4* and vacuum infiltrated in either the absence or presence of DEX. In particular, total leaf RNA was extracted after 6 hours from infiltration, i.e., at the stage of maximal accumulation of *PRPS1* and *PRPL4* transcripts (see Fig. 4 A) and at the beginning of evident changes in protein pattern accumulation (see Fig. 4 B and C), and subjected to Illumina sequencing. Principal component analyses (PCA) of *indPRPS1* and *indPRPL4* samples showed a clear separation between the untreated and treated samples (Fig. S6), despite the short induction time. The EdgeR package was used to identify differentially expressed genes (DEGs, listed in Table S2), obtained by comparing data from *indPRPS1*-DEX with *indPRPS1*+DEX, and *indPRPL4*-DEX with *indPRPL4*+DEX (Fig. 7 A). Overall, 431 DEGs in *indPRPS1* upon DEX induction and 328 in *indPRPL4* were identified. Among them, 124 DEGs were in common between the two datasets. Next, the obtained DEGs were divided into up and down regulated genes both in *indPRPS1* and *indPRPL4* datasets, obtaining *indPRPS1*UP, *indPRPL4*UP, *indPRPS1*DOWN and *indPRPL4*DOWN lists, which were further compared to isolate unique DEGs in each group (Fig. 7 B, see also Table S2). As a result, among the up-regulated DEGs, 161 were uniquely found in *indPRPS1* (Table S2 A) and 159 DEGs in *indPRPL4* (Table S2 B), while 107 DEGs were up-regulated in both lines (Table S2 C). Among the down-regulated DEGs, 146 were unique for *indPRPS1* line (Table S2 D), 45 unique DEGs for *indPRPL4* (Table S2 E) and only 14 were commonly down-regulated (Table S2 F). Furthermore, among the 149 down-regulated DEGs in *indPRPS1*, 3 were upregulated in *indPRPL4* (Table S2 G).

To investigate the biological functions activated or repressed by the overexpression of either *PRPS1* or *PRPL4* genes, the unique DEGs found up- or down-regulated in *indPRPS1* or *indPRPL4* were analysed with agriGO v2.0 online tool (Tian *et al.*, 2017). Next further analysis by REVIGO (Supek et al., 2011) was preformed to retrieve Biological Process Gene Ontology terms and group them into functional categories (Fig. 8; Table S3, S4, S5). The 161 DEGs up-regulated in *indPRPS1* produced strongly enriched GO terms associated with responses to endogenous factors or involvement in flowering and seeds production, such as "photoperiodism, flowering" (GO:0048573), "response to karrikin" (GO:0080167), "vegetative to reproductive phase transition of meristem" (GO:0010228) or "cellular response to hormone stimulus" (GO:0032870) (Fig. 8 A; see also Table S3). On the other hand, the repressed biological functions found in *indPRPS1* were related to the

production of secondary metabolites, defence against herbivores and oxidative stress such as "glucosinolate biosynthetic process" (GO:0019761), "sulfur compound biosynthetic process" (GO:0044272), "cell redox homeostasis" (GO:0045454) and "response to wounding" (GO:0009611), to cite a few of them (Fig. 8 B; see also Table S4). Interestingly, the high enrichment in GO terms associated with flowering and reproductive phase transition is in good agreement with the anticipated flowering phenotype, calculated as number of rosette leaves at bolting, observed when *PRPS1* transcripts are overexpressed (Fig. 9). In particular, in the case of plants cultivated on soil under growth chamber conditions, Arabidopsis Col-0 bolted with an average of about 10-11 rosette leaves while the *oePRPS1* line showed an anticipated flowering time, bolting at the stage of 8 rosette leaves, comparable to *prps1-1* behaviour (Fig 9 A, B). The same anticipated flowering time occurred under short day growth conditions, with the wild-type bolting at 54 leaves while the overexpressing line flowered at 37 rosette leaves on average (Fig 9 C). A similar observation was made when *indPRPS1* line was grown on MS medium supplemented with 1% (w/v) sucrose and DEX, in which its number of leaves at bolting was 5, similarly to *oePRPS1* (Fig. 9 D). Instead, when *indPRPS1* was grown on MS medium without DEX, the number of leaves at bolting was about 6-7, comparable to what observed in *indPRPL4* and Col-0 plants.

Conversely, the analysis of the activated biological processes in *indPRPL4* showed a strong enrichment in GO terms associated with abiotic stress responses and protein homeostasis such as "response to hydrogen peroxide" (GO:0042542), "response to high light intensity" (GO:0009644), "response to heat" (GO:0009408), "response to oxidative stress" (GO:0006979) and "protein folding" (GO:0006457) (Fig. 8 C; see also Table S5). These activated cellular pathways are in agreement with the observed increased levels of CLPB3, HSP90-1 and HSC70-4 proteins in *indPRPL4* line upon induction with DEX (see Fig. S7). In particular, CLPB3 protein abundance and even more the abundance of HSP90-1 and HSC70-4 proteins largely increased already at 3 HAI in *indPRPL4* leaf disks, unlike in *indPRPS1* samples, possibly generated by the overload of the plastid folding machinery caused by PRPL4 abundance and the consequent activation of chloroplast UPR. Interestingly, the unique down-regulated DEGs found in *indPRPL4* leaf disks resulted in no significantly enriched GO terms.

Short-term induction of *PRPS1* and *PRPL4* gene expression induces different changes in proteomic profiles

To further investigate the molecular responses following the DEX-mediated induction of *PRPS1* and *PRPL4* genes, a proteomic analysis was performed on leaf tissue harvested from *indPRPS1* and

indPRPL4 plants and vacuum infiltrated either in the absence or presence of DEX and sampled, as in the case of transcriptome analysis, after 6 hours of induction. PCA analysis revealed that dexamethasone-mediated induction led to significant changes also at proteomic level (Fig. S8). Comparing induced (+DEX) and control groups (-DEX), the abundances of 58 and 77 proteins were altered in *indPRPS1* and *indPRPL4* samples, respectively (T Student's test, FDR < 0.05; listed in Table S6). The minimal overlapping between the two datasets (only two common proteins) confirms the different cellular responses following the induction of *PRPS1* and *PRPL4* genes (Fig. 10 A). In particular, 27 and 31 proteins were up- and down-accumulated in *indPRPS1* leaf discs, whereas 45 and 32 proteins were up- and down-accumulated in *indPRPL4* samples, respectively (Fig. 10 B).

GO enrichment analysis of differentially abundant proteins (DAPs) found in *indPRPS1* samples revealed over-represented GO terms only among the down-accumulated proteins, probably due to the small size of the data set. The enriched Biological Process terms were "translational elongation" (GO:0009658) and "chloroplast organization" (GO:0006414) (Table S7). Among the enriched Cellular Component terms, "ribosome-associated quality control (RQC) complex" (GO:1990112), "transcriptionally active chromatin" (GO:0035327) and "chloroplast stroma" (GO:0009570) were found (Table S8). All DAPs were grouped based on their GO annotations (Fig. 11). Proteins up-regulated in response to *PRPS1* induction were mainly involved in "anatomical structure development" (GO:0048856), "catabolic process" (GO:0009056) and "response to light stimulus" (GO:0009416) (Fig. 11 A). In addition, the up-accumulated proteins in *indPRPS1* plantlets were mainly located in "nucleus" (GO:0005634) and "cytoplasm" (GO:0005737) (Fig. 11 B). Down-regulated DAPs produced GO annotations such as "biosynthetic processes" (GO:0009058), "RNA binding" (GO:0003729), "translation" (GO:0006412) and "post-embryonic development" (GO:0009791) (Fig. 11 A). Among down-regulated proteins detected in *indPRPS1* samples we found the regulator of fatty-acid composition 3 (RFC3; AT3G17170) which plays an important role in the plastid rRNA processing (Nagashima *et al.*, 2020). Many of these down-regulated proteins were located in chloroplast and nucleus (Fig. 11 B).

The significantly enriched GO terms retrieved by analysing the up-regulated proteins detected in *indPRPL4* samples were mainly associated with mitochondrial electron transport chain and mitochondrial ribosomes (Table S9). Moreover, GO annotation revealed that several DAPs in *indPRPL4* seedlings belong to "response to stress" (GO:0006950), as also detected by the transcriptome analysis (Fig. 11 C). The GO annotation tool allowed to locate DAPs in *indPRPL4* plants especially in the nucleus, chloroplast and cytoplasm (Fig. 11 D). Overall, our results, in agreement with transcriptomic analysis, point out very specific proteomic changes following the alteration of the two ribosomal proteins PRPS1 and PRPL4. In fact, the induction of *PRPS1* leads to

575 a general repression of translation, transcription and chloroplast organization. Conversely, the
576 increased amount of PRPL4 protein promotes the cellular stress response, leading to a positive
577 regulation of proteins involved in RNA metabolism and translation, with a major contribution also
578 given by components of the mitochondrial metabolism.

579

Discussion

Altered *PRPS1* expression impairs chloroplast biogenesis

PRPS1 is a nuclear gene encoding the S1 protein of the plastid 30S small ribosomal subunits. Reduced expression of *PRPS1* gene results in diminished plastid translation and decreased photosynthetic efficiency (Romani *et al.*, 2012; Yu *et al.*, 2012), while its disruption arrests embryo development at the globular stage in Arabidopsis (see Fig. 1) and prevents greening of seedlings in rice (*albino seedling lethality 4*; Zhou et al., 2021). Clearly, these observations indicate that *PRPS1* is an essential gene required during early stages of chloroplast biogenesis, as reported in the case of other essential nuclear genes coding for plastid ribosomal proteins (Bryant et al., 2011; Lloyd and Meinke, 2012; Romani et al., 2012). The apparent discrepancy between the early block of embryo development in Arabidopsis and the arrest of seedling greening in rice is in agreement with previous findings (Hess *et al.*, 1994; Zubko & Day, 1998; Ostheimer *et al.*, 2003; Asakura & Barkan, 2006) and compatible with the essential nature of fatty acid biosynthesis during chloroplast biogenesis. In particular, the lack of the plastid-encoded accD-subunit of the multimeric acetyl-CoA carboxylase required for fatty acid biosynthesis is responsible for the lethality of Arabidopsis embryos defective in plastid translation (Bryant *et al.*, 2011). In contrast, grass species contain a plastid-located monomeric acetyl-CoA carboxylase that, differently from Arabidopsis, is encoded in the nucleus and translated in the cytosol (Schulte *et al.*, 1997; Chalupska *et al.*, 2008). Therefore, fatty acid biosynthesis (and embryogenesis) can continue even when plastid protein synthesis is affected in these species.

Intriguingly, the reduced accumulation of S1 protein can also be obtained when *PRPS1* gene expression, and the consequent transcript accumulation, is both constitutively increased in *oePRPS1* and *indPRPS1* + DEX seedlings (Fig. 2) and induced in *indPRPS1* leaf discs for 24 hours (Fig. 4). This finding, together with the very limited increase in transcript accumulation observed in *oePRPS1* and *indPRPS1* + DEX seedlings, indicates the existence of post-transcriptional regulatory mechanisms aimed to prevent PRPS1 over-accumulation, as shown previously (Yu *et al.*, 2012). The strict control on *PRPS1* gene expression and protein accumulation appears to be rather specific and certainly it does not apply to *PRPL4*, a nuclear gene encoding a core subunit of the 50S plastid ribosome, also essential for embryo development and plant viability (Bryant *et al.*, 2011; Romani *et al.*, 2012). In fact, *oePRPL4* and *indPRPL4* + DEX lines were able to accumulate 25-30 times more transcripts, together with the double amount of PRPL4 protein, in comparison to Col-0 and *indPRPL4* - DEX controls (Fig. 2, Fig. 4).

Furthermore, the constitutive over-expression of *PRPS1* gene, driven in 16 DAS *oePRPS1* and *indPRPS1* + DEX plantlets, resulted in the impairment of chloroplast differentiation and physiology, leading to a virescent phenotype visible in the emerging leaves and in the younger portions of the leaves, corresponding to the tissue proximal to the petiole. In particular, transmission electron microscopy (TEM) observations of the chlorotic tissues revealed the presence of cells displaying misshapen chloroplasts with altered thylakoid membrane ultrastructure and large plastoglobuli in the stroma (Fig. 3), reported to be associated with the degradation of chlorophylls and thylakoids in response to abiotic and biotic stresses or during senescence (Rottet *et al.*, 2015; Van Wijk & Kessler, 2017; Zechmann, 2019). Moreover, the presence of vesicles budding from chloroplasts and containing electron dense material, together with the observation of entire round chloroplasts inside the vacuole (Fig. 3), indicates the ongoing chloroplast degradation, similarly to what reported in literature (Woodson, 2016; Zhuang and Jiang, 2019; Tadini et al., 2020; Jeran et al., 2021). Coherently, the relative expression of *ATI1* and *ATG8f* genes, involved in ATG-dependent micro-autophagy, was enhanced upon PRPS1 attempted over-accumulation (Fig. 3, Fig. S1 A), whereas the expression of genes involved in ATG-independent micro-autophagy was mildly stimulated in *oePRPS1* (Fig. S1 B) (Lemke *et al.*, 2021). Overall, these observations indicate that the reduced accumulation PRPS1 severely jeopardizes chloroplast integrity during leaf development, leading to the dismantling of damaged and misshapen chloroplasts with the final aim to remove reactive oxygen species–producing chloroplasts and redistributing nutrients to other tissues (Woodson, 2022).

A fully functional proteostasis machinery is needed to control PRPS1 accumulation in chloroplast stroma

All our attempts to increase the abundance of PRPS1 protein failed (Fig. 2 and Fig. 4; Tadini *et al.*, 2016) and, together with that, the accumulation of other plastid ribosomal proteins, such as PRPL4 and PRPS5, was reduced, as observed in *indPRPS1* + DEX leaf discs (Fig. 4), indicating that the decreased abundance of PRPS1 protein has a deleterious effect on plastid ribosome stability. In agreement with that, the pulse-labelling experiment conducted on *indPRPS1* leaf material infiltrated with DEX for 6 hours showed a severe inhibition of plastid protein translation and a larger fraction of PRPS1 protein freely associated to mRNA and not bound to actively translating ribosomes (Fig. 4). These findings explain the defects in leaf greening observed in the different Arabidopsis lines (Fig. 1 and Fig. 2) and support the role of PRPS1 as a stringently regulated translation factor rather

than a "real" ribosomal protein, given its weakly and reversible association with the 30S subunit, similarly to previous observations in *E. coli* (Delvillani *et al.*, 2011).

S1 protein is the closest PRPS1 homologue in *E. coli*, and it is encoded by the essential gene *rpsA* (Kitakawa & Isono, 1982). To gain possible insights on PRPS1 function, we attempted to rescue *E. coli* cell lethality due to S1 depletion and to phenocopy the bacteriostatic effects of S1 overaccumulation, by modulating the level of PRPS1 protein in *E. coli* cells (Fig. 5). Our data clearly showed that PRPS1 is not able to functionally replace the endogenous S1, as cells depleted of *rpsA* but with moderate amount of PRPS1, failed to grow (Fig. 5). According to previous studies, S1 protein exerts its functions in relationship with the specializations of its six S1 domains (Salah *et al.*, 2009). The interactions with the ribosome relies on S1 domains 1 and 2 (Giorginis & Subramanian, 1980), whereas the ability to bind mRNAs has been associated with the S1 domains 3, 4 and 5 (Subramanian, 1983). As for domain 6, if removed together with S1 domain 5, the initiation of translation is hampered (Boni *et al.*, 2000; Salah *et al.*, 2009) and together with domain 4, it is implicated in ribosome dimerization and hibernation in stationary phase (Beckert *et al.*, 2018). According to our *in silico* analysis, S1 domains 1 and 2 of PRPS1 appeared to be more similar to the respective domains 1 and 2 of S1, while domain 3 clustered together with domains 3, 4 and 5 of S1 (Fig. S3). The fact that PRPS1 is a smaller protein and possesses three out of the six S1 domains identified in S1, of which none could be associated with those required for translation initiation in *E. coli*, could explain the inability of PRPS1 to functionally replace S1 protein. Nonetheless, PRPS1 overaccumulation blocked cells growth as much as S1 (Fig. 5, Fig. S4). It has been shown that S1 over accumulation inhibits translation since the excess of "free" S1 interacts with mRNAs, preventing the ribosome loading (Delvillani et al., 2011; Boni et al., 2001, Skorski et al., 2006; Skouv et al., 1990). However, PRPS1 was found both in ribosome-bound and -unbound fractions, suggesting that, although PRPS1 can interact with the ribosome core in *E. coli* cells, this interaction is rather unfruitful. In this scenario PRPS1 would be able to inhibit *E. coli* growth by competing with the endogenous S1 protein and inhibiting ribosome activity (Fig. S4). Nevertheless, PRPS1 is likely capable of binding *E. coli* mRNAs with the S1 domains 2 and 3, since *E. coli* and plastid mRNAs share similar 5' UTRs with AU-rich sequences (Hirose & Sugiura, 2004), making *E. coli* transcripts inaccessible to ribosomes and acting as a negative modulator of translation initiation. The inhibitory role of PRPS1 protein on *E. coli* protein synthesis is corroborated further by the fact that the accumulation of PRPS1 upon overexpression reaches very rapidly the plateau level and concomitantly leads to the decreased accumulation of S1 protein over time (Fig. 5 C), mimicking the role of S1 as feedback effector of its own regulation at the translational level (Skouv *et al.*, 1990).

Such regulatory mechanism has a different spatial constraint in photosynthetic eukaryotes due to the physical separation of the nuclear/cytosolic compartments, where the *PRPS1* transcripts and the precursor protein are synthesized, and the chloroplast stroma where the mature PRPS1 protein plays its functions. While the limited accumulation of *PRPS1* transcripts observed upon constitutive expression allows us to hypothesize the existence of a cytosolic post-transcriptional regulatory mechanism (Wu *et al.*, 2019), our data strongly support the activation of a chloroplast stroma post-translational regulatory mechanism, in response to *PRPS1* overexpression, mediated by the plastid proteostasis machinery (Fig. 6). In chloroplasts, the major soluble stromal protease is the CLP complex, composed of multiple nuclear-encoded subunits with the addition of ClpP1 subunit, the only one to be plastid-encoded (van Wijk, 2015). Consequently, ClpP1 abundance is susceptible to genetic defects in plastid gene expression or to drugs inhibiting plastid translation (Llamas *et al.*, 2017). The co-infiltration of DEX with the plastid translational inhibitor lincomycin allowed a larger accumulation of PRPS1 protein (Fig. 6 A). Accordingly, an increased PRPS1 protein accumulation (Fig. 6 C) could be achieved by introgressing the *prps1-1* knock-down allele into *prpl11-1* genetic background, in which the chloroplast translation is reduced (Pesaresi *et al.*, 2001). This is also in line with the restoration of PRPS1 protein accumulation observed in *prps1 gun1* and *prps1 rh50* double mutants, as GUN1 stimulates the activity of the Nuclear-Encoded Polymerase (NEP) that, among other plastid house-keeping genes, is responsible of the transcription of *clpP1*, while RH50 is involved in plastid ribosome assembly and plastid translation (Tadini *et al.*, 2016, 2020c,a,b; Paieri *et al.*, 2018). Intriguingly, GUN1 was also found to physically interact with the plastid protein homeostasis machinery, including ClpC subunits (Tadini *et al.*, 2016). Furthermore, a comparable increase in PRPS1 levels were also observed in the double mutants *prps1-1 clpc1-1* and *prps1-1 clpd-1* (Fig. 6 C), in which the two plastid chaperones required by CLP protease to interact with the substrates are missing (Pulido *et al.*, 2016). These pieces of evidence strongly point towards CLP protease complex as one of the main regulators of PRPS1 protein abundance in Arabidopsis chloroplasts.

Our findings are also in agreement with previous reports. In particular, by combining transcriptomic and proteomic analyses, Wu et al., 2019 were able to show that plastid ribosomal proteins are regulated post-translationally, suggesting a protein degradation-based mechanism. Moreover, in *Chlamydomonas*, *CreS1* expression is induced by light, while CreS1 protein levels remain constant, pointing also in this case to the post-translational regulation of CreS1 abundance (Merendino *et al.*, 2003).

On the other hand, the constitutive over-accumulation of PRPL4 protein upon induction didn't affect neither the plastid translation nor the chloroplast ultrastructure (Fig. 2, Fig. 3, Fig. 4).

712 Interestingly, chaperones both resident in the cytoplasm and in plastids were progressively up-
713 regulated as PRPL4 levels increased, indicating the activation of protein homeostasis mechanisms to
714 cope with the increased protein amount (Fig. S7). These different responses to the overexpression of
715 two plastid ribosomal proteins could be due to their intrinsic features and activities, having PRPS1
716 mRNA-binding properties which, if not kept under strict control, would have dramatic consequences
717 on chloroplast functionality.

718

719 **_PRPS1_ overexpression promotes early flowering while PRPL4 overaccumulation triggers**
720 **cpUPR**

721 The switch from vegetative growth to reproductive growth is a pivotal event in plant
722 development, mostly dependent on the environmental stimuli such as day length (photoperiodic
723 flowering) and temperature (vernalization) that plants perceive to determine the proper timing to
724 assure successful reproduction, and ultimately the survival of the species (Freytes *et al.*, 2021).
725 However, plants subjected to a variety of stressful conditions can anticipate their flowering through
726 a new category of flowering response, known as stress-induced flowering, aimed to guarantee species
727 survival when they cannot adapt to unfavourable conditions (Takeno, 2016). Although the
728 mechanistic details behind the stress-induced flowering are still not fully understood, hormones seem
729 to be at least partially involved in these pathways as they are produced under stress and regulate gene
730 expression to cope with it (Takeno, 2016; Kazan & Lyons, 2016). This seems to be the case of plants
731 subjected to prolonged *PRPS1* overexpression and characterised by an early flowering phenotype
732 regardless of day length (Fig. 9). In these plants, the stress seems to be caused by the reduced
733 chloroplast protein synthesis and the consequent accumulation of damaged proteins and, possibly, by
734 low sucrose concentration due to the reduced photosynthetic performance (see Fig. 2; Bolouri
735 Moghaddam and Van den Ende, 2013). Consistently, the transcriptomic profile of Arabidopsis lines
736 characterised by the short-term induction of *PRPS1* gene highlighted that the early nuclear gene
737 expression response to PRPS1 imbalance in chloroplasts is characterised by a robust enrichment of
738 up-regulated genes associated with the reproductive phase transition and the cellular response to
739 hormones, such as "photoperiodism, flowering", "vegetative to reproductive phase transition of
740 meristem" and "cellular response to hormone stimulus" (Fig. 8 and Table S3), and by the concomitant
741 repression, amongst others, of genes involved in "cell redox homeostasis", "response to wounding",
742 "response to oxidative stress", "response to water deprivation". Accordingly, the circadian clock
743 regulators *RVE8* and *CO*, the *IDD8* transcription factor and the Gibberellic acid enzyme *ga3ox1*, all
744 positive modulators of flowering, are among the up-regulated genes. On the other hand, the

745 tetratricopeptide thioredoxin-like protein *TTL4*, required for osmotic stress tolerance, *BASS5* and
746 *BCAT4*, involved in glucosinolate biosynthesis, *PTR3*, required for defences against pathogens, and
747 the transcription factor *NAC019*, involved in the response to dehydration, were found to be down-
748 regulated upon *PRPS1* induction (Tran *et al.*, 2004; Schuster *et al.*, 2006; Karim *et al.*, 2007; Sawada
749 *et al.*, 2009; Lakhssassi *et al.*, 2012). Interestingly, the mass spectrometry analysis of the tissue
750 overexpressing *PRPS1* detected the increased accumulation of far-red insensitive 219 (FIN219;
751 AT2G46370) and the phytochrome associated protein phosphatase 2C (PAPP2C; AT1G22280), both
752 directly involved in the response to red, or far red light and in flower development (Hsieh *et al.*, 2000;
753 Phee *et al.*, 2008); while chloroplast-located proteins involved in "RNA metabolism" and
754 "translation" where down-regulated.

755 In contrast, the results obtained from the transcriptomic and proteomic analyses performed on
756 *indPRPL4* + DEX leaf discs showed markedly different results (Fig. 7-8, Fig. 10-11). The
757 overaccumulation of PRPL4 promoted abiotic stress responses and protein homeostasis such as
758 "response to hydrogen peroxide", "response to high light intensity", "response to heat", "response to
759 oxidative stress" and "protein folding" (Fig. 8 C). In particular, transcription factors involved in stress
760 responses such as *DREB2A*, *DREB2C* and *WRKY26* (Sakuma *et al.*, 2006; Chen *et al.*, 2010; Li *et al.*,
761 2011), were found to be upregulated, together with proteins directly involved in proteostasis
762 maintenance, such as small HSPs, CLPB1 cytosolic unfoldase and the co-chaperone HOP3 (Sun *et*
763 *al.*, 2001; Mishra & Grover, 2016; Fernández-Bautista *et al.*, 2017; Toribio *et al.*, 2020). Interestingly,
764 *GOLS1* gene coding for a key enzyme of raffinose family sugar synthesis, shown to enhance plant
765 resistance to oxidative damage, was also up-regulated (Panikulangara *et al.*, 2004; Nishizawa *et al.*,
766 2008). These findings together with the increased accumulation of CLPB3, HSP90-1 and HSC70-4
767 proteins over time (see Fig. S7), corroborate the hypothesis that PRPL4 over-accumulation
768 contributes to generate pressure on the plastid folding machinery that, in turns, activates retrograde
769 signalling pathways aimed at triggering a chloroplast-related UPR. It can be envisaged that the
770 activated cpUPR contributes to the limited increase of PRPL4 protein abundance in Arabidopsis
771 chloroplasts, i.e., two folds higher upon 24 HAI with respect to 0 HAI, despite the 30-fold increase
772 of PRPL4 transcripts (Fig. 4 A and C).

773 Taken together these observations highlight the activation of different nuclear and cellular
774 responses upon up-regulation of *PRPS1* and *PRPL4* gene expression and the consequent alteration of
775 plastid protein homeostasis. Whereas the *PRPS1*-related response mainly relies on chloroplast
776 breakdown with degradation and loss of chloroplast proteins, nucleic acids, pigments, lipids, and
777 polysaccharides, aimed to promote the remobilization of resources, such as carbon and nitrogen, in
778 favour of the anticipated reproductive phase, i.e. an escape strategy from a stress condition, the

779 *PRPL4*-related response consists in the activation of a stress pathway, compatible with the chloroplast
780 UPR.

781 **Author Contributions**

782 L.T. and P.P. designed the study. N.J., S.F., and L.T. took care of the isolation and the phenotypical
783 characterization of mutants and transgenic lines. L.T. and N.J. performed the molecular
784 characterization of plant lines and bacterial strains. S.M. and N.J. carried out the characterization of
785 embryo-lethal mutants. A.C., N.J. and F.Z. performed analyses of transcriptomic data. G.D., E.C.,
786 M.M. and C.V. performed proteomic analyses. L.T., N.J., F.B. and P.P. drafted the manuscript. L.T.,
787 N.J. and P.P. coordinated the study and took care of the final version of the manuscript. All authors
788 have read and agreed to the published version of the manuscript.

789 **Data Availability**

790 The data that support the findings of this study are openly available in Gene Expression Omnibus at
791 https://www.ncbi.nlm.nih.gov/geo/, reference number GSE205271, and in ProteomeXchange
792 Consortium at http://www.proteomexchange.org/, reference number PXD034479.

793 **Funding**

794 This research was funded by MUR—Ministero dell'Università e della Ricerca, grant number PRIN-
795 2017 2017FBS8YN.

796 **Acknowledgments**

797 We are grateful to James Friel for critical reading of the manuscript and English editing. We are
798 thankful to Lucio Conti and Cecilia Zumajo for fruitful discussion on flowering time regulatory
799 mechanisms. We are also grateful to Norma Lattuada, Roberto Ferrari, Valerio Paravicini and Mario
800 Beretta for excellent technical assistance. NoLimits platform at University of Milano is acknowledged
801 for TEM analyses.

802 **Conflicts of interest**

803 The authors declare no conflicts of interest.

804
805
806
807

Figure Legend

Figure 1 – Molecular description of *prps1-2* allele and the corresponding embryo-lethal phenotype. A) Schematic representation of *PRPS1* gene. Exons are indicated as numbered white boxes, and introns as black lines. Positions of start and stop codons with respect to the transcription initiation site, as well as the CRISPR/Cas9-induced deletion (*prps1-2*), are indicated. The *PRPS1* reading frame and corresponding amino acids in wild-type and *prps1-2* mutant are also reported. B) Sequencing electropherogram showing the single nucleotide deletion (coding strand) in *prps1-2* hetero- and homozygous mutants with respect to Col-0. The red arrowhead indicates the position of the CRISPR/Cas9-induced deletion. "N" readings in *PRPS1/prps1-2* lines results from double peaks, generated by Cas9-induced deletion in one of the two homologous chromosomes. C) Morphological characteristics of developing seeds in siliques at 10 Days After Fertilization (DAF) of Col-0, heterozygous *PRPS1/prps1-2* and *prps1-2* complemented with *pPRPS1::PRPS1* genomic locus. Around one quarter of white seeds are clearly distinguishable among the green seeds of *PRPS1/prps1-2* siliques. Bars = 2 mm. D) Cleared whole mount of Col-0, heterozygous *PRPS1/prps1-2* and *prps1-2 pPRPS1::PRPS1* complemented seeds containing embryos at the globular stage (3 DAF). Bars = 20 µm.

Figure 2 – Visible and molecular phenotypes of plantlets carrying altered amount of PRPS1 and PRPL4 proteins. A) Visible phenotypes and photosynthetic efficiency (F_V/F_M) of 16 Days After Sowing (DAS) plantlets grown on MS medium devoid (- DEX) or supplemented (+ DEX) with 2 µM dexamethasone. On the left (bright field), the visible phenotypes shown by Col-0, the knock-down *prps1-1* mutant, *oePRPS1* and *oePRPL4* constitutive over-expressing lines, *indPRPL4* and *indPRPS1* inducible lines. On the right panel (F_V/F_M), the photosynthetic efficiency of each genotype is shown both as false colour imaging and average values ± standard deviations. Statistical significance calculated via Student's t-test (*** indicates $P < 0.001$; N.S. not significant). Scale bar = 1 cm. B) Immunoblots of total protein extracts from Col-0, *prps1-1*, *oePRSP1*, *indPRPS1*, *oePRPL4* and *indPRPL4* 16 DAS plants grown on MS medium devoid (- DEX) or supplemented (+ DEX) with 2 µM dexamethasone. PRPS1 and PRPL4 specific antibodies were used for immuno-decoration. Coomassie Brilliant Blue (C.B.B.) stained gels are shown as loading control. Numbers show the relative protein abundance with respect to Col-0 (indicated as 100). Standard deviation was below ± 15%. One filter out of three biological replicates is shown. C) Relative expression values of *PRPS1* and *PRPL4* genes determined by qRT-PCR analyses of total RNA extracted from Col-0, *prps1-1*, *oePRSP1*, *indPRPS1*, *oePRPL4* and *indPRPL4* 16 DAS plants grown on MS medium devoid (- DEX)

or supplemented (+ DEX) with 2 µM dexamethasone. Results of one out of three biological replicates are shown. Error bars indicate standard deviations of three technical replicates.

Figure 3 - TEM micrographs of chloroplasts in mesophyll cells of Col-0 (A) control, *prps1-1* (B), *indPRPS1* (C, G, H, I, J), *indPRPL4* (D, E), *oePRPL4* (F) and *oePRPS1* (K, L) leaves obtained from 16 DAS plantlets grown on MS medium supplemented, or not, with DEX. The young portion of leaves, proximal to the petiole, showing the yellow to pale-green phenotype in *oePRPS1* and *indPRPS1* lines, was used for the analyses. S: starch granules; White arrowhead: thylakoid membranes; BV budding vesicles; P: Plastoglobules.

Figure 4 – Molecular features of *indPRPS1* and *indPRPL4* lines upon DEX-induced gene expression. A) Relative expression values of *PRPS1* and *PRPL4* genes determined by qRT-PCR analyses of total RNA extracted from *indPRPS1* (circles, blue) and *indPRPL4* (squares, green) leaf discs sampled at 0, 3, 6 and 24 Hours After Infiltration (HAI) with 2 µM dexamethasone (DEX). Data from one out of three biological replicates are shown. Error bars indicate standard deviations of three technical replicates. B) Immunoblots of total protein extracts from *indPRPS1* leaf discs sampled at 0, 3, 6 and 24 HAI with 2 µM DEX. Filters were incubated with antibodies raised against PRPS1, PRPL4 and PRPS5 plastid ribosomal proteins. C.B.B.-stained gels are shown as loading control. Numbers show the relative protein abundance with respect to 0 HAI (indicated as 100). Data from one out of three biological replicates are shown. Standard deviation was below 15%. C) Immunoblots of total protein extracts from *indPRPS4* leaf discs, sampled and analysed as in B, used as control. D) Total protein extracts from Col-0 and *indPRPS1* leaf discs previously incubated in DEX-containing MS medium for 6 hours and then infiltrated with ^{35}S-Methionine in the presence of cycloheximide, an inhibitor of cytosolic protein synthesis. The leaf proteins were sampled 15 and 30 minutes after labelling (MAL). RbcL and D1/D2 proteins signals are indicated. The ponceau-stained filter is shown as loading control. E) *indPRPS1* ± DEX (6 HAI) leaf material was subjected to sucrose gradient fractionation aimed to isolate PRPS1-contaning complexes. Filters were immuno-decorated with PRPS1 antibody to show the accumulation of PRPS1 in Low Molecular Weight (LMW) and High Molecular Weight (HMW) fractions. C.B.B.-stained gels are shown as loading control. F) Quantification of PRPS1 accumulation in LMW (1-5) and HMW (6-9) fractions as evaluated by Image Lab software on representative blots.

873 **Figure 5 –** Comparison of PRPS1 and S1 protein activities in *E. coli* cells. A) Schematic
874 representation of S1 and PRPS1 proteins. S1 domains are depicted as pink boxes, while the
875 chloroplast transit peptide (cTP) of PRPS1 protein as green box. Numbers indicate the position of
876 amino acid residues. Domain predictions are based on InterPro online tool
877 (https://www.ebi.ac.uk/interpro/). B) OD_{600} measurements of *E. coli indrpsA* (white symbols) and
878 *indPRPS1* (blue symbols) strains grown under Depletion (0.4% glucose; squares), Complementation
879 (0.4% glucose + 0.01 mM IPTG; triangles) or Overexpression (1% arabinose + 1 mM IPTG; circles)
880 conditions. Strains were sampled at 0, 45, 90, 135, 180 and 225 Minutes After Induction (MAI). Data
881 from one out of three biological replicates are reported. C) Immunoblots of total protein extracts from
882 *indrpsA* and *indPRPS1 E. coli* strains grown as described above sampled at 0, 45, 90, 135, 180 and
883 225 MAI, using S1 and PRPS1 specific antibodies. C.B.B.-stained gels are added as loading controls.
884 Numbers show the relative protein abundance with respect to 0 MAI. Data from one out of three
885 biological replicates are shown. Standard deviation was below 15%.

886 **Figure 6 –** PRPS1 protein accumulation and the stromal CLP protease. A) Immunoblots of total
887 protein extracts from *indPRPS1* leaf discs sampled at 0, 3, 6 and 24 HAI with 2 μM dexamethasone
888 alone (+ DEX) or supplemented with 550 μM lincomycin (+ DEX + LIN). Filters were incubated
889 with antibodies raised against PRPS1 protein. C.B.B.-stained gels are shown as loading control.
890 Numbers below the immunoblots show the relative protein abundance with respect to 0 HAI
891 (indicated as 100). Data are derived from one out of three biological replicates. Standard deviation
892 was below 15%. B) Visible phenotypes and photosynthetic efficiency (Fv/F_M) of 16 Days After
893 Sowing (DAS) seedlings grown on soil. On top (bright field) panel, visible phenotypes of Col-0 and
894 *prps1-1*, *prpl11-1*, *clpc1-1*, *clpd-1*, *prps1-1 prpl11-1*, *prps1-1 clpc1-1* and *prps1-1 clpd-1* mutants are
895 shown. On the bottom panel (Fv/F_M), the photosynthetic efficiency of each genotype is shown both
896 as false colour imaging and average values ± standard deviations. Scale bar = 1 cm C) Immunoblot
897 of total protein extracts from Col-0 and *prps1-1*, *prpl11-1*, *clpc1-1*, *clpd-1*, *prps1-1 prpl11-1*, *prps1-*
898 *1 clpc1-1* and *prps1-1 clpd-1* mutants obtained by using a PRPS1 specific antibody. C.B.B.-stained
899 gels are shown as loading control. Numbers below the immunoblot show the relative protein
900 abundance with respect to Col-0. Standard deviation was below 15%.

901

902 **Figure 7 –** Comparison of RNAseq transcriptomes from *indPRPS1* and *indPRPL4* lines infiltrated or
903 not with DEX. A) Venn diagram showing the number of DEGs found in *indPRPS1* and *indPRPL4*
904 upon induction. B) Venn diagram showing the distribution of DEGs resulted from the comparison of
905 *indPRPS1*UP, *indPRPL4*UP, *indPRPS1*DOWN and *indPRPL4*DOWN lists. Unique DEGs in each
906 group are in bold. Group A: Unique up-regulated DEGs found in *indPRPS1*; Group B: Unique up-

regulated DEGs found in *indPRPL4*; Group C: Common up-regulated DEGs found in *indPRPS1* and *indPRPL4*; Group D: Unique down-regulated DEGs found in *indPRPS1*; Group E: Unique down-regulated DEGs found in *indPRPL4*; Group F: Common down-regulated DEGs found in *indPRPS1* and *indPRPL4*; Group G: up-regulated DEGs found in *indPRPL4* but down-regulated in *indPRPS1*.

Figure 8 – Analysis of the biological functions activated or repressed by the short-term overexpression of *PRPS1* and *PRPL4* genes. Significantly enriched GO terms identified through agriGO v2.0 and REVIGO online tools retrieved from A) unique up-regulated DEGs found in *indPRPS1*; B) unique down-regulated DEGs found in *indPRPS1;* C) unique up-regulated DEGs found in *indPRPL4*.

Figure 9 – Flowering time determination in Col-0, *prps1-1*, *oePRPS1*, *indPRPS1* (± DEX) and *indPRPL4* (± DEX) lines. A) Pictures of representative plants at bolting grown on soil in long day conditions. B) Average numbers ± standard deviations of leaves at bolting observed in Col-0, *prps1-1* and *oePRPS1* plants grown on soil in long day conditions. C) Average numbers ± standard deviations of leaves at bolting observed in Col-0, *prps1-1* and *oePRPS1* plants grown on soil in short day conditions. D) Average numbers ± standard deviations of leaves at bolting observed in Col-0, *oePRSP1*, *indPRPS1* and *indPRPL4* plants grown on MS medium devoid (- DEX) or supplemented (+ DEX) with 2 µM dexamethasone in long day conditions. Statistical significance was calculated via Student's t-test (*** indicates $P < 0.001$).

Figure 10 – Comparison of proteome from *indPRPS1* and *indPRPL4* lines infiltrated or not with DEX. A) Venn diagram showing the number of DAPs found in *indPRPS1* and *indPRPL4* upon induction. B) Venn diagram showing the distribution of DAPs resulted from the comparison of *indPRPS1*UP, *indPRPL4*UP, *indPRPS1*DOWN and *indPRPL4*DOWN lists.

Figure 11 – Protein categorization based on Biological Process GO terms of DAPs found in *indPRPS1* (A) and *indPRPL4* (C) samples and based on Cellular Content GO terms found of *indPRPS1* (B) and *indPRPL4* (D) samples. Blue and red bars correspond to proteins that were up or down accumulated, respectively.

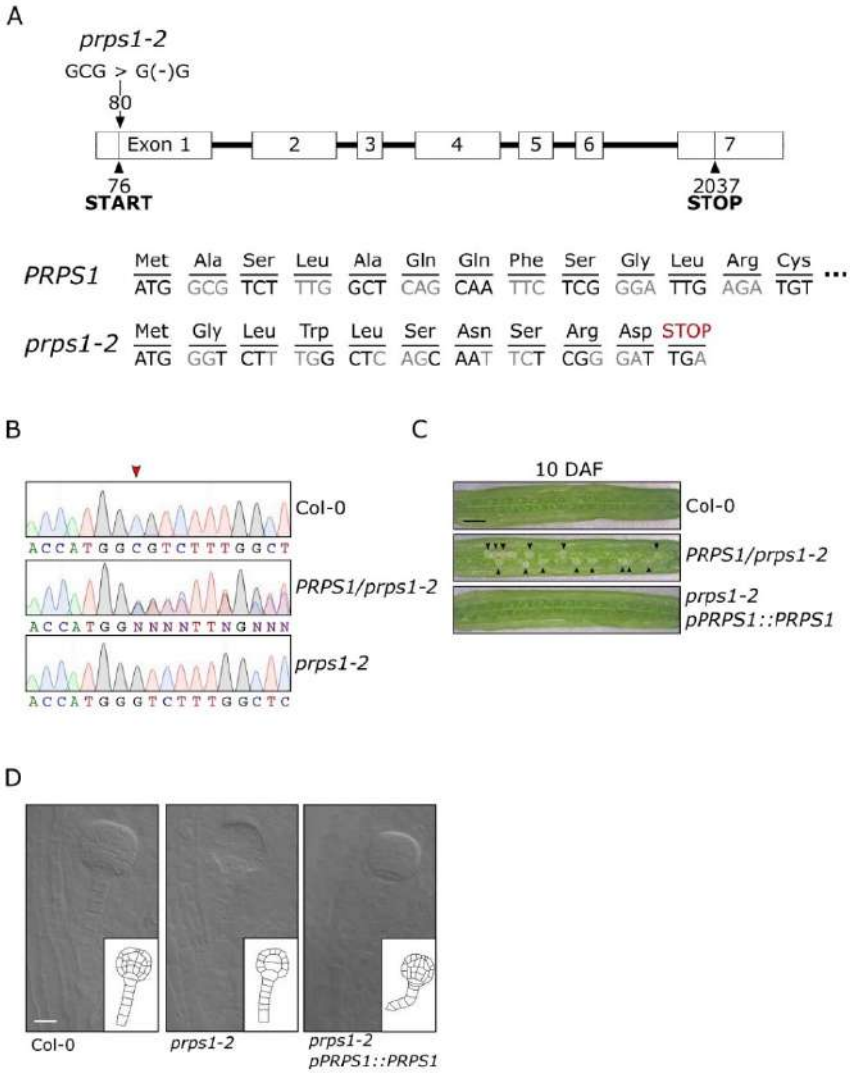

Figure 1

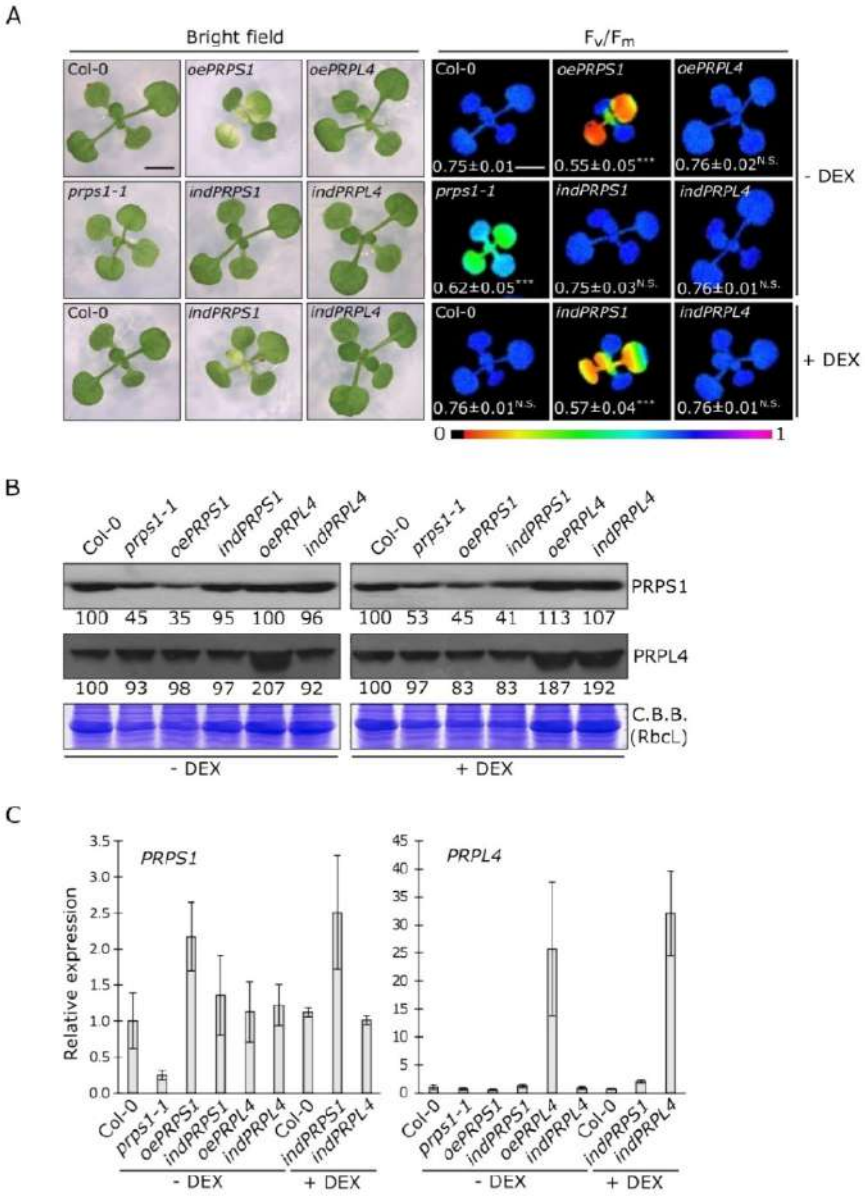

940

941 **Figure 2**

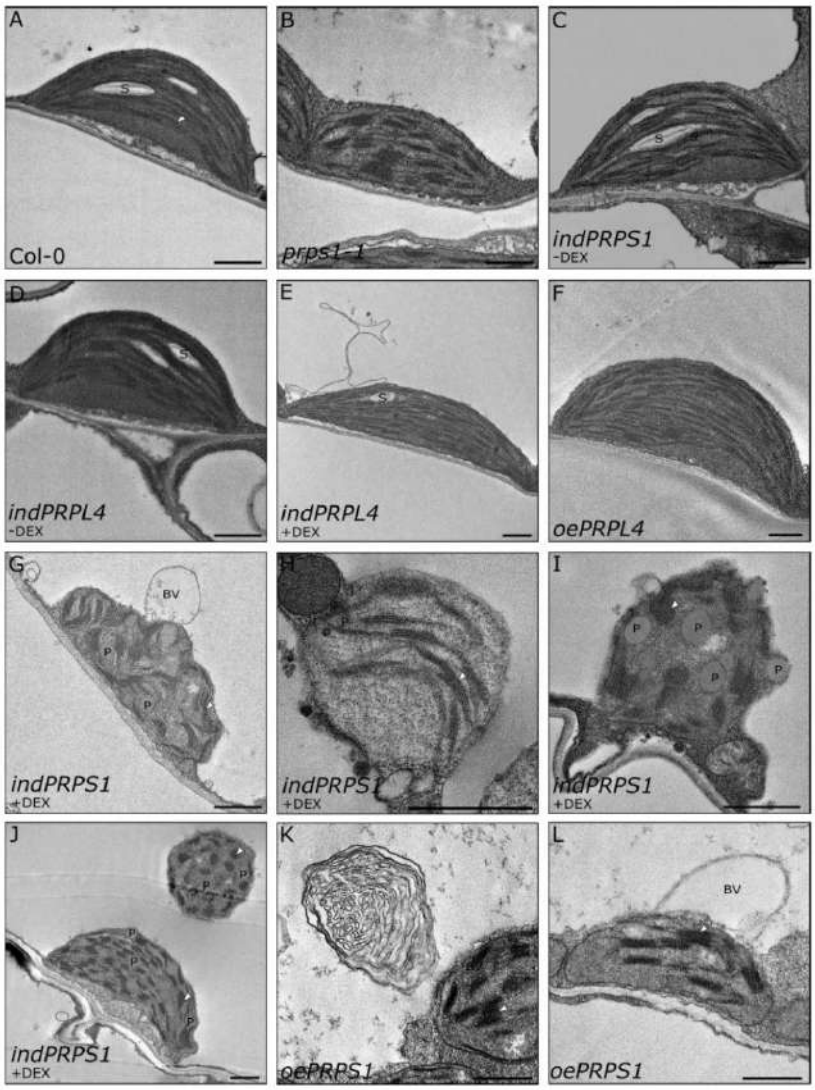

Figure 3

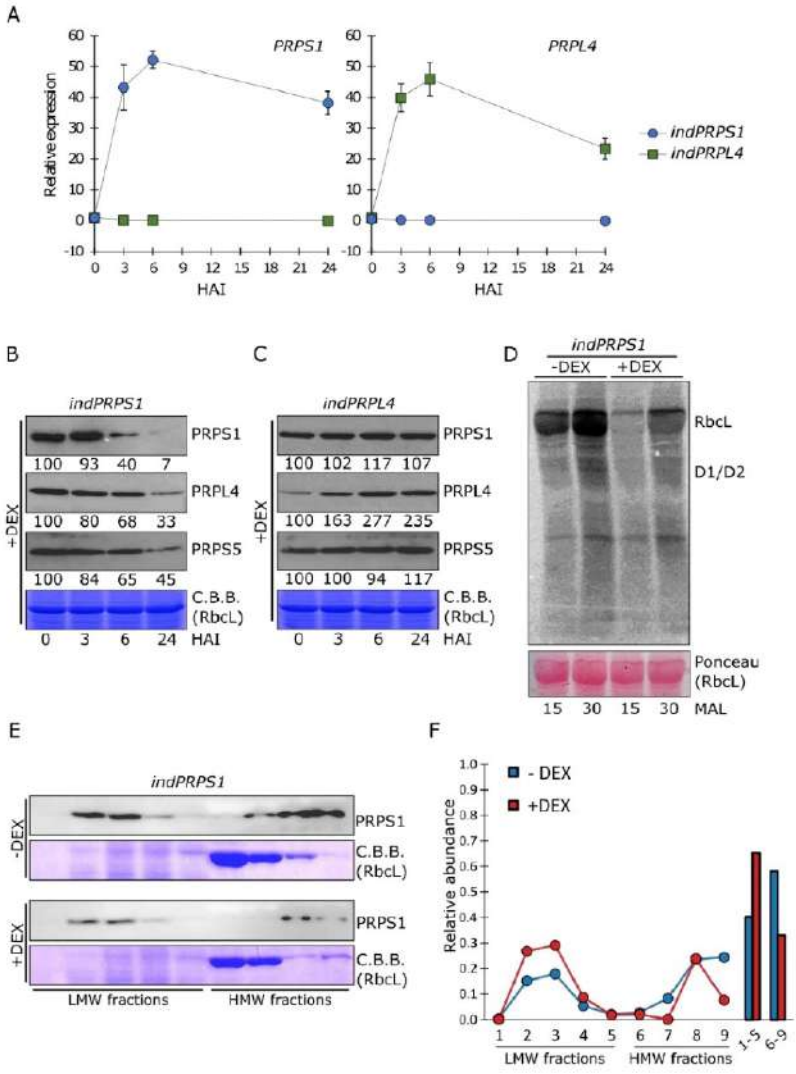

Figure 4

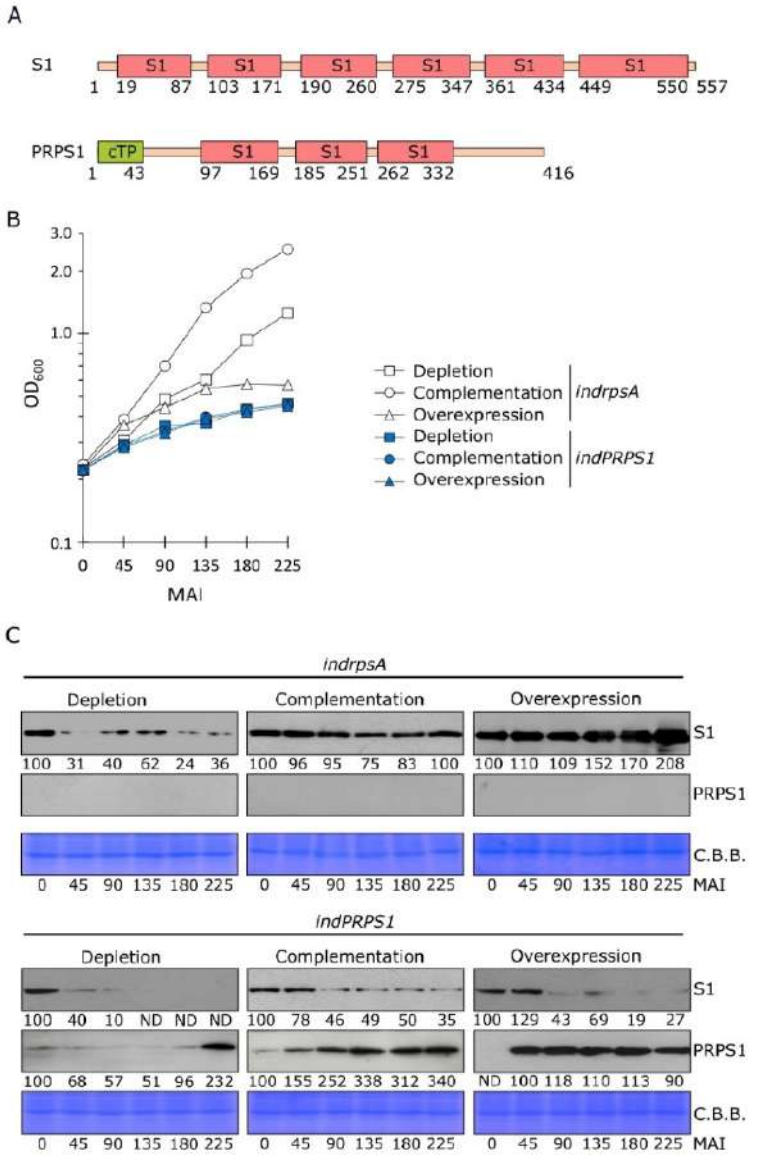

Figure 5

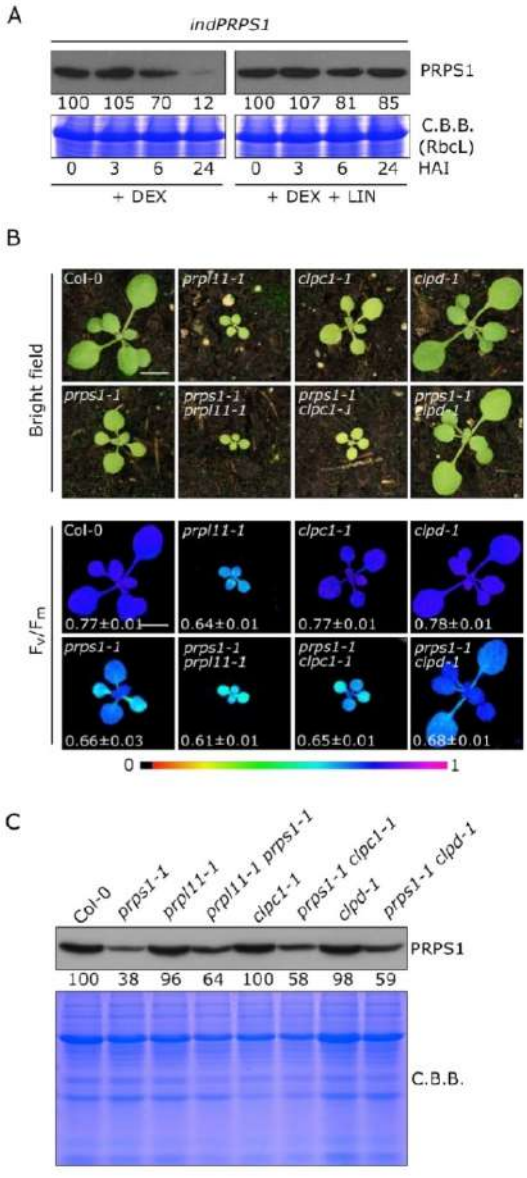

948

949 **Figure 6**

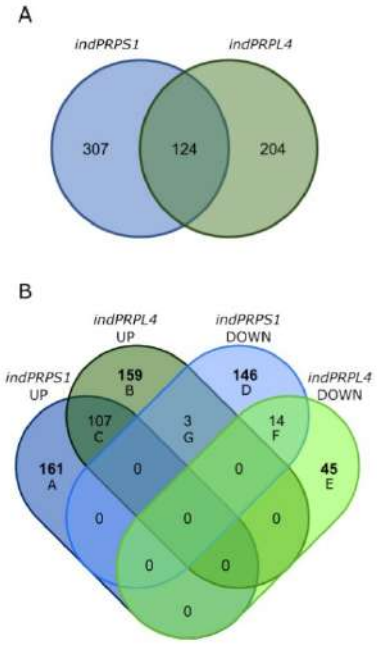

Figure 7

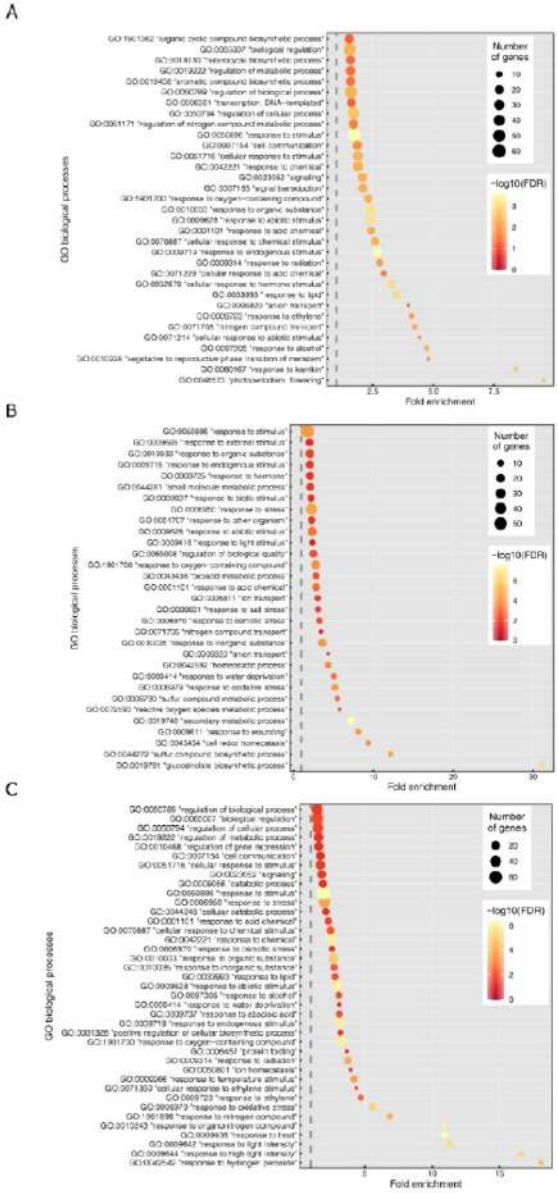

Figure 8

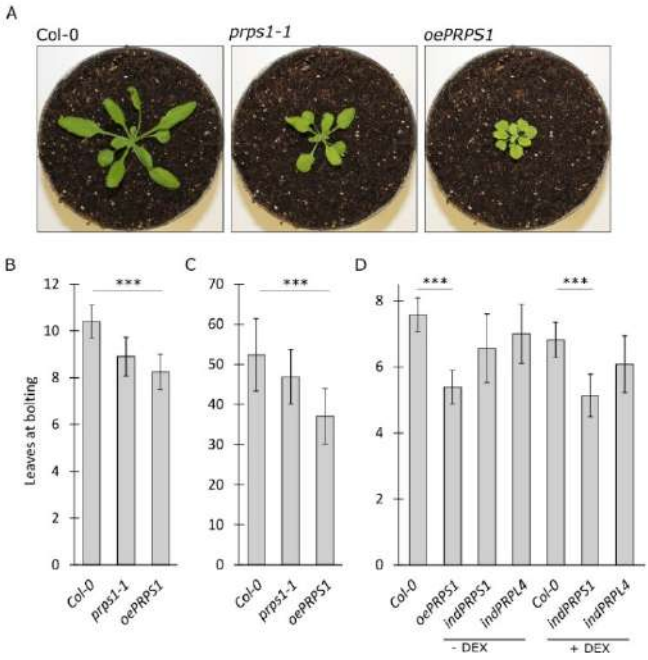

Figure 9

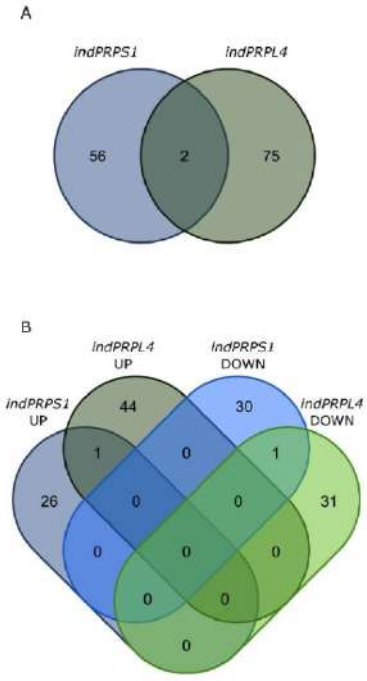

Figure 10

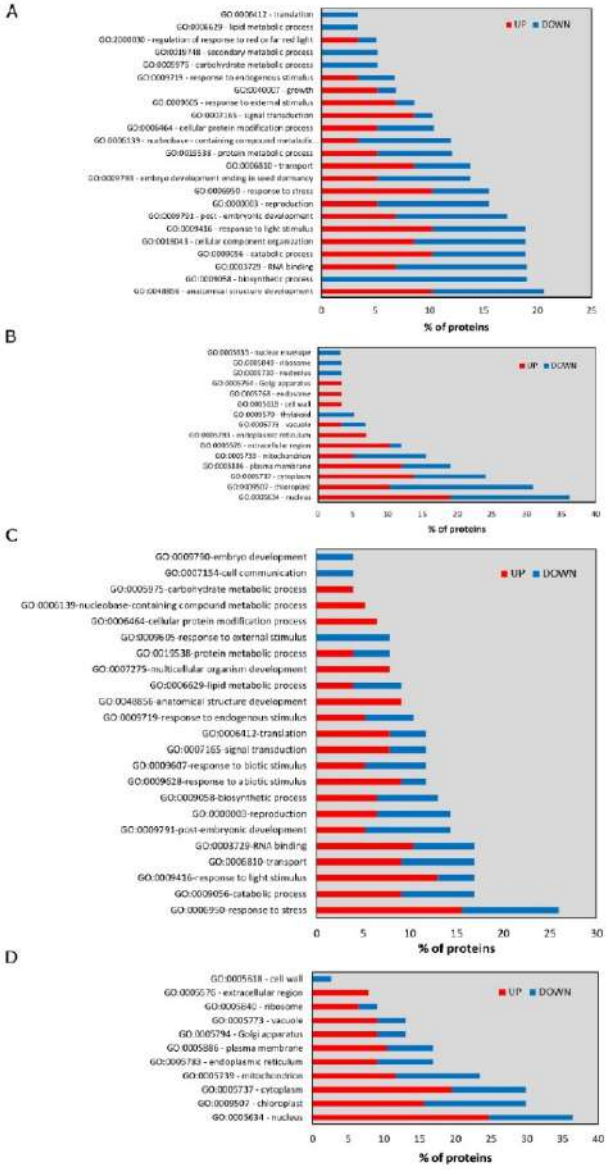

Figure 11

961 ## References

962 **Ahmed T, Yin Z, Bhushan S. 2016**. Cryo-EM structure of the large subunit of the spinach
963 chloroplast ribosome. *Scientific Reports* **6**: 1–13.

964 **Arcus V. 2002**. OB-fold domains: A snapshot of the evolution of sequence, structure and function.
965 *Current Opinion in Structural Biology* **12**: 794–801.

966 **Asakura Y, Barkan A. 2006**. Arabidopsis orthologs of maize chloroplast splicing factors promote
967 splicing of orthologous and species-specific group II introns. *Plant Physiology* **142**: 1656–1663.

968 **Barkan A. 1998**. Approaches to investigating nuclear genes that function in chloroplast biogenesis
969 in land plants. *Methods in Enzymology* **297**: 38–57.

970 **Beckert B, Turk M, Czech A, Berninghausen O, Beckmann R, Ignatova Z, Plitzko JM, Wilson**
971 **DN. 2018**. Structure of a hibernating 100S ribosome reveals an inactive conformation of the
972 ribosomal protein S1. *Nature Microbiology* **3**: 1115–1121.

973 **Bieri P, Leibundgut M, Saurer M, Boehringer D, Ban N. 2017**. The complete structure of the
974 chloroplast 70S ribosome in complex with translation factor pY. *The EMBO Journal* **36**: 475–486.

975 **Bolouri Moghaddam MR, Van den Ende W. 2013**. Sugars, the clock and transition to flowering.
976 *Frontiers in Plant Science* **4**.

977 **Boni I V., Artamonova VS, Dreyfus M. 2000**. The last RNA-binding repeat of the Escherichia coli
978 ribosomal protein S1 is specifically involved in autogenous control. *Journal of Bacteriology* **182**:
979 5872–5879.

980 **Briani F, Curti S, Rossi F, Carzaniga T, Mauri P, Dehò G. 2008**. Polynucleotide phosphorylase
981 hinders mRNA degradation upon ribosomal protein S1 overexpression in Escherichia coli. *RNA* **14**:
982 2417–2429.

983 **Bryant N, Lloyd J, Sweeney C, Myouga F, Meinke D. 2011**. Identification of nuclear genes
984 encoding chloroplast-localized proteins required for embryo development in Arabidopsis. *Plant*
985 *Physiology* **155**: 1678–1689.

986 **Bubunenko MG, Schmidt J, Subramanian AR. 1994**. Protein substitution in chloroplast ribosome
987 evolution a eukaryotic cytosolic protein has replaced its organelle homologue (L23) in spinach.
988 *Journal of Molecular Biology* **240**: 28–41.

989 **Bycroft M, Hubbard TJP, Proctor M, Freund SMV, Murzin AG. 1997**. The solution structure of
990 the S1 RNA binding domain: a member of an ancient nucleic acid-binding fold. *Cell* **88**: 235–242.

991 **Byrgazov K, Grishkovskaya I, Arenz S, Coudevylle N, Temmel H, Wilson DN, Djinovic-Carugo**
992 **K, Moll I. 2015**. Structural basis for the interaction of protein S1 with the Escherichia coli ribosome.
993 *Nucleic Acids Research* **43**: 661–673.

994 **Chalupska D, Lee HY, Faris JD, Evrard A, Chalhoub B, Haselkorn R, Gornicki P. 2008**. Acc
995 homoeoloci and the evolution of wheat genomes. *Proceedings of the National Academy of Sciences*
996 *of the United States of America* **105**: 9691–9696.

997 **Chen H, Hwang JE, Lim CJ, Kim DY, Lee SY, Lim CO. 2010**. Arabidopsis DREB2C functions
998 as a transcriptional activator of HsfA3 during the heat stress response. *Biochemical and Biophysical*
999 *Research Communications* **401**: 238–244.

1000 **Cifuentes-Goches JC, Hernández-Ancheyta L, Guarneros G, Oviedo N, Hernández-Sánchez J.**
1001 **2019**. Domains two and three of Escherichia coli ribosomal S1 protein confers 30S subunits a high
1002 affinity for downstream A/U-rich mRNAs. *Journal of Biochemistry* **166**: 29–40.

1003 **Colombo M, Tadini L, Peracchio C, Ferrari R, Pesaresi P. 2016**. GUN1, a Jack-Of-All-Trades in
1004 Chloroplast Protein Homeostasis and Signaling. *Frontiers in Plant Science* **7**.

1005 **Czechowski T, Stitt M, Altmann T, Udvardi MK, Scheible WR. 2005**. Genome-wide
1006 identification and testing of superior reference genes for transcript normalization in arabidopsis. *Plant*
1007 *Physiology* **139**: 5–17.

1008 **Delvillani F, Papiani G, Dehó G, Briani F. 2011**. S1 ribosomal protein and the interplay between
1009 translation and mRNA decay. *Nucleic Acids Research* **39**: 7702–7715.

1010 **Duval M, Korepanov A, Fuchsbauer O, Fechter P, Haller A, Fabbretti A, Choulier L, Micura**
1011 **R, Klaholz BP, Romby P, *et al.* 2013**. Escherichia coli Ribosomal Protein S1 Unfolds Structured
1012 mRNAs Onto the Ribosome for Active Translation Initiation. *PLoS Biology* **11**: e1001731.

1013 **Fernández-Bautista N, Fernández-Calvino L, Muñoz A, Castellano MM. 2017**. HOP3, a member
1014 of the HOP family in Arabidopsis, interacts with BiP and plays a major role in the ER stress response.
1015 *Plant Cell and Environment* **40**: 1341–1355.

1016 **Franzetti B, Carol P, Maches R. 1992**. Characterization and RNA-binding properties of a
1017 chloroplast S1-like ribosomal protein. *Journal of Biological Chemistry* **267**: 19075–19081.

1018 **Freytes SN, Canelo M, Cerdán PD. 2021**. Regulation of Flowering Time: When and Where?
1019 *Current Opinion in Plant Biology* **63**.

1020 **Giorginis S, Subramanian AR. 1980**. The major ribosome binding site of Escherichia coli ribosomal

protein S1 is located in its N-terminal segment. *Journal of Molecular Biology* **141**: 393–408.

Graf M, Arenz S, Huter P, Dönhöfer A, Nováček J, Wilson DN. 2017. Cryo-EM structure of the spinach chloroplast ribosome reveals the location of plastid-specific ribosomal proteins and extensions. *Nucleic Acids Research* **45**: 2887–2896.

Hajnsdorf E, Boni I V. 2012. Multiple activities of RNA-binding proteins S1 and Hfq. *Biochimie* **94**: 1544–1553.

Hess WR, Hoch B, Zeltz P, Hübschmann T, Kössel H, Börner T. 1994. Inefficient rpl2 splicing in barley mutants with ribosome-deficient plastids. *Plant Cell* **6**: 1455–1465.

Hirose T, Sugiura M. 2004. Multiple elements required for translation of plastid atpB mRNA lacking the Shine-Dalgarno sequence. *Nucleic Acids Research* **32**: 3503–3510.

Hsieh HL, Okamoto H, Wang M, Ang LH, Matsui M, Goodman H, Deng XW. 2000. FIN219, an auxin-regulated gene, defines a link between phytochrome A and the downstream regulator COP1 in light control of Arabidopsis development. *Genes and Development* **14**: 1958–1970.

Jeran N, Rotasperti L, Frabetti G, Calabritto A, Pesaresi P, Tadini L. 2021. The PUB4 E3 ubiquitin ligase is responsible for the variegated phenotype observed upon alteration of chloroplast protein homeostasis in arabidopsis cotyledons. *Genes* **12**: 1387.

Kalapos MP, Paulus H, Sarkar N. 1997. Identification of ribosomal protein S1 as a poly(A) binding protein in Escherichia coli. *Biochimie* **79**: 493–502.

Karim S, Holmström KO, Mandal A, Dahl P, Hohmann S, Brader G, Palva ET, Pirhonen M. 2007. AtPTR3, a wound-induced peptide transporter needed for defence against virulent bacterial pathogens in Arabidopsis. *Planta* **225**: 1431–1445.

Kazan K, Lyons R. 2016. The link between flowering time and stress tolerance. *Journal of Experimental Botany* **67**: 47–60.

Kitakawa M, Isono K. 1982. An amber mutation in the gene rpsA for ribosomal protein S1 in Escherichia coli. *Molecular and General Genetics MGG* **185**: 445–447.

Kmiec B, Teixeira PF, Glaser E. 2014. Shredding the signal: Targeting peptide degradation in mitochondria and chloroplasts. *Trends in Plant Science* **19**: 771–778.

Lakhssassi N, Doblas VG, Rosado A, del Valle AE, Posé D, Jimenez AJ, Castillo AG, Valpuesta V, Borsani O, Botella MA. 2012. The Arabidopsis TETRATRICOPEPTIDE THIOREDOXIN-LIKE gene family is required for osmotic stress tolerance and male sporogenesis. *Plant Physiology*

1051 **158**: 1252–1266.

1052 **Lemke MD, Fisher KE, Kozlowska MA, Tano DW, Woodson JD. 2021**. The core autophagy
1053 machinery is not required for chloroplast singlet oxygen-mediated cell death in the Arabidopsis
1054 thaliana plastid ferrochelatase two mutant. *BMC Plant Biology* **21**: 1–20.

1055 **Li B, Dewey CN. 2011**. RSEM: Accurate transcript quantification from RNA-Seq data with or
1056 without a reference genome. *BMC Bioinformatics* **12**: 1–16.

1057 **Li S, Fu Q, Chen L, Huang W, Yu D. 2011**. Arabidopsis thaliana WRKY25, WRKY26, and
1058 WRKY33 coordinate induction of plant thermotolerance. *Planta* **233**: 1237–1252.

1059 **Liu W, Liu Z, Mo Z, Guo S, Liu Y, Xie Q. 2021**. ATG8-Interacting Motif: Evolution and Function
1060 in Selective Autophagy of Targeting Biological Processes. *Frontiers in Plant Science* **12**: 2671.

1061 **Llamas E, Pulido P, Rodriguez-Concepcion M. 2017**. Interference with plastome gene expression
1062 and Clp protease activity in Arabidopsis triggers a chloroplast unfolded protein response to restore
1063 protein homeostasis. *PLoS Genetics* **13**: 1–28.

1064 **Mache R. 1990**. Chloroplast ribosomal proteins and their genes. *Plant Science* **72**: 1–12.

1065 **Merendino L, Falciatore A, Rochaix JD. 2003**. Expression and RNA binding properties of the
1066 chloroplast ribosomal protein S1 from Chlamydomonas reinhardtii. *Plant Molecular Biology* **53**:
1067 371–382.

1068 **Mi H, Ebert D, Muruganujan A, Mills C, Albou LP, Mushayamaha T, Thomas PD. 2021**.
1069 PANTHER version 16: A revised family classification, tree-based classification tool, enhancer
1070 regions and extensive API. *Nucleic Acids Research* **49**: D394–D403.

1071 **Michaeli S, Honig A, Levanony H, Peled-Zehavi H, Galili G. 2014**. Arabidopsis ATG8-
1072 INTERACTING PROTEIN1 is involved in autophagy-dependent vesicular trafficking of plastid
1073 proteins to the vacuole. *The Plant Cell* **26**: 4084–4101.

1074 **Mishra RC, Grover A. 2016**. ClpB/Hsp100 proteins and heat stress tolerance in plants. *Critical*
1075 *Reviews in Biotechnology* **36**: 862–874.

1076 **Murzin AG. 1993**. OB(oligonucleotide/oligosaccharide binding)-fold: Common structural and
1077 functional solution for non-homologous sequences. *EMBO Journal* **12**: 861–867.

1078 **Nagashima Y, Ohshiro K, Iwase A, Nakata MT, Maekawa S, Horiguchi G. 2020**. The bRPS6-
1079 family protein RFC3 prevents interference by the splicing factor CFM3b during plastid rRNA
1080 biogenesis in Arabidopsis thaliana. *Plants* **9**.

Nishizawa A, Yabuta Y, Shigeoka S. 2008. Galactinol and raffinose constitute a novel function to protect plants from oxidative damage. *Plant Physiology* **147**: 1251–1263.

Nishizawa A, Yabuta Y, Yoshida E, Maruta T, Yoshimura K, Shigeoka S. 2006. Arabidopsis heat shock transcription factor A2 as a key regulator in response to several types of environmental stress. *Plant Journal* **48**: 535–547.

Ostheimer GJ, Williams-Carrier R, Belcher S, Osborne E, Gierke J, Barkan A. 2003. Group II intron splicing factors derived by diversification of an ancient RNA-binding domain. *EMBO Journal* **22**: 3919–3929.

Paieri F, Tadini L, Manavski N, Kleine T, Ferrari R, Morandini P, Pesaresi P, Meurer J, Leister D. 2018. The DEAD-box RNA helicase RH50 is a 23S-4.5S rRNA maturation factor that functionally overlaps with the plastid signaling factor GUN1. *Plant Physiology* **176**: 634–648.

Panikulangara TJ, Eggers-Schumacher G, Wunderlich M, Stransky H, Schöffl F. 2004. Galactinol synthase1. A novel heat shock factor target gene responsible for heat-induced synthesis of raffinose family oligosaccharides in arabidopsis. *Plant Physiology* **136**: 3148–3158.

Paradiso A, Domingo G, Blanco E, Buscaglia A, Fortunato S, Marsoni M, Scarcia P, Caretto S, Vannini C, de Pinto MC. 2020. Cyclic AMP mediates heat stress response by the control of redox homeostasis and ubiquitin-proteasome system. *Plant Cell and Environment* **43**: 2727–2742.

Pérez-Martín M, Pérez-Pérez ME, Lemaire SD, Crespo JL. 2014. Oxidative stress contributes to autophagy induction in response to endoplasmic reticulum stress in chlamydomonas reinhardtii. *Plant Physiology* **166**: 997–1008.

Perez-Riverol Y, Csordas A, Bai J, Bernal-Llinares M, Hewapathirana S, Kundu DJ, Inuganti A, Griss J, Mayer G, Eisenacher M, *et al.* 2019. The PRIDE database and related tools and resources in 2019: Improving support for quantification data. *Nucleic Acids Research* **47**: D442–D450.

Pesaresi P, Varotto C, Meurer J, Jahns P, Salamini F, Leister D. 2001. Knock-out of the plastid ribosomal protein L11 in Arabidopsis: Effects on mRNA translation and photosynthesis. *The Plant Journal* **27**: 179–189.

Phee BK, Kim J Il, Shin DH, Yoo J, Park KJ, Han YJ, Kwon YK, Cho MH, Jeon JS, Bhoo SH, *et al.* 2008. A novel protein phosphatase indirectly regulates phytochrome-interacting factor 3 via phytochrome. *Biochemical Journal* **415**: 247–255.

Pulido P, Llamas E, Llorente B, Ventura S, Wright LP, Rodríguez-Concepción M. 2016. Specific Hsp100 Chaperones Determine the Fate of the First Enzyme of the Plastidial Isoprenoid Pathway for Either Refolding or Degradation by the Stromal Clp Protease in Arabidopsis. *PLoS Genetics* **12**.

Ramundo S, Casero D, Muhlhaus T, Hemme D, Sommer F, Crevecoeur M, Rahire M, Schroda M, Rusch J, Goodenough U, *et al.* 2014. Conditional Depletion of the Chlamydomonas Chloroplast ClpP Protease Activates Nuclear Genes Involved in Autophagy and Plastid Protein Quality Control. *The Plant Cell* **26**: 2201–2222.

Ramundo S, Rochaix JD. 2014. Chloroplast unfolded protein response, a new plastid stress signaling pathway? *Plant Signaling and Behavior* **9**: 1–3.

Robinson MD, McCarthy DJ, Smyth GK. 2009. edgeR: A Bioconductor package for differential expression analysis of digital gene expression data. *Bioinformatics* **26**: 139–140.

Romani I, Tadini L, Rossi F, Masiero S, Pribil M, Jahns P, Kater M, Leister D, Pesaresi P. 2012. Versatile roles of Arabidopsis plastid ribosomal proteins in plant growth and development. *Plant Journal* **72**: 922–934.

Rottet S, Besagni C, Kessler F. 2015. The role of plastoglobules in thylakoid lipid remodeling during plant development. *Biochimica et Biophysica Acta - Bioenergetics* **1847**: 889–899.

Sakuma Y, Maruyama K, Qin F, Osakabe Y, Shinozaki K, Yamaguchi-Shinozaki K. 2006. Dual function of an Arabidopsis transcription factor DREB2A in water-stress-responsive and heat-stress-responsive gene expression. *Proceedings of the National Academy of Sciences of the United States of America* **103**: 18822–18827.

Salah P, Bisaglia M, Aliprandi P, Uzan M, Sizun C, Bontems F. 2009. Probing the relationship between gram-negative and gram-positive S1 proteins by sequence analysis. *Nucleic Acids Research* **37**: 5578–5588.

Samalova M, Brzobohaty B, Moore I. 2005. pOp6/LhGR: a stringently regulated and highly responsive dexamethasone-inducible gene expression system for tobacco. *The Plant Journal* **41**: 919–935.

Sasaki I, Bertani G. 1965. Growth abnormalities in Hfr derivatives of Escherichia coli strain C. *Journal of general microbiology* **40**: 365–376.

Sawada Y, Toyooka K, Kuwahara A, Sakata A, Nagano M, Saito K, Hirai MY. 2009.

Arabidopsis bile acid:sodium symporter family protein 5 is involved in methionine-derived glucosinolate biosynthesis. *Plant and Cell Physiology cell physiology* **50**: 1579–1586.

Schägger H, von Jagow G. 1987. Tricine-sodium dodecyl sulfate-polyacrylamide gel electrophoresis for the separation of proteins in the range from 1 to 100 kDa. *Analytical Biochemistry* **166**: 368–379.

Schulte W, Töpfer R, Stracke R, Schell J, Martini N. 1997. Multi-functional acetyl-CoA carboxylase from Brassica napus is encoded by a multi-gene family: Indication for plastidic localization of at least one isoform. *Proceedings of the National Academy of Sciences of the United States of America* **94**: 3465–3470.

Schuster J, Knill T, Reichelt M, Gershenzon J, Binder S. 2006. BRANCHED-CHAIN AMINOTRANSFERASE4 is part of the chain elongation pathway in the biosynthesis of methionine-derived glucosinolates in Arabidopsis. *The Plant Cell* **18**: 2664–2679.

Sjögren LLE, MacDonald TM, Sutinen S, Clarke AK. 2004. Inactivation of the clpC1 gene encoding a chloroplast Hsp100 molecular chaperone causes growth retardation, leaf chlorosis, lower photosynthetic activity, and a specific reduction in photosystem content. *Plant Physiology* **136**: 4114–4126.

Skouv J, Schnier J, Rasmussen MD, Subramanian AR, Pedersen S. 1990. Ribosomal protein S1 of Escherichia coli is the effector for the regulation of its own synthesis. *Journal of Biological Chemistry* **265**: 17044–17049.

Sørensen MA, Fricke J, Pedersen S. 1998. Ribosomal protein S1 is required for translation of most, it not all, natural mRNAs in Escherichia coli in vivo. *Journal of Molecular Biology* **280**: 561–569.

Subramanian AR. 1983. Structure and Functions of Ribosomal Protein S1. *Progress in Nucleic Acid Research and Molecular Biology* **28**: 101–142.

Sugita M, Sugita C, Sugiura M. 1995. Structure and expression of the gene encoding ribosomal protein S1 from the cyanobacterium Synechococcus sp. strain PCC 6301: striking sequence similarity to the chloroplast ribosomal protein CS1. *Molecular and General Genetics MGG* **246**: 142–147.

Sukhodolets M V., Garges S, Adhya S. 2006. Ribosomal protein S1 promotes transcriptional cycling. *RNA* **12**: 1505–1513.

Sun W, Bernard C, Van Cotte B De, Van Montagu M, Verbruggen N. 2001. At-HSP17.6A, encoding a small heat-shock protein in Arabidopsis, can enhance osmotolerance upon

overexpression. *The Plant Journal* **27**: 407–415.

Supek F, Bošnjak M, Škunca N, Šmuc T. 2011. Revigo summarizes and visualizes long lists of gene ontology terms. *PLoS ONE* **6**: e21800.

Tadini L, Ferrari R, Lehniger M-K, Mizzotti C, Moratti F, Resentini F, Colombo M, Costa A, Masiero S, Pesaresi P. 2018. Trans-splicing of plastid rps12 transcripts, mediated by AtPPR4, is essential for embryo patterning in Arabidopsis thaliana. *Planta* **248**: 257–265.

Tadini L, Jeran N, Peracchio C, Masiero S, Colombo M, Pesaresi P. 2020a. The plastid transcription machinery and its coordination with the expression of nuclear genome: Plastid-Encoded Polymerase, Nuclear-Encoded Polymerase and the Genomes Uncoupled 1-mediated retrograde communication. *Philosophical Transactions of the Royal Society B: Biological Sciences* **375**: 20190399.

Tadini L, Jeran N, Pesaresi P. 2020b. GUN1 and Plastid RNA Metabolism: Learning from Genetics. *Cells* **9**: 2307.

Tadini L, Peracchio C, Trotta A, Colombo M, Mancini I, Jeran N, Costa A, Faoro F, Marsoni M, Vannini C, *et al.* 2020c. GUN1 influences the accumulation of NEP-dependent transcripts and chloroplast protein import in Arabidopsis cotyledons upon perturbation of chloroplast protein homeostasis. *The Plant Journal* **101**: 1198–1220.

Tadini L, Pesaresi P, Kleine T, Rossi F, Guljamow A, Sommer F, Mühlhaus T, Schroda M, Masiero S, Pribil M, *et al.* 2016. GUN1 Controls Accumulation of the Plastid Ribosomal Protein S1 at the Protein Level and Interacts with Proteins Involved in Plastid Protein Homeostasis. *Plant physiology* **170**: 1817–30.

Tadini L, Romani I, Pribil M, Jahns P, Leister D, Pesaresi P. 2012. Thylakoid redox signals are integrated into organellar-gene-expression-dependent retrograde signaling in the prors1-1 mutant. *Frontiers in Plant Science* **3**: 1–13.

Takeno K. 2016. Stress-induced flowering: The third category of flowering response. *Journal of Experimental Botany* **67**: 4925–4934.

Theobald DL, Mitton-Fry RM, Wuttke DS. 2003. Nucleic acid recognition by OB-fold proteins. *Annual Review of Biophysics and Biomolecular Structure* **32**: 115–133.

Tian T, Liu Y, Yan H, You Q, Yi X, Du Z, Xu W, Su Z. 2017. AgriGO v2.0: A GO analysis toolkit for the agricultural community, 2017 update. *Nucleic Acids Research* **45**: W122–W129.

Tiller N, Bock R. 2014. The translational apparatus of plastids and its role in plant development. *Molecular Plant* **7**: 1105–1120.

Toribio R, Mangano S, Fernández-Bautista N, Muñoz A, Castellano MM. 2020. HOP, a Co-chaperone Involved in Response to Stress in Plants. *Frontiers in Plant Science* **11**: 1657.

Tran LSP, Nakashima K, Sakuma Y, Simpson SD, Fujita Y, Maruyama K, Fujita M, Seki M, Shinozaki K, Yamaguchi-Shinozaki K. 2004. Isolation and functional analysis of arabidopsis stress-inducible NAC transcription factors that bind to a drought-responsive cis-element in the early responsive to dehydration stress 1 promoter. *The Plant Cell* **16**: 2481–2498.

Vannini C, Domingo G, Fiorilli V, Seco DG, Novero M, Marsoni M, Wisniewski-Dye F, Bracale M, Moulin L, Bonfante P. 2021. Proteomic analysis reveals how pairing of a Mycorrhizal fungus with plant growth-promoting bacteria modulates growth and defense in wheat. *Plant Cell and Environment* **44**: 1946–1960.

van Wijk KJ. 2015. Protein Maturation and Proteolysis in Plant Plastids, Mitochondria, and Peroxisomes. *Annual Review of Plant Biology* **66**: 75–111.

Van Wijk KJ, Kessler F. 2017. Plastoglobuli: Plastid Microcompartments with Integrated Functions in Metabolism, Plastid Developmental Transitions, and Environmental Adaptation. *Annual Review of Plant Biology* **68**: 253–289.

Wiśniewski JR. 2019. Filter Aided Sample Preparation – A tutorial. *Analytica Chimica Acta* **1090**: 23–30.

Woodson JD. 2016. Chloroplast quality control - balancing energy production and stress. *The New phytologist* **212**: 36–41.

Woodson JD. 2022. Control of chloroplast degradation and cell death in response to stress. *Trends in Biochemical Sciences*.

Wu GZ, Meyer EH, Richter AS, Schuster M, Ling Q, Schöttler MA, Walther D, Zoschke R, Grimm B, Jarvis RP, *et al.* 2019. Control of retrograde signalling by protein import and cytosolic folding stress. *Nature Plants* **5**: 525–538.

Yamaguchi K, Von Knoblauch K, Subramanian AR. 2000. The plastid ribosomal proteins. IDENTIFICATION OF ALL THE PROTEINS IN THE 30 S SUBUNIT OF AN ORGANELLE RIBOSOME (CHLOROPLAST)*. *Journal of Biological Chemistry* **275**: 28455–28465.

Yamaguchi K, Subramanian AR. 2003. Proteomic identification of all plastid-specific ribosomal

proteins in higher plant chloroplast 30S ribosomal subunit. *European journal of biochemistry* **270**: 190–205.

Yin T, Pan G, Liu H, Wu J, Li Y, Zhao Z, Fu T, Zhou Y. 2012. The chloroplast ribosomal protein L21 gene is essential for plastid development and embryogenesis in Arabidopsis. *Planta* **235**: 907–921.

Yu HD, Yang XF, Chen ST, Wang YT, Li JK, Shen Q, Liu XL, Guo FQ. 2012. Downregulation of chloroplast RPS1 negatively modulates nuclear heat-responsive expression of HsfA2 and its target genes in Arabidopsis. *PLoS Genetics* **8**.

Zechmann B. 2019. Ultrastructure of plastids serves as reliable abiotic and biotic stress marker. *PLoS ONE* **14**.

Zhou K, Zhang C, Xia J, Yun P, Wang Y, Ma T, Li Z. 2021. Albino seedling lethality 4; Chloroplast 30S Ribosomal Protein S1 is Required for Chloroplast Ribosome Biogenesis and Early Chloroplast Development in Rice. *Rice* **14**: 1–12.

Zhuang X, Jiang L. 2019. Chloroplast degradation: Multiple routes into the vacuole. *Frontiers in Plant Science* **10**: 359.

Zoschke R, Bock R. 2018. Chloroplast translation: Structural and functional organization, operational control, and regulation. *Plant Cell* **30**: 745–770.

Zubko MK, Day A. 1998. Stable albinism induced without mutagenesis: A model for ribosome-free plastid inheritance. *The Plant Journal* **15**: 265–271.